Université de Montréal

Azabicycloalkanone Synthesis by Transannular Cyclization

Par

Nagavenkata Durga Prasad Atmuri

Département de chimie

Faculté des arts et des sciences

Mémoire présenté à la Faculté des études supérieures et postdoctorales

En vue de l'obtention de grade de

Maîtrise ès sciences (M.Sc.)

en chimie

Décembre 2014

Acknowledgments

First and foremost, I offer my sincerest gratitude to my supervisor, Prof. William D. Lubell for giving me a wonderful opportunity, to build my career in the filed of Organic and Medicinal chemistry. Prof. Lubell supported me throughout my thesis with his patience and knowledge whilst allowing me the room to work in my own way.

I must also acknowledge to the Department of Chemistry, Université de Montréal for providing me excellent facilities to pursue my passion. I wish to express my sincere gratitude to my colleagues for helpful discussions and comments concerning chemistry. Mildred Bien-Aimé is thanked for help with technical issues. I am grateful to Dr. A. Fürtös, K. Venne, and M-C. Tang from the Regional Laboratory for Mass Spectrometry, Sylvie Bilodeau, Antoine Hamel and Cedric Malveau from the Regional Laboratory for NMR Spectroscopy and Francine Belanger-Gariepy from the Regional Laboratory for X-ray Analysis, at the Université de Montréal, for their assistance in compound analyses.

I would like to acknowledge the funding agencies that supported my research including the Natural Sciences and Engineering Research Council of Canada (NSERC), the Canadian Institutes of Health Research (CIHR, grant #TGC-114046 and CIP-79848), the Global Alliance to Prevent Prematurity and Stillbirth, an initiative of Seattle Children's, the Bill & Melinda Gates Foundation, the March of Dimes, and the Canadian Foundation for Innovation. The Shastri Indo-Canadian institute is specially thanked for providing me with a Quebec Tuition Fee Exemption grant to study at the Université de Montréal.

I would like to thank my parents. They probably don't completely understand what I have done these last two years, but without their constant love and support, I would not be here today. I would also like to thank my wife, sister, grandparents and the rest of my family for everything they have done for me over the years.

Résumé

Une stratégie de synthèse efficace de différents composés de type azabicyclo[X.Y.0]alkanone fonctionnalisés a été développée. La stratégie synthétique implique la préparation de dipeptides par couplage avec des motifs vinyl-, allyl-, homoallyl- et homohomoallylglycine suivi d'une réaction de fermeture de cycle par métathèse permettant d'obtenir des lactames macrocycliques de 8, 9 et 10 membres, qui subissent une iodolactamisation transannulaire menant à l'obtention de mimes peptidiques bicycliques portant un groupement iode.

Des couplages croisés catalysés par des métaux de transition ont été développés pour la synthèse d'acides aminés ω-insaturés énantiomériquement purs à partir de l'iodoanaline.

L'étude du mécanisme suggère que l'iodure subit une attaque du coté le moins stériquement encombré de la lactame macrocyclique insaturée pour mener à l'obtention d'un intermédiaire iodonium. La cyclisation se produit ensuite par une route minimisant les interactions diaxiales et la tension allylique.

L'iodolactamisation des différentes lactames macrocycliques insaturées a mené à l'obtention regio- et diastéréosélective d'acides aminés 5,5- et 6,6-iodobicycicliques. De plus, une imidate azabicyclo[4.3.1]alkane pontée de type anti-Bredt fut synthétisée à partir d'une lactame macrocyclique insaturé à neuf membres.

Les analyses cristallographiques et spectroscopiques des macrocycles à 8, 9 et 10 membres, du composé iodobicyclique 5,5 ainsi que de l'imidate pontée, montrent bien le potentiel de ces dipeptides rigidifiés de servir en tant que mimes des résidus centraux de tours β de type I, II', II et VI.

Mot-clés : **(**Cyclisation transannulaire, Acide aminé Azabicyclo[X.Y.0]alkanone, Iodolactamisation, Quinolozidinone, Pyrrolizidinone, Indolizidinone.)

Abstract

An efficient strategy has been developed for the synthesis of different functionalized azabicyclo[X.Y.0]alkanone amino acids. The synthetic sequence features preparation of dipeptides by coupling respectively vinyl-, allyl-, homoallyl- and homohomoallylglycine building blocks, followed by ring closing metathesis to produced 8-, 9-, and 10-member unsaturated macrocyclic lactams, and transannular iodolactamization to make the bicyclic dipeptide surrogates bearing iodine on the lactam ring. Transition metal cross-coupling methods were developed to make enantiomerically pure ω-unsaturated amino acid building blocks from iodoalanine. Mechanistic considerations suggest that attack of iodine from the least hindered face of the unsaturated macrocyclic lactam provides an iodonium intermediate and cyclization occurs by a route that minimizes allylic strain and diaxial interactions. Iodolactamization of the unsaturated macrocyclic lactams gave regio- and diastereoselectively fused 5,5- and 6,6-iodo-bicylic amino acids. Moreover, an anti-Bredt bridgehead imidate azabicyclo[4.3.1]alkane was synthesized from a 9-membered unsaturated macrocyclic lactam precursor. X-ray crystallographic and spectroscopic analyses of the 8-, 9-, and 10-member macrocycles, as well as the 5,5-bicycle and bridgehead imidate demonstrate the potential of these constrained dipeptides to mimic the central residues of ideal type I, II', II and VI β-turn geometry.

Keywords: (Transannular cyclizations, Azabicyclo[X.Y.Z]alkanone amino acid, Iodolactamization, Quinolozidinone, Pyrrolizidinone, Indolizidinone.)

Table of contents

List of Figures

CHAPTER 1

CHAPTER 2

CHAPTER 4

List of Schemes

CHAPTER 1

CHAPTER 2

CHAPTER 3

CHAPTER 4

List of Tables

List of Abbrivations

$[\alpha]_D$	Optical Rotation
lit.	literature
μ	micro
m	multiplet (spectral)
M	molar
Me	methyl
mg	milligram
min	minutes
MHz	megahertz
mL	millilitre
mmol	millimole
mp	melting point
MS	mass spectrometry
MW	molecular weight
NMR	nuclear magnetic resonance
IR	Infrared
J	coupling constant
ppm	part per milliom
R_f	retention factor (in chromatography)
s	singlet
t	triplet
DMSO-d_6	hexadeuterodimethyl sulfoxide
br	broad (spectral)
TFA	trifluoroacetic acid

μL	Microlitre
THF	tetrahydrofuran
TLC	thin layer chromatography
m-CPBA	meta-chloroperbenzoic acid
DIPEA	diisopropylethylamine
DMF	*N*,*N*-dimethylformamide
Fmoc	9-fluorenylmethyloxycarbonyl
HATU	*O*-(7-azabenzotriazole-l-yl)-1,1,3,3-tetramethyluronium hexafluorophosphate
LHMDS	lithium hexamethyldisilazane
ee	enantiomeric excess
HRMS	high-resolution mass spectrometry
Dmb	2,4-dimethoxybenzyl
9-BBN	9-borabicyclo[3.3.1]nonane
PhF	9-phenyl fluoren-9-yl
RCM	ring closing metathesis

CHAPTER 1

INTRODUCTION

Introduction

1.1 Peptides and Secondary Structure

Peptides control many physiological processes in the human body, serving as hormones, neurotransmitters, enzyme substrates, as well as neuro- and immunomodulators.[1] Binding often to membrane-bound receptors, peptides control a number of functions including metabolism, immune defense, digestion, respiration, and reproduction.

The secondary structure of a protein refers the local folding pattern of the polypeptide backbone, which may be stabilized by hydrogen bonds between amide N-H and C=O groups, as well as hydrophobic interactions. Various types of secondary structure have been discovered, the most common of which are the α-helix, β-sheet and turn conformations. Secondary structures such as turns are often essential components for peptide and protein biology, because they are often located on the protein surface and act as molecular recognition sites.[2,3] The β-turn is a structural motif common to many biologically active, cyclic peptides and has been postulated in many cases to be the biologically active conformer of linear peptides. The β-turn is composed of four amino acids (residues *i* to *i*+3), which reverse the direction of the peptide chain placing the α-carbons of the first and fourth residues at a distance of ≤7Å. Different β-turns are classified according to the conformations of their central amino acid residues as described by the dihedral angles ϕ and ψ (Figure 1.1).[4]

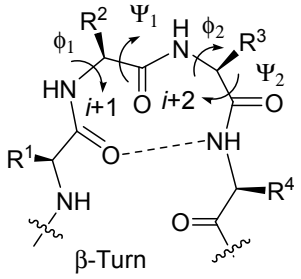

Type β Turn	ϕ^{i+1}, deg	ψ^{i+1}, deg	ϕ^{i+2}, deg	ψ^{i+2}, deg
I	–60	–30	–90	0
I’	60	30	90	0
II	–60	120	80	0

II’	60	–120	–80	0
VIa	–60	120	–90	0
VIb	–120	120	–60	0
IV	–60	–1	–50	20
VIII	–60	–30	–120	120

Figure 1.1 Representative β-turns and their torsional angles[4]

Peptides are attractive starting points for drug discovery, because they are essential for most biochemical processes. Unfortunately, the attributes of potency and specificity exhibited by these structures are compromised due to short biological half-lives, poor oral bioavailability, and rapid metabolism. To overcome these obstacles, medicinal chemists have committed to design and synthesize non-peptidic molecules, which display pharmacological activity like the native peptides at their receptors. These nonpeptidic compounds are referred to as peptidomimetics. In addition to mimicking the activity of native peptides and serving for example as receptor agonists, peptidomimetics may act as enzyme inhibitors as well as receptor antagonists. The design of such peptidomimetics remains a challenge because of the absence of lead structures as well as structural information concerning the receptors to which they may bind.

The small molecule, opioid natural product morphine (**1.2**) may be considered as a peptidomimetic, because of its structural and functional resemblance to endogenous opioid peptides such as enkephalin (**1.1**) and β-endorphin (**1.3**, Figure 1.2). For example, the morphine phenol and the tyrosine residue in the peptide opioids may interact with the opioid receptors in a similar fashion to elicit comparable responses.[5] The structural relationships between the morphine skeleton and enkephalins remain however unknown.[6]

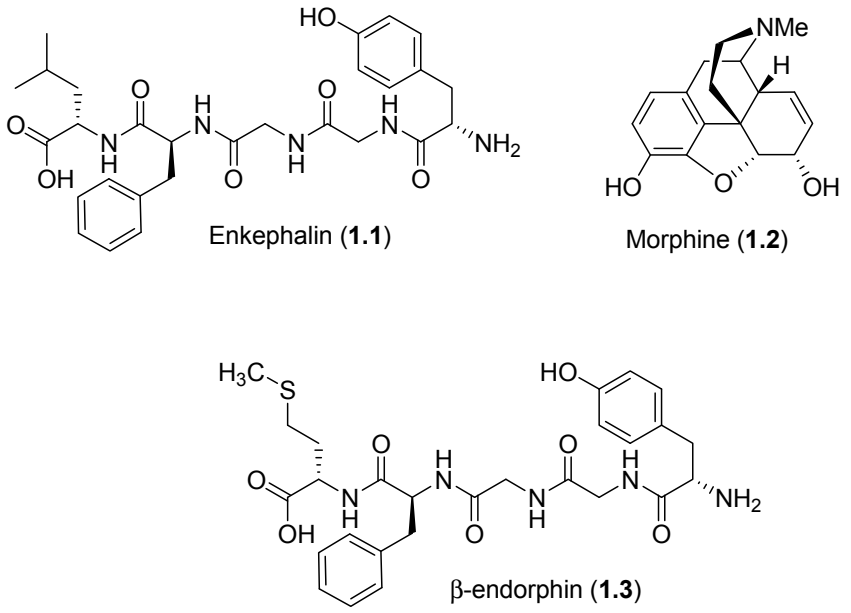

Figure 1.2 Examples of peptide and non-peptide opioid receptor ligands

1.2 Peptidomimetics

Peptidomimetics are compounds which retain the ability of the natural peptide or protein to interact with the biological target in 3D space and produce target specific biological effects. Peptidomimetics are valuable tools for structure-activity relationship studies in drug discovery.

Different categories have been used to describe different types of peptidomimetics.[7,8] For example, pseudopeptides have close structural similarity to natural peptides yet possess functional groups that improve properties and enhance contacts with receptor binding sites. Some units may mimic short portions of peptide secondary structure, such as a β-turn. Pseudopeptides are often employed to generate lead compounds. Functional mimetics have been commonly identified by molecular modeling and high throughput screening. Small non-peptide molecules that bind to a peptide receptor, such as morphine, functional mimetics can have very different structures from natural peptides. Topographical mimetics are synthesized by structure based drug design employing novel templates that may have structures unrelated

to the original peptide. Topographical mimetics contain the essential groups for recognition oriented on a novel non-peptide scaffold.

1.3 Designing of Peptidomimetics

The de novo design of small molecule peptidomimetics is still in its infanacy; instead, a more hierarchical approach is often pursued to obtain non-peptide ligands. Starting from the parent peptide, structure-activity relationship studies are typically performed to define the minimal active sequence and major pharmacophore elements responsible for biological activity. Several methods for the synthesis of peptidomimetics are discussed below.

1.3.1 Side-chain modifications

Side chain function and orientation are often essential for interaction with the receptor. Techniques for side chain substitution are often employed to explore the importance of side chain composition and conformation. For example, proline derivatives substituted at the 3-position have been synthesized to restrain the orientation of the amino acid side chain with respect to the peptide backbone.[9] For example, 3-propylproline (3PP) **1.5** was synthesized as a norleucine analogue and incorporated in a C-terminal tetrapeptide analog of cholecystokinin (CCK) providing improved affinity for the central CCK receptor (Figure 1.3).[10]

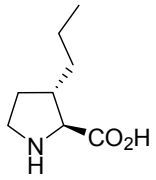

1.5

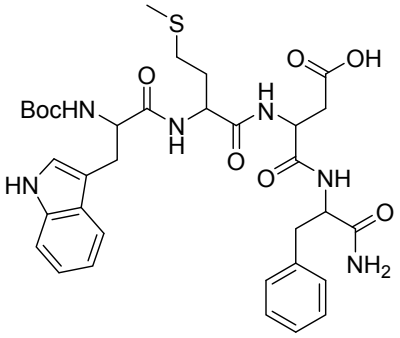

BocTrp-Met-Asp-Phe-NH_2

CCK Tetrapeptide Analogues

1.6

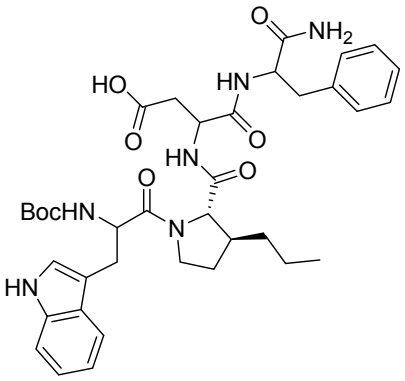

BocTrp-Pro-Asp-Phe-NH_2

Replacing the methionine residue with 3PP

1.7

Figure 1.3 Comparison of activities of tetrapeptides 1.6 & 1.7-advanatages of a proline substitution.

1.3.2 Peptide Backbone Modification

Peptide backbone modifications have been synthesized through changes of a single amino acid or many residues. Replacement of peptide bonds by non-peptide analogs has also been utilised to modify the backbone of peptides. Common backbone modifications are shown below (Figure 1.4).[11]

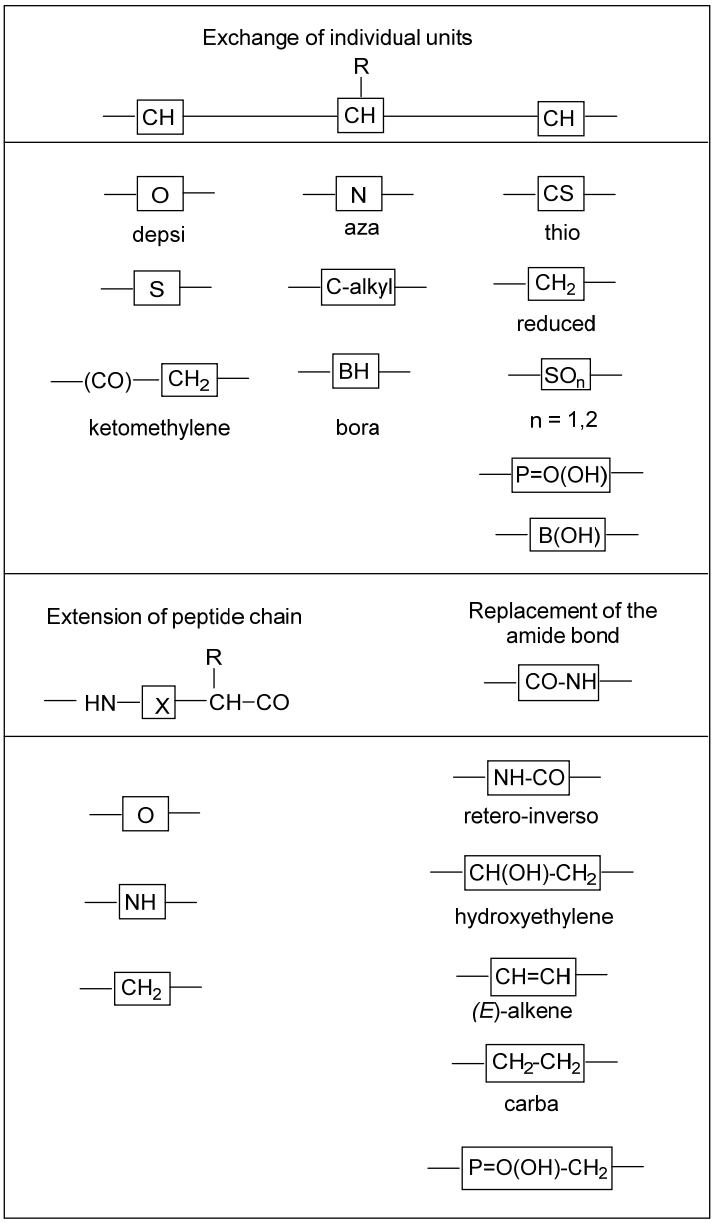

Figure 1.4 General peptide backbone modifications[11]

1.3.3 Constrained dipeptide analogues

Bridging between two neighbouring amino acids in a peptide may lead to a constrained dipeptide mimetic with limited conformational flexibility. Such constrained dipeptides can be used to explore the importance of specific peptide conformations for activity.

1.8
cyclo-(Ala-Sar)$_3$

1.9
Dipeptide lactam

Figure 1.5 Freidinger's initial application of dipeptide lactams

Studying C3 symmetric cyclic hexapeptides, typified by cyclo-(Ala-Sar)$_3$, because of their effects on feed efficiency of ruminant animals in which their cation binding properties shift ruminant stomach bacterial fermentation toward the production of less volatile products, Freidinger and co-workers employed the Merck Molecular Modeling System to design analogs possessing lactam bridges from the α-carbon of alanine to the nitrogen of the preceeding sarcosine residue. Although lactam rings were known in β-lactam antibiotics, such as pencillin, which may be considered a dipeptide-based natural product, their employment in the comformational constraint of alternative peptide structures had yet to be pioneered.[12]

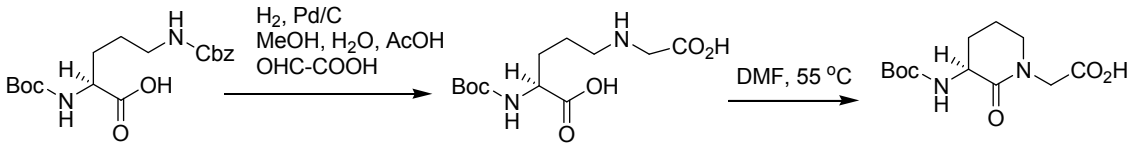

1.10 **1.11** **1.12**

Scheme 1.1 Synthesis of a lactam amino acid

Starting from orthogonally protected ornithine, the dipeptide lactam was constructed by a reductive amination lactam cyclization route (Scheme 11), and incorporated subsequently into peptides using conventional coupling conditions.[12] Notably, contrained variant **1.9** of the parent cyclo-(Ala-Sar)$_3$ **1.8** exhibited similar efficacy in the ruminant fermentation assay.

1.3.5 Global Restrictions of Conformations

Global restrictions in the conformation of a peptide are achieved by limiting flexibility through cyclizations. For example, head-to-tail cyclic peptides have typically rigid conformations, increased metabolic stability, superior bioavailability and higher cell permeability.[3,6] Alternative side chain-to-side chain and side chain-to-backbone bridges have also been used to increase the conformational rigidity of peptide structures with notable success.[11]

1.4 Azabicycloalkanone amino acids

Azabicyclo[X.Y.0]alkanone amino acids can serve as conformationally rigid peptide scaffolds that may mimic secondary stuctures such as β-turns (Figure 1.6).[13]

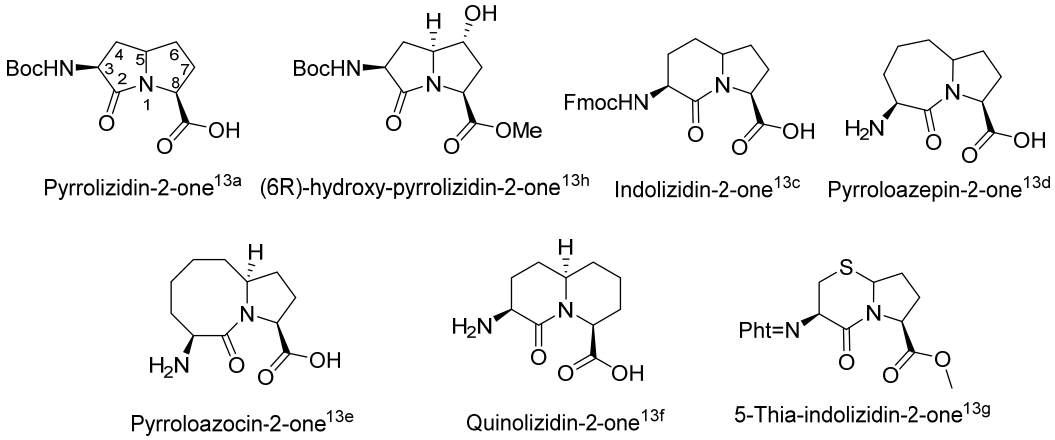

Figure 1.6 Different ring size azabicyclo[X.Y.0]amino acid structures

Their heterocyclic framework can rigidify the backbone dihedral angle geometry and side-chain conformations to specific orientations useful for investigating structure-activity relationships.[14] New methods are in demand to make these restrained dipeptide scaffolds for applications in peptide science and medicinal chemistry towards drug discovery.[15] Sets of azabicyclo[X.Y.0]alkanone amino acid derivatives, such as fused 5,5-, 6,5-, 7,5- and 6,6-ring systems, would be useful for drug discovery because they may be systematically employed to identify the backbone geometry responsible for peptide activity.

Examples of peptide mimics containing azabicyclo[X.Y.0]alkanone amino acids include PDC113.824 (**1.17**), which possesses a (3*S*,6*S*,9*S*)-indolizidin-2-one amino acid (I2aa, Figure 1.7) that orients pharmacophores to modulate the prostaglandin F2α receptor by a biased allosteric mechanism that ultimately delays labor in animal models.[16,17] Furthermore, the I2aa analog **1.20** and pyrroloazepinones **1.19** and **1.21**, all block inhibitor of apoptosis proteins (IAPs) and have been used to develop anticancer therapeutics.[18] Peptide analog **1.18** acts as a potent bradykinin B2 receptor antagonist.[19] Azabicyclo[5.3.0]alkanone amino acid analog **1.22** exhibits selective $\alpha_v\beta_3/\alpha_v\beta_5$ integrin receptor antagonism (Figure 1.7).[20]

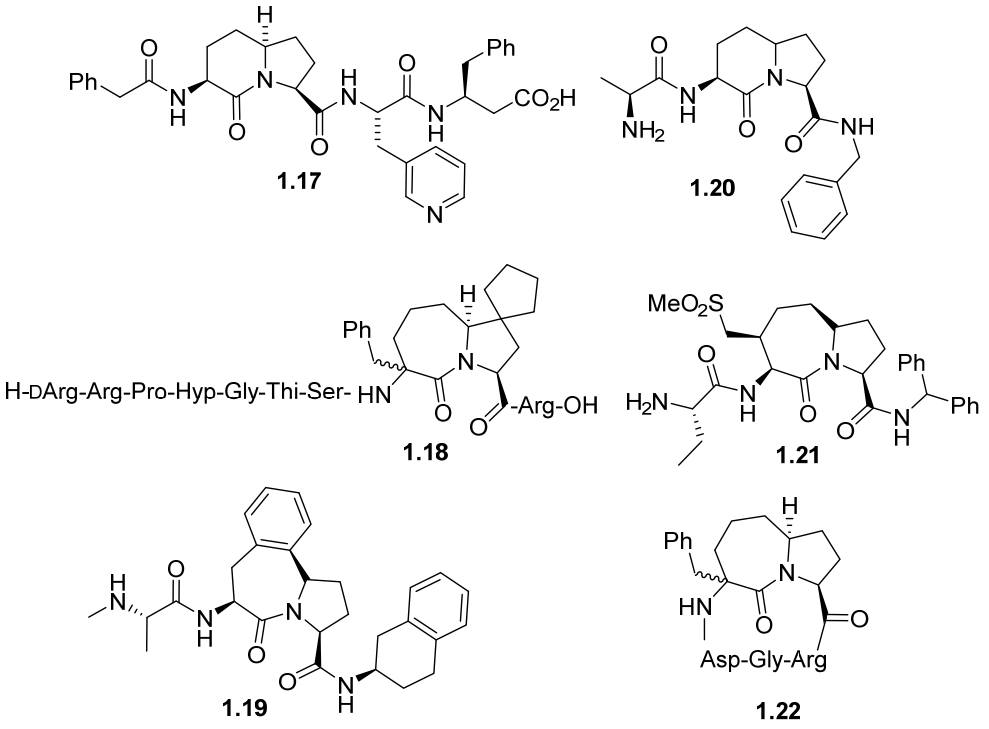

Figure 1.7 Biologically active azabicyclo[X.Y.0]alkanone amino acid analogs

1.5 Azabicyclo[X.Y.0]alkanone Synthesis

Azabicycloalkanone amino acids posessing different ring sizes have attracted interest to develop probes for studying structure-activity relationships of various biologically relevant peptides. The synthesis of these constrained dipeptides is however challenging and requires typically multiple-step processes to make specific analogs, which are often obtained as

stereoisomeric mixtures.[21] The preparation of azabicycloalkanone amino acids has been reviewed.[22] Representative approaches are shown below to illustrate the challenges of constructing different bicyclic ring systems with stereocontrol and potential for adding side chains on the ring carbons.

1.5.1 Azabicyclo[3.2.0]alkan-2-one Amino Acid

Molecular modelling studies indicated that fused γ-lactam-azetidine analogues (e.g., **1.34**) have pyramidalized lactam distortions similar to those observed in penicillins (Scheme 1.2).[23] Towards the synthesis of such an azabicyclo[3.2.0]alkan-2-one amino acid derivative, bromination of glutaric anhydride **1.23** gave α,α'-dibromo diacid **1.24**, which on esterification and treatment with bezylamine provided diastereomeric azetidine **1.27**. The diasteromers were separated after reduction of the methyl ester. Oxidation of alcohol **1.29**, olefination and catalytic reduction gave azetidine **1.31**, which was converted to the γ-lactam **1.32**. Amination of the 3-position was accomplished using LiHMDS and *o*-(diphenylphosphinoyl)hydroxylamine to provide amino ester **1.33**, which was transformed into *N*-phenacetyl counterpart **1.34**.[24]

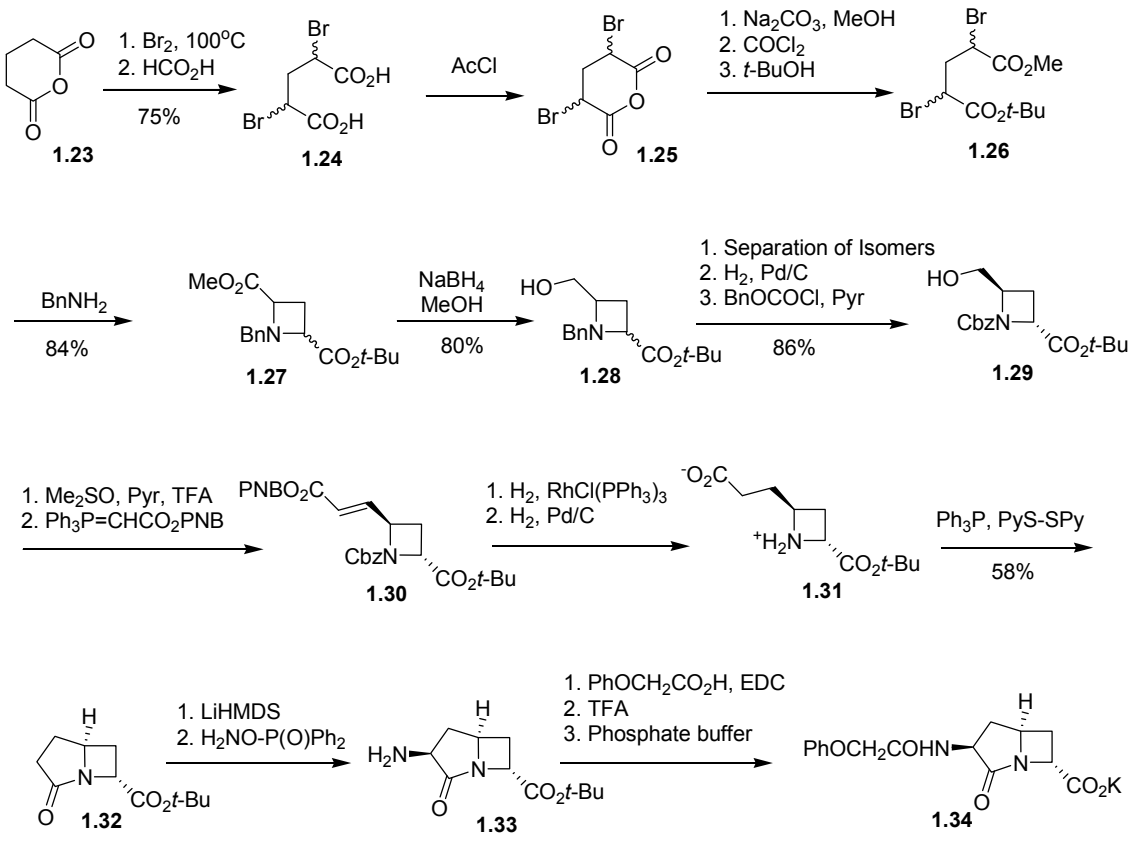

Scheme 1.2 Synthesis of azabicyclo[3.2.0]alkanone amino acid

1.5.2 Azabicyclo[3.3.0]alkan-2-one amino acid (Pyrrolizidinone type)

γ-Lactam analogues of penicillanic acid were pursued by a 1,3-dipolar cycloaddition strategy. Nitrone **1.35** reacted with methyl acrylate to give a regioisomeric mixture of isoxazolidine diastereomers **1.36** and **1.37** (Scheme 1.3). Reductive cleavage of the N-O bond, lactam formation, alcohol activation and introduction of the amine group via displacement with azide ion gave the bicyclic lactams.[25]

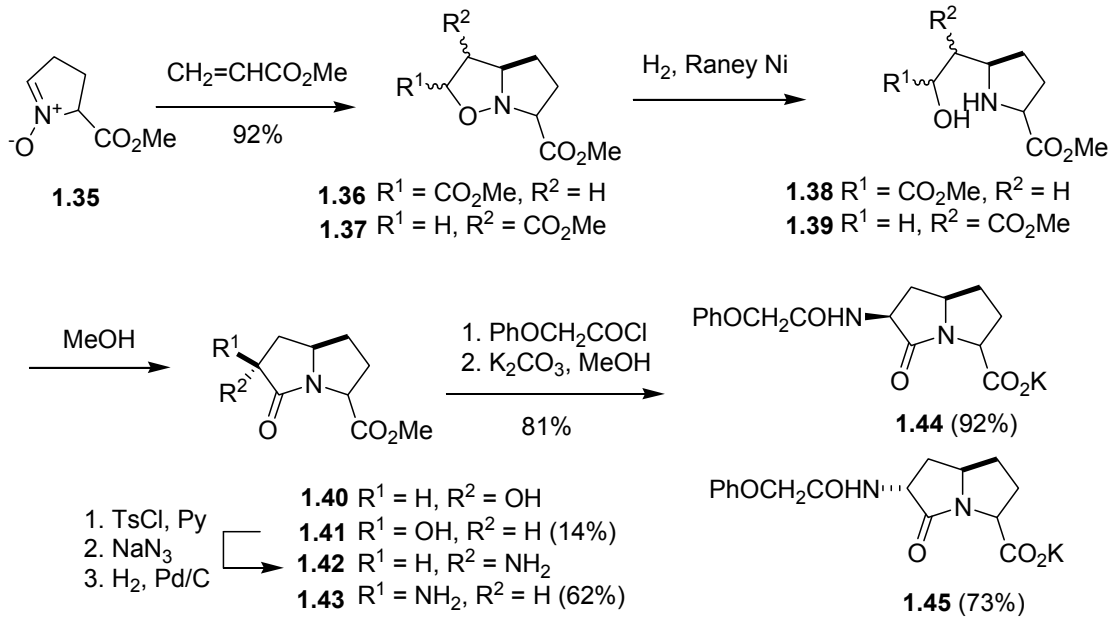

Scheme 1.3 Synthesis of Azabicyclo[3.3.0]alkan-2-one amino acid

1.5.3 Synthesis of Enantiopure C6-Functionalized Pyrrolizidinone Amino Acids

Enantiopure 6-hydroxy pyrrolizidinone amino acid **1.55** was synthesized in seven steps from (2*S*)-α-*tert*-butyl *N*-(PhF)aspartate *β*-aldehyde **1.46**, which was prepared in four steps from L-aspartate.[26] Acyloin condensation of aldehyde **1.46** gave α-hydroxy ketone **1.48** (Scheme 1.4). Alcohol acetylation, reductive amination, ester group exchange and lactam cyclization then gave protected 6-hydroxy pyrrolizidinone amino acid **1.55**.[13h]

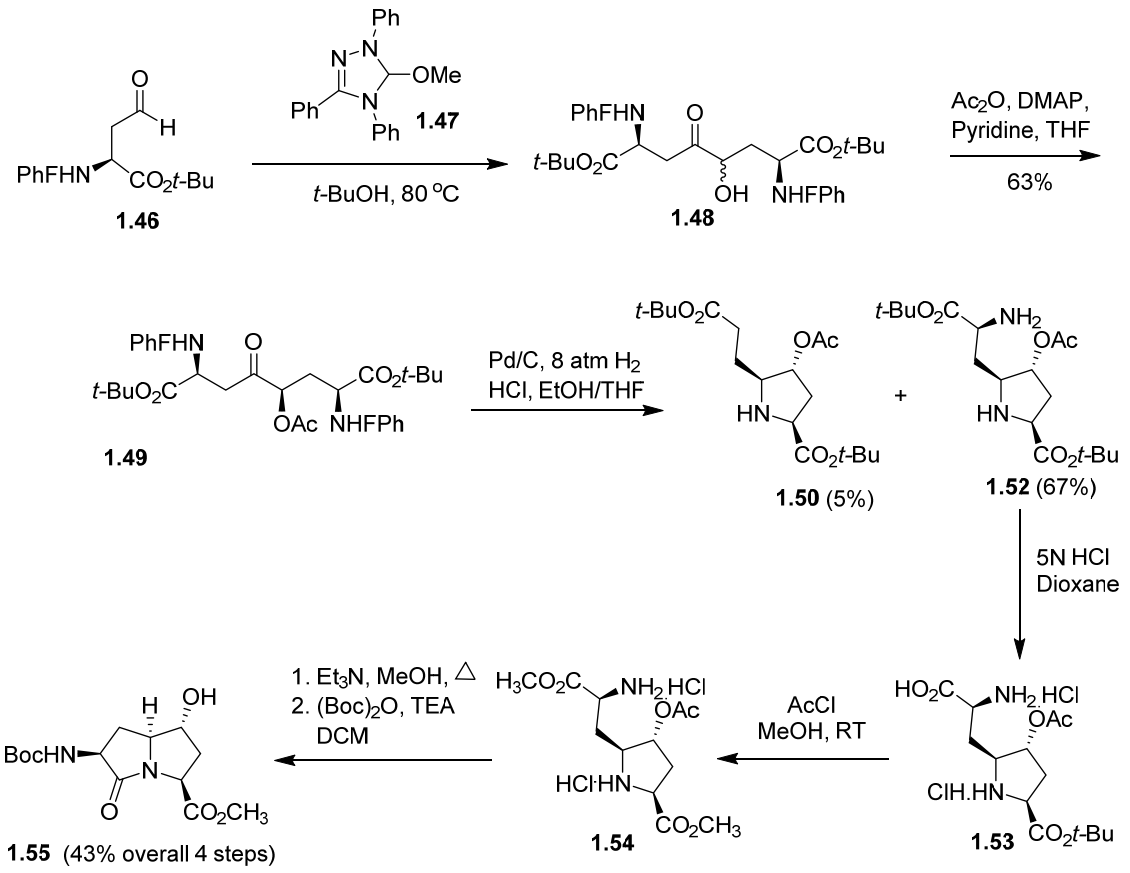

Scheme 1.4 Synthesis of C6-Functionalized azabicyclo[3.3.0]alkanone amino acid

1.5.4 Azabicyclo[4.3.0]alkanone Amino Acid (Indolizidinone-type)

The Claisen condensation of *N*-(PhF)glutamate **1.56**, followed by saponification and decarboxylation gave symmetric diaminoazelate **1.58**, which underwent diastereoselective reductive amination and lactam cyclization to provide protected indolizidinone amino acid in 39% overall yield (Scheme 1.5).[27]

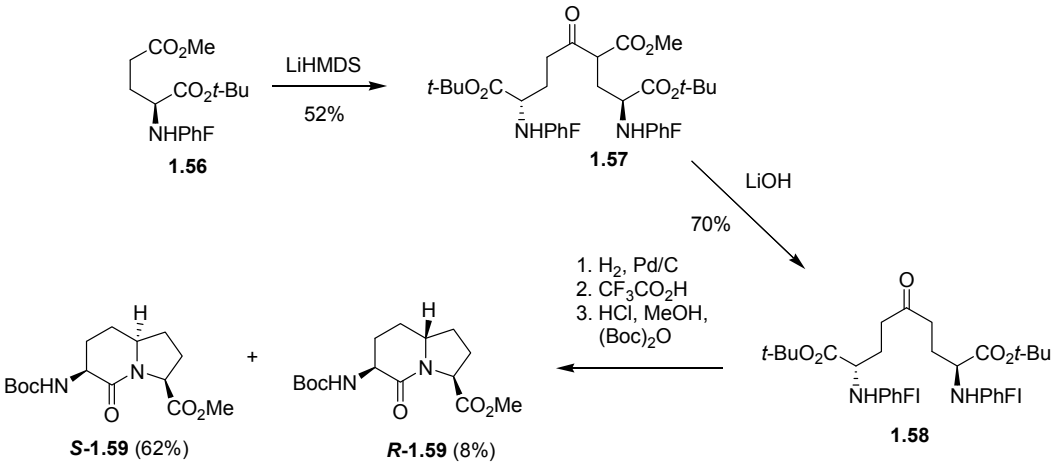

Scheme 1.5 Synthesis of protected azabicyclo[4.3.0]alkanone amino acid

1.5.5 Azabicyclo[4.4.0]alkan-2-one Amino Acid (Quinolizidinone-type)

The first successful synthesis of a quinolizidinone amino acid was accomplished in seven steps and 40% overall yield from L-pyroglutamic acid.[28] Pyroglutamic acid **1.60** was protected with benzyl bromide in the presence of diisopropylethylamine (DIEA) in DCM, followed by di-*tert*-butyl dicarbonate in presence of DMAP, and Et_3N in acetonitrile to give **1.61**. β-Ketophosphonate **1.62** was obtained by the addition of the lithium anion of dimethyl methylphosphonate to benzyl *N*-(Boc)pyroglutamate **1.61** in toluene in 74% yield. α,β-Unsaturated ketone **1.64** was obtained by the Horner-Wadsworth-Emmons olefination of *N*-(PhF)aspartate β-aldehyde **1.63** with β-ketophosphonate **1.62**. Ketone **1.64** underwent reductive amination on treatment with palladium-on-carbon to give pipecolate **1.65** as a single diastereomer. Without further purification pipecolate **1.65** was converted quantitatively to protected quinolizidinone amino acid **1.66** using diphenylphosphoryl azide and DIEA in CH_2Cl_2.[28]

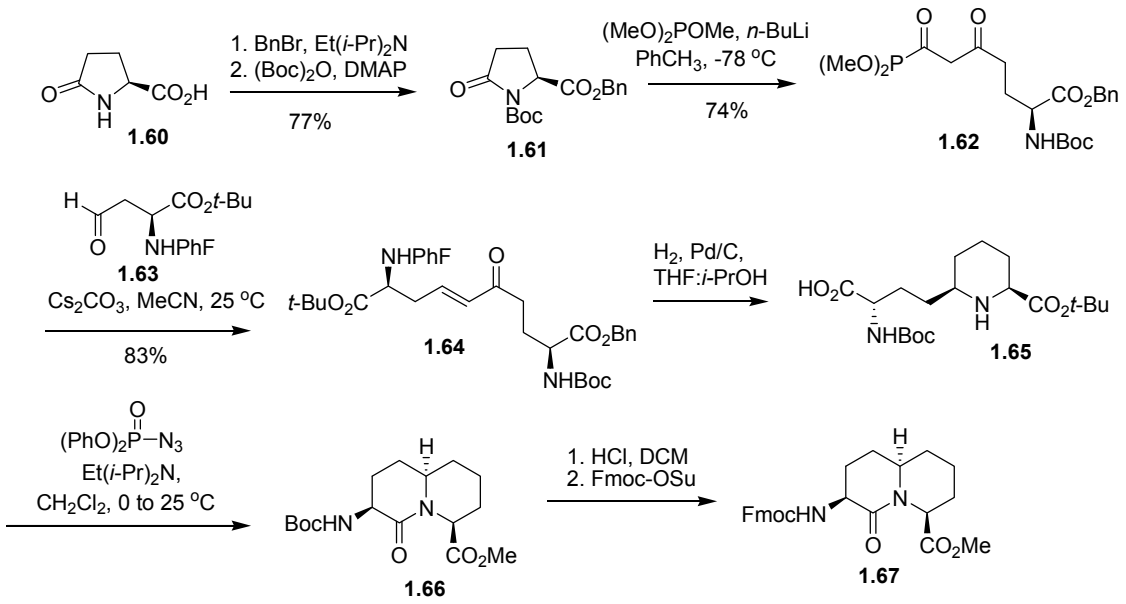

Scheme 1.6 Synthesis of azabicyclo[4.4.0]alkanone amino acid

1.5.6 Azabicyclo[5.3.0]alkanone Amino Acids (Pyrroloazepinone-type)

Ketone **1.68** (Scheme 1.7) was transformed into its corresponding allylic alcohol by reduction with sodium borohydride in the presence of cerium trichloride in MeOH:THF to provide **1.69** as a 1:1 mixture of diastereomers in 86% yield (Scheme 1.7).[28] Treatment of the alcohol with methanesulfonyl chloride and triethylamine in DCM, afforded cyclization to 5-alkylprolines **1.70** in 91% yield. The *E*-olefin geometry of alcohol **1.69** excluded the attack of the N-(PhF)amine onto the methanesulfonate such that *N*-(Boc)prolines **1.70** was formed exclusively. Removal of the PhF and benzyl groups with concurrent double bond reduction was achieved by catalytic hydrogenation of **1.70** in a THF/methanol solution. *N*-Acylation with Fmoc-OSu in an acetone/water solution gave prolines **1.71** in 81% overall yield from **1.70**. Alkylative esterification with allyl iodide in MeCN afforded ester **1.72** in 86% yield under reflux. Simultaneous removal of the Boc group and *tert*-butyl ester with HCl in DCM, followed by lactam cyclization with HATU in presence of DIEA gave (7*S*)- and (7*R*)-**1.74** in a 2:1 diastereomeric ratio. Pyrroloazepin-2-one *N*-(Fmoc)amino acids (7*S*)- and (7*R*)-**1.75** were finally synthesized by palladium-catalyzed hydrostannolytic cleavage of their respective allyl esters (7*S*)- and (7*R*)-**1.74** in yields of 88% and 99% after chromatography.[28]

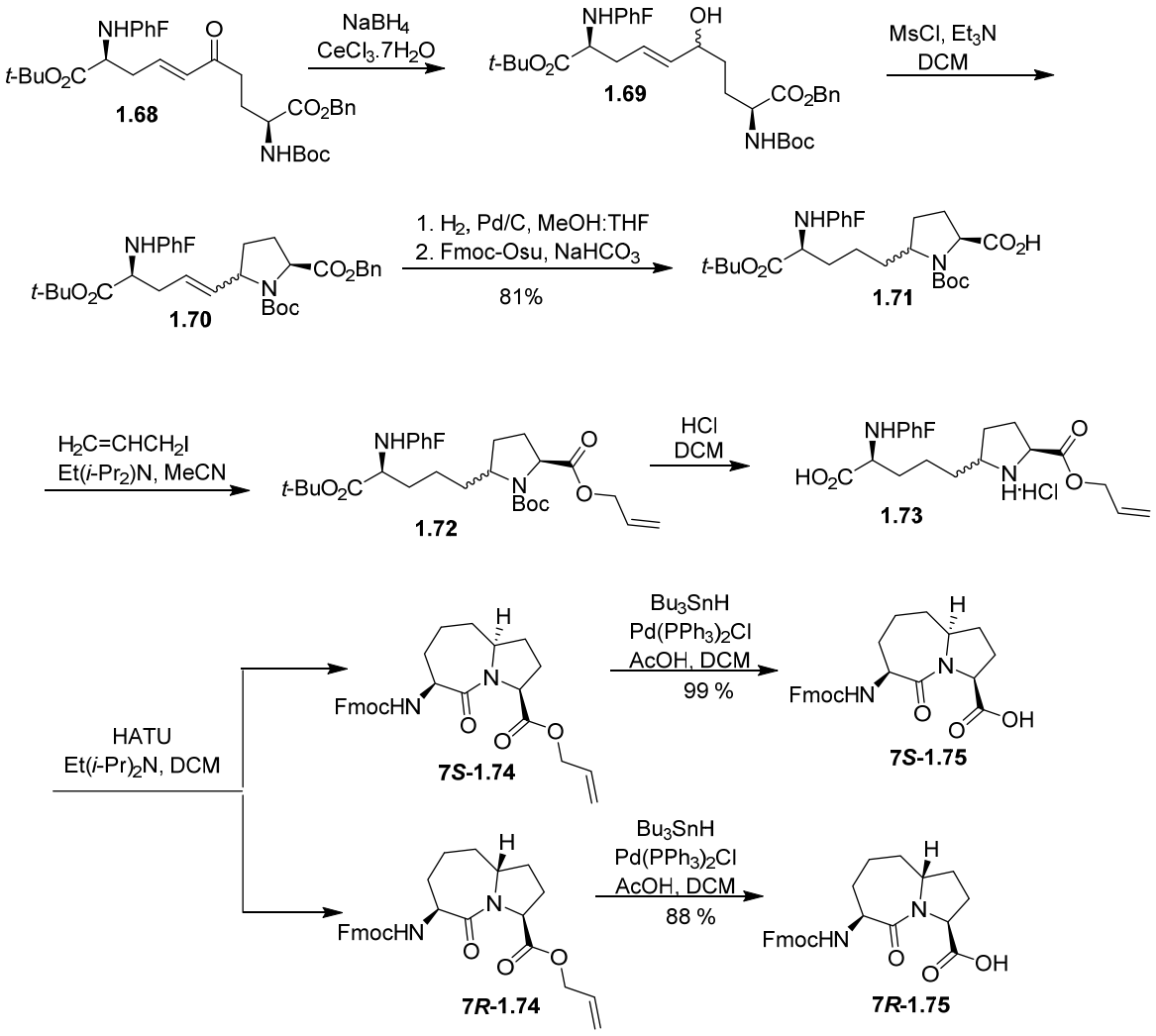

Scheme 1.7 Synthesis of azabicyclo[5.3.0]alkanone amino acid

1.5.7 Azabicyclo[5.4.0]alkanone Amino Acids

Dipeptide aldehyde **1.79** was converted into enamide **1.80** using catalytic TFA (Scheme 1.8).[15a] Bicycle **1.83** was constructed from **1.80** by an iminium ion cyclization, followed by reducing double bond using different reducing agents.

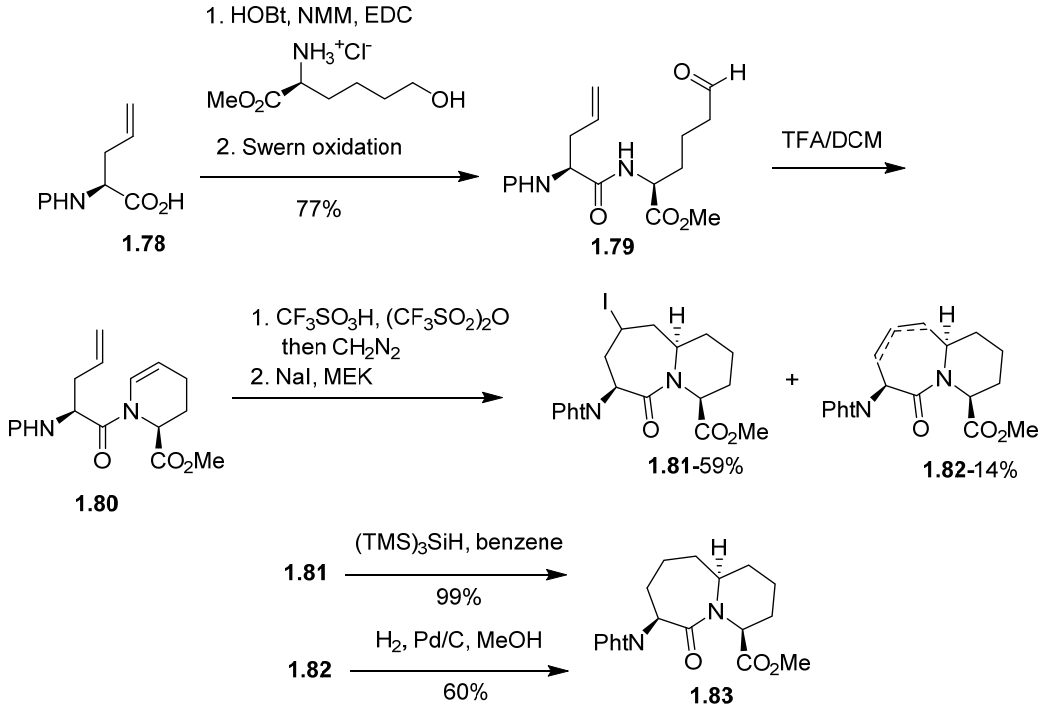

Scheme 1.8 Synthesis of azabicyclo[5.4.0]alkanone amino acid

1.5.8 Synthesis of α-Thrombin inhibitory activity of Indolizidinone

Stephen Hanessian et. al., developed a constrained mimic consisting of indolizidinone nucleus with strategically situated substituents acting as inhibitors of α-Thrombin.[29,30] The synthesis was starts with L-pyroglutamic acid. The enantiopure precursor **1.85** (scheme1.9) was efficiently prepared from L-pyroglutamic acid **1.84** in six steps. Hydrogenation of **1.85** to the saturated lactones, followed by removal of the Boc protecting group with bromocatechol borane gave the lactone **1.86** ref. Ring expansion of lactone to lactam and protection of hydroxyl group gives indolizidinone **1.87**. C-terminal branching was introduced by using *t*-butyl lithium and benzyl bromide gave the product as a single isomer **1.88**. Reformation of the enolate under the same conditions and trapping with the Davis oxaziridine reagent led to **1.89** as a single isomer having the desired configuration at C-3 (*vide infra*). Cleavage of the PMB group with DDQ, Barton-McCombie deoxygenation, and acetylation gave the indolizidinone **1.89**. Deprotection of the primary silyl ether, and oxidation of the

alcohol to the corresponding acid **1.90**. Deacylation and amide formation gave the desired prototype **1.91**.

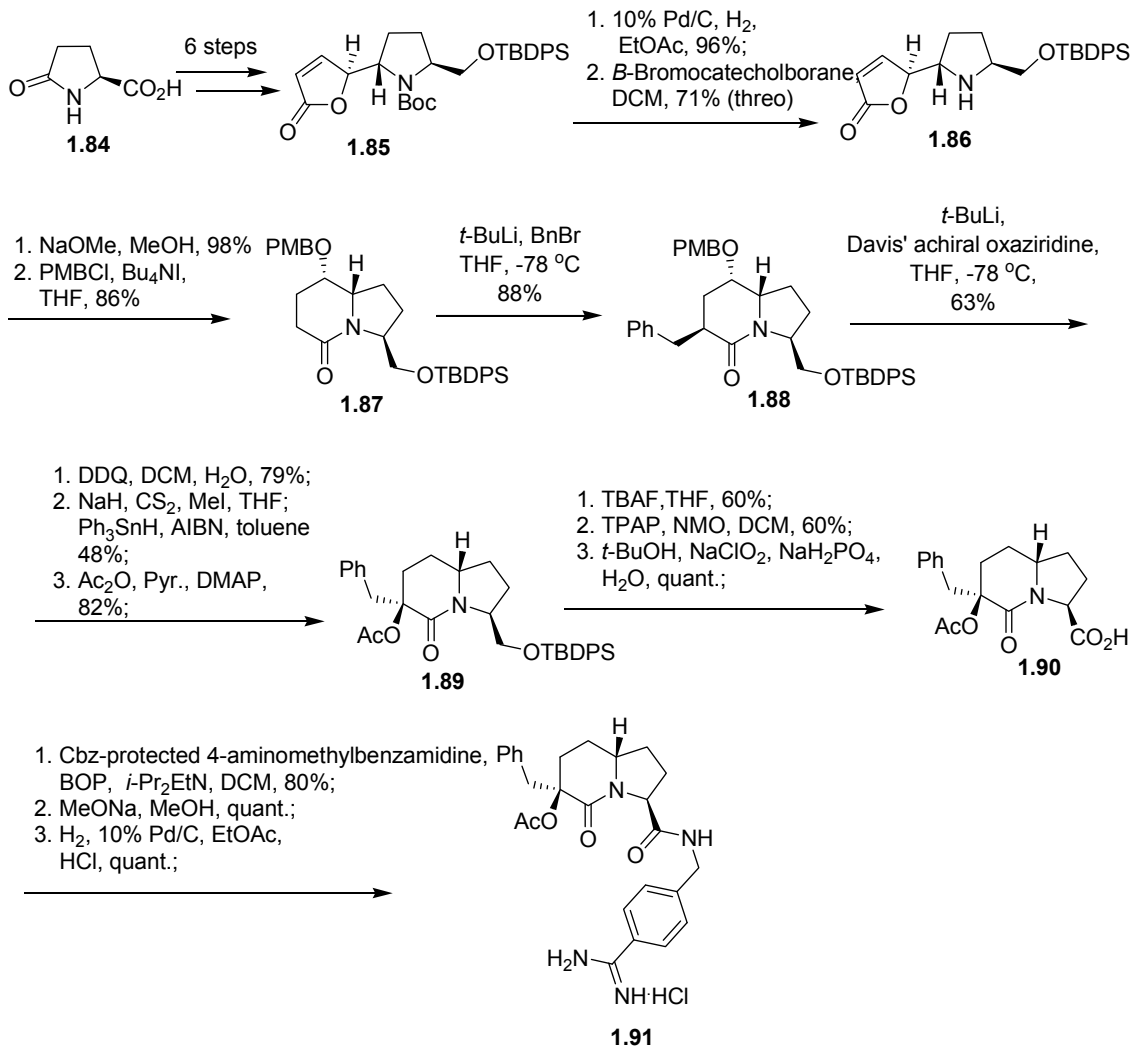

Scheme 1.9 Synthesis of Indolizidinone derivatives

1.6 Transannular cyclization

Seeking a more general method for making azabicycloalkane amino acids, ideally with potential for amending a diverse array of side chain functionality onto the ring system, our laboratory has pursued a route featuring ring-closing metathesis and electrophilic transanular cyclization. Transannular reactions of amine nucleophiles onto macrocyclic olefins and epoxides have been used for stereoselective construction of bicyclic amines.[31] Fewer examples have been reported of cyclizations of macrocyclic lactams.[32] Ring closing

metathesis (RCM) of dipeptides composed of various ω-unsaturated amino acids may give access to a diverse variety of unsaturated macrocycles of different ring-sizes for subsequent electrophilic transanular cyclizations using electrophiles to afford sets of azabicycloalkanones by a common method.[32a,33]

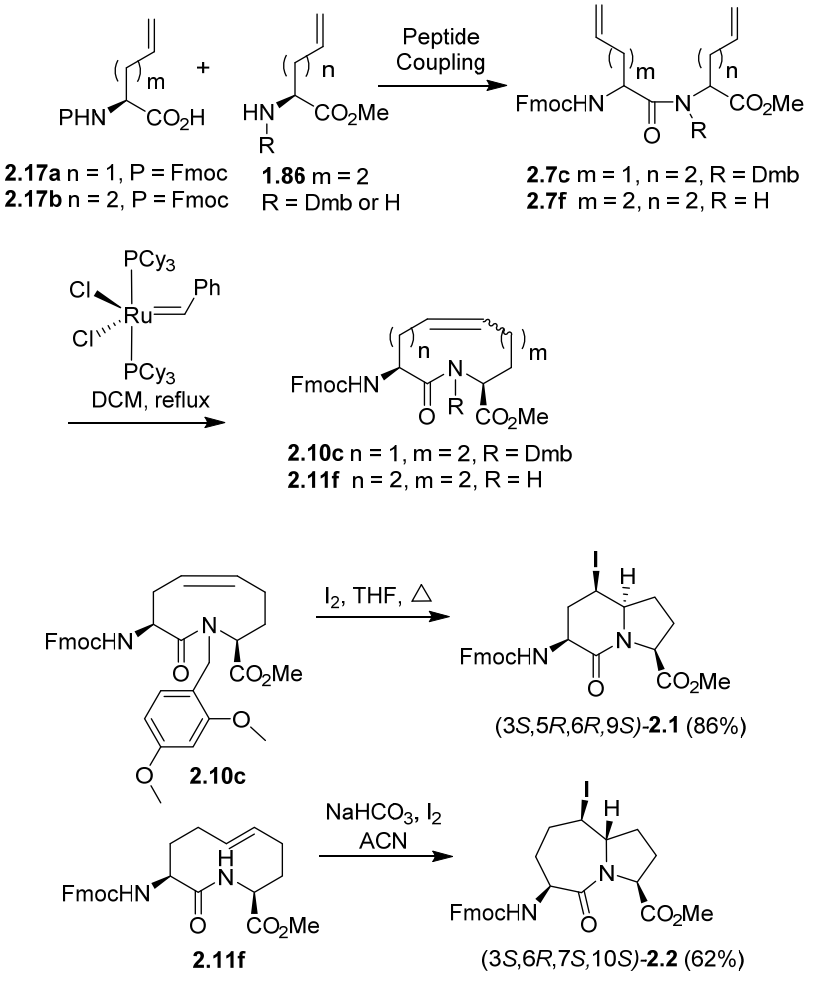

Scheme 1.10 Synthesis of azabicyclo[4.3.0] and [5.3.0]alkanone amino acid

The RCM / electrophilic transanular cyclization strategy was initially developed by employing dipeptides derived from allyl-, and homoallyl-glycine (Scheme 1.9). Iodo-azabicyclo[4.3.0] and [5.3.0]alkanones **2.1** and **2.2** were prepared selectively from dipeptides **2.7c** (Dmb = 2,4-dimethoxybenzyl) and **2.7f** by ring-closing metathesis to provide

respectively the 9- and 10-membered macrocyclic dipeptides **2.10c** and **2.11f**,[33] which on treatment with iodine gave the bicycles **2.1** and **2.2** as single diastereomers.[34,32a]

1.7 Side chain diversification

The importance of side chains in recognition events of turn sites of bioactive peptides inspires the synthesis of azabicycloalkanone mimics possessing functional groups on different ring positions. In this light, the iodide substituent from the transannular reaction may be employed as a handle to introduce functional groups onto the bicycle.

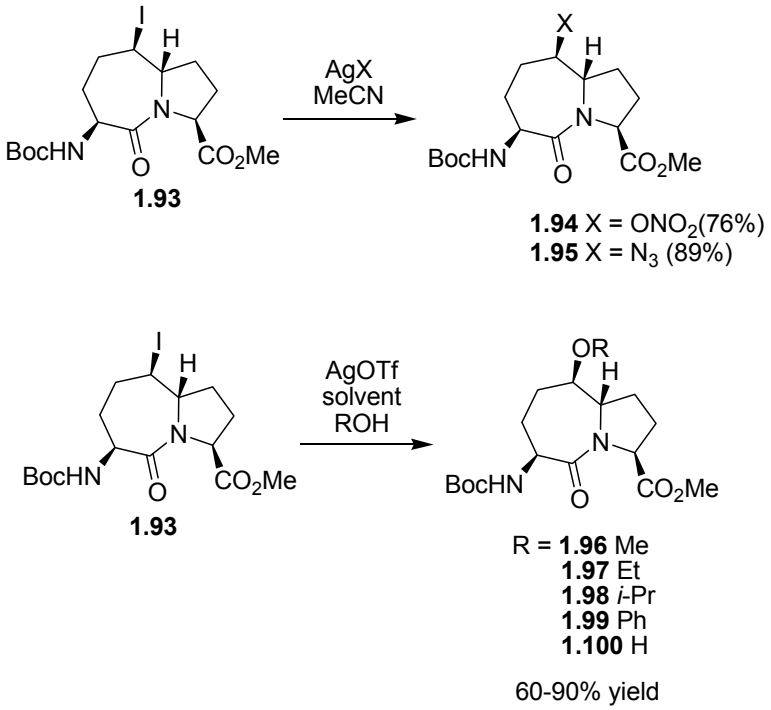

Scheme 1.11 Synthesis of substituted azabicyclo[5.3.0]alkanone amino acids

For example, 6-iodo-azabicyclo[5.3.0]alkanone was successfully converted into a series of substituted analogs by nucleophilic displacements of the iodide using silver salts (Scheme 1.10).[34] Employing silver triflate to assist displacement of iodide **1.93** with alcohols and phenol a series of ethers (**1.96-1.100**) were produced by a diastereoselective S_N1 displacement. Similarly, silver azide gave the corresponding azide **1.95**. Further side chain diversifications may be useful for creating libraries of turn mimics for studying side chain structure-activity relationships of biologically active peptides.

1.8 Synthesis of Bulding Blocks

Vinylglycine, allylglycine, homoallylglycine and 2-Aminohept-6-enoate are the important building blocks in this transannular cyclization approach. Although many approaches exist for the synthesis of such unsaturated amino acid building blocks, these routes demand often multiple steps to give enantiomerically pure products. Examples of such routes that were initially employed to develop the RCM / electrophilic transannular cyclization route are discussed below.

1.8.1 Synthesis of Allylglycine

Allylglycine was initially prepared from β-methyl *N*-(PhF)aspartate **1.101**.[33] Esterification using *O*-*tert*-butyl trichloroacetimidate in dichloromethane gave α-tert-butyl ester **1.102** in 84% yield. The methyl ester of aspartate **1.102** was selectively reduced with DIBAL-H to provide homoserine **1.103**, which was subsequently oxidized to aldehyde **1.104** in 91% yield.[26] The Wittig reaction of aldehyde **1.104** and the ylide generated from treatment of methyltriphenylphosphonium bromide with KHMDS in THF gave in 95% yield *N*-(PhF)allylglycine *tert*-butyl ester **1.105**, which was converted to allylglycine hydrochloride by treating with TFA, followed by conversion of the trifluoroacetate salt to the hydrochloride using aq HCl and freeze-drying (Scheme 1.11).[33]

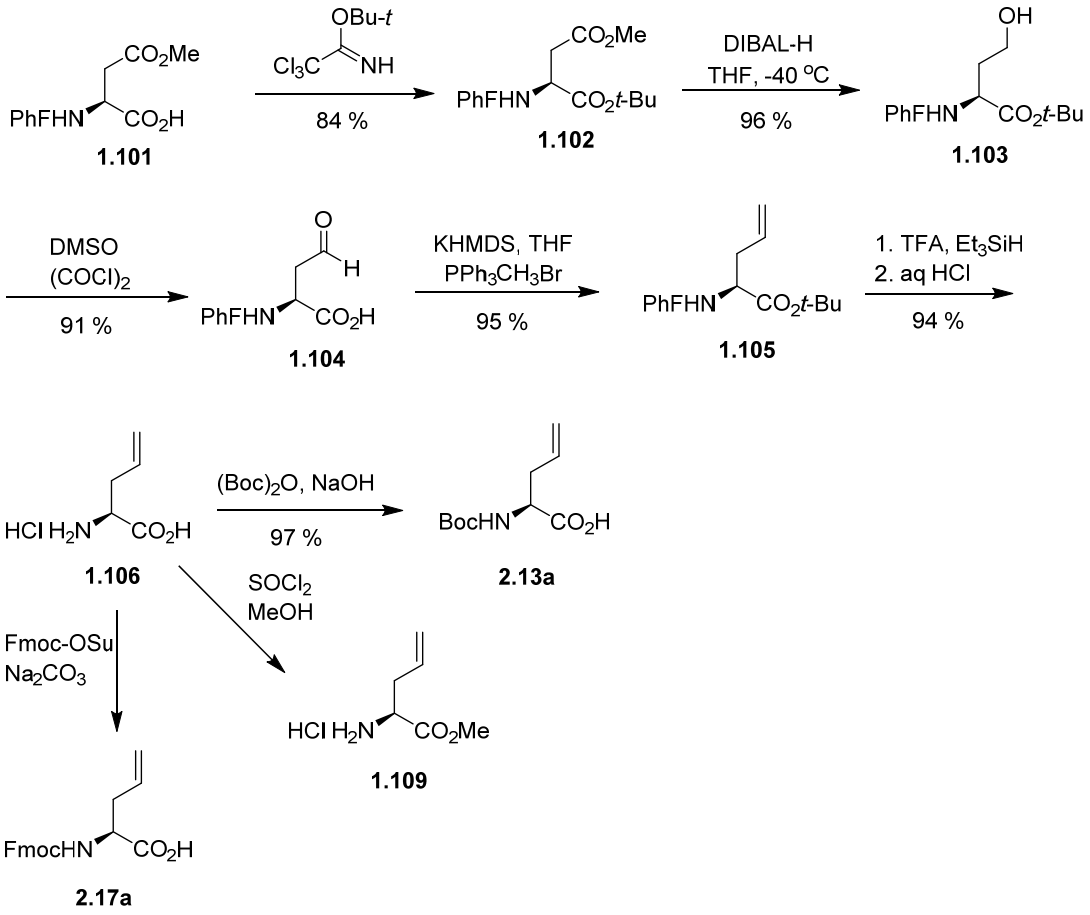

Scheme 1.12 Synthesis of Allylglycine

N-(Boc)- and *N*-(Fmoc)allylglycines **1.128** and **1.125** were then prepared by the protection of **1.106** with $(Boc)_2O$ **1.128** and FmocOSu, **1.125** respectively, under basic conditions. Allylglycine methyl ester hydrochloride **1.109** was quantitatively obtained by the treatment of **1.106** with methanol and thionyl chloride.[33]

1.8.2 Synthesis of 2-Aminohex-6-enoate

Homoallylglycine was preparared from *N*-(Boc)serine methyl ester **1.110**.[34] The application of the Apple reaction converted alcohol **1.110** into iodide **2.12**.[35] Iodoalanine **2.12** was converted into organozinc reagent using activated zinc dust in DMF. The excess zinc dust was allowed to settle and the supernatant was then removed by syringe and added to a pre-mixed DMF solution of CuBr·DMS (0.13 eq.) and allyl chloride at –15°C. After

subsequent purification by flash chromatography *N*-(Boc)homoallylglycine methyl ester **2.14** was isolated in 60% yield (Scheme 1.12).[36]

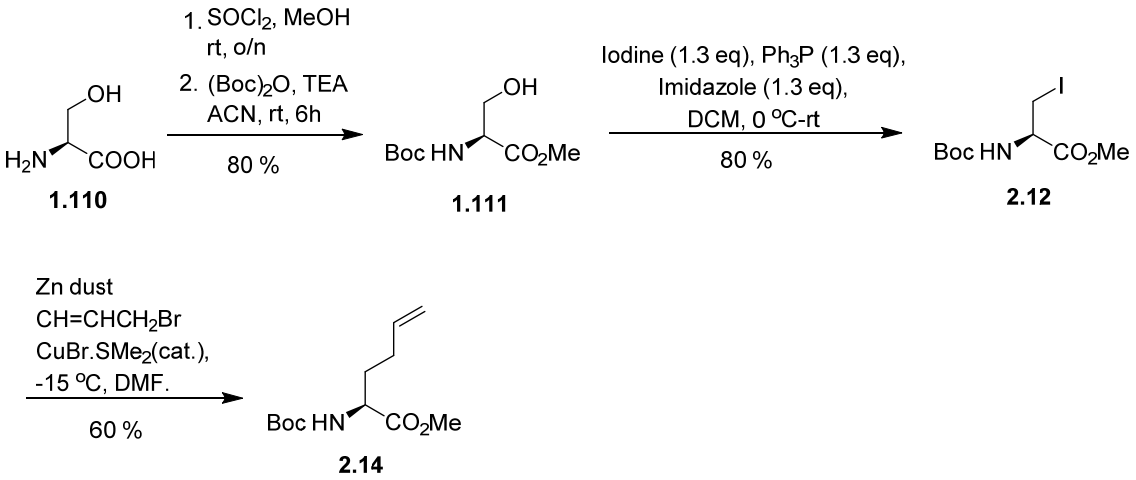

Scheme 1.13 Synthesis of 2-Aminohex-6-enoate

1.8.3 Synthesis of 2-Aminohept-6-enoate

2-Aminohept-6-enoate was prepared by the method of Belokon starting from L-proline **1.114**.[37] (*S*)-*O*-(*N*-Benzylprolylamino)benzophenone was treated with glycine in presence of nickel nitrate hexahydrate to give Ni(II) complex **1.117** (Scheme 1.13). Diastereoselective alkylation with bromopent-4-ene and sodium hydroxide gave the alkylated nickel complex **1.118**, which was treated with 6N HCl to release 2-Aminohept-6-enoate. 2-Aminohept-6-enoate methyl ester hydrochloride was quantitatively obtained by the treatment with methanol and thionyl chloride, and protected with di-*tert*-butyldicarbonate to give *N*-(Boc)homohomoallylglycine methyl ester **2.15**.[38]

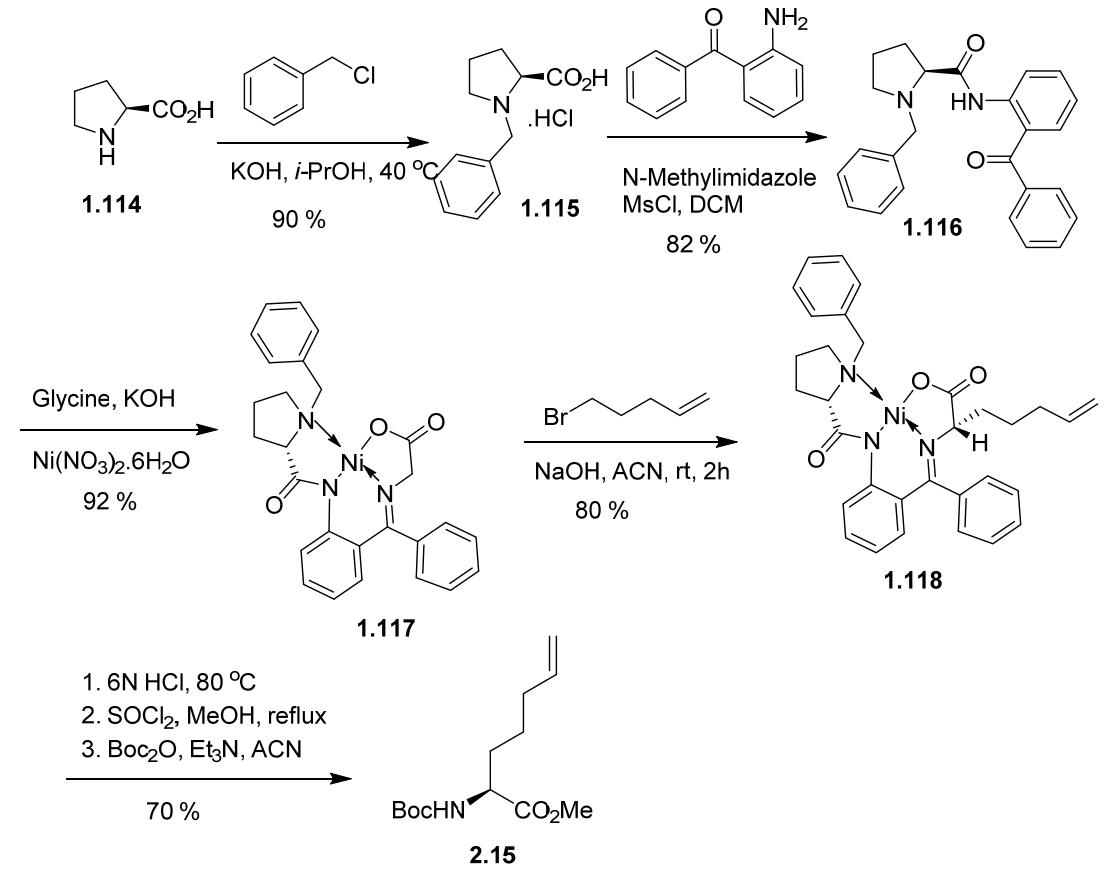

Scheme 1.14 Synthesis of 2-Aminohept-6-enoate

1.8.4 Synthesis of Vinylglycine

Although a variety of methods have provided to prepare Vinylglycine.[39,40,41] *N*-(Fmoc)methionine methyl ester **1.121** was prepared by oxidation to the corresponding sulfoxide with $NaIO_4$ and pyrolysis by heating in xylene at reflux (Scheme 1.14).[42,43]

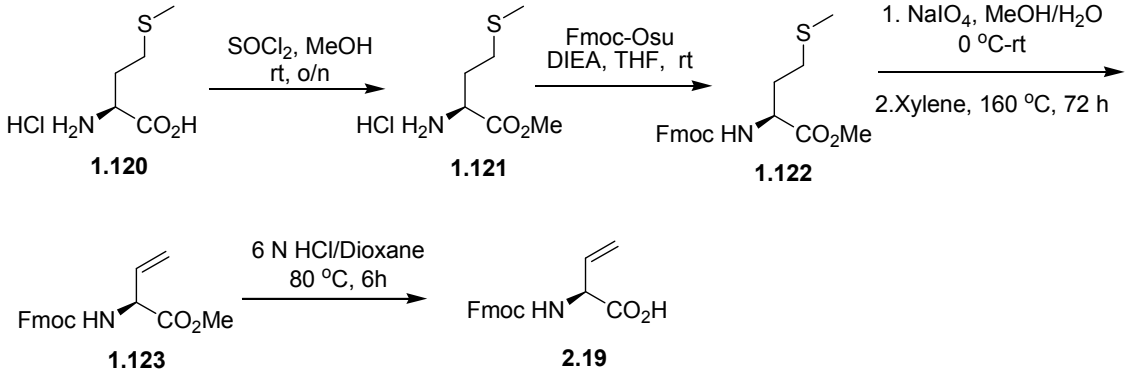

Scheme 1.15 Synthesis of Vinylglycine

1.9 Aim of the project

The goal of this research project is to develop new methodology for the synthesis of different ring size iodo-azabicyclo[X.Y.0]alkanes from 8-, 9- and 10- member unsaturated macrocyclic lactams via transannular iodolactamization.

Our aim is build based on the earlier success in transannular cyclization[32a] to develop a methodology to occur different ring size azabicycloakanones with iodine handle. Employing previously unexplored vinylglycine and homohomoallylglycine along with allyglycine and homoallyglycine, macrocycles will be prepared from dipeptides (Chapter 2) using RCM employing Grubbs first generation catalyst. Azabicyclo[X.Y.0]alkanes were then pursued from the macrocycles by transannular iodolactamization.

In addition, one synthetic challenge that needs to be addressed was accessibility of allylglycine and 2-Aminohept-6-enoate. These starting materials are commercially available, but prohibitively costly to be incorporated in a large scale synthesis. To avoid, which we sought to develop a methodology to access these compounds. For that we aimed an efficient atom economical routes to make valuable building blocks such as *N*-(Boc)allylglycine methyl ester and *N*-(Boc)homohomoallylglycine methyl ester, starting materials for the synthesis of different ring size macrocyclic lactams (Chapter 2 & Chapter 3).

Moreover, Considering that both bicycle and macrocycle constraints serve to rigidify the peptide backbone efforts have focused to get X-ray structural data of macrocycle and bicycle products has furnished both understanding of the conformational preferences of these peptidomimetics as well as insight into the mechanism of the transannular cyclization.

1. 10 References

1. Krogsgaard-Larsen, P., *A textbook of drug design and development*. Harwood Academic Pub1991.

2. Beeley, N. R., *Drug Discovery Today* **2000,** *5*, 354-363.

3. Sewald, N.; Jakubke, H.-D., *Peptides: chemistry and biology*. Wiley-Vch Weinheim 2002; Vol. 2.

4. Hutchinson, E. G.; Thornton, J. M., *Protein Sci.* **1994,** *3*, 2207-2216.

5. (a) Childers, S. R.; Creese, I.; Snowman, A. M.; Snyder, S. H., *Eur. J. Pharmacol.* **1979,** *55*, 11-18; (b) Aubry, A.; Birlirakis, N.; Sakarellos-Daitsiotis, M.; Sakarellos, C.; Marraud, M., *Biopolymers* **1989,** *28*, 27-40.

6. Giannis, A.; Kolter, T., *Angew. Chem. Int. Ed.* **1993,** *32*, 1244-1267.

7. Ripka, A. S.; Rich, D. H., *Curr. Opin. Chem. Biol.* **1998,** *2*, 441-452.

8. Bursavich, M. G.; Rich, D. H., *J. Med. Chem.* **2002,** *45*, 541-558.

9. Chung, J. Y.; Wasicak, J. T.; Arnold, W. A.; May, C. S.; Nadzan, A. M.; Holladay, M. W., *J. Org. Chem.* **1990,** *55*, 270-275.

10. Holladay, M. W.; Lin, C. W.; May, C. S.; Garvey, D. S.; Witte, D. G.; Miller, T. R.; Wolfram, C. A.; Nadzan, A. M., *J. Med. Chem.* **1991,** *34*, 455-457.

11. Gante, J., *J. Angew. Chem. Int. Ed.* **1994,** *33*, 1699-1720.

12. Freidinger, R. M., *J. Med. Chem.* **2003,** *46*, 5553-5566.

13. (a) Dietrich, E.; Lubell, W. D., *J. Org. Chem.* **2003,** *68*, 6988-6996; (b) Boeglin, D.; Hamdan, F. F.; Melendez, R. E.; Cluzeau, J.; Laperriere, A.; Héroux, M.; Bouvier, M.; Lubell, W. D., *J. Med. Chem.* **2007,** *50*, 1401-1408; (c) Mandal, P. K.; Kaluarachchi, K. K.; Ogrin, D.; Bott, S. G.; McMurray, J. S., *J. Org. Chem.* **2005,** *70*, 10128-10131; (d) Seide, W.; Watson, S. E., *Synth. Commun.* **2005,** *35*, 995-1002; (e) Chen, J.; De, B.; Demuth, T.; Laufersweiler, M.; O'Neil, S.; Oppong, K.; Soper, D.; Wang, Y.; Wos, J., Novel interleukin-1beta converting enzyme inhibitors. Google Patents 2003; (f) Kaul, R.; Brouillette, Y.; Sajjadi, Z.; Hansford, K. A.; Lubell, W. D., *J. Org. Chem.* **2004,** *69*, 6131-6133; (g) Siddiqui, M. A.; Préville, P.; Tarazi, M.; Warder, S. E.; Eby, P.; Gorseth, E.; Puumala, K.; DiMaio, J., *Tetrahedron Lett.* **1997,** *38*, 8807-8810; (h) Rao, M. H. R.; Pinyol, E.; Lubell, W. D., *J. Org. Chem.* **2007,** *72*, 736-743.

14. (a) Haubner, R.; Schmitt, W.; Hölzemann, G.; Goodman, S. L.; Jonczyk, A.; Kessler, H., *J. Am. Chem. Soc.* **1996,** *118*, 7881-7891; (b) Nagai, U.; Sato, K.; Nakamura, R.; Kato, R., *Tetrahedron* **1993,** *49*, 3577-3592.

15. (a) Hanessian, S.; McNaughton-Smith, G.; Lombart, H.-G.; Lubell, W. D., *Tetrahedron* **1997,** *53*, 12789-12854; (b) Vagner, J.; Qu, H.; Hruby, V. J., *Curr. Opin. Chem. Biol.* **2008,** *12*, 292-296.

16. Bourguet, C. B.; Goupil, E.; Tassy, D.; Hou, X.; Thouin, E.; Polyak, F.; Hébert, T. E.; Claing, A.; Laporte, S. A.; Chemtob, S., *J. Med. Chem.* **2011,** *54*, 6085-6097.

17. Bourguet, C. B.; Claing, A.; Laporte, S. A.; Hébert, T. E.; Chemtob, S.; Lubell, W. D., *Can. J. Chem.* **2014,** *92*, 1031-1040.

18. (a) Sun, H.; Nikolovska-Coleska, Z.; Yang, C.-Y.; Xu, L.; Liu, M.; Tomita, Y.; Pan, H.; Yoshioka, Y.; Krajewski, K.; Roller, P. P., *J. Am. Chem. Soc.* **2004,** *126*, 16686-16687; (b) Zhang, B.; Nikolovska-Coleska, Z.; Zhang, Y.; Bai, L.; Qiu, S.; Yang, C.-Y.; Sun, H.; Wang, S.; Wu, Y., *J. Med. Chem.* **2008,** *51*, 7352-7355.

19. Alcaro, M. C.; Vinci, V.; D'Ursi, A. M.; Scrima, M.; Chelli, M.; Giuliani, S.; Meini, S.; Di Giacomo, M.; Colombo, L.; Papini, A. M., *Bioorg. Med. Chem. Lett.* **2006,** *16*, 2387-2390.

20. Belvisi, L.; Bernardi, A.; Colombo, M.; Manzoni, L.; Potenza, D.; Scolastico, C.; Giannini, G.; Marcellini, M.; Riccioni, T.; Castorina, M., *Biorg. Med. Chem.* **2006,** *14*, 169-180.

21. (a) Cordero, F. M.; Valenza, S.; Machetti, F.; Brandi, A., *Chem. Commun.* **2001**, 1590-1591; (b) Fustero, S.; Mateu, N.; Albert, L.; Aceña, J. L., *J. Org. Chem.* **2009,** *74*, 4429-4432; (c) Vartak, A. P.; Skoblenick, K.; Thomas, N.; Mishra, R. K.; Johnson, R. L., *J. Med. Chem.* **2007,** *50*, 6725-6729.

22. Khashper, A.; Lubell, W. D., *Org. Biomol. Chem.* **2014**.

23. Baldwin, J. E.; Adlington, R. M.; Jones, R. H.; Schofield, C. J.; Zaracostas, C.; Greengrass, C. W., *Tetrahedron* **1986,** *42*, 4879-4888.

24. Baldwin, J. E.; Adlington, R. M.; Jones, R. H.; Schofield, C. J.; Zarocostas, C.; Greengrass, C. W., *J. Chem. Soc., Chem. Commun.* **1985**, 194-196.

25. Baldwin, J. E.; Chan, M. F.; Gallacher, G.; Otsuka, M.; Monk, P.; Prout, K., *Tetrahedron* **1984,** *40*, 4513-4525.

26. Gosselin, F.; Lubell, W. D., *J. Org. Chem.* **1998,** *63*, 7463-7471.

27. Lombart, H.-G.; Lubell, W. D., *J. Org. Chem.* **1994,** *59*, 6147-6149.

28. Gosselin, F.; Lubell, W. D., *J. Org. Chem.* **2000,** *65*, 2163-2171.

29. Hanessian, S.; Balaux, E.; Musil, D.; Olsson, L.-L.; Nilsson, I., *Bioorg. Med. Chem. Lett.* **2000,** *10*, 243-247.

30. Hanessian, S.; Therrien, E.; Granberg, K.; Nilsson, I., *Bioorg. Med. Chem. Lett.* **2002,** *12*, 2907-2911.

31. (a) Sudau, A.; Münch, W.; Bats, J. W.; Nubbemeyer, U., *Chem. Eur. J.* **2001,** *7*, 611-621; (b) White, J. D.; Hrnciar, P., *J. Org. Chem.* **2000,** *65*, 9129-9142; (c) White, J. D.; Hrnciar, P.; Yokochi, A. F., *J. Am. Chem. Soc.* **1998,** *120*, 7359-7360; (d) Jensen, T.; Mikkelsen, M.; Lauritsen, A.; Andresen, T. L.; Gotfredsen, C. H.; Madsen, R., *J. Org. Chem.* **2009,** *74*, 8886-8889; (e) Brock, E. A.; Davies, S. G.; Lee, J. A.; Roberts, P. M.; Thomson, J. E., *Org. Lett.,* **2012,** *14*, 4278-4281; (f) Brock, E. A.; Davies, S. G.; Lee, J. A.; Roberts, P. M.; Thomson, J. E., *Org. Lett.,* **2011,** *13*, 1594-1597.

32. (a) Surprenant, S.; Lubell, W. D., *Org. Lett.,* **2006,** *8*, 2851-2854; (b) Edstrom, E. D., *J. Am. Chem. Soc.* **1991,** *113*, 6690-6692; (c) Edwards, O.; Paton, J.; Benn, M.; Mitchell, R.; Watanatada, C.; Vohra, K., *Can. J. Chem.* **1971,** *49*, 1648-1658; (d) Diederich, M.; Nubbemeyer, U., *Chem. Eur. J.* **1996,** *2*, 894-900; (e) Edstrom, E. D., *Tetrahedron Lett.* **1991,** *32*, 5709-5712.

33. Kaul, R.; Surprenant, S.; Lubell, W. D., *J. Org. Chem.* **2005,** *70*, 3838-3844.

34. Godina, T. A.; Lubell, W. D., *J. Org. Chem.* **2011,** *76*, 5846-5849.

35. Trost, B. M., *Science* **1983,** *219*, 245-250.

36. Rodríguez, A.; Miller, D. D.; Jackson, R. F., *Org. Biomol. Chem.* **2003,** *1*, 973-977.

37. Belokon, Y. N.; Zel'tser, I.; Bakhmutov, V.; Saporovskaya, M.; Ryzhov, M.; Yanovskii, A.; Struchkov, Y. T.; Belikov, V., *J. Am. Chem. Soc.* **1983,** *105*, 2010-2017.

38. Traoré, M.; Mietton, F.; Maubon, D. l.; Peuchmaur, M.; Francisco Hilário, F.; Pereira de Freitas, R.; Bougdour, A.; Curt, A. l.; Maynadier, M.; Vial, H., *J. Org. Chem.* **2013,** *78*, 3655-3675.

39. Itaya, T.; Shimizu, S.; Nakagawa, S.; Morisue, M., *Chem. Pharm. Bull.* **1994,** *42*, 1927-1930.

40. Marcovici-Mizrahi, D.; Gottlieb, H. E.; Marks, V.; Nudelman, A., *J. Org. Chem.* **1996,** *61*, 8402-8406.

41. (a) Dondoni, A.; Giovannini, P. P.; Perrone, D., *J. Org. Chem.* **2005,** *70*, 5508-5518; (b) Berkowitz, D. B.; Bose, M.; Choi, S., *Angewandte Chemie* **2002,** *114*, 1673-1677; (c) Berkowitz, D. B.; Maiti, G., *Org. Lett.,* **2004,** *6*, 2661-2664.

42. Organ, M. G.; Xu, J.; N'Zemba, B., *Tetrahedron Lett.* **2002,** *43*, 8177-8180.

43. Sicherl, F.; Cupido, T.; Albericio, F., *Chem. Commun.* **2010,** *46*, 1266-1268.

CHAPTER 2

Article: Insight Into Transannular Cyclization Reactions To Synthesize Azabicyclo[X.Y.Z]alkanone Amino Acid Derivatives From 8-, 9- and 10-Member Macrocyclic Dipeptide Lactams

N. D. Prasad Atmuri and William D. Lubell*

J. Org. Chem. 2015, 80, 4904-4918

2.1 ABSTRACT:

An efficient method for synthesizing different functionalized azabicyclo[X.Y.0]alkanone amino acid derivatives has been developed employing electrophilic transannular cyclizations of 8-, 9- and 10-member unsaturated macrocycles to form fused 5,5-, 6,5-, 7,5- and 6,6-fused bicylic amino acids, respectively. Macrocycles were obtained by a sequence featuring peptide coupling of vinyl, allyl, homoallyl, and homohomoallyl-glycine building blocks followed by ring closing metathesis. X-ray crystallographic analyses of the 8-, 9- and 10-member macrocycle lactam starting materials as well as several bicyclic amino acid products provided insight into their conformational preferences as well as the mechanism for the diastereoselective formation of specific azabicycloalkanone amino acids by way of transannular iodolactamization reactions.

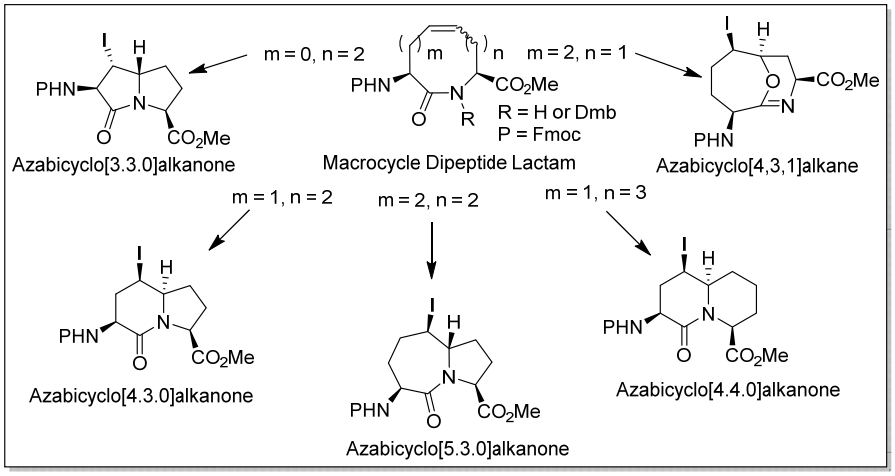

Figure 2.1 Iodo-azabicyclo[X.Y.Z]alkane synthesis

2.2 Introduction

Azabicyclo[X.Y.0]alkane structures, such as pyrrolizidines, indolizidines and qunolizidines, are found in numerous biologically active alkaloid natural products.[1,2] The related azabicyclo[X.Y.0]alkanone amino acid counterparts are rigid dipeptide surrogates that have been employed to study conformation-activity relationships of biologically active peptides.[3,4] Inherent in the syntheses of both classes of heterocycle has been the stereocontrolled

construction of the bicyclic ring system in a way that provides for effective introduction of ring functionality. Among various synthetic strategies,[5] transannular reactions featuring amine nucleophiles reacting on macrocycle olefin and epoxide precursors have exhibited considerable utility for the stereoselective construction of the bicyclic amines,[6,7] albeit few examples of the related cyclizations of macrocyclic lactams have been reported.[8] In both cases, regioselective formation of specific bicycles has often been observed to occur with high diastereoselectivity. Limited mechanistic understanding exists however to predict the outcome of such transannular cyclization reactions, because they have been typically performed on a restricted number of ring sizes with substituents that have varied greatly both in functional group and location. Generally, in cycloalkanes of 8 to 11 ring atoms, unfavourable interactions of ring substituents can cause significant strain, so-called "Prelog strain".[9,10] Moreover, nitrogen lone pair electrons have been reported to prefer an anti-orientation with respect to the olefin pi-bond to minimize repulsive interactions.[11] Such steric and electronic interactions serve likely in part as driving forces for preferred macrocycle conformations and favoured regioselective cyclizations.

In the interest of developing a general strategy for synthesizing azabicyclo[X.Y.0]alkanone amino acids of varying ring sizes, we have pursued electrophilic transannular lactamizations of unsaturated macrocyclic dipeptides.[8a] This strategy is appealing, because a variety of macrocycles may be generated by coupling various ω-unsaturated amino acids, followed by ring-closing metathesis (RCM, Figure 2.2). Moreover, after transannular iodolactamization, the resulting iodide has served as a handle for introducing various side chain functional groups onto the bicyclic system.[12]

Considering that both bicycle and macrocycle constraints serve to rigidify the peptide backbone,[5c,13] efforts have focused on studying the synthesis and conformational analysis of a series of ring systems in which the same dipeptide motif is maintained as the ring size and olefin orientation are modulated. Employing X-ray crystallography and NMR spectroscopy,

insight has now been gained with respect to the conformational preferences of the macrocycle and bicycle dipeptide motifs, as well as the regioselective nature of the transannular lactamization. Exploring five different macrocycles, we have found conditions to prepare regioselectively and stereoselectively five distinct bicyclic dipeptide mimics validating the effectiveness of this approach for peptidomimetic synthesis.

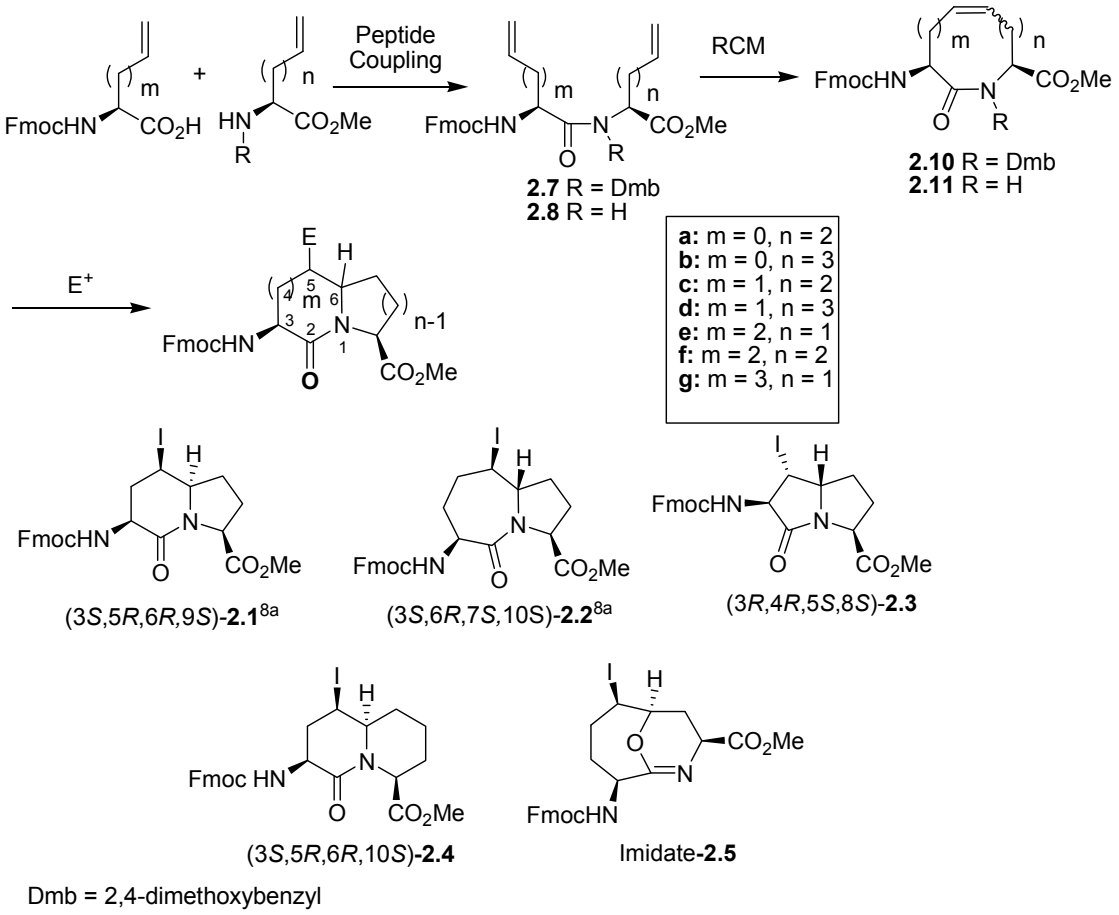

Figure 2.2. General synthetic plan for making azabicyclo[X.Y.0]alkanones and representative examples of previously prepared bicycles **2.1** and **2.2**, as well as new examples **2.3-2.5** prepared herein.

2.3 Results and Discussion

Iodo-azabicyclo[4.3.0] and [5.3.0]alkanones **2.1** and **2.2** were previously made by the diastereoselective iodolactamization of 9- and 10-member macrocycles *Z*-**2.10c** and *E*-**2.11f**,

respectively (Figure 1).[8a,12,14] Macrocycles *Z*-**2.10c** and *E*-**2.11f** had been made from allyl-, and homoallyl-glycine building blocks.[14] Herein, vinyl- and homohomoallylglycines were added to provide a set of four ω-unsaturated amino acids for RCM / electrophilic transannular cyclizations that have now given access to the new 5,5- and 6,6-fused bicyclic ring systems **2.3** and **2.4**, as well as anti-Bredt imidate **2.5** (Figure 2.2). The latter bridge-head imidate represents a rare substituted heterocycle example that challenges Bredt's rules.[15] From all five of these related transannular cyclizations, only a single heterocyclic system was typically formed diastereoselectively.

The enantiomerically pure ω-unsaturated amino acid starting materials with lengths of four to seven carbons were synthesized efficiently by atom economical routes. Many synthetic approaches exist for making these building blocks;[14,16,17] however, they require often long reaction sequences, especially in the cases of 2-aminopent-4-enoate (allylglycine), and 2-aminohept-6-enoate (homohomoallylglycine).

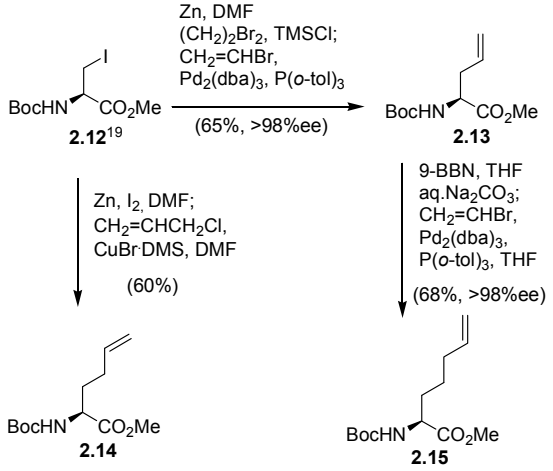

Scheme 2.1. Synthesis of 2-amino pent-4-, hex-5- and hept-6-enoates **2.13-2.15**.

Inspired by the relatively efficient synthesis of methyl 2-*N*-(Boc)aminohex-5-enoate **2.14**,[18] which featured the copper-catalyzed cross-coupling of allyl chloride and the zincate derived from iodoalanine **2.12** (Scheme 1),[19] related transition-metal cross-coupling methods were developed to make the higher and lower amino acid homologues. Methyl 2-*N*-(Boc)aminopent-4-enoate **2.13** and methyl 2-*N*-(Boc)aminohept-6-enoate **2.15** were thus

respectively prepared by using vinyl bromide in the Pd-catalyzed reactions on the zincate derived from iodoalanine **2.12** and the boronate derived from **2.13**.

Starting from L-serine as chiral educt, protected enantiomerically pure ω-unsaturated amino acids with chain lengths of 5-7 carbons were prepared by a common sequence. Methyl *N*-(Boc)iodoalanine (**2.12**, Scheme 1) was assembled in three steps from serine and used in the synthesis of the 5- and 6-carbon analogs.[19] On treatment with zinc, iodoalanine **2.12** was converted to the corresponding zincate which was coupled with vinyl bromide and $Pd_2(dba)_3$,[20] or allyl chloride and CuBr•DMS,[18] respectively to give pentenoate and hexenoate **2.13** and **2.14** in 65% and 60% yields, Heptenoate **2.15** was synthesized from pentenoate **2.13** in 68% yield by hydroboration of terminal alkene using 9-borabicyclo[3.3.1]nonane (9-BBN) and cross-coupling to vinyl bromide using $Pd_2(dba)_3$.

After syntheses of pentenoate **2.13** and heptenoate **2.15**, their enantiomeric purity was respectively evaluated by conversion to diastereomeric dipeptides on removal of the Boc group with HCl gas in dichloromethane, and coupling to L- and D-*N*-(Boc)alanine with HATU (Supporting Information). Examination of the diastereotopic methyl ester singlets by ^{1}H NMR spectroscopy in CD_3CN during incremental addition of the (*S,R*)- into the (*S,S*)-diastereomer demonstrated in both cases a >99:1 dr. Hence, pentenoate **2.13** and heptenoate **2.15**, both are assumed to be of >98% enantiomeric purity.

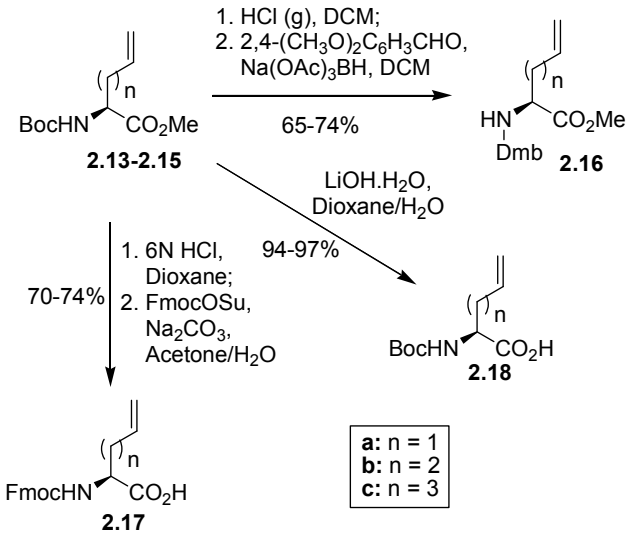

Scheme 2.2. Protecting group shuffle to make Boc, Fmoc and Dmb building blocks

Suitably protected 2-*N*-(Dmb)amino ester **2.16** and 2-*N*-(Boc)- and (Fmoc)amino acids **2.17** and **2.18** were prepared from 2-*N*-(Boc)amino esters **2.13-2.15** using previously described protocols (Scheme 2.2).[14] 2-*N*-(Fmoc)Aminobut-3-enoic acid (vinylglycine **2.19**) was synthesized as previously described.[21,22]

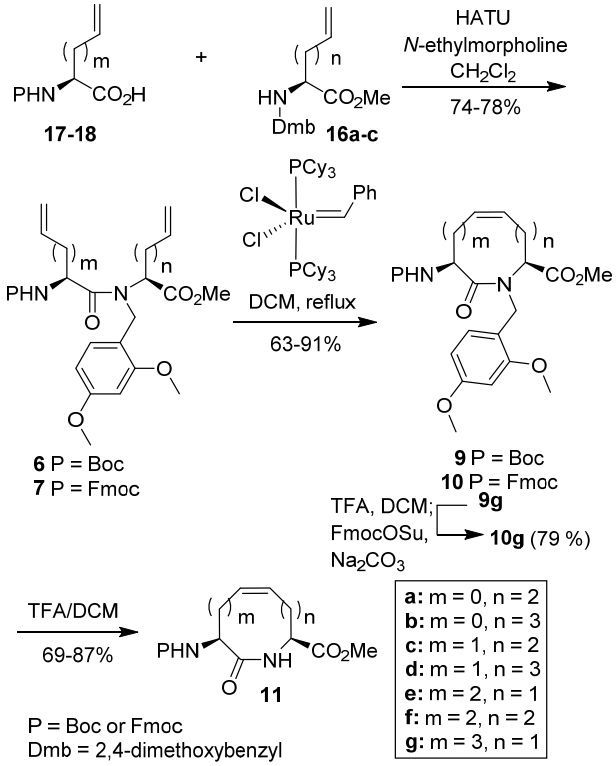

Scheme 2.3. Syntheses of dipeptides **2.6** and **2.7**, and macrocycles **2.9-2.11**

Dipeptides **6** and **7** were synthesized by coupling ester **2.16** and acids **2.17** and **2.18** using HATU and *N*-ethylmorpholine in 70-80% yield (Scheme 2.3).[14] Double bond migration occurred during coupling of but-3-enoic acid **2.19** to 2-*N*-(Dmb)hex-5-oate **2.16b** using HATU and DIEA and gave dehydropeptide **2.20** (Scheme 4). Double bond migration was avoided by converting vinylglycine **19** to the corresponding acid chloride, which reacted with **2.16b** and **2.16c** in the absence of base to afford dipeptides **2.7a** and **2.7b** in 50-60% yield. Macrocycles **2.9** and **2.10** were prepared from dipeptides **2.6** and **2.7** in 60-90% yields in solution using RCM employing Grubbs first generation catalyst in dichloromethane at reflux

(Scheme 3).[23,24] Dehydroamino acid analog **2.20** failed to react using the first generation of Grubbs catalyst, but could be converted to dehydro azepinone **2.21** with Grubbs second generation catalyst (Scheme 4).[25] In spite of the acid sensitivity of the Dmb group, the Boc group could be selectively removed from macrocycle **2.9g** using 50% TFA in DCM for 2h to afford the corresponding amine, which was converted to its Fmoc counterpart **2.10g**, using Fmoc-OSu and Na_2CO_3 (Scheme 2.3).[14] To remove the Dmb group, *N*-(Fmoc)amino lactams **2.10** were treated with 50% TFA:DCM for 18h and afforded macrocycles **2.11** in 70-80% yields. In the case of 10 member *N*-(Dmb)lactam **2.10d**, starting material was however not consumed even after treatment for 3 days, when lactam **2.11d** was afforded in 69% yield after chromatography. The olefin and amide isomer geometries of macrocycles **2.9**-**2.11** were established by NMR spectroscopy and X-ray analysis (*vide infra*).

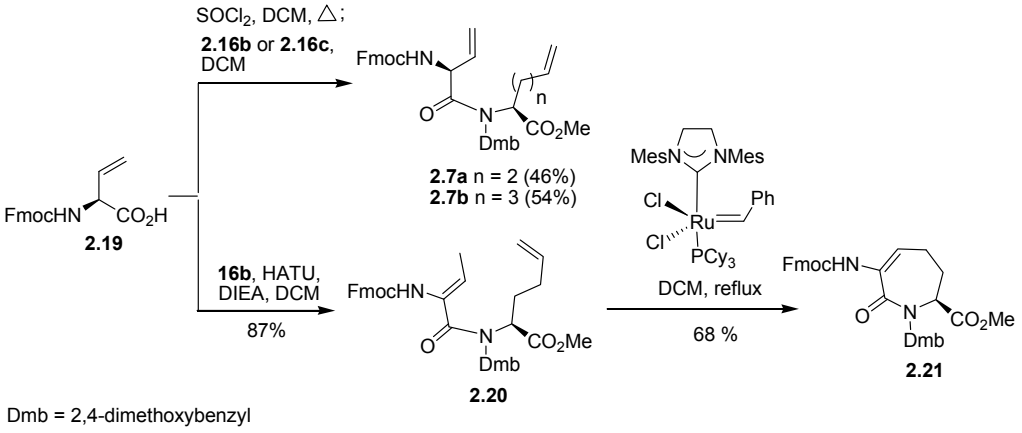

Scheme 2.4. Coupling with vinylglycine **2.19** and synthesis of dehydro azepinone **2.21**

Transannular cyclization of 8-member macrocyclic lactam *Z*-**2.10a** was initially studied by treating with iodine in THF and MeCN at room temperature to reflux; however, only loss of the Dmb group was observed and macrocycle *Z*-**2.11a** was isolated. 8-Member lactam *Z*-**2.11a** proved resistant to transannular iodoamidation using I_2 in THF buffered with $NaHCO_3$, as well as using I_2 in acetonitrile at reflux. Transannular cyclization was achieved by treating *Z*-**2.11a** with diacetoxyiodobenzene (DIB, 1.5 equiv.) and 4 equivalents of iodine in acetonitrile at reflux for 30 min (Scheme 2.5). Although DIB has been used in oxidative

cyclizations of *o*-hydroxy styrenes to benzofurans, to the best of our knowledge, this is the first use of this reagent in a transannular iodolactamization. (3*R*,4*R*,5*S*,8*S*)-Pyrrolizidinone **2.3** was isolated as a single diastereomer in 62% yield after chromatography (Scheme 2.5). In the mechanism for the formation of **3**, hypervalent iodine may activate the double bond as a three-membered iodonium species **2.22**,[26] which undergoes intramolecular reaction with the amide nitrogen to form intermediate **2.23**. Displacement of the hypervalent iodine by the neighboring carbamate may occur by way of an oxazole intermediate **2.24**, which is opened by iodide to give iodopyrrolizidinone **3** with retention of configuration. The structure of **2.3** was confirmed by NMR spectroscopy and X-ray diffractometry as described below.

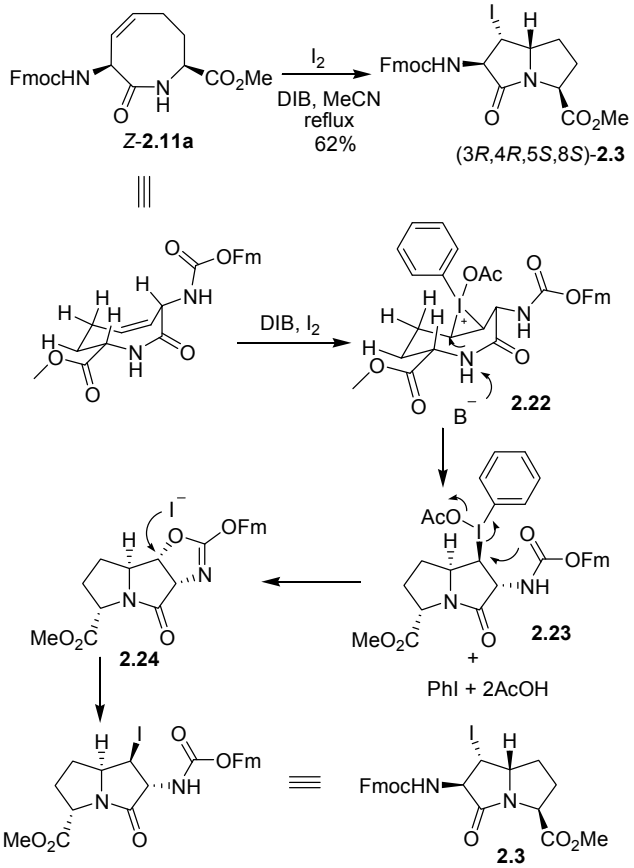

Scheme 2.5. Proposed mechanism for the synthesis of iodo-azabicyclo[3.3.0]alkanone amino ester **2.3**

Although the related double bond isomer *Z*-**2.10c** (m = 1, n = 2) underwent iodolactamization to provide iodo-indolizidinone 2.**1** in 86% yield using I_2 in THF at 80 °C

(Figure 2.2),[8a] treatment of unsaturated macrocycle lactam *Z*-**2.10e** (m = 2, n = 1) under analogous conditions only caused removal of the Dmb group to provide lactam *Z*-**2.11e**. Moreover, attempts to induce transannular cyclization of 9-membered lactam *Z*-**2.11e** using alternative conditions (I_2 in MeCN;[12] DIB and I_2 in MeCN, rt to reflux; Lewis base catalyzed[27] iodolactamization using $Ph_3P{=}S$, NIS/DCM) produced a relatively less polar spot on TLC compared to the iodo bicycles. The reaction proceeded cleanly and the starting material was all consumed within 1 h as indicated by TLC. After the usual aqueous work up with $Na_2S_2O_3$, and purification by silica gel chromatography in the dark, imidate **2.5** was characterized using NMR spectroscopy and X-ray crystallography (Scheme 2.6). Imidate formation has been observed commonly in halocyclizations of linear unsaturated amides, and avoided using methods employing *N*,*O*-bis-silylation, *N*-tosyl and *N*-alkoxycarbonyl substitution, as well as strong bases.[28] On the other hand, transannular iodolactamization has favoured azabicycloalkanone.[8b,12] Albeit light sensitive, imidate **2.5** is a unique anti-Bredt heterocycle formed by attack of the lactam oxygen on iodonium intermediate **2.25**.[29,30]

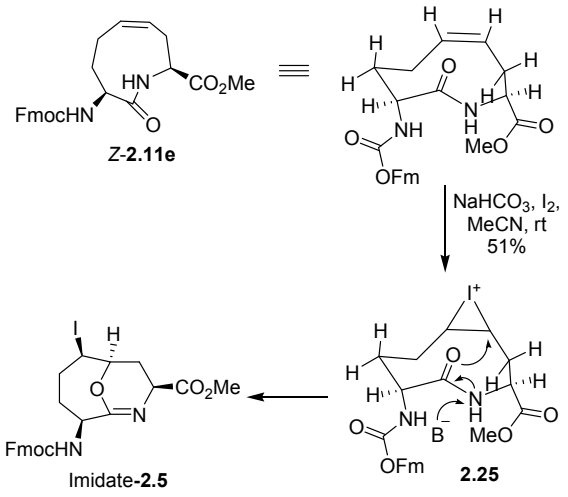

Scheme 2.6. Synthesis of azabicyclo[4,3,1]alkane **2.5**.

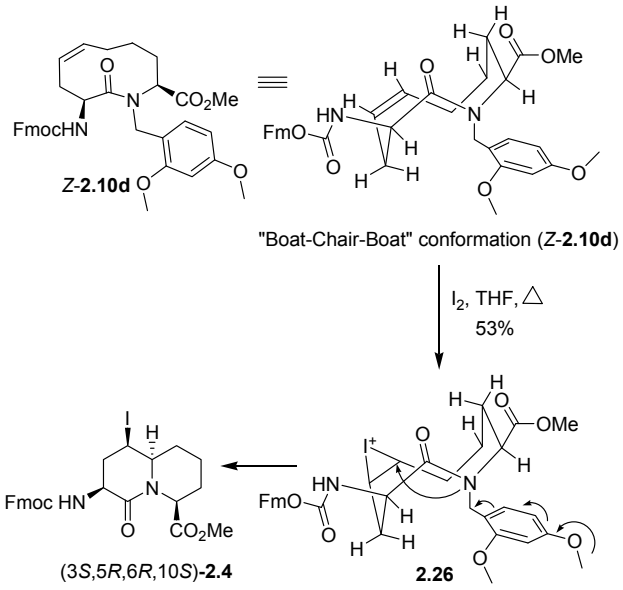

Scheme 2.7. Synthesis of iodo-azabicyclo[4.4.0]alkanone amino ester **2.4**.

Previously, iodo-azabicyclo[5.3.0]alkanone **2.2** (Figure 2.1) was prepared diastereoselectively from 10-member lactam *E*-**2.11f** (m = 2, n = 2) using 4 equivalents of I_2 in THF at reflux.[8a] Iodolactamization of 10-member *N*-(Dmb)lactam *Z*-**2.10d** (m = 1, n = 3) has now given diastereoselective access to the first example of a substituted quinolizidinone amino acid, (3*S*,5*R*,6*R*,10*S*)-5-iodo-azabicyclo[4.4.0]alkanone **2.4** in 53% yield using I_2 in THF at reflux (Scheme 2.7).

2.4 Stereochemical assignment using NMR spectroscopy

The assignment of the structure and stereochemistry of bicycles **2.3**-**2.5** was accomplished by 2D NMR spectroscopy and X-ray crystallography (Supporting Information). Typically, a COSY spectrum was used to assign the ring proton through-bond connectivities starting from the down field carbamate NH proton. The observation of magnetisation transfer between the peptide backbone protons and ring protons in the NOESY and ROESY spectra was then used to assign relative stereochemistry at the ring-fusion and iodide bearing carbons (Figure 2.3). For example, (4*R*, 5*S*)-4-iodopyrrolizidinone *N*-(Fmoc)amino ester **2.3** exhibited a transfer of magnetisation between the backbone C3α and the ring C6α protons in C_6D_6. A second long range NOE between the ring C4 and C6 β-protons established the relative stereochemistry of

the iodide bearing carbon. Long range transfer of magnetization was observed between the ring fusion C6 and backbone C3 and C10 protons in the ROESY spectrum of (3*S*,5*R*,6*R*,10*S*)-5-iodoquinolizidinone **2.4**. The stereochemistry of the ring-fusion carbon of pyrrolizidinone **2.3** and the iodide-bearing carbon of **2.4** were subsequently inferred based on mechanistic considerations that placed the protons from the *cis*-double bond of the macrocycle on the same face of the bicycle.

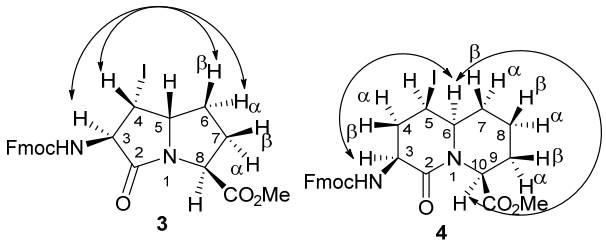

Figure 2.3. NOESY and ROESY correlations used to assign relative configurations of bicycles **2.3** and **2.4.**

Although through-bond couplings of azabicyclo[4,3,1]alkane **2.5** could be used to assign all of the ring protons, no clear long range NOEs were observed to assign relative stereochemistry. In the infrared spectrum of **2.5**, a C=N stretching band at 1657 cm^{-1} was observed indicative of imidate structure. Examination of the coupling pattern (ddd, J = 2.7, 5.4, 11.0 Hz) for the proton on the iodide-bearing carbon, before and after saturation of the neighboring bridge-head proton, and application of Karplus equation[31] gave torsion angels that were consistent with those observed in the crystal structure.

2.5. Crystal structures of 8-, 9- and 10-member macrocyclic dipeptide lactams

Lactams *Z*-**2.11a,** *Z*-**2.11e** and *Z*-**2.10d** were crystallized by a common method (Supporting Information). In all three cases, the *Z*-double bond geometry was observed. In 8-member lactam *Z*-**2.11a**, the *cis*-*E*-amide isomer was observed, as was previously described in the X-ray structure of the related olefin regioisomer 8-member macrocycle **2.27** (Table 2.1).[32] On the other hand, the *trans*-*Z*-amide isomer was detected in the crystal structures of 9- and 10-member lactams *Z*-**2.11e** and *Z*-**2.10d**.

Examination of the backbone dihedral angles found in the crystal structures of lactams *Z*-**2.11a,** *Z*-**2.11e** and *Z*-**2.10d** may provide understanding of their potential for mimicry of natural peptide structures, albeit ^{1}H NMR spectroscopy of macrocyclic lactams *Z*-**2.11e** and *Z*-**2.10d** did show doubling of some peaks indicative of conformational isomers in $CDCl_3$. The torsion angles of lactams *Z*-**2.11a,** *Z*-**2.11e** and *Z*-**2.10d** were compared with those for ideal turn and sheet structures (Table 1).[33] Notably, 8-member lactam *Z*-**2.11a** possesses similar dihedral angle geometry as observed for the central residues of an ideal type VIb β-turn, similar to its olefin regioisomer **2.27**. The torsion angle values of 9-member lactam *Z*-**2.11e** are similar to an ideal type I β-turn. Previously, 10-member lactam **2.28** possessing a *trans*-olefin geometry had also been found to exhibit backbone dihedral angles similar to an ideal type I β-turn (Table 2.1). In the case of 10-member lactam *Z*-**2.10d**, which possesses a *cis*-olefin at a different ring position, the backbone conformation was more similar to an ideal type II β-turn, albeit the dihedral angles of the *N*-terminal residue resembled an extended parallel β-pleated sheet. In sum, lactams *Z*-**2.11a,** *Z*-**2.11e** and *Z*-**2.10d** appear to have potential for mimicry of three different β-turn conformations.

2.7. Crystal structures of azabicyclo[X.Y.Z]alkanes 2.3 and 2.5

The stereochemical assignments made for iodo-pyrrolizidinone **2.3** were confirmed by the X-ray structure. The dihedral angle values of the peptide backbone in the 5,5-fused bicycle **2.3** resembled an extended rather than a turn structure. In this respect, the peptide backbone geometry in azabicyclo[3.3.0]alkanone **2.3** differed from those observed in X-ray analyses of larger azabicyclo[4.3.0]alkanone and iodo-azabicyclo[5.3.0]alkanone (**2.2**) amino esters counterparts, which were respectively similar to ideal type II' and type I β-turns.[34,12] In addition, the X-ray structure of 4-iodo-pyrrolizidinone **2.3** exhibited different dihedral angles than that of the related 6-hydroxy pyrrolizidinone, which closely resembled a type II' β-turn (Table 1).[5a]

In the X-ray structure of cyclic imidate **2.5**, the *Z-anti*-periplanar isomer was observed. Although related structures of such anti-Bredt heterocycles were not found, the bond lengths of bridging imidate **2.5** (C-O: 1.39; C=N: 1.24) compared well with those from crystal structures of cyclic imidates (C-O: 1.36±0.2 ; C=N: 1.25±0.01),[35,36] indicating that little distortion was induced by the bridge-head geometry of **2.5**. In addition, the dihedral angle values of **2.5** resembled that of an ideal type II β turn.

2.6. Mechanistic considerations

Transannular iodolactamizations have been studied using a series of related macrocycles of 8-10 ring atoms. In spite of the structural similarities of the starting macrocycle lactams, many factors may influence this reaction including ring conformation and cyclization conditions. In related iodolactamizations, regioselectivity has previously been considered to be a consequence of macrocycle conformation.[37] In this light, the flexibility of the macrocycle ring may contribute to mixtures of bicyclic products, yet ring substituents that orient to avoid allylic strain with the olefin substituents and diaxial interactions will reduce significantly the number of cyclization pathways. Typically, a relaxed conformer may orient the lactam and olefin to give regio- and stereoselective pathways.[37,8f,8d] In such cases, the iodide substituent ends up on the lactam ring. In one case, a thermodynamically less stable 9-member lactam has been found to give an alternative regio- and stereochemical indolizidinone featuring a five-member lactam and a piperidine ring bearing the iodide.[37] In addition, 9-member lactam *Z*-**2.11e** gave imidate **2.5** instead of a fused 7,4-bicycle with the iodide on the 7-member lactam or a 6,5-bicycle with the iodide on the 5-member pyrrolidine.

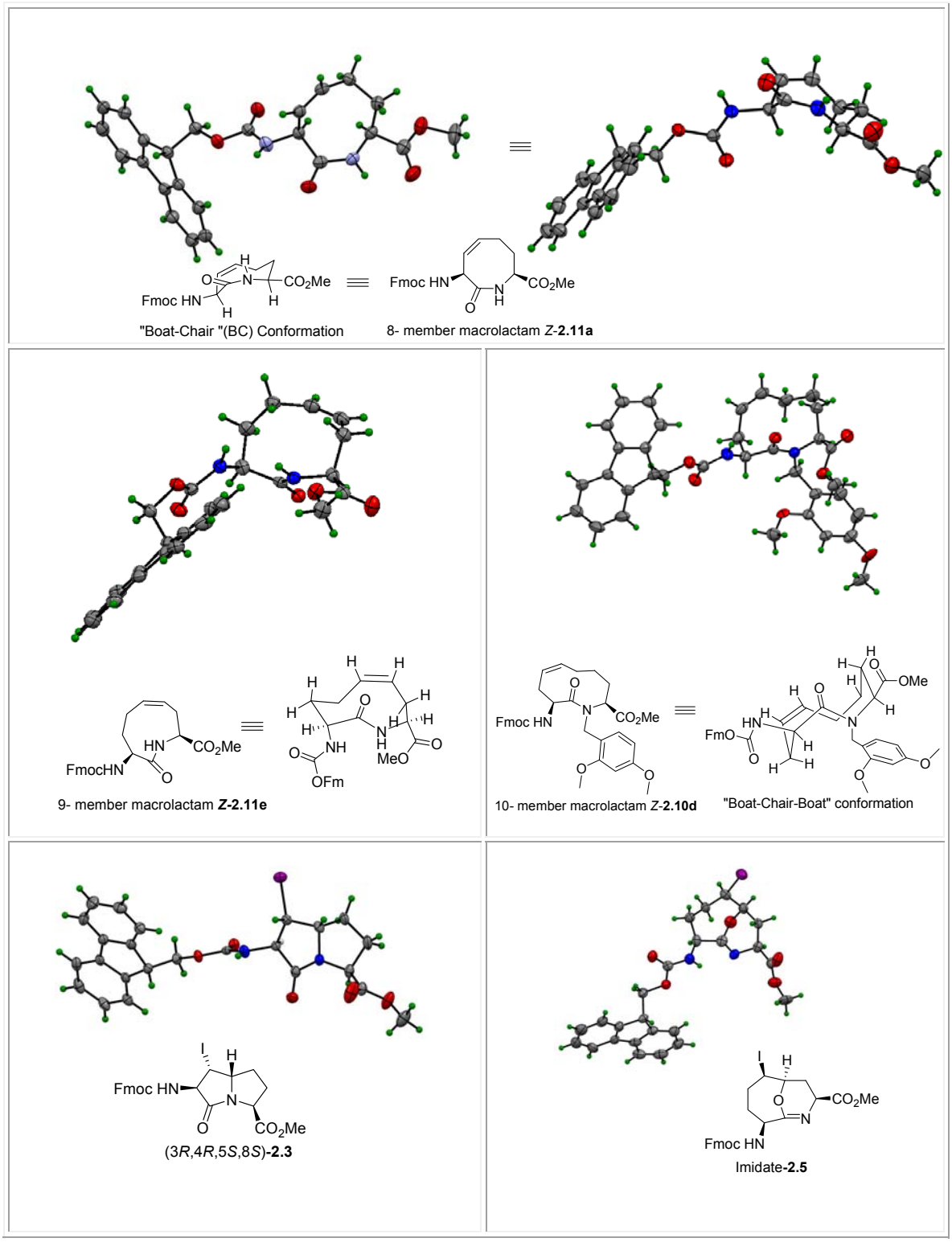

Figure 2.4. X-Ray structures of macrocycle dipeptide lactams and iodo-azabicyclo[X.Y.Z]alkanes (C, gray; H, green; N, blue; O,red)

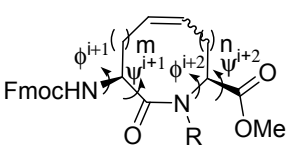

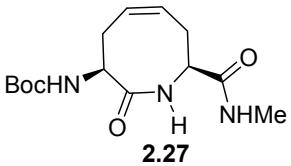

2.27

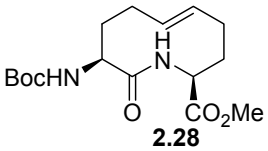

2.28

Type β Turn[33]		ϕ_1, deg	ψ_1, deg	ϕ_2, deg	ψ_2, deg
I		–60	–30	–90	0
II		–60	120	80	0
II'		60	–120	–80	0
Vib		–135	135	–75	160
Anti Parallel β Sheet[38]		ϕ = –140		ψ = 135	
Parallel β Sheet[38]		ϕ = –120		ψ = 115	
Peptidomimetic dihedral angles		ϕ^{i+1}, deg	ψ^{i+1}, deg	ϕ^{i+2}, deg	ψ^{i+2}, deg
8-member lactam *Z*-**2.11a**		–142	156	–158	172
8-member lactam **2.27**[32]		–93	177	–148	90
9-member lactam *Z*-**2.11e**		–109	–27	–145	–28
10-member lactam *Z*-**2.10d**		–161	171	63	23
10-member lactam *E*-**2.28**[39]	chair-chair	–107	–1	–130	23
	chair-boat	120	–64	–131	–43
4-Iodo-azabicyclo[3.3.0]alkanone **2.3**		–120	–140	–109	173
6-Hydroxy-azabicyclo[3.3.0]alkanone[5a]		14	–141	–40	133
Iodo-azabicyclo[5.3.0]alkanone **2.2**[8a]		–138	–64	–49	136
Azabicyclo[4,3,1]alkane **2.5**		–166	–1	175	74

Table 2.1. Comparison of dihedral angles of macrocycle and bicycle peptidomimetics with ideal secondary structures

Although electrophile-induced intramolecular cyclization reactions may proceed by formation of a dihalide that is subsequently displaced by the lactam to form the ring,[8e] cyclizations of macrocycles *Z*-**2.11a,** *Z*-**2.11e** and *Z*-**2.10d** are presumed to proceed by way of iodonium-like intermediates based on their stereochemical outcomes.[40] The ambidentate nucleophilic nature of the amide group has been observed to give imidates in iodocyclizations of simpler olefins,[41,42] and such *O*-selectivity has been explained on the basis of hard-soft acid-base theory considering the iodine-olefin π-complex to be a hard electrophile.[43,44] However, transannular attack of oxygen would result in an anti-Bredt bridge-head heterocycle,[45] which may be relatively disfavored due to ring strain. Given the choices between placing iodide on the non-lactam ring, forming a strained *N*-acyl azetidine or forming the anti-Bredt imidate, the latter product **5** was favored.

Bond distance	**8-member *Z*-2.11a**	**9-member *Z*-2.11e**	**10-member *Z*-2.10d**
N to C^N	3.11	3.23	3.45
N to C^{CO}	3.40	3.01	3.47
O to C^N	3.14	3.33	3.29
O to C^{CO}	4.12	3.38	3.63

Table 2.2. Comparison of Transannular distances in macrocyclic lactams

Notably, the respective proximities of the amide nitrogen and oxygen to the double bond carbons on the amine (C^N) and carbonyl (C^{CO}) sides of the macrocycle did not correlate with the mode of cyclization except in the case of the 8-member lactam going to the fused 5,5-bicycle (Table 2.2).

A working hypothesis for the selectivity of the transannular iodolactamization begins with a favored macrocycle conformation that minimizes ring strain. Approach of iodine to the less sterically hindered face of the olefin provides the iodonium intermediate, which is typically attacked on the carbon (C^N) on the amide nitrogen side of the macrocycle to provide a bicycle

having the iodide on the lactam ring. Attack of the iodonium carbon (C^{CO}) on the carbonyl side of the macrocycle is likely disfavored due to the need to avoid allylic strain between the carboxylate and the lactam carbonyl as well as potential diaxial interactions between the carboxylate and the iodide. In the case of **5**, the combination of the factors mentioned above and ring strain to make a 4-member azetidine, lead to a preferred attack by oxygen giving the imidate. Computational analyses are currently being pursued to provide additional support of these mechanistic considerations.

2.8. Conclusions

A variety of azabicyclo[X.Y.0]alkanone amino acids have been prepared using a common approach featuring effective assembly of macrocyclic lactams of 8-10 member ring sizes by the synthesis and coupling of ω-unsaturated amino acids, RCM of their dipeptide derivatives, followed by regio- and stereoselective electrophilic transannular cyclization. Employing X-ray crystallographic and NMR spectroscopic analyses, we have demonstrated that the macrocycle and bicyclic structures offer ample potential to mimic peptide secondary structures, in particular type I, II' and VI β-turn geometry contingent on ring size. Moreover, such conformational analyses have also provided insight into the mechanism of transannular iodolactamization. Considering the potential of this method for making effectively a series of related dipeptide mimics to explore peptide conformation-activity relationships, as well as opportunity for replacing the iodide with other side chains to examine functional group influences on activity, this method should have significant impact on peptidomimetic approaches for studying biologically active peptides particularly for the discovery of therapeutic agents.

2.9. Experimental Section

2.9.1. General Methods

Unless otherwise noted, all reactions were performed under argon atmosphere and distilled solvents were transferred by syringe. Anhydrous CH_2Cl_2 (DCM), THF and diethyl ether were obtained by passage through a solvent filtration system (GlassContour, Irvine, CA). Final reaction mixture solutions were dried over anhydrous $MgSO_4$ or Na_2SO_4, filtered and rotary-evaporated under reduced pressure. Flash chromatography[46] was on 230–400 mesh silica gel, and thin-layer chromatography was performed on silica gel 60 F254 plates. Specific rotations, $[\alpha]_D$ values, were calculated from optical rotations measured at 20 °C in $CHCl_3$ or MeOD at the specified concentrations (*c* in g/100 ml) using a 1-dm cell (*l*) on a Polarimeter, using the general formula: $[\alpha]^{20}_D = (100 \times \alpha)/(l \times c)$. Accurate mass measurements were performed on a LC-MSD instrument from electrospray ionization (ESI-TOF) mode. Sodium adducts [M + Na]+ were used for empirical formula confirmation. ^{1}H NMR spectra were measured in $CDCl_3$ (7.26 ppm), CD_3OD (3.31 ppm) or DMSO-d_6 (2.50 ppm). ^{13}C NMR spectra were measured in $CDCl_3$ (77.16 ppm) or DMSO-d_6 (39.52 ppm). ^{1}H NMR spectra for the dipeptides **2.7a, 2.7b, 2.6d, 2.7d, 2.6g, 2.11g, 2.11d** and **2.20** were recorded at 100 °C to coalesce signals due to conformational isomers. Coupling constant *J* values are measured in Hertz (Hz) and chemical shift values in parts per million (ppm). Infrared spectra were recorded in the neat on an FT-IR apparatus. Synthesis and characterization of compounds 2.7e, 2.10e, 2.11e, 2.17a, 2.17b, 2.16a and 2.16b has been previously reported.[14]

(*S*)-Methyl 2-*N*-(Boc)aminopet-4-enoate (2.13)

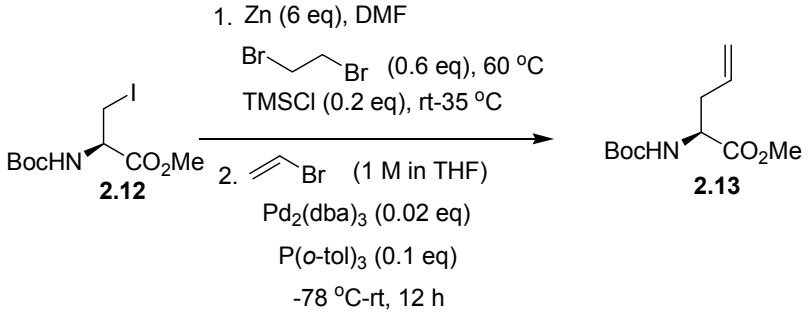

To a stirred solution of zinc dust (11.92 g, 182.3 mmol, 6 eq) in dry DMF (20 mL), 1,2-dibromoethane (1.57 mL, 3.42 g, 18.2 mmol, 0.6 eq) was added via a syringe. The resulting mixture was heated to 60 °C, stirred for 45 min, cooled to room temperature, and the slurry was treated with chlorotrimethylsilane (0.77 mL, 6.0 mmol). After stirring for 40 min at room temperature, the activated zinc was treated with a solution of methyl (*R*)-*N*-(Boc)iodoalaninate (**2.12**, 10 g, 30.39 mmol,) in dry DMF (20 mL), heated to 35 °C and stirred for 60 min, when insertion was judged complete by TLC analysis [(2:1 hexanes/ethyl acetate) using 254 nm UV light to visualize the starting material **2.12** (R_f = 0.7) and organozinc reagent (R_f = 0.1)]. After complete zinc insertion, the reaction mixture was cooled to room temperature, charged with $Pd_2(dba)_3$ (779 mg, 0.85 mmol, 0.028 eq) and tri(*o*-tolyl)phosphine (925 mg, 3.03 mmol, 0.1 eq), cooled to –78 °C, and treated drop-wise via a cannula with a solution of vinyl bromide in THF (1 M, 42.5 mL, 42.5 mmol, 1.4 eq). After complete addition of the vinyl bromide solution, the cold bath was removed, and the reaction mixture was allowed to warm to room temperature with stirring for 12 h. The reaction mixture was diluted with ethyl acetate (200 mL) and water (200 mL), and filtered through a pad of Celite™. The pad was washed with ethyl acetate (300 mL). The filtrate and washings were combined and transferred to a separating funnel. The organic layer was separated. The aqueous layer was extracted with ethyl acetate (2 x 200 mL). The combined organic layers were washed with brine (400 mL), dried over anhydrous sodium

sulfate, filtered, and concentrated under reduced pressure to give 8.2 g of brown oil, which was purified by column chromatography on silica gel (8% to 10% EtOAc in hexane) to give olefin **2.13** (4.50 g, 19.64 mmol, 65%) as a brown oil: R_f = 0.29 (9:1 hexanes: ethyl acetate, visualized as a UV inactive and $KMnO_4$ active spot on heating), $[\alpha]_D^{20}$ +20.2 (*c* 1.5, $CHCl_3$); FT-IR (neat) ν_{max} 2978, 1744, 1712, 1499, 1437, 1365, 1159, 1021, 868, 779 cm^{-1}; ^1H NMR (500 MHz, $CDCl_3$) δ: 5.63-5.71 (m, 1H), 5.09-5.12 (m, 2H), 5.03-5.04 (br d, 1H), 4.34-4.37 (m, 1H), 3.71 (s, 3H), 2.50-2.55 (m, 1H), 2.42-2.47 (m, 1H), 1.41 (s, 9H); ^{13}C NMR (125 MHz, $CDCl_3$) δ 172.7, 155.3, 132.4, 119.1, 79.9, 53.0, 52.3, 36.9, 28.4; HRMS (ESI-TOF) m/z: [M+Na]+ Calcd for $C_{11}H_{19}NO_4Na$, 252.1215; Found 252.1217. Anal. Calcd for $C_{11}H_{19}NO_4$: C, 57.62; H, 8.35; N, 6.11. Found: C, 57.13; H, 8.51; N, 5.93. Attempts to ascertain the enantiomeric purity of olefin **2.13**, as well as the hydrochloride **2.30** obtained on treating **2.13** with HCl gas in dichloromethane, both were unsuccessful using super-critical fluid chromatography on a chiral column. To assess enantiomeric purity, diastereomeric amides were synthesized as described below. The crude residue was examined by ^1H NMR spectroscopy in CD_3CN at 700 MHz. Incremental addition of (*S,R*)-**2.31** into (*S,S*)-**2.31** and observation of the methyl ester singlets at 3.697 and 3.691 ppm demonstrated the diastereomers were of >99:1 dr. Hence, olefin **2.13** is assumed to be of >98% enantiomeric purity.

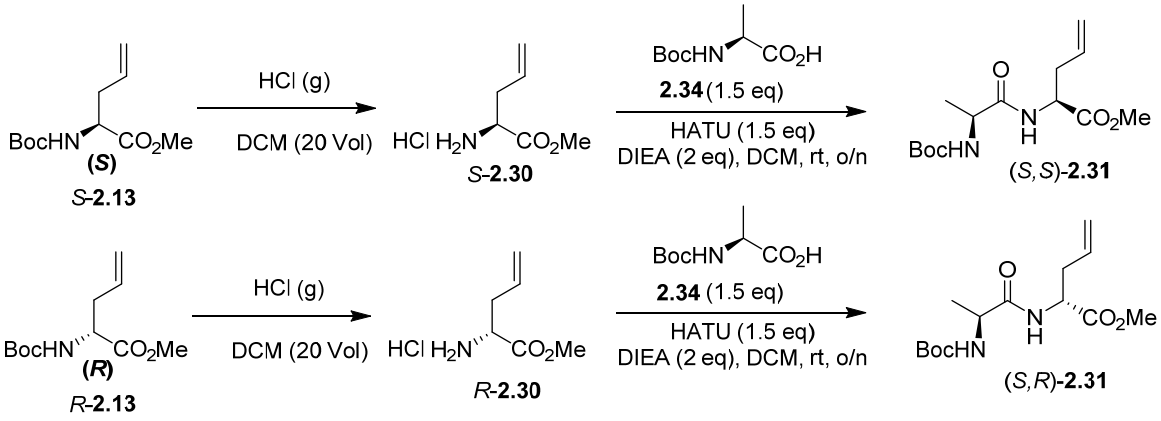

(*S*)-Methyl 2-aminopent-4-enoate hydrochloride (**2.30**). Dry HCl gas was bubbled into a stirred solution of methyl (*S*)-2-*N*-(Boc)aminopent-4-enoate (**2.13**, 70 mg, 0.30 mmol) in dichloromethane at room temperature. Consumption of **2.13** was observed by TLC after 3h. The resulting solution was concentrated under reduced pressure to give (*S*)-**2.30** as a brown solid: ^{1}H NMR (400 MHz, CD_3OD) δ: 2.68-2.75 (m, 2H), 3.86 (s, 3H), 4.16-4.19 (m, 1H), 5.27-5.33 (m, 2H), 5.77-5.81 (m, 1H). (*R*)-Methyl 2-aminopent-4-enoate hydrochloride *R*-**2.30** was made by an analogous method from *R*-**13** as that used to prepare *S*-**2.30**.

(*S,S*)-Methyl *N*-(Boc)alaninyl-2-aminopent-4-enoate (*S,S*-**2.31**). A stirred solution of Boc-L-Ala (**2.34**, 86 mg, 0.45 mmol, 1.5 equiv) in DCM (5 mL) was treated with amine hydrochloride (*S*)-**2.30** (50 mg, 0.30 mmol, 1 equiv), DIEA (78 mg, 0.6 mmol, 2 equiv), and HATU (173 mg, 0.45 mmol, 1.5 equiv), stirred at room temperature for 16 h, diluted with DCM (~10 mL) and washed with saturated aqueous $NaHCO_3$. The layers were separated. The aqueous layer was extracted with DCM (~10 mL). The combined organic layers were washed with brine, dried over anhydrous sodium sulfate, filtered, and concentrated under reduced pressure to give (*S,S*)-**2.31** as brown oil, which was analyzed without further purification.

(*S,S*)-**2.31**: ^{1}H NMR (400 MHz, CD_3CN) δ: 1.27-1.28 (d, J = 7.2, 3H), 1.44 (s, 9H), 2.43-2.51 (m, 1H), 2.53-2.60 (m, 1H), 3.71 (s, 3H), 4.06-4.10 (m, 1H), 4.44-4.49 (m, 1H), 5.10-5.19 (m, 2H), 5.63 (br s, 1H), 5.72-5.82 (m, 1H), 6.91 (br s, 1H);

(*S,R*)-**2.31** was made by the analogous method used to prepare (*S,S*)-**2.31** using *R*-**2.30**. (*S,R*)-**2.31**: ^{1}H NMR (400 MHz, CD_3CN) δ: 1.26-1.28 (d, J = 7.2, 3H), 1.44 (s, 9H), 2.42-2.50 (m, 1H), 2.53-2.60 (m, 1H), 3.70 (s, 3H), 4.05-4.09 (m, 1H), 4.44-4.49 (m, 1H), 5.10-5.18 (m, 2H), 5.62 (br s, 1H), 5.68-5.81 (m, 1H), 6.90 (br s, 1H).

(*S*)-Methyl 2-*N*-(Boc)aminohept-6-enoate (2.15)

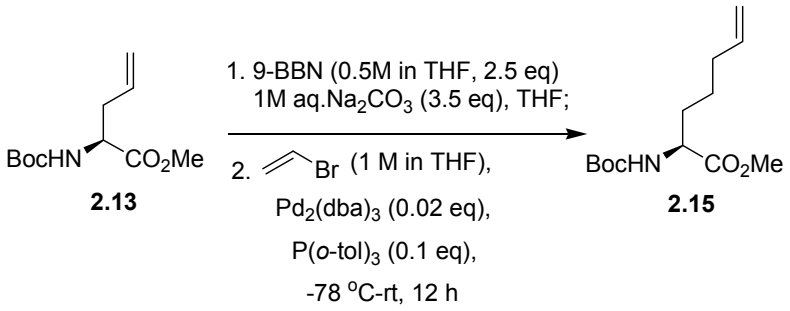

A solution of 9-BBN in THF (0.5 M, 109 mL) was added to a 0 °C solution of methyl pent-4-enoate **2.13** (5 g, 21.8 mmol) in anhydrous THF (40 mL). The mixture was warmed to room temperature, stirred for 3 h, and quenched with 1M aqueous Na_2CO_3 in H_2O (76.3 mL) with agitation using argon bubbles for 20 min. To a second round bottomed flask containing a stirred suspension of $Pd_2(dba)_3$ (393 mg, 0.43 mmol) and tri (*o*-tolyl)phosphine (663 mg, 2.18 mmol) in THF at –78 °C, a 1M solution of vinyl bromide in THF (87 ml, 87 mmol) was added, followed by the degassed solution of boronate. The resulting mixture was stirred at room temperature overnight, quenched with water (100 mL) and extracted using ethyl acetate (150 mL x 2). The combined organic extracts were washed with brine (100 mL) and dried over anhydrous Na_2SO_4, filtered, and concentrated under reduced pressure to give 7.8 g of brown oil, which was twice purified by column chromatography on silica gel using 4-6% EtOAc in hexane. Evaporation of the collected fractions gave olefin **2.15** (3.81 g, 14.81 mmol, 68%) as a light brown oil: R_f = 0.29 (9:1 hexanes/ethyl acetate, visualized as a UV inactive and $KMnO_4$ active spot on heating); $[\alpha]_D^{22}$ +14.6 (*c* 1, $CHCl_3$); FT-IR (neat) ν_{max} 2977, 1742, 1712, 1501, 1365, 1160. 1050, 909 cm^{-1}; ^1H NMR (400 MHz, $CDCl_3$) δ 5.70-5.80 (m, 1H), 4.93-5.01 (m, 3H), 4.27-4.28 (m, 1H), 3.71 (s, 3H), 2.00-2.09 (m, 2H), 1.74-1.82 (m, 1H), 1.56-1.65 (m, 1H), 1.37-1.48 (m, 11H); ^{13}C NMR (100 MHz, $CDCl_3$) δ 173.5, 155.5, 138.1, 115.2, 79.9, 53.4, 52.3, 33.2, 32.3, 28.3, 24.7; HRMS (ESI-TOF) m/z: [M+Na]+ Calcd for $C_{13}H_{23}NO_4Na$, 280.1519; Found 280.1533.

Attempts to ascertain the enantiomeric purity of olefin **2.15**, as well as the hydrochloride **2.32** that was obtained on treating **2.15** with HCl gas in dichloromethane, both were unsuccessful using SFC on a chiral column. To assess enantiomeric purity, diastereomeric amides were synthesized as described below. Crude residue was examined by ^{1}H NMR spectroscopy in CD_3CN at 700 MHz. Incremental addition of (*S,R*)**-2.33** into (*S,S*)**-2.33** and observation of the methyl ester singlets at 3.6578 and 3.6622 ppm demonstrated the diastereomers were of >99:1 dr. Hence, olefin **2.15** is assumed to be of >98% enantiomeric purity.

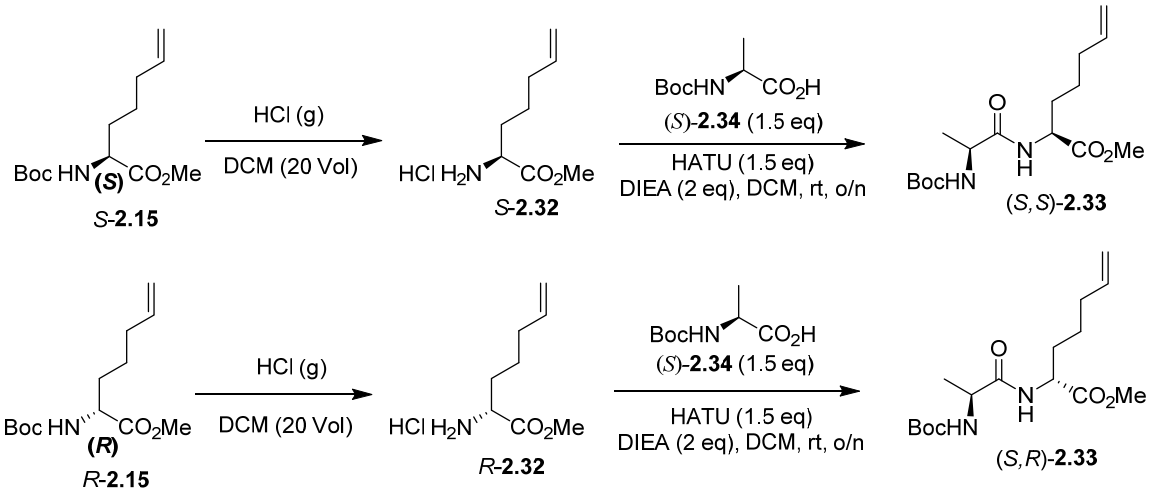

(*S*)-Methyl 2-aminohept-6-enoate hydrochloride (*S*-**2.32**). Dry HCl gas was bubbled into a stirred solution of (*S*)-methyl 2-*N*-(Boc)aminohept-6-enoate (*S*-**2.15**, 100 mg, 0.38 mmol) in dry dichloromethane at room temperature. Consumption of *S*-**2.15** was observed by TLC after 3h. The resulting solution was concentrated under reduced pressure to give (*S*)**-2.32** as a white solid: ^{1}H NMR (500 MHz, $CDCl_3$) δ 5.78-5.86 (m, 1H), 4.99-5.09 (m, 2H), 4.06-4.09 (t, 1H, J = 6.4 Hz), 3.85 (s, 3H), 2.11-2.16 (m, 2H), 1.86-1.99 (m, 2H), 1.45-1.63 (m, 2H); (*R*)-Methyl 2-aminohept-6-enoate hydrochloride *R*-**32** was made by the analogous method from *R*-**15** as that used to prepare *S*-**2.32**.

(*S*,*S*)-Methyl *N*-(Boc)alaninyl-2-aminohept-6-enoate (*S,S*)**-2.33.** A stirred solution of Boc-L-Ala (**2.34**, 87 mg, 0.46 mmol, 1.5 equiv) in DCM (5 mL) was treated with amine hydrochloride (*S*)**-2.32** (60 mg, 0.31 mmol, 1 equiv), DIEA (80 mg, 0.62 mmol, 2 equiv), and HATU (180 mg, 0.45 mmol, 1.5 equiv), stirred at room temperature for 16 h, diluted with DCM (~10 mL) and washed with saturated aqueous $NaHCO_3$. The layers were separated. The aqueous layer was extracted with DCM (~10 mL). The combined organic layers were washed with brine, dried over anhydrous sodium sulfate, filtered, and concentrated under reduced pressure to give (*S,S*)**-2.33** as brown oil, which was analyzed without further purification. (*S,S*)**-2.33**: ^{1}H NMR (700 MHz, CD_3CN) δ: 6.86 (br s, 1H), 5.77-5.83 (m, 1H), 5.57 (br s, 1H), 4.99-5.03 (m, 1H), 4.94-4.96 (m, 1H), 4.34-4.37 (m, 1H), 4.03-4.05 (m, 1H), 3.65 (s, 3H), 2.03-2.06 (m, 2H), 1.75-1.80 (m, 1H), 1.61-1.68 (m, 1H), 1.38-1.42 (m, 11H), 1.24-1.25 (d, J = 7.1 Hz, 3H). Amide (*S,R*)**-2.33** was made by the analogous method used to prepare (*S,S*)**-2.33** using *R*-**2.32**. Amide (*S,R*)**-2.33**: ^{1}H NMR (700 MHz, CD_3CN) δ: 6.86 (br s, 1H), 5.76-5.82 (m, 1H), 5.57 (br s, 1H), 5.01-5.02 (m, 1H), 4.99-5.00 (m, 1H), 4.33-4.36 (m, 1H), 4.01-4.03 (m, 1H), 3.66 (s, 3H), 2.01-2.08 (m, 2H), 1.75-1.80 (m, 1H), 1.60-1.66 (m, 1H), 1.39-1.40 (m, 11H), 1.24-1.25 (d, J = 7.1 Hz, 3H).

(*S*)-2-Aminopent-4-enoic acid hydrochloride (2.29)

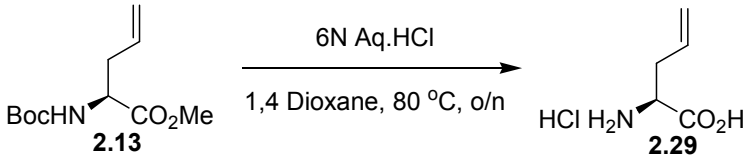

A stirred solution of methyl (*S*)-2-*N*-(Boc)aminopent-4-enoate (**2.13**, 4 g, 17.4 mmol) in 1,4-dioxane at 0 °C was treated with 6N HCl (80 mL), heated to 80 °C overnight, cooled and evaporated to a reside that was dissolved in water and washed with dichloromethane. The aqueous layer was concentrated to off white solid **2.29** (2.51 g, 16.61 mmol, 95%): mp 206-208,

$[\alpha]_D^{20}$ +7.6 (*c* 1, CH_3OH); FT-IR (neat) ν_{max} 2914, 1730, 1490, 1427, 1215, 1174, 1124, 993, 933, 873 cm^{-1}; ^1H NMR (400 MHz, $CDCl_3$) δ 5.76-5.87 (m, 1H), 5.26-5.34 (m, 2H), 4.06-4.09 (m, 1H), 2.63-2.79 (m, 2H); ^{13}C NMR (100 MHz, $CDCl_3$) δ 171.1, 131.8, 121.4, 53.4, 35.7 ; HRMS (ESI-TOF) m/z: [M–H]– Calcd for $C_5H_9ClNO_2$ 150.0327; Found 150.0330.

(*S*)-Methyl 2-(2,4-dimethoxybenzylamino)hept-6-enoate (2.16c)

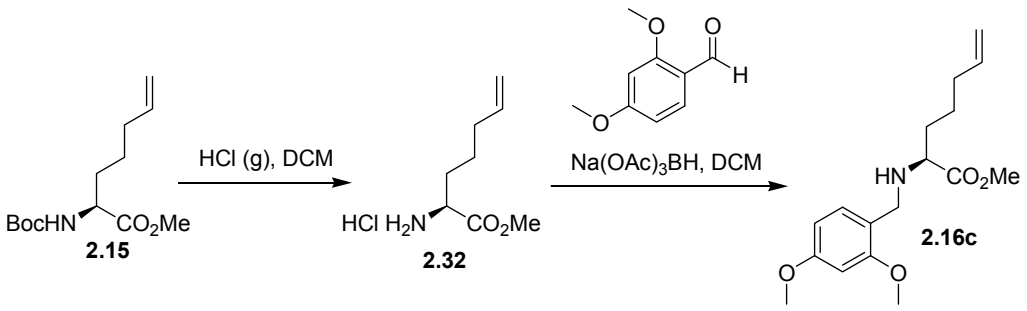

A stirred solution of (*S*)-methyl 2-*N*-(Boc)aminohept-6-enoate (**2.15**, 3 g, 11.7 mmol) in dichloromethane (60 mL) was treated with HCl gas bubbles for 3 h. The volatiles were removed by rotary evaporation to give (*S*)-methyl 2-aminohept-6-enoate hydrochloride (**2.32**, 2.19 g, 11.34 mmol, 97 %) as white solid: mp 112-114 °C; $[\alpha]_D^{24}$ +24.6 (*c* 1, $CHCl_3$); FT-IR (neat) ν_{max} 2922, 2134, 1745, 1438, 1234, 912 cm^{-1}; ^1H NMR (500 MHz, CD_3OD) δ 5.78-5.86 (m, 1H), 4.99-5.09 (m, 2H), 4.06-4.09 (t, 1H, J = 6.4 Hz), 3.85 (s, 3H), 2.11-2.16 (m, 2H), 1.86-1.99 (m, 2H), 1.45-1.63 (m, 2H); ^{13}C NMR (125 MHz, CD_3OD) δ 170.9, 138.6, 116.0, 53.9, 53.6, 34.0, 30.9, 25.1; HRMS (ESI-TOF) m/z: [M+H]+ Calcd for $C_8H_{16}NO_2$ 158.1175; Found 158.1179.

Amino ester hydrochloride **2.32** (2 g, 10.35 mmol) was partitioned between a saturated $NaHCO_3$ solution (50 mL) and CH_2Cl_2 (50 mL). The aqueous phase was extracted with CH_2Cl_2 (2 x 50 mL), and the combined organic layers were washed with 30 mL of brine, dried over Na_2SO_4, filtered, and concentrated to a volume of ~30 mL. The solution of freebase was treated with 2,4-

dimethoxybenzaldehyde (2.23 g, 13.45 mmol) and $NaBH(OAc)_3$ (3.28 g, 15.5 mmol), stirred for 18 h at room temperature, treated with 40 mL of saturated $NaHCO_3$, and stirred for 30 min. The aqueous layer was separated and washed with 20 mL of CH_2Cl_2. The combined organic layers were washed with brine, dried over $MgSO_4$, filtered, and concentrated to a residue that was purified by chromatography on silica gel (20-25% EtOAc in hexane) to give N-(Dmb)amino ester **2.16c** (2.09 g, 6.80 mmol, 65%) as colorless oil: R_f = 0.35 (7:3 hexanes/ethyl acetate, visualized by UV), $[\alpha]_D^{20}$ –3.1 (*c* 1, $CHCl_3$); FT-IR (neat) ν_{max} 2943, 1732, 1612, 1587, 1505, 1457, 1437, 1287, 1260, 1206, 1154, 1035, 913 cm^{-1}; ^1H NMR (500 MHz, $CDCl_3$) δ 7.11-7.12 (d, 1H, *J* = 8.25 Hz), 6.40-6.42 (m, 2H), 5.71-5.78 (m, 1H), 4.91-4.99 (m, 2H), 3.79 (s, 3H), 3.78 (s, 3H), 3.68-3.71 (d, 1H, *J* = 13.2 Hz), 3.64 (s, 3H), 3.61-3.64 (d, 1H, *J* = 13.2 Hz), 3.22-3.25 (t, 1H, *J* = 6.65 Hz), 1.99-2.01 (m, 2H), 1.59-1.65 (m, 2H), 1.39-1.46 (m, 2H); ^{13}C NMR (125 MHz, $CDCl_3$) δ 175.9, 160.1, 158.6, 138.3, 130.3, 120.5, 114.7, 103.7, 98.5, 60.7, 55.4, 55.3, 51.5, 47.1, 33.5, 33.0, 25.0; HRMS (ESI-TOF) m/z: [M+Na]+ Calcd for $C_{17}H_{25}NO_4Na$, 330.1675; Found 330.1691.

(*S*)-2-*N*-(Boc)Aminopent-4-enoic acid (2.18a)

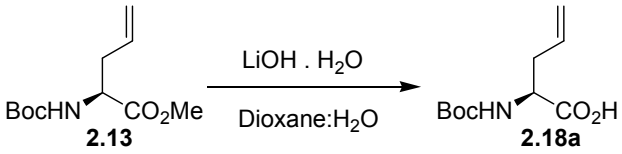

2.13 **2.18a**

A solution of methyl (*S*)-2-*N*-(Boc)aminopent-4-enoate (**2.13**, 1.2 g, 5.23 mmol) in 1:1 H_2O:dioxane (48 mL) was treated with $LiOH•H_2O$ (219 mg, 5.23 mmol), stirred for 3 h, and evaporated to a residue that was partitioned between H_2O (20 mL) and EtOAc (20 mL). The aqueous phase was acidified with 1 M HCl to pH 4 and extracted twice with EtOAc (20 mL). The combined organic extracts were washed with brine, dried over Na_2SO_4, filtered, and

concentrated to afford acid **2.18a** (1.09 g, 5.06 mmol, 97%) as colorless oil: $[\alpha]_D^{22}$ +12.3 (*c* 1, $CHCl_3$); FT-IR (neat) ν_{max} 2978, 1698, 1699, 1507, 1393, 1367, 1248, 1158, 1050, 869, 754 cm^{-1}; ^1H NMR (500 MHz, CD_3OD) δ 5.74-5.83 (m, 1H,), 5.07-5.15 (m, 2H), 4.13-4.16 (m, 1H), 2.52-2.53 (m, 1H), 2.38-2.42 (m, 1H), 1.44 (s, 9H); ^{13}C NMR (125 MHz, CD_3OD) δ 175.4, 157.9, 134.7, 118.5, 80.5, 54.6, 37.1, 28.7; HRMS (ESI-TOF) m/z: [M+Na]+ Calcd for $C_{10}H_{17}NO_4Na$, 238.1049; Found 238.1050.

(*S*)-2-*N*-(Boc)aminohept-6-enoic acid (2.18c)

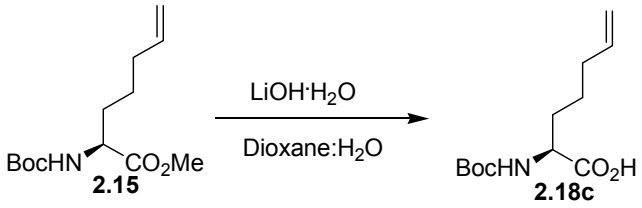

Employing the procedure described for acid **2.8a**, methyl hept-6-enoate **2.15** (500 mg, 1.94 mmol) was converted to acid **2.18c** (445 mg, 1.83 mmol, 94%): a colorless oil; $[\alpha]_D^{20}$ +11.5 (*c* 1, $CHCl_3$); FT-IR (neat) ν_{max} 2977, 2929, 1711, 1508, 1393, 1367, 1245, 1160, 910 cm^{-1}; ^1H NMR (500 MHz, CD_3OD) δ 5.76-5.84 (m, 1H,), 4.94-5.04 (m, 2H), 4.05-4.08 (m, 1H), 2.03-2.12 (m, 2H), 1.77-1.84 (m, 1H), 1.59-1.67 (m, 1H), 1.51-1.46 (m, 2H), 1.44 (s, 9H); ^{13}C NMR (125 MHz, CD_3OD) δ 176.3, 158.1, 139.4, 115.3, 80.4, 54.7, 34.3, 32.3, 28.7, 26.2; HRMS (ESI-TOF) m/z: [M-H] Calcd for $C_{12}H_{20}NO_4Na$, 242.1397; Found 242.1409.

(*S*,*S*)-Methyl 2-(Fmoc)aminobut-3-enoyl-*N*-(2,4-dimethoxybenzyl)-2-aminohex-5-enoate (2.7a)

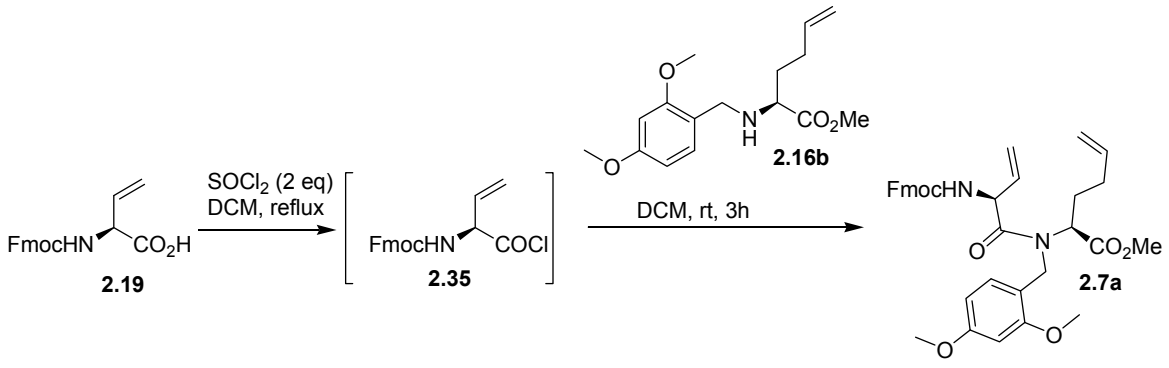

(*S*)-*N*-(Fmoc)Vinylglycine (**19**, 2.47 g, 7.64 mmol) was treated with thionyl chloride (1.1 mL, 15.32 mmol) in DCM at 0 ºC. The resulting solution was then heated to a reflux for 3 h, cooled and the volatiles were evaporated. The residue was dissolved and evaporated 3 times from DCM. Without further purification, acid chloride **2.35** was dissolved in DCM (20 mL), cooled to 0 °C, and treated with *N*-(Dmb)homoallylglycine (**2.16b**, 1.5 g, 5.12 mmol). The resulting mixture was stirred at room temperature for 3 h. The volatiles were evaporated and the residue was taken up in a minimum volume of DCM, applied onto a silica gel column and eluted with 30-40% EtOAc/Hexanes to give **2.7a** (1.42 g, 2.37 mmol, 46%) as a colorless oil that solidified on standing: R_f = 0.52 (4:6 EtOAc/Hexanes, visualized by UV); $[\alpha]_D^{24}$ –40.1 (*c* 1, $CHCl_3$); FT-IR (neat) ν_{max} 2947, 1719, 1647, 1612, 1588, 1506, 1207, 1156, 1032, 759, 738 cm^{-1}; ^1H NMR (500 MHz, DMSO-d_6, 100 °C) δ: 7.84-7.85 (d, 2H, *J* = 7.5 Hz), 7.67-7.70 (t, 2H, *J* = 6.7 Hz), 7.38-7.42 (m, 2H), 7.29-7.32 (m, 2H), 7.18 (br s, 1H), 7.04 (br s, 1H), 6.55 (d, 1H, *J* = 2.0 Hz), 6.46-6.48 (dd, 1H, *J* = 2.2 Hz), 5.87-5.95 (m, 1H), 5.63-5.71 (m, 1H), 5.23-5.29 (m, 2H), 5.18-5.20 (br t, 1H), 4.92-4.93 (m, 1H), 4.90-4.91 (m, 1H), 4.55-4.58 (d, 1H, *J* = 16.4 Hz), 4.39-4.43 (m, 1H), 4.28-4.35 (m, 2H), 4.20-4.23 (m, 2H), 3.77 (s, 3H), 3.75 (s, 3H), 3.50 (s, 3H), 1.91-2.04 (m, 3H), 1.65-1.71 (m, 1H); ^{13}C NMR (125 MHz, DMSO-d_6, 100 °C) δ 170.1, 169.8, 160.1, 157.9, 154.6, 143.4, 143.3, 140.2, 137.1, 133.5, 129.5, 127.2, 126.4, 124.6, 124.5, 119.3, 117.0,

114.5, 104.5, 98.2, 78.6, 65.6, 57,.5 54.9, 54.8, 53.7, 50.9, 46.4, 29.4, 27.6; HRMS (ESI-TOF) m/z: [M+Na]+ Calcd for $C_{35}H_{38}N_2O_7Na$, 621.2571; Found 621.2562.

(*S*,*S*)-Methyl 2-(Fmoc)aminobut-3-enoyl-*N*-(2,4-dimethoxybenzyl)-2-aminohept-6-enoate (2.7b)

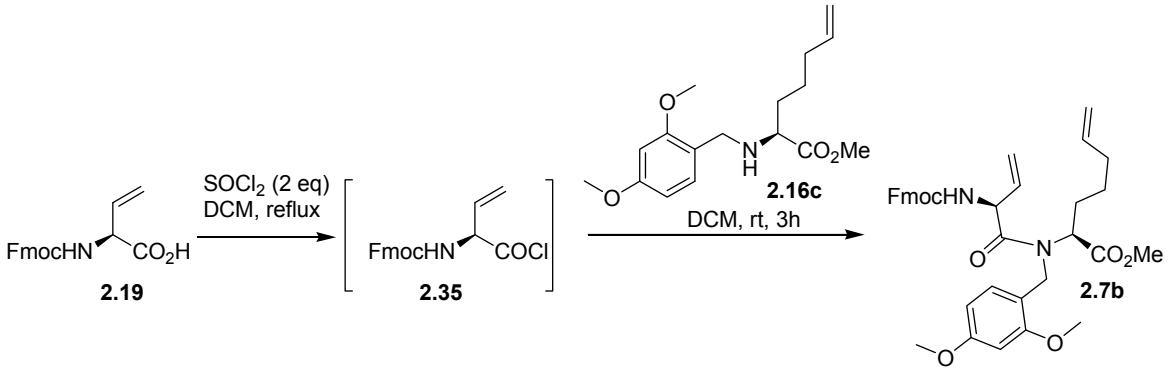

As described for the synthesis of dipeptide **2.7a**, (*S*)-2-*N*-(Fmoc)aminobut-3-enoic acid (**2.19**, 785 mg, 2.43 mmol) was coupled with *N*-(Dmb)-2-aminohept-6-enoate (**2.16c**, 500 mg, 1.62 mmol). The residue was purified by chromatography on silica gel (30-40% EtOAc in hexane) to give dipeptide **2.7b** (540 mg, 0.88 mmol, 54%) as a colorless oil: R_f = 0.55 (4:6 EtOAc:Hexanes, visualized by UV); $[\alpha]_D^{20}$ –30.6 (*c* 1, $CHCl_3$); FT-IR (neat) ν_{max} 2947, 1719, 1647, 1612, 1588, 1506, 1207, 1156, 1032, 916, 758, 738 cm^{-1}; ^1H NMR (500 MHz, DMSO-d_6, 100 °C) δ: 7.84-7.85 (d, 2H, *J* = 7.5 Hz), 7.67-7.70 (t, 2H, *J* = 6.6 Hz), 7.38-7.42 (m, 2H), 7.29-7.32 (m, 2H), 7.18-7.19 (m, 1H), 7.03 (br s, 1H) 6.55-6.56 (m, 1H), 6.45-6.47 (m, 1H), 5.84-5.96 (m, 1H), 5.62-5.71 (m, 1H), 5.24-5.29 (m, 2H), 5.17-5.20 (m, 1H), 4.88-4.94 (m, 2H), 4.53-4.57 (d, 1H, *J* = 16.4), 4.41-4.44 (m, 1H), 4.20-4.35 (m, 4H), 3.75 (s, 3H), 3.78 (s, 3H), 3.51 (s, 3H), 1.81-1.97 (m, 3H), 1.55-1.67 (m, 1H), 1.17-1.37 (m, 2H); ^{13}C NMR (125 MHz, DMSO-d_6, 100 °C) δ 170.2, 160.1, 157.7, 154.6, 143.4, 143.3, 140.3, 137.6, 133.6, 129.4, 127.0, 126.4, 124.6, 124.5,

119.3, 117.0, 114.0, 104.5, 98.2, 78.6, 65.6, 57.9, 54.9, 54.8, 53.7, 50.9, 46.4, 45.3, 32.1, 27.7, 24.7; HRMS (ESI-TOF) m/z: [M+Na]+ Calcd for $C_{36}H_{40}N_2O_7Na$, 635.2727; Found 635.2738.

(*Z*,*S*)-Methyl 2-*N*-(Fmoc)aminobut-2-enoyl-*N*-(2,4-dimethoxybenzyl)-2-aminohex-5-enoate (2.20)

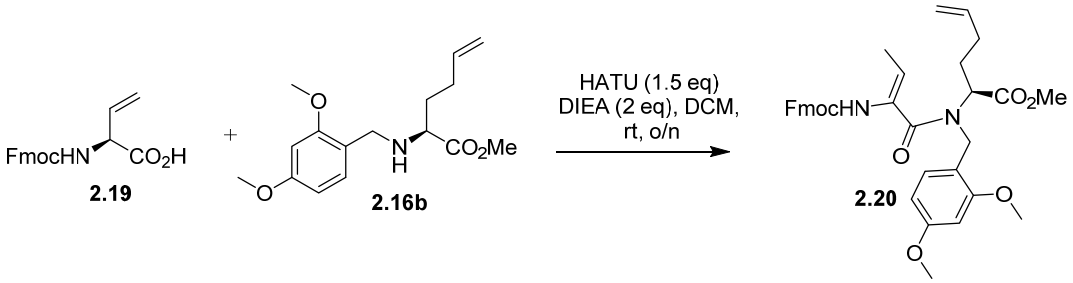

N-(Fmoc)Vinylglycine (**2.19**, 274 mg, 0.85 mmol) and methyl *N*-(Dmb)pent-4-enoate (**2.16b**, 170 mg, 0.57 mmol) were dissolved in DCM (10 mL), treated with DIEA (147 mg, 1.14 mmol) and HATU (323.1 mg, 0.85 mmol), stirred for 24 h, and diluted with water. The aqueous layer was extracted with DCM (3 x 50 mL). The combined organic layers were washed with brine (50 mL), dried over anhydrous sodium sulfate, filtered, and concentrated under reduced pressure. The residue was purified by column chromatography on silica gel (30-40% EtOAc in hexane) to give dipeptide **2.20** (302 mg, 0.50 mmol, 87%) as colorless gummy oil: R_f = 0.27 (4.5:5.5 EtOAc/Hexanes, visualized by UV); $[\alpha]_D^{20}$ –63.2 (*c* 1, $CHCl_3$); FT-IR (neat) ν_{max} 2945, 1716, 1611, 1506, 1448, 1206, 1108, 1032, 757, 738 cm^{-1}; ^1H NMR (500 MHz, DMSO-d_6, 100 °C) δ: 8.68 (br, s, 1H), 7.85-7.86 (d, 2H, *J* = 7.6 Hz), 7.71-7.72 (m, 2H), 7.40-7.43 (t, 2H, *J* = 7.4 Hz), 7.31-7.34 (m, 2H), 7.25-7.27 (d, 1H, *J* = 8.5 Hz), 6.52-6.53 (d, 1H, *J* = 2.4 Hz), 6.44-6.46 (dd, 1H, *J* = 2.4 Hz), 5.60-5.68 (m, 1H), 5.45-5.49 (m, 1H), 4.84-4.89 (m, 2H), 4.56-4.59 (d, 1H, *J* = 16 Hz), 4.47-4.50 (d, 1H, *J* = 15.9 Hz), 4.355-4.356 (d, 1H, *J* = 0.8 Hz), 4.34 (s, 1H), 4.23-4.26 (t, 1H, *J* = 13.9 Hz), 4.16 (br s, 1H), 3.77 (s, 3H), 3.7 (s, 3H), 3.51 (s, 3H), 1.88-2.07 (m, 3H),

1.71-1.81 (m, 1H), 1.64-1.66 (d, 3H, J = 7 Hz); ^{13}C NMR (125 MHz, DMSO-d_6, 100 °C) δ 170.5, 168.1, 159.6, 157.5, 153.3, 143.3, 143.3, 140.3, 137.3, 130.6, 129.3, 127.0, 126.4, 124.6, 119.4, 118.4, 117.2, 114.2, 104.6, 98.0, 78.6, 65.7, 58.2, 54.9, 54.8, 50.8, 46.4, 29.6, 27.9, 11.2; HRMS (ESI-TOF) m/z: [M+Na]+ Calcd for $C_{35}H_{38}N_2NaO_7$, 621.2571; Found 621.2573.

(*S*,*S*)-Methyl 2-*N*-(Boc)aminopent-4-enoyl-*N*-(2,4-dimethoxybenzyl)-2-aminohept-6-enoate (2.6d)

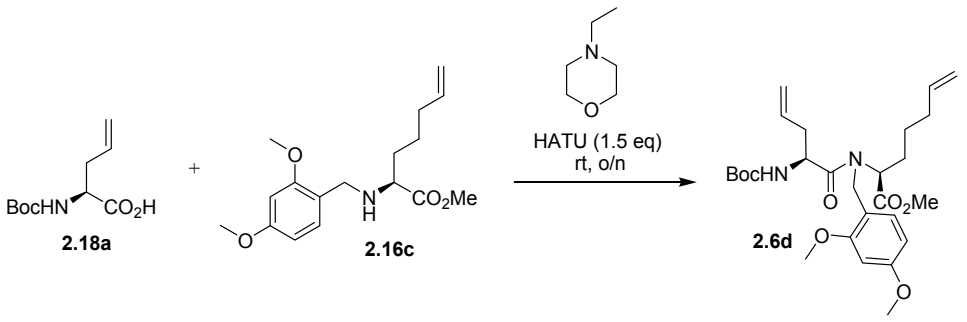

N-(Boc)Allylglycine **2.18a** (522 mg, 2.43 mmol) and *N*-(Dmb)amino ester **2.16c** (500 mg, 1.62 mmol) were dissolved in DCM (10 mL), treated with *N*-ethylmorpholine (373 mg, 3.24 mmol) and HATU (923 mg, 2.43 mmol), stirred for 24 h, and diluted with water. The aqueous layer was extracted with DCM (3 x 50 mL). The combined organic layers were washed with brine (50 mL), dried over anhydrous sodium sulfate, filtered, and concentrated under reduced pressure. The residue was purified by chromatography on silica gel (30-35% EtOAc in hexane) to give dipeptide **2.6d** (610 mg, 1.21 mmol, 74%) as colorless gummy oil: R_f = 0.67 (4:6 EtOAc:Hexanes, visualized by UV); $[\alpha]_D^{20}$ –33.1 (*c* 1, $CHCl_3$); FT-IR (neat) ν_{max} 2975, 2932, 1739, 1708, 1639, 1613, 1507, 1437, 1208, 1158, 1033, 753 cm^{-1}; ^{1}H NMR (500 MHz, DMSO-d_6, 100 ^{o}C) δ: 7.16 (br s, 1H), 6.56 (s, 1H), 6.47-6.49 (d, 1H, J = 7.7 Hz), 6.20 (brs, 1H), 5.63-5.77 (m, 2H), 5.01-5.09 (m, 2H), 4.88-4.95 (m, 2H), 4.61-4.62 (m, 2H), 4.43-4.48 (m, 1H), 4.23

(br s, 1H), 3.80 (s, 3H), 3.77 (s, 3H), 3.51 (s, 3H), 2.30-2.39 (m, 2H), 1.86-1.95 (m, 3H), 1.58-1.70 (m, 1H), 1.39 (s, 9H), 1.20-1.26 (m, 2H); ^{13}C NMR (125 MHz, DMSO-d$_6$, 100 ^{o}C) δ 171.6, 170.3, 160.1, 157.9, 154.2, 137.6, 133.5, 129.6, 116.8, 116.6, 114.0, 104.5, 98.2, 78.6, 77.9, 58.5, 54.9, 54.8, 50.8, 50.1, 36.1, 32.2, 28.1, 27.6, 24.6; HRMS (ESI-TOF) m/z: [M+Na]+ Calcd for $C_{27}H_{40}N_2NaO_7$, 527.2727; Found 527.2732.

(*S*,*S*)-Methyl 2-*N*-(Fmoc)aminopent-4-enoyl-*N*-(2,4-dimethoxybenzyl)-2-aminohept-6-enoate (2.7d)

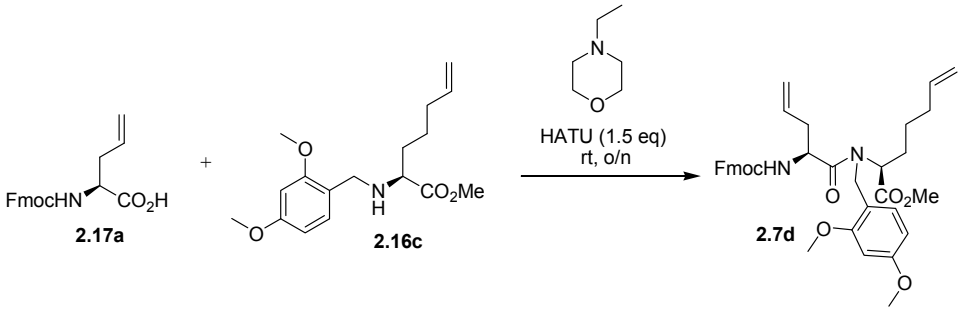

Employing the protocol described for the synthesis of dipeptide **2.6d**, (*S*)-2-*N*-(Fmoc)aminopent-4-enoic acid (**2.17a**, 1.147 g, 3.40 mmol) was coupled with *N*-(Dmb)aminohept-4-enoate (**2.16c**, 700 mg, 2.27 mmol). The residue was purified by chromatography on silica gel (30-40% EtOAc in hexane) to give dipeptide **2.7d** (1.080 g, 1.72 mmol, 76%) as colorless gummy oil: R_f = 0.57 (4:7 EtOAc:Hexanes, visualized by UV); $[\alpha]_D^{20}$ –39.7 (*c* 1, $CHCl_3$); FT-IR (neat) ν_{max} 2923, 1718, 1638, 1612, 1588, 1506, 1437, 1207, 1156, 758, 739538 cm^{-1}; ^{1}H NMR (500 MHz, DMSO-d$_6$, 100 °C) δ: 7.82-7.85 (d, 2H, *J* = 7.5 Hz), 7.67-7.68 (m, 2H), 7.38-7.42 (m, 2H), 7.29-7.32 (t, 2H, *J* = 7.4 Hz), 7.15 (br s, 1H), 6.96 (br s, 1H), 6.54-6.55 (m, 1H), 6.44-6.46 (m, 1H), 5.62-5.75 (m, 2H), 5.02-5.10 (m, 2H), 4.87-4.93 (m, 2H), 4.67 (br s, 2H), 4.41 (br s, 1H), 4.28-4.34 (m, 2H), 4.19-4.22 (t, 2H, *J* = 13.9), 3.77 (s, 3H), 3.74 (s, 3H), 3.49 (s, 3H), 2.36-2.41 (m,

2H), 1.81-1.93 (m, 3H), 1.56-1.67 (m, 1H), 1.16-1.27 (m, 2H); ^{13}C NMR (125 MHz, DMSO-d$_6$, 100 °C) δ 171.5, 170.3, 160.1, 158.0, 154.9, 143.4, 140.2, 137.7, 133.4, 129.5, 127.0, 126.4, 124.6, 119.4, 116.9, 114.0, 104.5, 98.2, 78.6, 66.2, 65.4, 57.8, 54.9, 54.8, 50.8, 50.5, 46.4, 45.1, 36.0, 32.1, 27.8, 24.6. HRMS (ESI-TOF) m/z: [M+Na]+ Calcd for $C_{37}H_{42}N_2O_7Na$, 649.2884; found 649.2873.

(*S*,*S*)-Methyl 2-*N*-(Boc)aminohept-6-enoyl-*N*-(2,4-dimethoxybenzyl)-2-aminopent-4-enoate (2.6g)

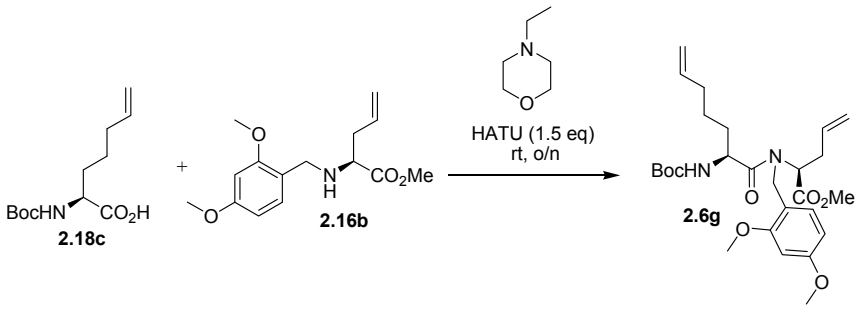

Employing the protocol described for the synthesis of dipeptide **2.6d**, (*S*)-2-*N*-(Boc)aminohept-6-enoic acid (**2.18c**, 521 mg, 2.14 mmol) was coupled with 2-*N*-(Dmb)aminopent-4-enoate **2.16b** (400 mg, 1.43 mmol). The residue was purified by chromatography on silica gel (30-40% EtOAc in hexane) to give dipeptide **2.16g** (561mg, 1.11 mmol, 78%) as colorless gummy oil: R_f = 0.72 (4:6 EtOAc:Hexanes, visualized by UV); $[\alpha]_D^{22}$ –52.5 (*c* 1, $CHCl_3$); FT-IR (neat) ν_{max} 2975, 2932, 1739, 1708, 1639, 1613, 1507, 1437, 1208, 1158, 1033, 753 cm^{-1}; ^{1}H NMR (500 MHz, DMSO-d$_6$, 100 °C) δ: 7.19 (br s, 1H), 6.56 (s, 1H), 6.47-6.49 (m, 1H), 6.16 (br s, 1H), 5.73-5.81 (m, 1H), 5.60-5.70 (m, 1H), 4.91-5.02 (m, 4H), 4.42-4.55 (m, 3H), 4.19-4.21 (m, 1H), 3.80 (s, 3H), 3.77 (s, 3H), 3.50 (s, 3H), 2.60-2.68 (m, 1H), 2.40-2.46 (m, 1H), 1.95-2.04 (m, 2H) 1.59-1.65 (m, 1H), 1.49-1.57 (m, 1H), 1.44-1.35 (m, 11H); ^{13}C NMR (125 MHz, DMSO-d$_6$, 100 °C) δ 172.1, 169.8, 160.1,154.3, 137.8, 134.5, 129.3, 116.3, 114.0, 104.4, 98.2, 78.6, 77.8, 57.8, 54.9,

54.8, 50.9, 50.3, 32.8, 32.7, 32.1, 31.5, 27.6, 23.8, 23.7. HRMS (ESI-TOF) m/z: [M+H]+ Calcd for $C_{27}H_{41}N_2O_7$, 505.2908; Found 505.2920.

(*S*)-Methyl 3-(Fmoc)amino-1-(2,4-dimethoxybenzyl)-2-oxo-5,6,7-tetrahydro-1H-azepine-7-carboxylate (2.21)

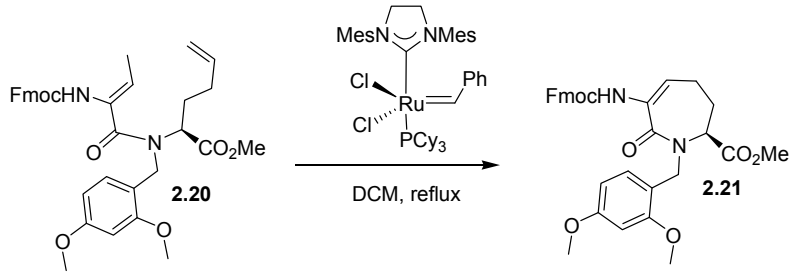

Dipeptide **2.20** (150 mg, 0.25 mmol) was dissolved in DCM (300 mL), treated with Grubbs 2nd generation catalyst (42 mg, 0.050 mmol), heated and stirred at reflux for 2 d. The volatiles were removed under reduced pressure and the residue was taken up in a minimum volume of DCM, applied onto a silica gel column and eluted with 35-40% EtOAc in hexanes. Evaporation of the collected fractions gave macrocycle **2.21** (95 mg, 68%) as white foam: R_f = 0.55 (4:6 EtOAc/Hexanes); $[\alpha]_D^{20}$ +31.8 (*c* 0.5, $CHCl_3$); FT-IR (neat) ν_{max} 2947, 1718, 1654, 1612, 1505, 1206, 1154, 1123, 1032, 758, 738 cm^{-1}; ^1H NMR (300 MHz, $CDCl_3$) δ: 7.75-7.77 (m, 2H); 7.59-7.63 (m, 2H), 7.37-7.43 (m, 2H), 7.27-7.34 (m, 3H), 7.05 (br s, 1H), 6.66 (br s, 1H), 6.45-6.49 (m, 2H), 5.16-5.20 (d, 1H, *J* = 14), 4.39-4.41 (m, 2H), 4.18-4.24 (m, 3H) 3.81 (s, 3H), 3.80 (s, 3H), 3.58 (s, 3H), 2.55-2.60 (m, 1H), 2.13-2.18 (m, 2H), 1.84-1.91 (m, 1H), ^{13}C NMR (75 MHz, $CDCl_3$) δ 171.8, 167.9, 161.0, 158.8, 153.6, 143.9, 143.9, 141.4, 141.4, 132.2, 131.5, 127.8, 127.8, 127.2, 125.2, 120.1, 120.0, 117.2, 116.2, 104.3, 98.5, 66.8, 59.5, 55.5, 55.3, 52.7, 47.2, 47.1, 32.8, 21.7; HRMS (ESI-TOF) m/z: [M+Na]+ Calcd for $C_{32}H_{32}N_2NaO_7$, 579.2107; Found 579.2101.

(3*S*,8*S*,*Z*)-Methyl 3-(Fmoc)amino-1-(2,4-dimethoxybenzyl)-2-oxo-1,2,3,6,7,8-hexahydroazocine-8-carboxylate (2.10a)

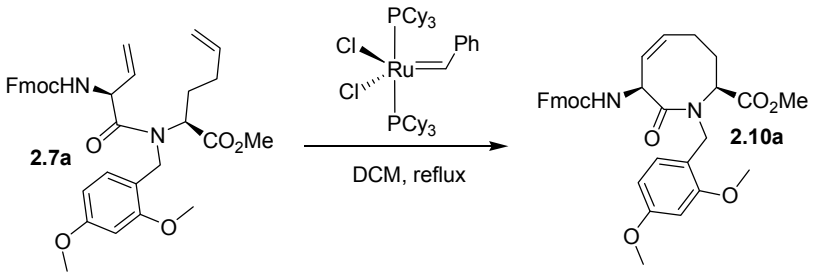

Dipeptide **2.7a** (1 g, 1.67 mmol) was dissolved in DCM (2 L), treated with Grubbs 1st generation catalyst (412 mg, 0.50 mmol), heated and stirred at reflux for 2 d. After two days, TLC showed remaining **2.7a**, and more catalyst (274 mg, 0.33 mmol) was added to the reaction mixture, which was heated at reflux and stirred 2 days. The volatiles were removed under reduced pressure. The residue was taken up in a minimum volume of DCM, applied onto a silica gel column and eluted with 35-40% EtOAc in hexanes. Evaporation of the collected fractions afforded macrocycle **2.10a** (605 mg, 1.06 mmol, 63%) as colourless gummy oil: R_f = 0.45 (4:6 EtOAc:Hexanes); $[\alpha]_D^{24}$ +8.7 (*c* 1, $CHCl_3$); FT-IR (neat) ν_{max} 2947, 1718, 1654, 1612, 1505, 1447, 1206, 1154, 1123, 738 cm^{-1}; ^1H NMR (300 MHz, $CDCl_3$) δ: 7.75-7.77 (d, 2H, *J* = 7.5 Hz), 7.61-7.63 (d, 2H, *J* = 7.4 Hz), 7.37-7.42 (t, 2H, *J* = 7.5 Hz), 7.28-7.33 (m, 2H), 7.16-7.19 (d, 1H, *J* = 8.3 Hz), 6.40-6.45 (m, 2H), 6.17-6.19 (d, 1H, *J* = 7 Hz), 5.67-5.79 (m, 2H), 5.28-5.31 (d, 1H, *J* = 7 Hz), 4.71-4.81 (m, 2H), 4.33-4.43 (m, 2H), 4.12-4.26 (m, 2H), 3.79 (s, 3H), 3.77 (s, 3H), 3.45 (s, 3H), 1.97-2.44 (m, 2H), 1.82-1.91 (m, 2H); ^{13}C NMR (75 MHz, $CDCl_3$) δ 171.4, 169.9, 160.0, 157.7, 155.9, 144.1, 143.9, 141.4, 131.3, 129.2, 128.1, 127.8, 127.2, 125.7, 120.0, 116.8, 104.1, 98.2, 67.3, 57.6, 55.5, 55.4, 53.7, 52.2, 47.2, 41.0, 28.3, 21.4. HRMS (ESI-TOF) m/z: [M+Na]+ Calcd for $C_{33}H_{34}N_2O_7Na$, 593.2258; found 593.2255.

(3*S*,9*S*,*Z*)-Methyl-3-(Fmoc)amino)-1-(2,4-dimethoxybenzyl)-2-oxo-1,2,3,6,7,8,9-heptahydro-1H-azonine-9-carboxylate (2.10b)

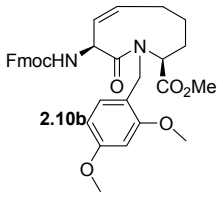

Dipeptide **2.7b** (200 mg, 0.32 mmol) was dissolved in DCM (400 mL), treated with Grubbs 1st generation catalyst (79 mg, 0.096 mmol), heated and stirred at reflux for 2 d, when TLC indicated remaining **2.7b** and another portion of catalyst (53 mg, 0.065 mmol) was added to the mixture which was heated at reflux and stirred for 1 day. The volatiles were removed under reduced pressure. The residue was taken up in a minimum volume of DCM, applied onto a silica gel column and eluted with 35-40% EtOAc in hexanes. Evaporation of the collected fractions afforded macrocycle **2.10b** (131 mg, 0.22 mmol, 69%) as colourless gummy oil: R_f = 0.37 (4:6 EtOAc:Hexanes); $[\alpha]_D^{20}$ +7.1 (*c* 0.22, $CHCl_3$); FT-IR (neat) ν_{max} 2946, 1718, 1637, 1612, 1587, 1505, 1447, 1288, 1206, 1034, 739 cm^{-1}; ^{1}HNMR (400 MHz, $CDCl_3$) δ: 7.75-7.77 (d, 2H, *J* = 7.4 Hz), 7.60-7.63 (m, 2H), 7.38-7.42 (t, 2H, *J* = 7.4 Hz), 7.30-7.33 (t, 2H, *J* = 7.4), 7.08-7.10 (d, 1H, *J* = 8.3 Hz), 6.35-6.42 (m, 3H), 5.69-5.73 (t, 1H, *J* = 7.8 Hz), 5.56-5.63 (m, 1H), 5.34-5.39 (t, 1H, *J* = 10 Hz), 4.87-4.91 (d, 1H, *J* = 15.1 Hz), 4.69-4.71 (d, 1H, *J* = 7.6 Hz), 4.36-4.38 (m, 2H), 4.22-4.31 (m, 2H), 3.76 (s, 3H), 3.78 (s, 3H), 3.59 (s, 3H), 2.62-2.73 (m, 1H), 2.23-2.2 6 (m, 1H), 2.06-2.11 (m, 1H), 1.63-1.69 (m, 1H), 1.47-1.57 (m, 1H), 1.31-1.39 (m, 1H); ^{13}C NMR (100 MHz, $CDCl_3$) δ 170.3, 170.0, 160.5, 158.3, 155.8, 144.0, 144.0, 141.4, 130.8, 130.7, 129.1, 127.7, 127.1, 125.3, 125.3, 120.1, 120.0, 117.5, 104.1, 98.1, 67.1, 55.4, 55.3, 55.2, 52.4, 50.4,

47.2, 41.6, 28.3, 24.5, 23.7; HRMS (ESI-TOF) m/z: [M+Na]+ Calcd for $C_{34}H_{36}N_2O_7Na$, 607.2414; found 607.2425.

(3*S*,10*S*,*Z*)-Methyl 3-*N*-(Boc)amino-1-(2,4-dimethoxybenzyl)-2-oxo-1,2,3,4,7,8,9,10-octahydroazecine-10-carboxylate (2.9d)

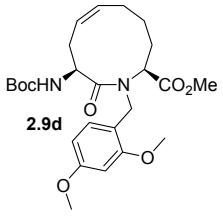

Dipeptide (**2.6d**, 600 mg, 1.18 mmol) was dissolved in DCM (1300 mL), treated with Grubbs 1st generation catalyst (189 mg, 0.23 mmol), heated and stirred at reflux for 2 d. The volatiles were removed under reduced pressure and the residue was taken up in a minimum volume of DCM, applied onto a silica gel column and eluted with 30-35% EtOAc in hexanes to afford macrocycle **2.9d** (490 mg, 1.02 mmol, 86%) as white solid: R_f = 0.55 (4:6 EtOAc:Hexanes); mp 81-83 °C; $[\alpha]_D^{20}$ +15.1 (*c* 1, $CHCl_3$); FT-IR (neat) ν_{max} 2944, 1706, 1644, 1612, 1490, 1433, 1363, 1209, 1157, 1130, 1030, 833 cm^{-1}; ^1H NMR (500 MHz, $CDCl_3$) δ: 7.04-7.06 (d, 1H, *J* = 8.2 Hz), 6.42-6.43 (d, 1H, *J* = 2.2 Hz), 6.34-6.39 (m, 1H), 5.85-5.86 (d, 1H, *J* = 7.1 Hz), 5.53-5.58 (m, 1H), 5.44-5.46 (m, 1H), 5.23 (br s, 1H), 4.97-4.99 (d, 1H, *J* = 14.2), 3.93-3.98 (m, 1H), 3.78 (s, 3H), 3.75 (s, 3H), 3.37-3.39 (d, 1H, *J* = 10.5 Hz), 3.30 (s, 3H), 2.79-2.81 (m, 1H), 2.44-2.45 (m, 1H), 2.25-2.37 (m, 2H), 2.02-2.05 (m, 1H), 1.93-1.96 (m, 1H), 1.65-1.66 (m, 1H), 1.46-1.41(m, 10H); ^{13}C NMR (125 MHz, $CDCl_3$) δ 170.2, 169.9, 160.5, 159.0, 154.2, 132.1, 130.5, 123.1, 115.2, 102.3, 97.4, 78.3, 76.3, 61.2, 54.5, 54.1, 50.7, 50.4, 49.8, 28.5, 27.5, 25.0, 22.3; HRMS (ESI-TOF) m/z: [M+Na]+ Calcd for $C_{25}H_{36}N_2O_7Na$, 499.2414; Found 499.2409.

(3*S*,10*S*,*Z*)-Methyl-3-(Fmoc)amino)-1-(2,4-dimethoxybenzyl)-2-oxo-1,2,3,4,7,8,9,10-octahydroazecine-10-carboxylate (2.10d)

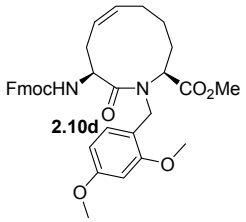

Dipeptide (**2.7d**, 1 g, 1.60 mmol) was dissolved in DCM (2000 mL), treated with Grubbs 1st generation catalyst (263.34 mg, 0.32 mmol), heated and stirred at reflux for 2 d. The volatiles were removed under reduced pressure and the residue was taken up in a minimum volume of DCM, applied onto a silica gel column and eluted with 35-40% EtOAc in hexanes to afford macrocycle **2.10d** (872 mg, 1.45 mmol, 91%) as white solid: R_f = 0.40 (4:6 EtOAc:Hexanes); mp 89-92 °C; $[\alpha]_D^{20}$ –5.8 (*c* 1, $CHCl_3$); FT-IR (neat) ν_{max} 3005, 1717, 1640, 1611, 1588, 1505, 1207, 1156, 1034, 758, 739, 542 cm^{-1}; ^1H NMR (400 MHz, $CDCl_3$) δ: 7.76-7.78 (d, 2H, *J* = 7.5 Hz), 7.62-7.65 (m, 2H), 7.38-7.42 (t, 2H, *J* = 7.4), 7.30-7.33 (m, 2H), 7.06-7.08 (d, 1H, *J* = 8.2 Hz), 6.38-6.43 (m, 2H), 6.17-6.19 (d, 1H, *J* = 6.5 Hz), 5.49-5.60 (m, 2H), 5.26-5.28 (m, 1H), 4.97-5.01 (d, 1H, *J* = 14.4), 4.34-4.47 (m, 2H), 4.22-4.26 (m, 1H), 3.99-4.02 (m, 1H), 3.79 (s, 3H), 3.73 (s, 3H), 3.39-3.44 (m, 1H), 3.33 (s, 3H), 2.80-2.90 (m, 1H), 2.40-2.52 (m, 2H), 2.27-2.36 (m, 1H), 1.84-2.09 (m, 3H), 1.67-1.74 (m, 1H); ^{13}C NMR (100 MHz, $CDCl_3$) δ 171.1, 170.5, 161.5, 159.9, 155.5, 144.1, 144.0, 141.4, 131.5, 127.8, 127.2, 127.1, 125.4, 125.3, 123.8, 120.1, 116.0, 103.5, 98.4, 66.8, 62.3, 55.5, 55.4, 55.4, 55.3, 52.0, 51.7, 47.4, 47.3, 26.0; HRMS (ESI-TOF) m/z: [M+Na]+ Calcd for $C_{35}H_{38}N_2O_7Na$, 621.2571; Found 621.2588.

(3*S*,10*S*,*Z*)- Methyl 3-*N*-(Boc)amino-1-(2,4-dimethoxybenzyl)-2-oxo-1,2,3,4,5,6,9,10-octahydroazecine-10-carboxylate (2.9g)

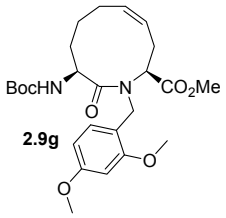

Dipeptide **2.6g** (550 mg, 1.09 mmol) was dissolved in DCM (1000 mL), treated with Grubbs 1st generation catalyst (173 mg, 0.21 mmol), heated and stirred at reflux for 2 d. The volatiles were removed under reduced pressure and the residue was taken up in a minimum volume of DCM, applied onto a silica gel column and eluted with 30-35% EtOAc in hexanes to afford macrocycle **2.9g** (460 mg, 0.96 mmol, 79 %) as white solid: R_f = 0.62 (4:6 EtOAc:Hexanes); mp 79-82 °C; $[\alpha]_D^{22}$ –40.5 (*c* 1, $CHCl_3$); FT-IR (neat) ν_{max} 2943, 1735, 1706, 1637, 1612, 1589, 1506, 1438, 1363, 1208, 1156, 1034, 750, 533 cm^{-1}; ^1H NMR (400 MHz, $CDCl_3$) δ: 7.03-7.05 (d, 1H, *J* = 8.16 Hz), 6.37-6.42 (m, 2H), 5.87-5.88 (d, 1H, *J* = 6.76 Hz), 5.48-5.60 (m, 2H), 5.02-5.05 (t, 1H, *J* = 6.36 Hz), 4.81-4.85 (d, 1H, *J* = 14.2 Hz), 3.78 (s, 3H), 3.75 (s, 3H), 3.44-3.49 (m, 1H), 3.42 (m, 3H), 3.26-3.35 (m, 1H), 2.46-2.55 (m, 1H), 2.25-2.31 (m, 1H), 1.98-2.04 (m, 1H), 1.84-1.93 (m, 2H), 1.74-1.78 (m, 1H), 1.39-1.53 (m, 11H); ^{13}C NMR (100 MHz, $CDCl_3$) δ 172.5, 170.8, 161.3, 159.9, 155.2, 135.3, 131.4, 125.0, 115.9, 103.4, 98.5, 79.2, 57.9, 55.4, 55.2, 51.8, 50.7, 50.1, 28.5, 27.7, 25.0, 24.1, 21.5; HRMS (ESI-TOF) m/z: [M+Na]+ Calcd for $C_{25}H_{36}N_2O_7Na$, 499.2414; Found 499.2409.

(3*S*,10*S*,*Z*)-Methyl-3-*N*-(Fmoc)amino-1-(2,4-dimethoxybenzyl)-2-oxo-1,2,3,4,5,6,,9,10-octahydroazecine-10-carboxylate (2.10g)

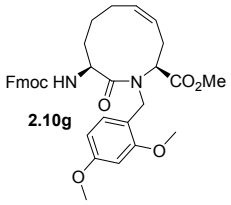

A stirred solution of Boc-protected dipeptide lactam **2.9g** (200 mg, 0.42 mmol) in 10 mL DCM was treated with TFA (4 mL) at 0 °C, stirred for 2h, and the volatiles were removed under reduced pressure to provide the trifluoroacetate salt, which was dissolved in 15 mL of a 1:1 water/acetone solution, and treated with Fmoc-OSu (138 mg, 0.42 mmol) and Na_2CO_3 (90 mg, 0.84 mmol). After stirring for 18h at room temperature, the mixture was diluted with water and acidified to pH 3-4 with 10% $KHSO_4$ solution. This aqueous solution was extracted with ethyl acetate (3 x 20 mL). The combined organic layers were washed with brine, dried over $MgSO_4$, filtered, and concentrated to a residue that was purified by chromatography on silica gel using 25-30% EtOAc in hexane as eluent. Evaporation of the collected fractions gave Fmoc-protected dipeptide lactam **2.10g** (151 mg, 0.25 mmol, 60%) as a colorless oil: R_f = 0.50 (4:6 EtOAc:Hexanes, visualized by UV); $[\alpha]_D^{20}$ –45.2 (*c* 0.5, $CHCl_3$); FT-IR (neat) ν_{max} 2944, 1715, 1636, 1612, 1588, 1506, 1440, 1207, 1156, 1130, 1035, 758, 739, 535 cm^{-1}; ^1H NMR (400 MHz, $CDCl_3$) δ: 7.76-7.78 (d, 2H, *J* = 7.5 Hz), 7.63-7.66 (t, 2H, *J* = 6.0 Hz), 7.39-7.42 (t, 2H, *J* = 7.4 Hz), 7.30-7.34 (m, 2H), 7.05-7.07 (d, 1H, *J* = 8.1 Hz), 6.39-6.43 (m, 2H), 6.21-6.23 (d, 1H, *J* = 6.7), 5.52-5.64 (m, 2H), 5.08-5.12 (m, 1H), 4.83-4.87 (d, 1H, *J* = 14.3 Hz), 4.41-4.46 (m, 1H), 4.33-4.39 (m, 1H), 4.22-4.26 (t, 1H, *J* = 7.2 Hz), 3.79 (s, 3H), 3.75 (s, 3H), 3.48-3.54 (m, 1H), 3.45 (s, 3H), 3.30-3.40 (m, 1H), 2.50-2.62 (m, 1H), 2.30-2.35 (m, 1H), 2.05-211 (m, 1H), 1.80-1.98 (m, 3H), 1.75-1.49 (m, 2H); ^{13}C NMR (100 MHz, $CDCl_3$) δ 172.1, 170.7, 161.4, 159.8, 155.5, 144.1, 144.1, 141.5, 135.3, 131.4, 127.8, 127.1, 125.4, 125.3, 125.1, 120.1, 120.0, 115.7,

103.5, 98.5, 66.9, 58.0, 55.4, 55.4, 51.9, 50.7, 50.6, 47.4, 27.5, 25.0, 24.2, 21.5; HRMS (ESI-TOF) m/z: [M+Na]+ Calcd for $C_{35}H_{38}N_2O_7Na$, 621.2571; Found 621.2576

(3*S*,8*S*,*Z*)- Methyl-3-*N*-(Fmoc)amino-2-oxo-1,2,3,6,7,8-hexahydroazocine-8-carboxylate (2.11a)

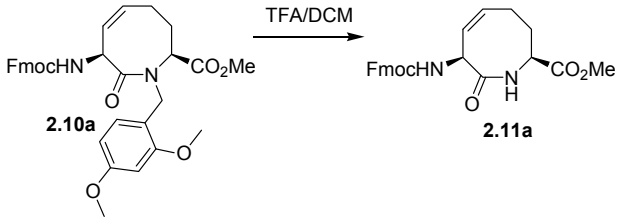

Lactam **2.10a** (155 mg, 0.27 mmol) was treated with TFA (2 mL) in DCM (5 mL) overnight. The volatiles were removed under vacuum and the residue was purified by chromatography on silica gel (40-50% EtOAc in hexane) to give macrocycle **2.11a** (97mg, 0.23 mmol, 85%) as white solid: R_f = 0.2 (1:1 EtOAc:Hexanes, visualized by UV); mp 183-185 °C, $[\alpha]_D^{24}$ +29.5 (*c* 1, $CHCl_3$); FT-IR (neat) ν_{max} 3377, 2955, 1728, 1696, 1663, 1528, 1432, 1255, 1050, 984, 721, 549 cm^{-1}; ^1H NMR (400 MHz, $CDCl_3$) δ: 7.74-7.76 (d, 2H, *J* = 7.5 Hz), 7.59-7.61 (m, 2H), 7.37-7.41 (t, 2H, *J* = 7.4 Hz), 7.29-7.32 (m, 2H), 6.17-6.19 (d, 1H, *J* = 7.7 Hz), 6.06-6.08 (d, 1H, *J* = 7.3 Hz), 5.77-5.84 (m, 1H), 5.63-5.68 (m, 1H), 5.15-5.19 (t, 1H, *J* = 6.5 Hz), 4.44-4.49 (m, 1H), 4.33-4.41 (m, 2H), 4.21-4.24 (t, 1H, *J* = 7.23 Hz), 3.79 (s, 3H), 2.46-2.51 (m, 2H), 2.16-2.21 (m, 1H), 1.56-1.65 (m, 1H); ^{13}C NMR (100 MHz, $CDCl_3$) δ 172.0, 171.8, 155.9, 144.0, 143.9, 141.4, 132.7, 129.2, 127.8, 127.2, 125.3, 125.2, 120.0, 67.3, 55.9, 53.2, 52.2, 47.2, 33.0, 25.5; HRMS (ESI-TOF) m/z: [M+Na]+ Calcd for $C_{24}H_{24}N_2O_5Na$, 443.1577; found 443.1581.

(3*S*,9*S*,*Z*)- Methyl 3-*N*-(Fmoc)amino-2-oxo-1,2,3,6,7,8,9-heptahydro-1H-azonine-9-carboxylate (2.11b)

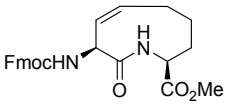

2.11b

Lactam **2.10b** (53 mg, 0.09 mmol) was treated as described for the synthesis of **2.11a** above with TFA (1 mL) in DCM overnight. Chromatography (30-40% EtOAc in hexane) gave **2.11b** (34 mg, 0.08 mmol, 87%) as white solid: R_f = 0.2 (1:1 EtOAc:Hexanes, visualized by UV); mp 202-204 °C; $[\alpha]_D^{20}$ +21.1 (*c* 1, $CHCl_3$); FT-IR (neat) ν_{max} 3325, 2922, 1736, 1660, 1521, 1434, 1318, 1240, 1204, 1032, 985, 882, 758 cm^{-1}; ^1H NMR (500 MHz, $CDCl_3$) δ: 7.75-7.76 (d, 2H, *J* = 7.5 Hz), 7.58-7.60 (m, 2H), 7.37-7.41 (t, 2H, *J* = 7.4 Hz), 7.29-7.32 (t, 2H, *J* = 7.4 Hz), 6.37-6.39 (d, 1H, *J* = 9.0 Hz), 6.13-6.14 (d, 1H, *J* = 5.9 Hz), 5.68-5.75 (m, 1H), 5.39-5.43 (m, 2H), 4.31-4.39 (m, 3H), 4.20-4.23 (t, 1H, *J* = 7.2 Hz), 3.80 (s, 3H), 2.80-2.91 (m, 1H), 2.29-2.40 (m, 1H), 1.93-2.01 (m, 2H), 1.76-1.82 (m, 1H), 162-1.71 (m, 1H); ^{13}C NMR (100 MHz, $CDCl_3$) δ 172.4, 169.8, 155.6, 144.0, 143.9, 141.4, 131.5, 128.1, 127.8, 127.2, 125.2, 120.0, 67.2, 53.1, 50.2, 50.2, 47.2, 34.1, 29.8, 25.6, 23.4; HRMS (ESI-TOF) m/z: [M+Na]+ Calcd for $C_{25}H_{26}N_2O_5Na$, 457.1733; Found 457.1745.

(3*S*,10*S*,*Z*)-Methyl-3-*N*-(Fmoc)amino-2-oxo-1,2,3,4,7,8,9,10-octahydroazecine-10-carboxylate (2.11d)

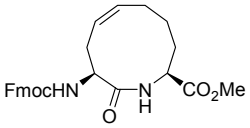

2.11d

Lactam **2.10d** (100 mg, 0.17 mmol) was treated with TFA (2 mL) in DCM (5 mL) for three days. The volatiles were removed under vacuum and the residue was purified by chromatography on silica gel (40-50% EtOAc in hexane) gave lactam **2.11d** (52 mg, 0.11 mmol, 69%) as white

solid: R_f = 0.2 (1:1 EtOAc:Hexanes, visualized by UV); $[\alpha]_D^{20}$ +48.1 (*c* 0.16, $CHCl_3$); FT-IR (neat) ν_{max} 3327, 2920, 1723, 1649, 1505, 1437, 1349, 1221, 1022, 756 cm^{-1}; ^1H NMR (500 MHz, 100 °C DMSO-d_6) δ: 7.86-7.87 (d, 2H, *J* = 7.5 Hz), 7.81-7.82 (m, 1H), 7.86-7.89 (d, 2H, *J* = 7.5 Hz), 7.40-7.43 (t, 2H, *J* = 7.4), 7.32-7.35 (m, 2H), 6.86 (br s, 1H), 5.35-5.46 (m, 2H), 4.34-4.40 (m, 2H), 4.23-4.26 (m, 1H), 4.08-4.18 (m, 2H) 3.65 (s, 3H), 2.36-2.39 (m, 1H), 2.27-2.28 (m, 1H), 1.97-2.15 (m, 2H), 1.66-1.91 (m, 3H), 1.55-1.57 (m, 1H); ^{13}C NMR (125 MHz, 100 °C DMSO-d_6) δ 172.0, 169.8, 144.4, 141.3, 134.3, 128.0, 127.5, 125.5, 123.8, 121.7, 120.6, 120.4, 120.3, 79.6, 66.4, 55.4, 54.3, 52.1, 47.5, 30.0, 26.1, 25.9, 25.6; HRMS (ESI-TOF) m/z: [M+Na]+ Calcd for $C_{26}H_{28}N_2O_5Na$, 471.1890; Found 471.1898.

(3*S*,10*S*,*Z*)-Methyl-3-*N*-(Fmoc)amino-2-oxo-1,2,3,4,5,6,9,10-octahydroazecine-10-carboxylate (2.11g)

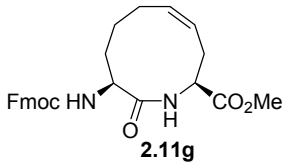

2.11g

Lactam **2.10g** (40 mg, 0.07 mmol) was treated as described for the synthesis of **2.11a** above with TFA (0.5 mL) in DCM overnight. Chromatography (40-50% EtOAc in hexane) gave lactam **2.11g** (24 mg, 0.05 mmol, 80%) as a white solid: R_f = 0.2 (1:1 EtOAc:Hexanes, visualized by UV); mp 210-215 °C; $[\alpha]_D^{22}$ +2.4 (*c* 0.16, $CHCl_3$); FT-IR (neat) ν_{max} 3296, 2926, 1726, 1685, 1643, 1527, 1438, 1247, 1105, 1031, 755, 736 cm^{-1}; ^1H NMR (500 MHz, 100 °C, DMSO-d_6) δ: 7.92 (br, s, 1H), 7.84-7.86 (d, 2H, *J* = 7.6 Hz), 7.67-7.69 (m, 2H), 7.39-7.42 (t, 2H, *J* = 7.4 Hz), 7.30-7.33 (t, 2H, *J* = 7. 5), 6.74 (br s, 1H), 5.48-5.53 (m, 1H), 5.34-5.41 (m, 1H), 4.32-4.33 (m, 2H), 4.21-4.24 (t, 1H, *J* = 6.9), 4.06-4.09 (m, 1H), 3.90 (br s, 1H), 3.65 (s, 3H), 2.75-2.82 (m,

1H), 2.42-2.43 (m, 1H), 2.12-2.20 (m, 1H), 1.83-1.89 (m, 2H), 1.74-1.78 (m, 2H), 1.44-1.48 (m, 1H); ^{13}C NMR (125 MHz, 100 °C, DMSO-d_6) δ 171.3, 170.4, 154.5, 143.4, 140.3, 134.4, 127.0, 126.5, 124.6, 124.2, 119.4, 65.4, 53.2, 51.7, 51.2, 46.5, 35.8, 29.4, 24.7, 23.7, 21.7, 16.5; HRMS (ESI-TOF) m/z: [M+Na]+ Calcd for $C_{26}H_{28}N_2O_5Na$, 471.1890; Found 471.1903.

(3*R*,4*R*,5*S*,8*S*)-Methyl 3-*N*-(Fmoc)amino-4-iodo-2-oxohexahydro-5H-pyrrolizine-8-carboxylate (2.3)

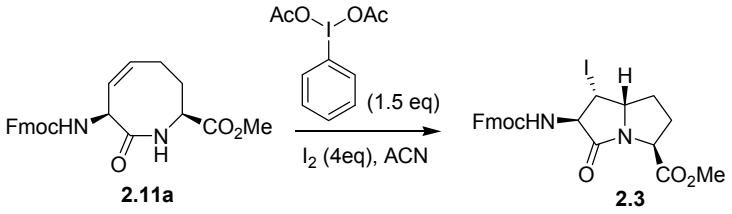

In the dark, a solution of macrocycle **2.11a** (100 mg, 0.24 mmol) in acetonitrile (4 mL) was treated with iodine (243 mg, 0.96 mmol) followed by diacetoxy iodobenzene (116 mg, 0.36 mmol). The resulting mixture was heated to 80°C for 30 min, cooled to room temperature, and the volatiles were evaporated under reduced pressure. The residue was chromatographed on silica gel (40-50% EtOAc in hexane) to give pyrrolizidinone **2.3** (81 mg, 0.15 mmol, 62%) as a light-sensitive white solid: R_f = 0.45 (3:2 EtOAc:Hexanes, visualized by UV); mp 94-96 °C; $[\alpha]_D^{20}$ –70.8 (*c* 1, $CHCl_3$); FT-IR (neat) ν_{max} 3374,1754, 1739, 1692, 1522, 1444, 1380, 1254, 1220, 1166, 1076, 1049, 818, 755, 741, 532 cm^{-1}; ^{1}H NMR (700 MHz, C_6D_6) δ: 7.57-7.58 (d, 2H, *J* = 7.7 Hz), 7.43-7.44 (m, 2H), 7.17-7.24 (m, 4H), 4.92-4.93 (d, 1H, *J* = 7.6 Hz), 4.49-4.51 (t, 1H, *J* = 7.4), 4.40-4.43 (t, 1H, *J* = 7.6 Hz), 4.34-4.35 (d, 2H, *J* = 6.5 Hz), 3.96-3.98 (t, 1H, *J* = 6.5 Hz), 3.90-3.92 (t, 1H, *J* = 6.6 Hz), 3.26-3.29 (m, 1H), 3.22 (s, 3H), 1.70-1.78 (m, 1H), 1.43-1.48 (m, 1H), 1.32-1.34 (m, 1H), 0.80-0.83 (m, 1H); ^{13}C NMR (175 MHz, C_6D_6) δ 172.0, 171.0, 156.2, 144.5, 144.4, 141.8, 127.4, 127.4, 125.5, 120.2, 67.0, 63.9, 62.6, 57.6, 51.8, 47.5, 33.5,

30.3, 30.0, 22.5; HRMS (ESI-TOF) m/z: [M+Na]+ Calcd for $C_{24}H_{23}IN_2O_5Na$, 569.0543; Found 569.0559.

Imidate-2.5

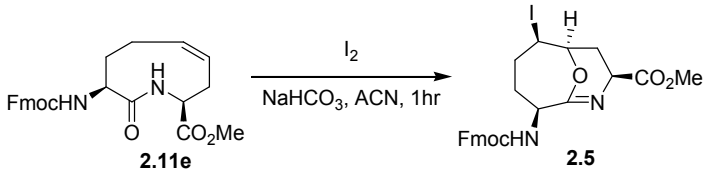

In the dark, a solution of macrocycle (**2.11e,** 50 mg, 0.11 mmol) in acetonitrile (4 mL) was treated with $NaHCO_3$ (27 mg, 0.33 mmol) followed by iodine (83.7 mg, 0.33 mmol) in three portions, stirred for 1h at rt, treated with 1M $Na_2S_2O_3$ until the purple solution became clear. The mixture was extracted quickly with ethyl acetate (3 x 10 mL). The organic extractions were washed with brine, dried and concentrated under reduced pressure to a residue that was chromatographed on silica gel (20-30% EtOAc in hexane). Evaporation of the collected fractions gave imidate **2.5** (33 mg, 0.06 mmol, 51%) as white solid: R_f = 0.45 (4.5:6.5 EtOAc:Hexanes, visualized by UV); mp 152-154 ^oC; $[\alpha]_D^{20}$ +48.4 (*c* 1, $CHCl_3$); FT-IR (neat) ν_{max} 3410, 2923, 1738, 1715, 1657, 1490, 1449, 1352, 1277, 1208, 1162, 1020, 958, 903, 739, 541 cm^{-1}; ^1H NMR (700 MHz, $CDCl_3$) δ: 7.76-7.77 (d, 2H, *J* = 7.4 Hz), 7.60-7.63 (m, 2H), 7.39-7.41 (m, 2H), 7.31-7.33 (m, 2H), 6.17-6.18 (d, 1H, *J* = 5.9 Hz), 4.89-4.93 (m, 1H), 4.67-4.69 (m, 1H), 4.38-4.39 (d, 2H, *J* = 7 Hz), 4.26-4.29 (m, 1H), 4.21-4.23 (t, 1H, *J* = 6.9), 3.95-3.97 (m, 1H), 3.85 (s, 3H), 2.69-2.73 (m, 1H), 2.12-2.17 (m, 2H), 2.03-2.10 (m, 1H), 1.94-1.98 (m, 2H); ^{13}C NMR (175 MHz, $CDCl_3$) δ 172.0, 164.8, 155.7, 144.1, 143.9, 141.4, 141.4, 127.8, 127.2, 125.3, 125.2, 120.1, 120.1, 67.1, 55.3, 52.7, 51.3, 47.3, 36.7, 33.2, 30.3, 30.1, 14.1; HRMS (ESI-TOF) m/z: [M+Na]+ Calcd for $C_{25}H_{25}IN_2O_5Na$, 583.0700; Found 583.0705.

(3*S*,5*R*,6*R*,10*S*)-Methyl 3-*N*-(Fmoc)-5-iodo-2-oxo-octahydro-6H-quinolizine-10-carboxylate (2.4)

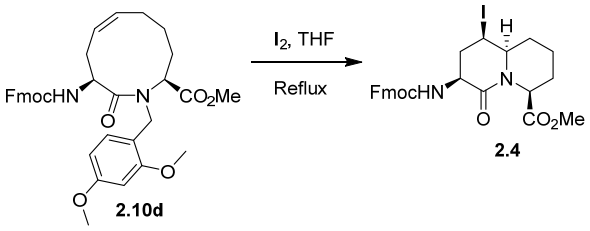

In the dark, a solution of macrocycle **2.10d** (300 mg, 0.50 mmol) in THF (10 mL) was treated with iodine (508 mg, 2 mmol), heated to 80 °C for 8 h, cooled to room temperature, and the volatiles were removed under reduced pressure to a residue that was chromatographed on silica gel (40-50% EtOAc in hexane) to give quinolizidinone **2.4** (151 mg, 0.26 mmol, 53%) as a white solid: R_f = 0.45 (3:2 EtOAc:Hexanes); mp 98-101 °C; $[\alpha]_D^{20}$ +16.2 (*c* 1, $CHCl_3$); FT-IR (neat) ν_{max} 2947, 1717, 1655, 1508, 1446, 1324, 1226, 738, 538 cm^{-1}; ^1H NMR (700 MHz, $CDCl_3$) δ: 7.75-7.76 (d, 2H, *J* = 7.1 Hz), 7.57-7.58 (d, 2H, *J* = 7.3 Hz), 7.38-7.40 (t, 2H, *J* = 7.4 Hz), 7.30-7.32 (t, 2H, *J* = 7.3 Hz), 5.75 (br s, 1H), 4.69-4.70 (m, 1H), 4.31-4.42 (m, 2H), 4.17-4.20 (m, 2H), 3.73 (s, 3H), 3.65-3.68 (m, 1H), 3.44-3.45 (m, 1H), 3.06-3.08 (m, 1H), 2.45-2.51 (m, 1H) , 2.24-2.25 (m, 1H), 2.06-2.09 (m, 1H), 1.94-1.98 (m, 1H), 1.83-1.89 (m, 1H) , 1.59-1.60 (m, 2H) ^{13}C NMR (175 MHz, $CDCl_3$) δ 169.6, 168.6, 156.2, 143.9, 143.8, 141.4, 141.4, 127.8, 127.2, 125.3, 120.1, 67.2, 62.9, 60.2, 52.6, 52.4,. 47.2, 37.7, 30.1, 24.8, 22.9, 20.3; HRMS (ESI-TOF) m/z: [M+Na]+ Calcd for $C_{26}H_{27}IN_2O_5Na$, 597.0856; Found 597.0861.

2.10. ACKNOWLEDGMENT

This work was supported by the Natural Sciences and Engineering Research Council of Canada (NSERC), the Canadian Institutes of Health Research (CIHR, grant #TGC-114046 and CIP-

79848), the Global Alliance to Prevent Prematurity and Stillbirth, an initiative of Seattle Children's, the Bill & Melinda Gates Foundation, the March of Dimes, and the Canadian Foundation for Innovation. The authors thank Dr. A. Fürtös, K. Venne, and M-C. Tang from the Regional Laboratory for Mass Spectrometry, Sylvie Bilodeau, Antoine Hamel and Cedric Malveau from the Regional Laboratory for NMR Spectroscopy, Francine Belanger-Gariepy from the Regional Laboratory for X-ray Analysis, at the Université de Montréal, for their assistance in compound analyses. Shastri Indo-Canadian institute is thanked for a Quebec Tuition Fee Exemption grant to N.D. Prasad Atmuri.

2.11. References

1. (a) Daly, J. W.; Spande, T. F.; Garraffo, H. M., *J. Nat. Prod.* **2005,** *68*, 1556-1575; (b)Nukui, S.; Sodeoka, M.; Sasai, H.; Shibasaki, M., *J. Org. Chem.* **1995,** *60*, 398-404; (c) Rawal, V. H.; Michoud, C., *Tetrahedron Lett.* **1991,** *32*, 1695-1698.

2. (a) Yang, C.-W.; Chen, W.-L.; Wu, P.-L.; Tseng, H.-Y.; Lee, S.-J., *Mol. Pharmacol.* **2006,** *69*, 749-758; (b) Michael, J. P., *Natural product reports* **2001,** *18*, 543-559; (c) Michael, J. P., *Natural product reports* **2002,** *19*, 719-741; (d) Grundon, M. F.; Saxton, J. E., *The Alkaloids*. Royal Society of Chemistry1971; Vol. 1; (e) Wei, L.; Shi, Q.; Bastow, K. F.; Brossi, A.; Morris-Natschke, S. L.; Nakagawa-Goto, K.; Wu, T.-S.; Pan, S.-L.; Teng, C.-M.; Lee, K.-H., *J. Med. Chem.* **2007,** *50*, 3674-3680.

3. (a) Sukhorukov, A. Y.; Boyko, Y. D.; Nelyubina, Y. V.; Gerard, S.; Ioffe, S. L.; Tartakovsky, V. A., *J. Org. Chem.* **2012,** *77*, 5465-5469; (b) Sun, H.; Nikolovska-Coleska, Z.; Yang, C.-Y.; Xu, L.; Liu, M.; Tomita, Y.; Pan, H.; Yoshioka, Y.; Krajewski, K.; Roller, P. P., *J. Am. Chem. Soc.* **2004,** *126*, 16686-16687; (c) Zhang, B.; Nikolovska-Coleska, Z.; Zhang, Y.; Bai, L.; Qiu, S.; Yang, C.-Y.; Sun, H.; Wang, S.; Wu, Y., *J. Med. Chem.* **2008,** *51*, 7352-7355;

(d) Vagner, J.; Qu, H.; Hruby, V. J., *Curr. Opin. Chem. Biol.* **2008,** *12*, 292-296; (e) Bourguet, C. B.; Claing, A.; Laporte, S. A.; Hébert, T. E.; Chemtob, S.; Lubell, W. D., *Can. J. Chem.* **2014,** *92*, 1031-1040; (f)Haubner, R.; Schmitt, W.; Hölzemann, G.; Goodman, S. L.; Jonczyk, A.; Kessler, H., *J. Am. Chem. Soc.* **1996,** *118*, 7881-7891; (g) Nogawa, T.; Kawatani, M.; Uramoto, M.; Okano, A.; Aono, H.; Futamura, Y.; Koshino, H.; Takahashi, S.; Osada, H., *The Journal of antibiotics* **2013**.

4. (a) Bourguet, C. B.; Goupil, E.; Tassy, D.; Hou, X.; Thouin, E.; Polyak, F.; Hébert, T. E.; Claing, A.; Laporte, S. A.; Chemtob, S., *J. Med. Chem.* **2011,** *54*, 6085-6097; (b) Hanessian, S.; McNaughton-Smith, G.; Lombart, H.-G.; Lubell, W. D., *Tetrahedron* **1997,** *53*, 12789-12854; (c) Becker, J. A.; Wallace, A.; Garzon, A.; Ingallinella, P.; Bianchi, E.; Cortese, R.; Simonin, F.; Kieffer, B. L.; Pessi, A., *J. Biol. Chem.* **1999,** *274*, 27513-27522; (d) Estiarte, M. A.; Rubiralta, M.; Diez, A.; Thormann, M.; Giralt, E., *J. Org. Chem.* **2000,** *65*, 6992-6999.

5. (a) Rao, M. H. R.; Pinyol, E.; Lubell, W. D., *J. Org. Chem.* **2007,** *72*, 736-743; (b) Polyak, F.; Lubell, W. D., *J. Org. Chem.* **1998,** *63*, 5937-5949; (c) Polyak, F.; Lubell, W. D., *J. Org. Chem.* **2001,** *66*, 1171-1180; (d) Salvati, M.; Cordero, F. M.; Pisaneschi, F.; Bucelli, F.; Brandi, A., *Tetrahedron* **2005,** *61*, 8836-8847; (e) Hanessian, S.; Chattopadhyay, A. K., *Org. Lett.* **2013,** *16*, 232-235.

6. Transannular cyclization reactions have been recently reviewed: Harutyunyan, S. R.; Rizzo, A., *Org. Biomol. Chem.* **2014**.

7. For examples of transannular aminations see: (a) White, J. D.; Hrnciar, P., *J. Org. Chem.* **2000,** *65*, 9129-9142; (b) White, J. D.; Hrnciar, P.; Yokochi, A. F., *J. Am. Chem. Soc.* **1998,** *120*, 7359-7360; (c) Jensen, T.; Mikkelsen, M.; Lauritsen, A.; Andresen, T. L.; Gotfredsen, C. H.; Madsen, R., *J. Org. Chem.* **2009,** *74*, 8886-8889; (d) Brock, E. A.; Davies, S. G.; Lee, J. A.;

Roberts, P. M.; Thomson, J. E., *Org. Lett.,* **2012,** *14*, 4278-4281; (e) Brock, E. A.; Davies, S. G.; Lee, J. A.; Roberts, P. M.; Thomson, J. E., *Org. Lett.,* **2011,** *13*, 1594-1597.

8. For examples of transannular amidations see: (a) Surprenant, S.; Lubell, W. D., *Org. Lett.,* **2006,** *8*, 2851-2854; (b) Edstrom, E. D., *J. Am. Chem. Soc.* **1991,** *113*, 6690-6692; (c) Edwards, O.; Paton, J.; Benn, M.; Mitchell, R.; Watanatada, C.; Vohra, K., *Can. J. Chem.* **1971,** *49*, 1648-1658; (d) Diederich, M.; Nubbemeyer, U., *Chem. Eur. J.* **1996,** *2*, 894-900; (e) Edstrom, E. D., *Tetrahedron Lett.* **1991,** *32*, 5709-5712; (f) Sudau, A.; Münch, W.; Bats, J. W.; Nubbemeyer, U., *Chem. Eur. J.* **2001,** *7*, 611-621.

9. (a) Prelog, V., *J. Chem. Soc.* **1950**, 420-428; (b) Brown, H. C.; Ichikawa, K., *Tetrahedron* **1957,** *1*, 221-230.

10. Still, W. C.; Galynker, I., *Tetrahedron* **1981,** *37*, 3981-3996.

11. Yoshikawa, K.; Bekki, K.; Karatsu, M.; Toyoda, K.; Kamio, T.; Morishima, I., *J. Am. Chem. Soc.* **1976,** *98*, 3272-3281.

12. Godina, T. A.; Lubell, W. D., *J. Org. Chem.* **2011,** *76*, 5846-5849.

13. (a) Liu, Y.; Bolen, D., *Biochemistry* **1995,** *34*, 12884-12891; (b) Bean, J. W.; Kopple, K. D.; Peishoff, C. E., *J. Am. Chem. Soc.* **1992,** *114*, 5328-5334.

14. Kaul, R.; Surprenant, S.; Lubell, W. D., *J. Org. Chem.* **2005,** *70*, 3838-3844.

15. Buchanan, G., *Chem. Soc. Rev.* **1974,** *3*, 41-63.

16. (a) Rémond, E.; Bayardon, J. R. M.; Ondel-Eymin, M.-J. L.; Jugé, S., *J. Org. Chem.* **2012,** *77*, 7579-7587; (b) Myers, A. G.; Gleason, J. L.; Yoon, T.; Kung, D. W., *J. Am. Chem. Soc.* **1997,** *119*, 656-673; (c) Xu, P.-F.; Lu, T.-J., *J. Org. Chem.* **2003,** *68*, 658-661; (d) Workman, J. A.; Garrido, N. P.; Sançon, J.; Roberts, E.; Wessel, H. P.; Sweeney, J. B., *J. Am. Chem. Soc.* **2005,** *127*, 1066-1067.

17. Traoré, M.; Mietton, F.; Maubon, D. l.; Peuchmaur, M.; Francisco Hilário, F.; Pereira de Freitas, R.; Bougdour, A.; Curt, A. l.; Maynadier, M.; Vial, H., *J. Org. Chem.* **2013,** *78*, 3655-3675.

18. Rodríguez, A.; Miller, D. D.; Jackson, R. F., *Org. Biomol. Chem.* **2003,** *1*, 973-977.

19. Trost, B. M.; Rudd, M. T., *Org. Lett.,* **2003,** *5*, 4599-4602.

20. Olsen, J. A.; Severinsen, R.; Rasmussen, T. B.; Hentzer, M.; Givskov, M.; Nielsen, J., *Bioorg. Med. Chem. Lett.* **2002,** *12*, 325-328.

21. Sicherl, F.; Cupido, T.; Albericio, F., *Chem. Commun.* **2010,** *46*, 1266-1268.

22. Organ, M. G.; Xu, J.; N'Zemba, B., *Tetrahedron Lett.* **2002,** *43*, 8177-8180.

23. Grubbs, R. H., *J. Angew. Chem. Int. Ed.* **2006,** *45*, 3760-3765.

24. Miller, S. J.; Grubbs, R. H., *J. Am. Chem. Soc.* **1995,** *117*, 5855-5856.

25. Wang, X.; Bowman, E. J.; Bowman, B. J.; Porco, J. A., *J. Angew. Chem. Int. Ed.* **2004,** *43*, 3601-3605.

26. Singh, F. V.; Wirth, T., *Synthesis* **2012,** *44*, 1171-1177.

27. Denmark, S. E.; Burk, M. T., Proc. Natl. Acad. Sci. U.S.A. **2010,** *107*, 20655-20660.

28. (a) Biloski, A. J.; Wood, R. D.; Ganem, B., *J. Am. Chem. Soc.* **1982,** *104*, 3233-3235; (b) Rajendra, G.; Miller, M. J., *J. Org. Chem.* **1987,** *52*, 4471-4477.

29. Tang, Y.; Li, C., *Tetrahedron Lett.* **2006,** *47*, 3823-3825.

30. Mehta, S.; Yao, T.; Larock, R. C., *J. Org. Chem.* **2012,** *77*, 10938-10944.

31. Karplus, M., *J. Am. Chem. Soc.* **1963,** *85*, 2870-2871.

32. Creighton, C. J.; Leo, G. C.; Du, Y.; Reitz, A. B., *Biorg. Med. Chem.* **2004,** *12*, 4375-4385.

33. Hutchinson, E. G.; Thornton, J. M., *Protein Sci.* **1994,** *3*, 2207-2216.

34. Lombart, H.-G.; Lubell, W. D., *J. Org. Chem.* **1996,** *61*, 9437-9446.

35. Sauvaître, T.; Barlier, M.; Herlem, D.; Gresh, N.; Chiaroni, A.; Guenard, D.; Guillou, C., *J. Med. Chem.* **2007,** *50*, 5311-5323.

36. Pandey, G., *Org. Lett.,* **2011,** *13*, 4672-4675.

37. Sudau, A.; Münch, W.; Nubbemeyer, U.; Bats, J. W., *J. Org. Chem.* **2000,** *65*, 1710-1720.

38. Richardson, J. S.; Richardson, D. C., Proc. Natl. Acad. Sci. U.S.A. **2002,** *99*, 2754-2759.

39. Fink, B. E.; Kym, P. R.; Katzenellenbogen, J. A., *J. Am. Chem. Soc.* **1998,** *120*, 4334-4344.

40. Wilson, S. R.; Sawicki, R. A., *J. Org. Chem.* **1979,** *44*, 287-291.

41. Bianchi, G.; Chiarini, M.; Marinelli, F.; Rossi, L.; Arcadi, A., *Adv. Synth. Catal.* **2010,** *352*, 136-142.

42. Padwa, A.; Hasegawa, T.; Liu, B.; Zhang, Z., *J. Org. Chem.* **2000,** *65*, 7124-7133.

43. Hu, T.; Liu, K.; Shen, M.; Yuan, X.; Tang, Y.; Li, C., *J. Org. Chem.* **2007,** *72*, 8555-8558.

44. Fujita, M.; Kitagawa, O.; Suzuki, T.; Taguchi, T., *J. Org. Chem.* **1997,** *62*, 7330-7335.

45. Detert, H.; Anthony-Mayer, C.; Meier, H., *Angew. Chem. Int. Ed.* **1992,** *31*, 791-792.

46. Still, W. C.; Kahn, M.; Mitra, A., *J. Org. Chem.* **1978,** *43*, 2923-2925.

CHAPTER 3

Article: Preparation of *N*-(Boc)allylglycine methyl ester using a zinc-mediated, Palladium-catalyzed cross-coupling reaction

N. D Prasad Atmuri and William D. Lubell*

Org. Synth. 2015, 92, 103-116

3.1 Introduction

In the field of peptide chemistry, unsaturated amino acids and their esters are useful starting materials for the synthesis of amino acids, constrained peptides and peptide mimics. Allylglycine esters have been used as versatile building blocks for the synthesis of macrocyclic dipeptide β-turn mimics,[4] azabicyclo[X.Y.0]alkanone amino acids,[5] the key intermediate of diaminopimelate metabolism L-tetrahydrodipicolinic acid,[6] potent macrocyclic HCV NS3 protease inhibitors,[7] bicyclic amino acid substrates for intramolecular Pauson-Khand cyclizations,[8] and anti-bacterial cyclic peptides.[9] The double bond of the unsaturated amino acid has been functionalized by various chemical processes, including Diels–Alder reactions,[10] and cycloadditions,[11] cross-metathesis,[12] as well as Heck[13] and Suziki-Miyaura cross coupling reactions.[14]

Although a variety of methods have provided allylglycinates in enantiomerically enriched forms,[3,15-25] they require often longer reaction sequences. Diastereoselective syntheses of allylglycinate have been achived using chiral auxiliaries which may be removed or destroyed,[23] such as ephedrine-derived imidazolidinone glycinimides,[22] menthone-derived nitrones,[18] and camphor-derived glycine derivatives.[17,20,24] Enantioselective approaches to allylglycinate have featured allylation of ketoester oximes employing chiral bis(oxazoline) ligands,[21] and allylation of *tert*-butyl glycinate using tartrate-derived and Cinchona alkaloid-derived quaternary ammonium phase-transfer catalysts.[19,28] In addition, allylglycinates have been prepared from amino acids as chiral educts. For example, glutamate served as starting material for the syntheisis of allyl 2-(Boc)amino-4-triphenylphosphonium butanoate, which reacted with various aldehydes and paraformaldehyde in Wittig-Horner-Wadsworth-Emmons reactions to yield unsaturated amino acids.[16] Similarly, ylide from methyltriphenylphosphonium bromide reacted with α-*tert*-butyl *N*-(PhF) aspartate β-aldehyde to provide protected allylglycinate.[4] In the

context of our research in peptide mimicry,[4,5] we required an efficient, atom economical route to enantiomerically pure allylglycine analogues. Building on the established precedent of zinc-mediated, palladuim-catalyzed cross-coupling reactions of commercially available and inexpensive *tert*-butyl (*R*)-1-(methoxycarbonyl)-2-iodoethylcarbamate,[2,15,26,27] this extension employs vinyl bromide to give effective access to allylglycine in enantiomerically pure form on multi-gram scale.

3.2 Results and discussion

The zinc insertion reaction of the alininyl iodide **1.112** are typically performed in DMF to thwart the chelation of the ester and carbamate functions with zinc, which has been suggested to promote β-elimination to the corresponding amino acrylate, particulary when performed in THF.[26] The organozinc intermediate is relatively stable towards air and moisture. Attempts to perform the related Kumuda coupling using vinylmagnesium bromide were unsuccessful and resulted in β-elimination affording amino acrylate. Negishi cross coupling of the alininyl zinc intermediate with vinyl bromide is effectively mediated by $Pd_2(dba)_3$ and tri-(*o*-tolyl)phosphine and has been examined at lower temperature to give the *N*-(Boc)-allylglycine methyl ester **1.108** with improved yield.

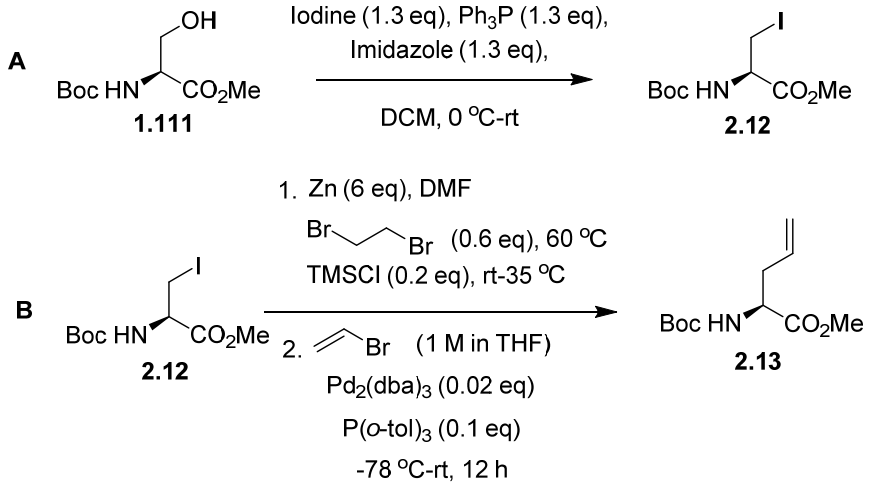

Scheme 3.1 Synthesis of Iodo alanine and *N*-(Boc)-allylglycine methyl ester

3.3 Procedure

A. *tert-Butyl (R)-1-(methoxycarbonyl)-2-iodoethylcarbamate* (**2.12**). A flame dried 1000-mL, three necked round-bottomed flask is equipped with a rubber septum, and a Teflon®-coated magnetic stir bar. The apparatus is purged with argon (Note 1). Keeping a positive flow of argon, the septum is removed temporarily and the flask is charged with triphenylphosphine (Note 2) (32.65 g, 124.5 mmol) and 400 mL of dichloromethane (Note 3). The solution is stirred at room temperature and 8.47 g (124.5 mmol) of imidazole (Note 2) is added in one portion. The solution is cooled in an ice bath to 0 °C and maintained at that temperature during the addition of iodine (31.59 g, 124.5 mmol) (Note 2) in four portions. The solution is warmed to room temperature, stirred for 10 min, and cooled to 0 °C. The reaction mixture is stirred in the dark. The septum is replaced with a dropping funnel, which is charged with *tert*-butyl (S)-1-(methoxycarbonyl)-2-hydroxyethylcarbamate (**1.111**, 21 g, 95.84 mmol, Note 4) in 100 mL of dichloromethane. To the reaction mixture at 0 °C, the solution of alcohol **1.111** in dichloromethane is added drop-wise over 60 min. The resulting slurry is stirred at 0 °C for 1 hr and at room temperature for 1.5 h (Note 5). The reaction mixture is filtered through silica gel using 50:50 ether:hexanes (~500 mL) as eluent and concentrated under reduced pressure to give 32.5 g of brown oil, which is purified by column chromatography (Note 6). Evaporation of the collected fractions provides colorless oil, which solidifies in the freezer (25.2 g, 76.59 mmol, 80%, Note 7).

B. *tert-Butyl (S)-1-(methoxycarbonyl)but-3-enylcarbamate* (**2.13**). A flame dried 250-mL, three necked round-bottomed flask is equipped with a reflux condenser [fitted with a three way stop cock connected to an argon balloon (Note 1)], a rubber septum, and a Teflon®-coated

magnetic stir bar. The apparatus is purged with argon. Keeping a positive flow of argon, the septum is removed temporarily and the flask is charged with zinc dust (11.92 g, 182.3 mmol, 6 eq) (Note 8). Dry DMF (20 mL) (Note 9) is then added to the flask via a syringe. 1,2-Dibromoethane (1.57 mL, 3.42 g, 18.2 mmol, 0.6 eq) (Note 10) is added next to the stirred suspension via a syringe. The mixture is stirred and heated to 60 °C and kept at 60 °C for 45 min (Note 11). The mixture is cooled to room temperature. Chlorotrimethyl silane (TMS-Cl; 0.77 mL, 6.0 mmol) (Note 12) is added via a syringe to the slurry, which is stirred for 40 min at room temperature (Note 13). A solution of *tert*-butyl (*R*)-1-(methoxycarbonyl)-2-iodoethylcarbamate (**2.12**, 10 g, 30.39 mmol, Note 14) in dry DMF (20 mL) is added via a syringe (Note 15) to the room temperature mixture of activated zinc, which is then heated to 35 °C and stirred for 60 min. The zinc insertion was judged complete by TLC analysis (Note 16). After complete zinc insertion, the reaction mixture is cooled to room temperature, and charged with $Pd_2(dba)_3$ (779 mg, 0.85 mmol, 0.028 eq) (Note 17) and tri(*o*-tolyl)phosphine (925 mg, 3.03 mmol, 0.1 eq) (Note 18). The resulting mixture is cooled to –78 ^{o}C. A solution of vinyl bromide (1 M in THF 42.5 mL, 42.5 mmol, 1.4 eq, Note 19) is added drop-wise via a cannula to the stirred –78 °C suspension. After the addition of the vinyl bromide is complete, the cold bath is removed and the reaction mixture is allowed to warm to room temperature with stirring for 12 h (Note 20). The reaction mixture is diluted with ethyl acetate (200 mL) and water (200 mL), and filtered through a pad of Celite™. The pad is washed with ethyl acetate (300 mL). The filtrate and washings are combined and transferred to a separating funnel. The organic layer is separated. The aqueous layer is extracted with ethyl acetate (2 x 200 mL). The combined organic layers are washed with brine (400 mL), dried over anhydrous sodium sulphate, filtered, and concentrated under reduced

pressure to give 8.2 g of brown oil, which is purified by column chromatography (Note 21). Evaporation of the collected fractions yields brown oil (4.50 g, 19.64 mmol, 65%, Note 22).

3.4 Notes

1. The submitters conducted this procedure under an atmosphere of argon.
2. Triphenylphosphine (99 %), imidazole (purity ≥99 %), and iodine (purity ≥99.9%) were obtained from Aldrich and used as provided.
3. The submitters used dry dichloromethane from a solvent filtration system (Glass Contour, Irvine, CA).
4. *tert*-Butyl (S)-1-(methoxycarbonyl)-2-hydroxyethylcarbamate (**1.111**) was prepared according to the procedure reported by Trost et al.[2.]

   Alcohol **1.111**: ^{1}H NMR (400 MHz, $CDCl_3$) δ 5.58-5.60 (broad d, 1H), 4.32 (br s, 1H), 3.90-3.91 (m, 1H), 3.82-3.84 (m, 1H), 3.73 (s, 3H), 3.19 (m, 1H), 1.40 (s, 9H). ^{13}C NMR (400 MHz, CDCl3) δ 171.5, 155.8, 80.3, 63.3, 55.7, 52.6, 28.06. HRMS calcd for $C_9H_{17}NO_5Na$, 242.0999; found 242.0996. $[\alpha]_D$ 10.5 (*c* 1.0, $CHCl_3$); LC-MS purity >99.5(Acq method, LC_20_95_10min_MeOH, column, polar RP 30X2.00mm, t_r = 3.85min). At the start of the addition of starting material **1.111**, the round bottomed flask was covered with aluminum foil and stirred in the dark until the reaction was complete, because iodide **2.12** is light sensitive.
5. TLC analysis was performed on Merck Aluminum silica gel plates 60 F_{254}. Reaction conversion was ascertained using the following procedure. The reaction mixture was spotted directly on the TLC plate, which was eluted with 8:2 hexanes/ethyl acetate, and visualized with 254 nm UV light and $KMnO_4$ stain after heating: starting material **1.111** (R_f = 0.075, a UV inactive and $KMnO_4$ active spot); iodide **2.12** (R_f = 0.55, a UV active and $KMnO_4$ active spot).

6. Iodoalanine **2.12** is purified on a silica column in a dark place. The crude residue is absorbed onto 70 g of silica gel, and added to a column (18.4 cm diameter x 20 cm length), which is packed with a slurry of 360 g of silica (high purity grade Silica gel particle size 230-400 mesh ASTM, Merck Ltd.) in hexanes (700 mL). An eluent of 5-7% diethyl ether in hexanes (~1000 mL) is first flushed through the column to remove the less polar spot tert-butyl 1-(methoxycarbonyl)vinylcarbamate. The eluent is switched to 10-13% diethyl ether/hexanes (~2500 mL) to elute the iodide (R_f = 0.55, 8:2 hexanes/ethyl acetate, visualized with 254 nm UV light and $KMnO_4$ stain on heating).
7. Iodide **2.12**: ^{1}H NMR (400 MHz, $CDCl_3$) δ: 5.40-5.42 (broad d, 1H), 4.45-4.47 (m, 1 H), 3.73 (s, 3 H), 3.50-3.54 (m, 2 H), 1.41 (s, 9 H). ^{13}C NMR (400 MHz, $CDCl_3$) δ: 169.9, 154.7, 80.2, 53.7, 52.9, 28.2, 7.69. HRMS calcd for $C_9H_{16}NIO_4Na$, 352.0016; found 352.0016. $[\alpha]_D$ 40.6 (*c* 1.0, $CHCl_3$). The enantiomeric purity of compound **2.12** was >98 % by SFC (eluent 10 % MeOH, pressure 150 bar, flow rate 3 mL/min, injection volume 25 μL into a 20 μL loop, column AD-H, 25 cm x 5 μm, column temp. 35 °C, t_r = 1.68 min); injection of a sample containing an incremental addition of 0.1 mg of the *R*-isomer (t_r = 2.25 min) into 10 mg of *S*-**2.12** established the limits of detection to be at least 1:99.
8. Zinc dust (particle size <10 μm, >98 %) was purchased and used as received from Aldrich chemical company.
9. The submitters used dry DMF from a solvent filtration system (Glass Contour, Irvine, CA).
10. 1,2-Dibromoethane was purchased from Baker Chemicals and used as received.
11. The submitters used an oil bath kept at 60 °C external temperature.
12. TMS-Cl (purity ≥97%) was purchased and used as received from Aldrich chemical company.
13. Evolution of gas was observed after the addition of TMS-Cl.

14. During addition of iodide **2.12**, the round bottomed flask was covered with aluminum foil and stirred in the dark until the reaction was complete, because iodide **2.12** is light sensitive.
15. The time for reagent addition varied with reaction scale. In the reported experiment, the addition was completed over 25 min.
16. The reaction flask was immersed in an oil bath having a bath temperature of 25 °C. Reaction conversion was monitored by TLC (2:1 hexanes/ethyl acetate) using 254 nm UV light to visualize the starting material (R_f = 0.7) and organozinc reagent (R_f = 0.2).
17. $Pd_2(dba)_3$ (purity 97%) was purchased and used as received from Aldrich chemical company.
18. Tri(*o*-tolyl)phosphine (purity ≥97%) was purchased and used as received from Aldrich chemical company.
19. Anhydrous THF (50 mL) in a flame-dried measuring cylinder fitted with a septum was cooled to –78 °C. On cooling, the volume of the THF contracted to 45 mL. Vinyl bromide gas was bubbled into the THF until the total volume rose from 45 mL to 48.1 mL yielding a 1M solution. Employment of vinyl bromide solutions of >1 molar augmented formation of methyl *N*-(Boc)alaninate and diminished iodide yield. Methyl *N*-(Boc)alaninate is removed by chromatography: TLC R_f = 0.21 (9:1 hexanes/ethyl acetate), visualized as a UV inactive and $KMnO_4$ active spot.
20. Reaction conversion is ascertained on an aliquot of the reaction mixture (100 μL), which was partitioned between ethyl acetate (200 μL) and water (500 μL). The ethyl acetate layer was analyzed by TLC using 9:1 hexanes/ethyl acetate as eluant, and the plate was visualized with 254 nm UV light as well as with $KMnO_4$ stain after heating: iodide **2.12** (R_f = 0.29, a UV and $KMnO_4$ active spot); olefin **2.13** (R_f = 0.29, a UV inactive and $KMnO_4$ active spot).

21. Olefin **2.13** is purified on a silica column. The residue is absorbed onto 30 g of silica gel. The column (18.4 cm diameter) is packed with slurry of 250 g of silica (high purity grade Silica gel particle size 230-400 mesh ASTM, Merck Ltd.) in hexanes (1000 mL). Elution with 2-5% ethyl acetate/hexanes removes first all non polar spots. Switching to 7-10% ethyl acetate in hexanes (~1000 mL) elutes the product (TLC R_f = 0.29, 9:1 hexanes/ethyl acetate), which is visualized as a UV inactive and KMnO4 active spot on heating.
22. *N*-(Boc)Allylglycine methyl ester (**2.13**): $[\alpha]_D$ +20.2 (c 1.5, $CHCl_3$); lit.[3] $[\alpha]_D$ +18.8 (c 1.0, $CHCl_3$); ^1H NMR (400 MHz, $CDCl_3$) δ: 1.44 (s, 9H), 2.48-2.55 (m, 2H), 3.75 (s, 3H), 4.38-4.39 (m, 1H), 5.04 (br s, 1H), 5.12-5.16 (m, 2H), 5.66-5.73 (m, 1H); ^{13}C NMR (400 MHz, $CDCl_3$) δ 28.5, 37.0, 52.4, 53.1, 80.1, 119.2, 132.6, 155.4, 172.8; HRMS calcd for $C_{11}H_{19}NO_4Na$, 252.1215; found 252.1217. Anal. Calcd for $C_{11}H_{19}NO_4$: C, 57.62; H, 8.35; N, 6.11. Found: C, 57.13; H, 8.51; N, 5.93.

    Establishment of enantiomeric purity of olefin **2.13** was shown in chapter 2

3.5 Handling and Disposal of Hazardous Chemicals

Persons with prior training in experimental organic chemistry must only perform the procedures in this article. All hazardous materials should be handled using the standard procedures for work with chemicals described in references such as "Prudent Practices in the Laboratory" (The National Academies Press, Washington, D.C., 2011 www.nap.edu). All chemical waste should be disposed of in accordance with local regulations. For general guidelines for the management of chemical waste, see Chapter 8 of Prudent Practices.

These procedures must be conducted at one's own risk. *Organic Syntheses, Inc*., its Editors, and its Board of Directors do not warrant or guarantee the safety of individuals using these

procedures and hereby disclaim any liability for any injuries or damages claimed to have resulted from or related in any way to the procedures herein.

3.6 References

1. N. D. Prasad Atmuri and William D. Lubell, Department of Chemistry, Université de Montréal, P.O. Box 6128, Succursal Centre-ville, Montréal, QC H3C 3J7, Canada. We thank the Natural Sciences and Engineering Research Council of Canada for financial support.
2. Trost, B. M.; Rudd, M. T. *Org. Lett.* **2003,** 5, 4599.
3. Collier, P. N.; Campbell, A. D.; Patel, I.; Taylor, R. J. *Tetrahedron* **2002**, 58, 6117.
4. Kaul, R.; Surprenant, S.; Lubell, W. D. *J. Org. Chem*. **2005**, 70, 3838.
5. Surprenant, S.; Lubell, W. D. *Org. Lett*. **2006**, 8, 2851.
6. Caplan, J. F.; Sutherland, A.; Vederas, J. C. *J. Chem. Soc., Perkin Trans. 1* **2001**, 2217.
7. Nair, L. G.; Bogen, S.; Bennett, F.; Chen, K.; Vibulbhan, B.; Huang, Y.; Yang, W.; Doll, R. J.; Shih, N.-Y.; Njoroge, F. G. *Tetrahedron Lett.* **2010**, 51, 3057.
8. Bolton, G. L.; Hodges, J. C.; Ronald Rubin, J. *Tetrahedron* **1997**, 53, 6611.
9. Boyle, T. P.; Bremner, J. B.; Coates, J.; Deadman, J.; Keller, P. A.; Pyne, S. G.; Rhodes, D. I. *Tetrahedron* **2008**, 64, 11270.
10. Kotha, S. *Acc. Chem. Res*. **2003,** 36, 342.
11. Avenoza, A.; Busto, J. H.; Canal, N.; Peregrina, J. M.; Pérez-Fernández, M. *Org. Lett.* **2005,** 7, 3597.
12. Wang, Z. J.; Jackson, W. R.; Robinson, A. J. *Org. Lett.* **2013**, 15, 3006.
13. Collier, P. N.; Patel, I.; Taylor, R. J. *Tetrahedron Lett.* **2002**, 43, 3401.
14. Krebs, A.; Ludwig, V.; Pfizer, J.; Dürner, G.; Göbel, M. W. *Chem-Eur. J.* **2004**, 10, 544.

15. A synthesis of methyl *N*-(Cbz)allyglycinate without experimental procedure is reported in: Olsen, J. A.; Severinsen, R.; Rasmussen, T. B.; Hentzer, M.; Givskov, M.; Nielsen, J. *Bioorg. Med. Chem. Lett.* **2002**, 12, 325.

16. Rémond, E.; Bayardon, J. r. m.; Ondel-Eymin, M.-J. l.; Jugé, S. *J. Org. Chem.* **2012,** 77, 7579.

17. Workman, J. A.; Garrido, N. P.; Sançon, J.; Roberts, E.; Wessel, H. P.; Sweeney, J. B. *J. Am. Chem. Soc.* **2005,** 127, 1066.

18. Katagiri, N.; Okada, M.; Morishita, Y.; Kaneko, C. *Tetrahedron* **1997,** 53, 5725.

19. Ohshima, T.; Shibuguchi, T.; Fukuta, Y.; Shibasaki, M. *Tetrahedron* **2004**, 60, 7743.

20. Yeh, T.-L.; Liao, C.-C.; Uang, B.-J. *Tetrahedron* **1997**, 53, 11141.

21. Hanessian, S.; Yang, R.-Y. *Tetrahedron Lett.* **1996,** 37, 8997.

22. Guillena, G.; Nájera, C. *J. Org. Chem*. **2000**, 65, 7310.

23. Myers, A. G.; Gleason, J. L. *Org. Synth*. **1999**, 76, 57.

24. Xu, P.-F.; Lu, T.-J. *J. Org. Chem*. **2003,** 68, 658.

25. Kitagawa, O.; Hanano, T.; Kikuchi, N.; Taguchi, T. *Tetrahedron Lett.* **1993**, 34, 2165.

26. Jackson, R. F.; Moore, R. J.; Dexter, C. S.; Elliott, J.; Mowbray, C. E. *J. Org. Chem.* **1998,** 63, 7875.

27. Carrillo-Marquez, T.; Caggiano, L.; Jackson, R. F.; Grabowska, U.; Rae, A.; Tozer, M. *J. Org. Biomol. Chem.* **2005**, 3, 4117.

28. Bojan, V.; Maja, G. –P.; Radomir, M.; Radomir, N. S. *Org. Lett.* **2014**, 16, 34.

CHAPTER 4

CONCLUSIONS & PERSPECTIVES

4.1 Conclusions

The development of a common synthetic approach for building a verity of iodo-azabicyco[X.Y.0]alkanes has been achieved by employing different ring-size macrocyclic lactams in transannular iodolactamization reactions. Isomeric unsaturated 8-, 9- and 10-member macrocyclic lactams were successfully assembled by a sequence featuring peptide coupling of vinyl-, allyl-, homoallyl- and homohomoallylglycine building blocks followed by ring closing metathesis. Novel iodo-substituted pyrrolizidinone and quinolizidinone were synthesized using this methodology. To make 4-iodo-pyrrolizidinone **2.3** (Chapter 2) a new method for iodolactamization was developed using diacetoxyidodobenzene and conditions that may have potential for inducing cyclizations of macrolactams resistant to conventional transannular reactions. Mechanistic considerations suggest that cyclization proceeds by attack of iodine from the least hindered face of the olefin and that cyclization onto the iodonium intermediate occurs by a route that minimizes allylic strain and diaxial interactions. X-ray crystallographic and spectroscopic analyses of the macrocyclic lactams, the bicycles, and bridgehead imidate **2.10d, 2.11a, 2.11e, 2.3** and **2.5** (Chapter 2) demonstrate the potential of these constrained dipeptides to mimic the central residues of ideal types of β-turn secondary structures. Both the bicycle and macrocycle constraints can thus serve to rigidify the backbone for studying peptide conformation-activity relationships. Moreover the iodide substitution on the azabicycloalkanes may function as a useful handle for the addition of side chain modifications to produce a broad verity of peptidomemitics.

Three relatively expensive building blocks, allylglycine, homoallylglycine and homohomoallylglycine, were prepared from L-serine using iodoalanine as a common intermediate. In particular, syntheses of *N*-(Boc)allyl and homohomoallylglycine methyl esters

were developed using transition metal cross-coupling methods. In summary, the above methodology and building blocks offer atom economical means for producing different ring-size macrocycles and iodo-azabycyclo[X.Y0]alkanes by a common synthetic strategy.

4.2 Future Work

Azabicyclo[X.Y.0]alkanones have provided conformationally rigid peptide mimics exhibiting significant biological activity. For example, in the mimic PDC113.824, (3*S*,6*S*,9*S*)-indolizidine-2-one amino acid (**1.17**, I2aa, Figure 4.1) plays a key role in orienting the pharmacophores to modulate the prostaglandin F2α receptor by a biased allosteric mechanism that ultimately delays labor in animal models.[1,2] Modification of the (3*S*,6*S*,9*S*)-indolizidin-2-one amino acid in PDC113.824 may thus be achieved by modifying the iodide of (3*S*,5*R*,6*R*,9*S*)**-2.1** (Chapter 2) to prepare analogs for studying effects on biological activity (Figure 4.1).

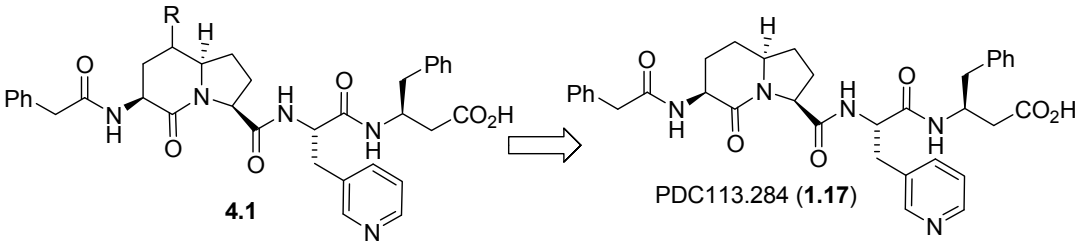

Figure 4.1 Substituted PDC113.284 targets

New fused bicyclic amino acid scaffolds may be pursued using different 8- and 9-member isomeric unsaturated macrocyclic lactams (Scheme 4.1). For example macrocyclic lactams **2.9b** and **4.3** may be prepared from *N*-(Fmoc)vinylglycinyl-*N*-(dimethoxybenzyl) homohomoallylglycine **2.7b** (Dmb = 2,4-dimethoxybenzyl) and *N*-(Fmoc)allylglycinyl-*N* (dimethoxybenzyl)allylglycine **4.2**[3] by ring-closing metathesis. The resulting macrocyclic lactams may then be subjected to transannular cyclizations to make azabicycles.

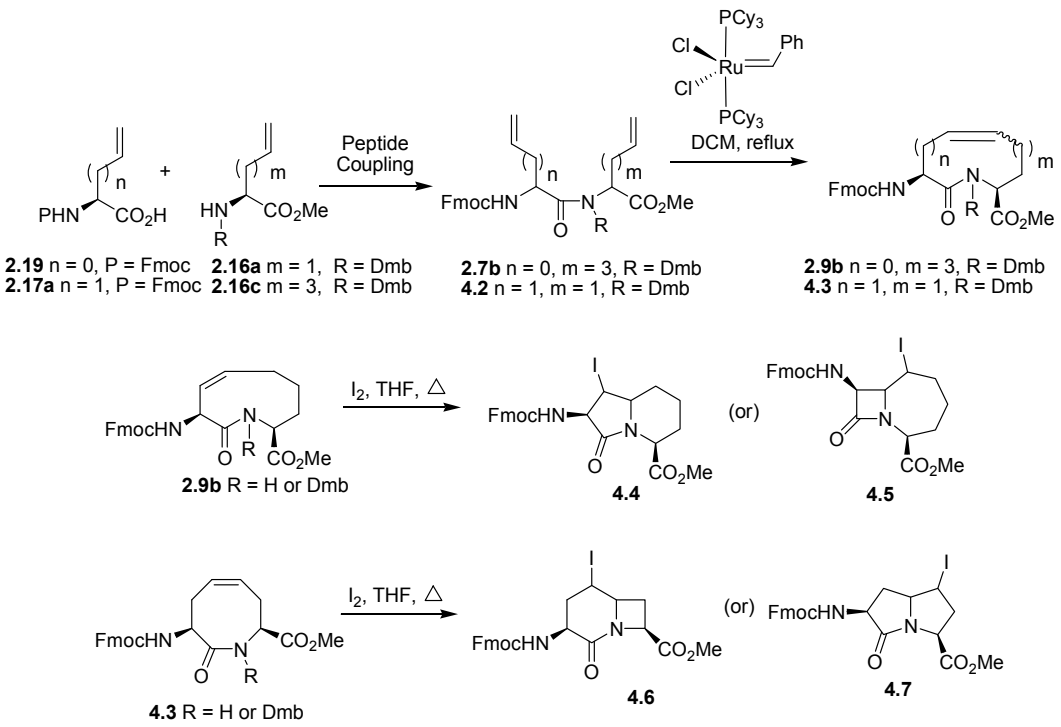

Scheme 4.1 Proposed fused ring systems from alternative macrocyclic lactams

Moreover, macrocyclic lactams that are resistant to transannular cyclization may be induced to react after olefin photochemical isomerization.[4,5] Further mechanistic insight may also be obtained by computational analysis.[6] Pursuing alternative bicycles, improved methods for their synthesis and mechanistic understanding of the factors governing stereo- and regiochemical transannular cyclizations, this study is well positioned for preparing different ring-size macrocycle and bicycle peptidomimetics. Realization of this strategy should have significant utility for medicinal chemistry studies of biologically active peptides.

4.3 References

1. Bourguet, C. B.; Goupil, E.; Tassy, D.; Hou, X.; Thouin, E.; Polyak, F.; Hébert, T. E.; Claing, A.; Laporte, S. A.; Chemtob, S., *J. Med. Chem.* **2011,** *54*, 6085-6097.

2. Bourguet, C. B.; Claing, A.; Laporte, S. A.; Hébert, T. E.; Chemtob, S.; Lubell, W. D., *Can. J. Chem.* **2014,** *92*, 1031-1040.

3. Kaul, R.; Surprenant, S.; Lubell, W. D., *J. Org. Chem.* **2005,** *70*, 3838-3844.

4. Royzen, M.; Yap, G. P.; Fox, J. M., *J. Am. Chem. Soc.* **2008,** *130*, 3760-3761.

5. Moran, J.; Dornan, P.; Beauchemin, A. M., *Org. Lett.,* **2007,** *9*, 3893-3896.

6. Fink, B. E.; Kym, P. R.; Katzenellenbogen, J. A., *J. Am. Chem. Soc.* **1998,** *120*, 4334-4344.

Appendix

Spectral data related to CHAPTER 2

^{1}H NMR 500 MHz
Solvent: $CDCl_3$

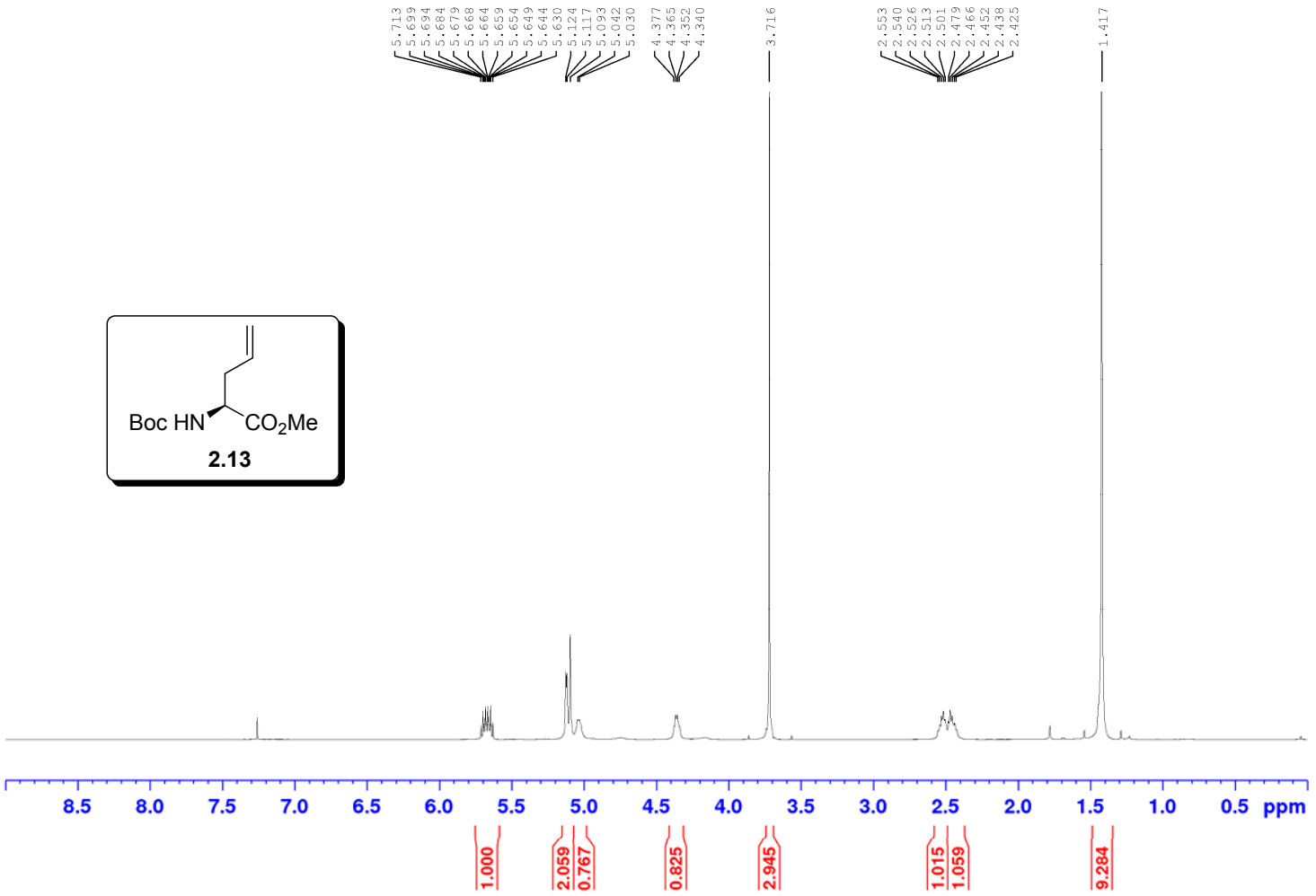

^{13}C NMR 500 MHz
Solvent: $CDCl_3$

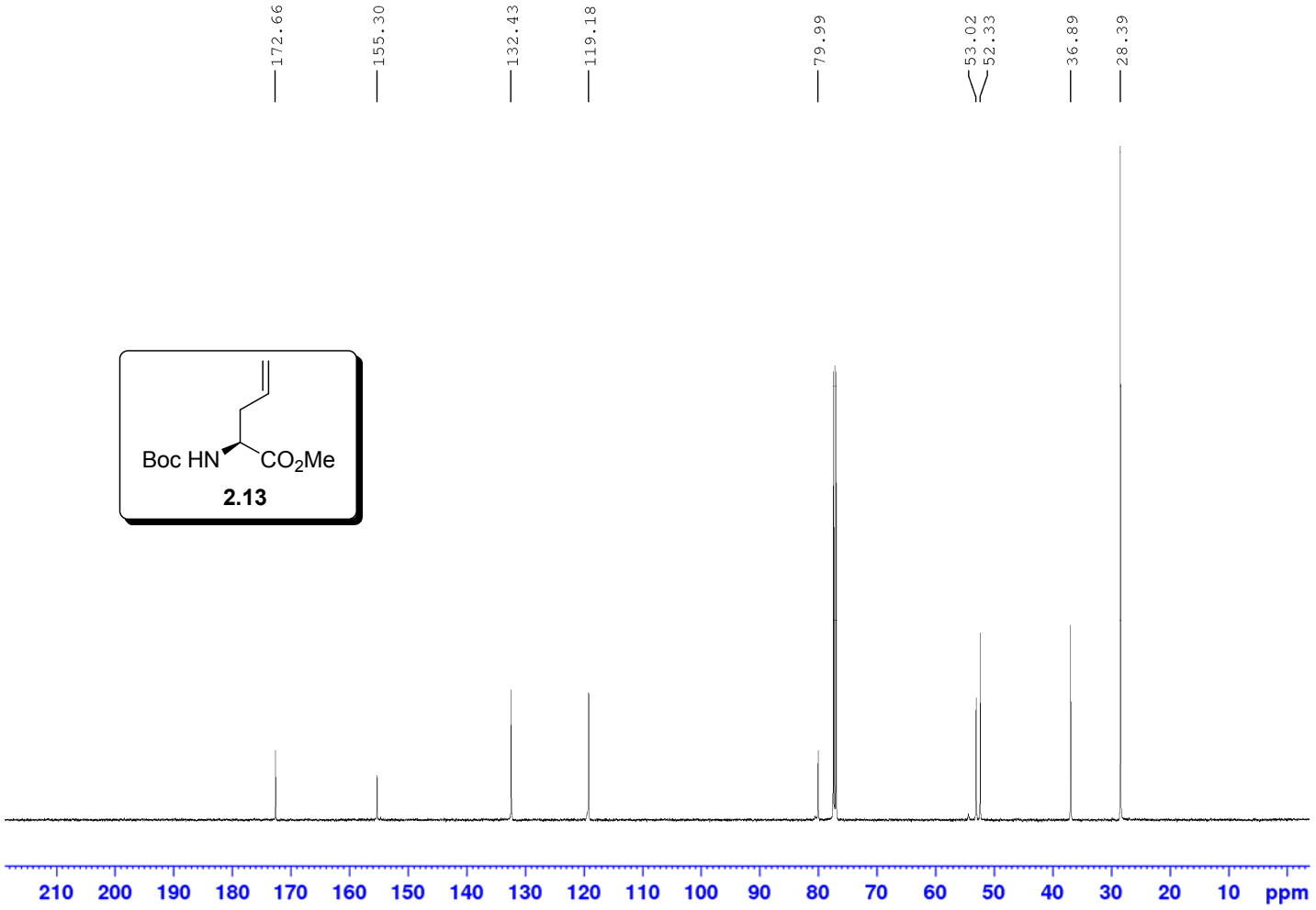

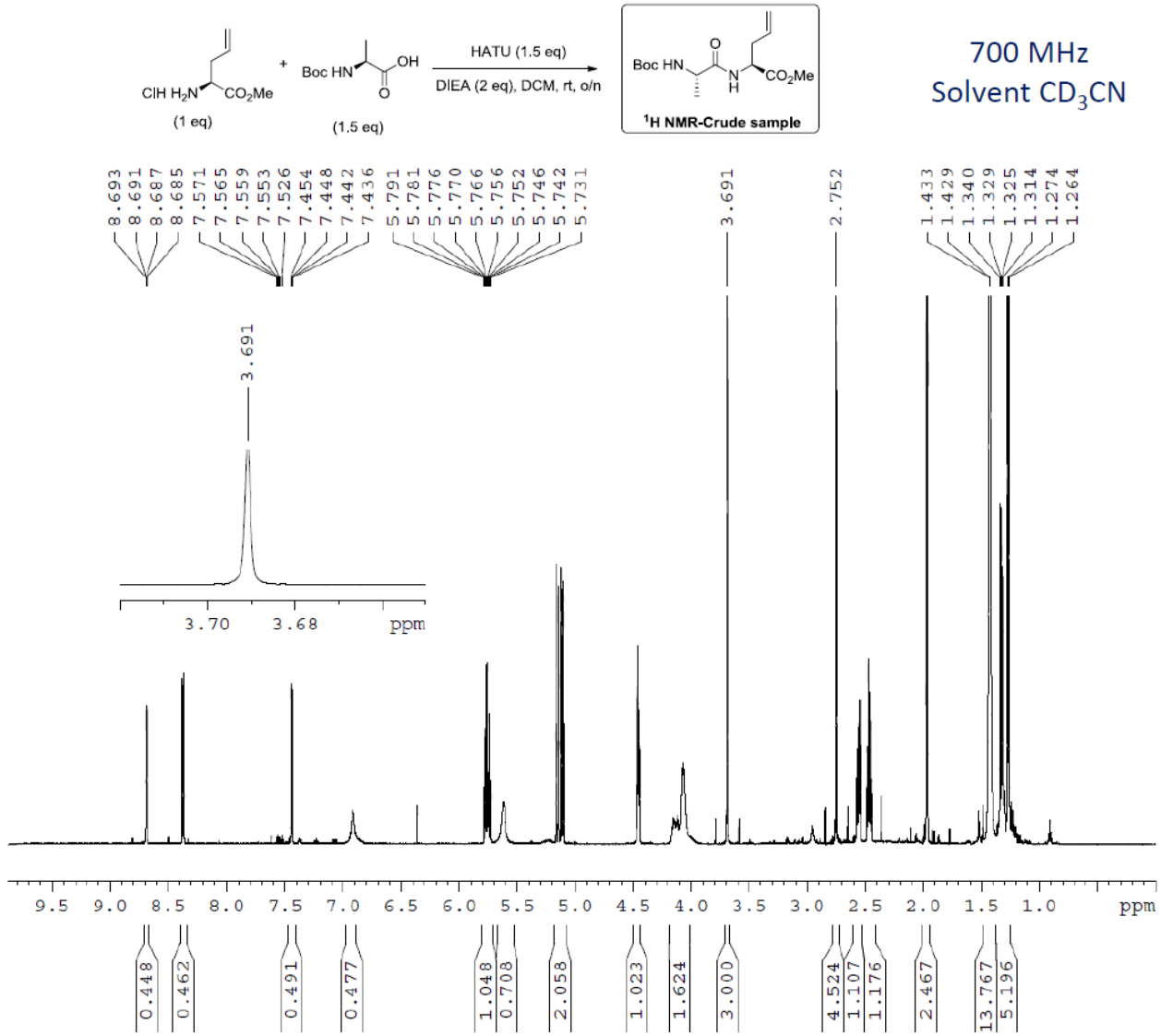
ClH H2N CO2Me
(1 eq)
+
Boc HN OH
O
(1.5 eq)
HATU (1.5 eq)
DIEA (2 eq), DCM, rt, o/n
Boc HN
O
N
H
CO2Me
1H NMR-Crude sample
700 MHz
Solvent CD3CN
8.693
8.691
8.687
8.685
7.571
7.565
7.559
7.553
7.526
7.454
7.448
7.442
7.436
5.791
5.781
5.776
5.770
5.766
5.756
5.752
5.746
5.742
5.731
3.691
2.752
1.433
1.429
1.340
1.329
1.325
1.314
1.274
1.264
3.70
3.68
ppm
9.5 9.0 8.5 8.0 7.5 7.0 6.5 6.0 5.5 5.0 4.5 4.0 3.5 3.0 2.5 2.0 1.5 1.0
ppm
0.448
0.462
0.491
0.477
1.048
0.708
2.058
1.023
1.624
3.000
4.524
1.107
1.176
2.467
13.767
5.196

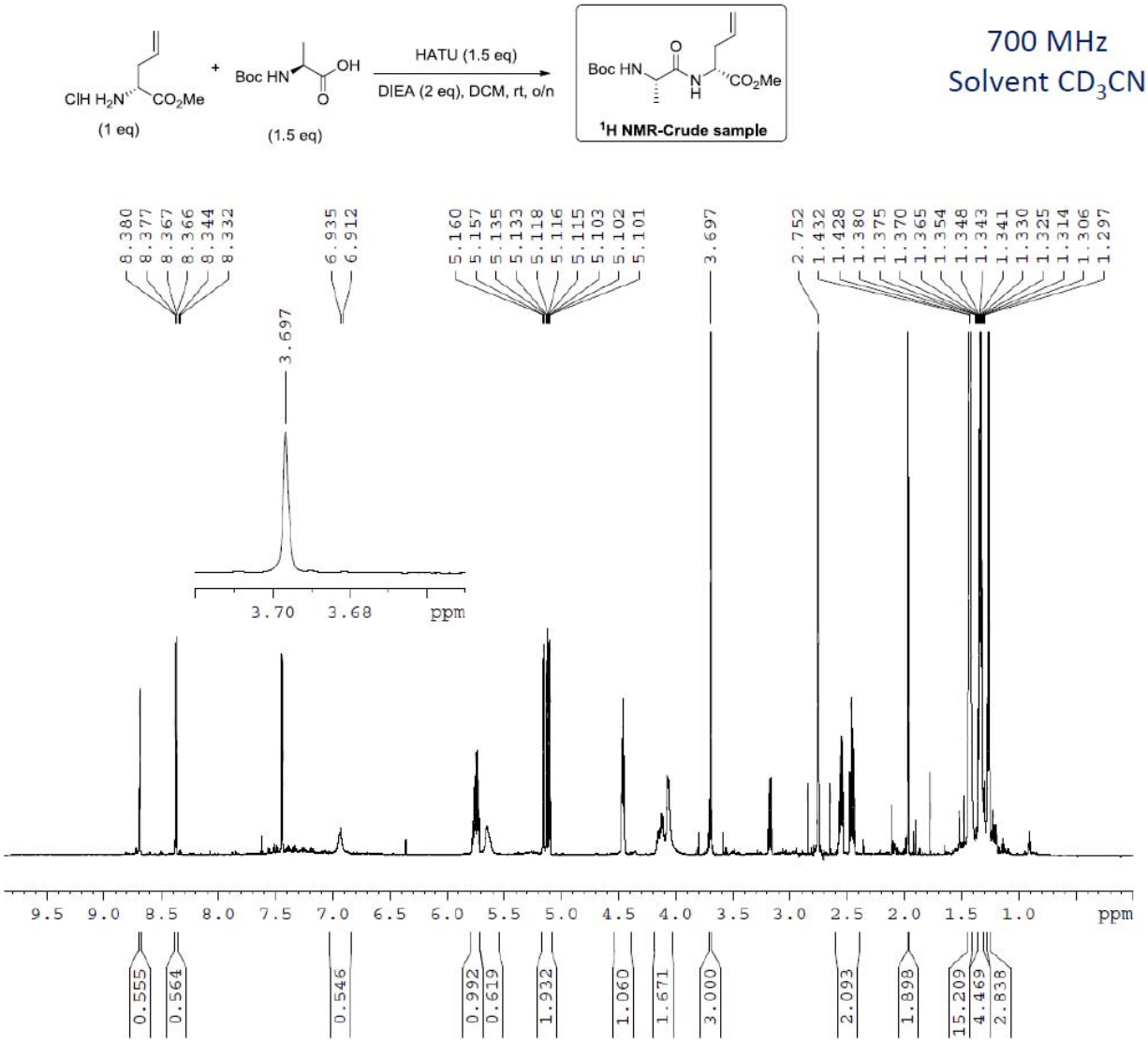
ClH H2N CO2Me
(1 eq)
Boc HN OH
O
(1.5 eq)
HATU (1.5 eq)
DIEA (2 eq), DCM, rt, o/n
Boc HN
N
H
CO2Me
1H NMR-Crude sample
700 MHz
Solvent CD3CN
8.380
8.377
8.367
8.366
8.344
8.332
6.935
6.912
5.160
5.157
5.135
5.133
5.118
5.116
5.115
5.103
5.102
5.101
3.697
2.752
1.432
1.428
1.380
1.375
1.370
1.365
1.354
1.348
1.343
1.341
1.330
1.325
1.314
1.306
1.297
3.70
3.68
ppm
9.5 9.0 8.5 8.0 7.5 7.0 6.5 6.0 5.5 5.0 4.5 4.0 3.5 3.0 2.5 2.0 1.5 1.0 ppm
0.555
0.564
0.546
0.992
0.619
1.932
1.060
1.671
3.000
2.093
1.898
15.209
4.469
2.838

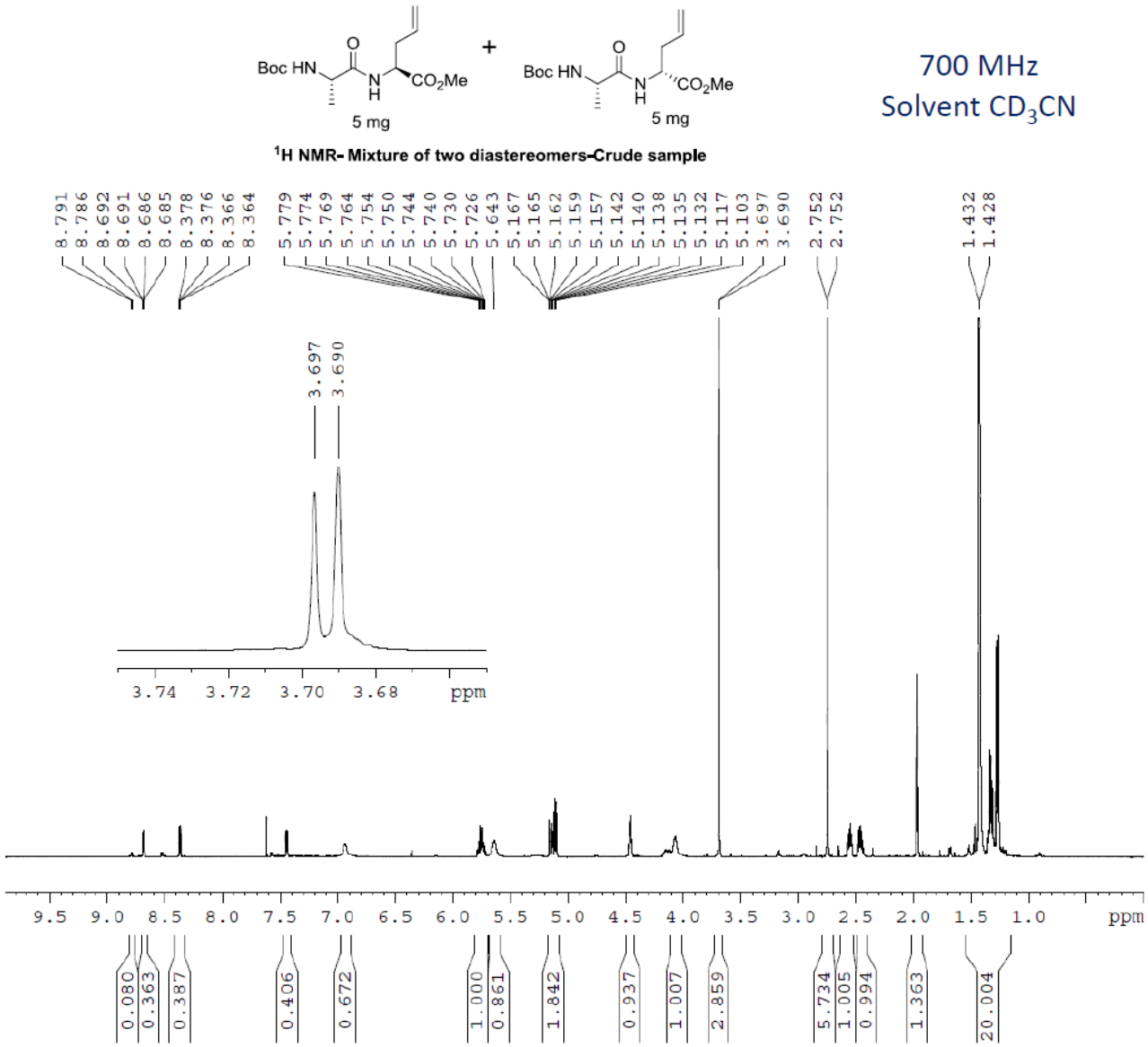
Boc HN
O
N
H
CO2Me
5 mg
+
Boc HN
O
N
H
CO2Me
5 mg
700 MHz
Solvent CD3CN
1H NMR- Mixture of two diastereomers-Crude sample
8.791
8.786
8.692
8.691
8.686
8.685
8.378
8.376
8.366
8.364
5.779
5.774
5.769
5.764
5.754
5.750
5.744
5.740
5.730
5.726
5.643
5.167
5.165
5.162
5.159
5.157
5.142
5.140
5.138
5.135
5.132
5.117
5.103
3.697
3.690
2.752
2.752
1.432
1.428
3.74
3.72
3.70
3.68
ppm
9.5
9.0
8.5
8.0
7.5
7.0
6.5
6.0
5.5
5.0
4.5
4.0
3.5
3.0
2.5
2.0
1.5
1.0
ppm
0.080
0.363
0.387
0.406
0.672
1.000
0.861
1.842
0.937
1.007
2.859
5.734
1.005
0.994
1.363
20.004

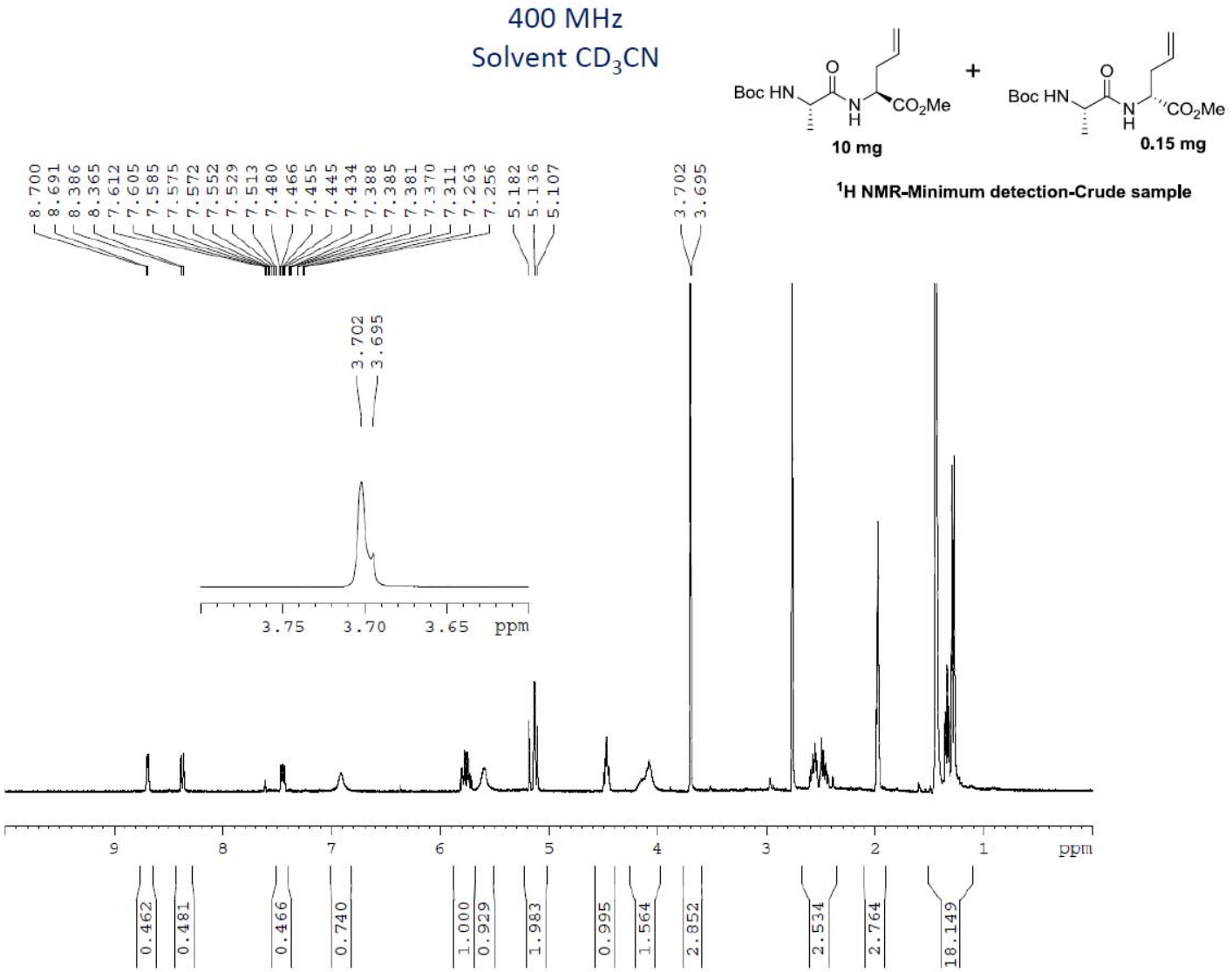
400 MHz
Solvent CD_3CN
Boc HN
CO_2Me
10 mg
+
Boc HN
CO_2Me
0.15 mg
^{1}H NMR-Minimum detection-Crude sample
8.700
8.691
8.386
8.365
7.612
7.605
7.585
7.575
7.572
7.552
7.529
7.513
7.480
7.466
7.455
7.445
7.434
7.388
7.385
7.381
7.370
7.311
7.263
7.256
5.182
5.136
5.107
3.702
3.695
3.75
3.70
3.65
ppm
9
8
7
6
5
4
3
2
1
ppm
0.462
0.481
0.466
0.740
1.000
0.929
1.983
0.995
1.564
2.852
2.534
2.764
18.149

^{1}H NMR 400 MHz
Solvent: CD_3CN

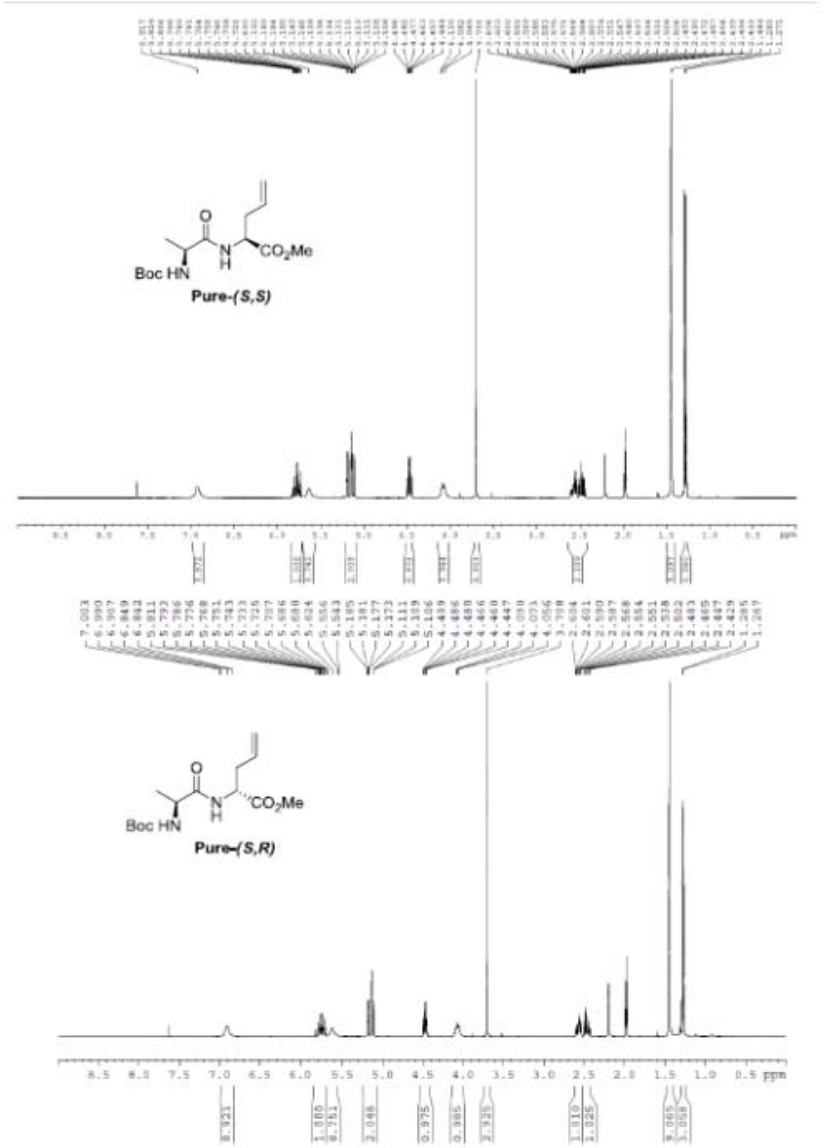

Laboratoire d'Analyse Élémentaire de l'Université de Montréal
Université de Montréal, Dépt. Chimie, Pavillon Roger-Gaudry, local A637 ou A634
2900 Edouard-Montpetit, Montréal (Qc), H3T 3J4

Tél. (514) 343-6111 ext. 3274 ou 3937

Dr. William D. Lubell, 18 févr. 2014

Voici les résultats d'analyses (C,H,N,S) pour l'échantillon soumis par Nagavenkata Durga prasad. A (LUB231).

Dossier:	LUB231
Identification de l'échantillon:	PRA-Boc-Allylgly
Formule moléculaire:	C11H19NO4
Nom de chimiste:	Nagavenkata Durga prasad. A
Nom de responsable:	William D. Lubell

Sample Name	% Nitrogen	% Carbon	% Hydrogen	% Sulphur
LUB231-1	5.91	57.04	8.45	0.00
LUB231-2	5.93	57.13	8.51	0.00

	% Nitrogen	% Carbon	% Hydrogen	% Sulphur
Moyenne	5.92	57.08	8.48	0.00
Théorie:	6.11	57.62	8.35	0.00

Technicienne:	Elena Nadezhina
Chimiste:	Francine Bélanger-Gariépy
Méthode utilisée:	140217E; Fisons
Date d'analyse:	February 18, 2014
Remarque:	The sample is liquid.

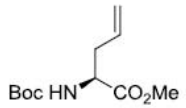

Chemical Formula: $C_{11}H_{19}NO_4$
Molecular Weight: 229.27
Elemental Analysis: C, 57.62; H, 8.35; N, 6.11; O, 27.91

^{1}H NMR 400 MHz
Solvent: $CDCl_3$

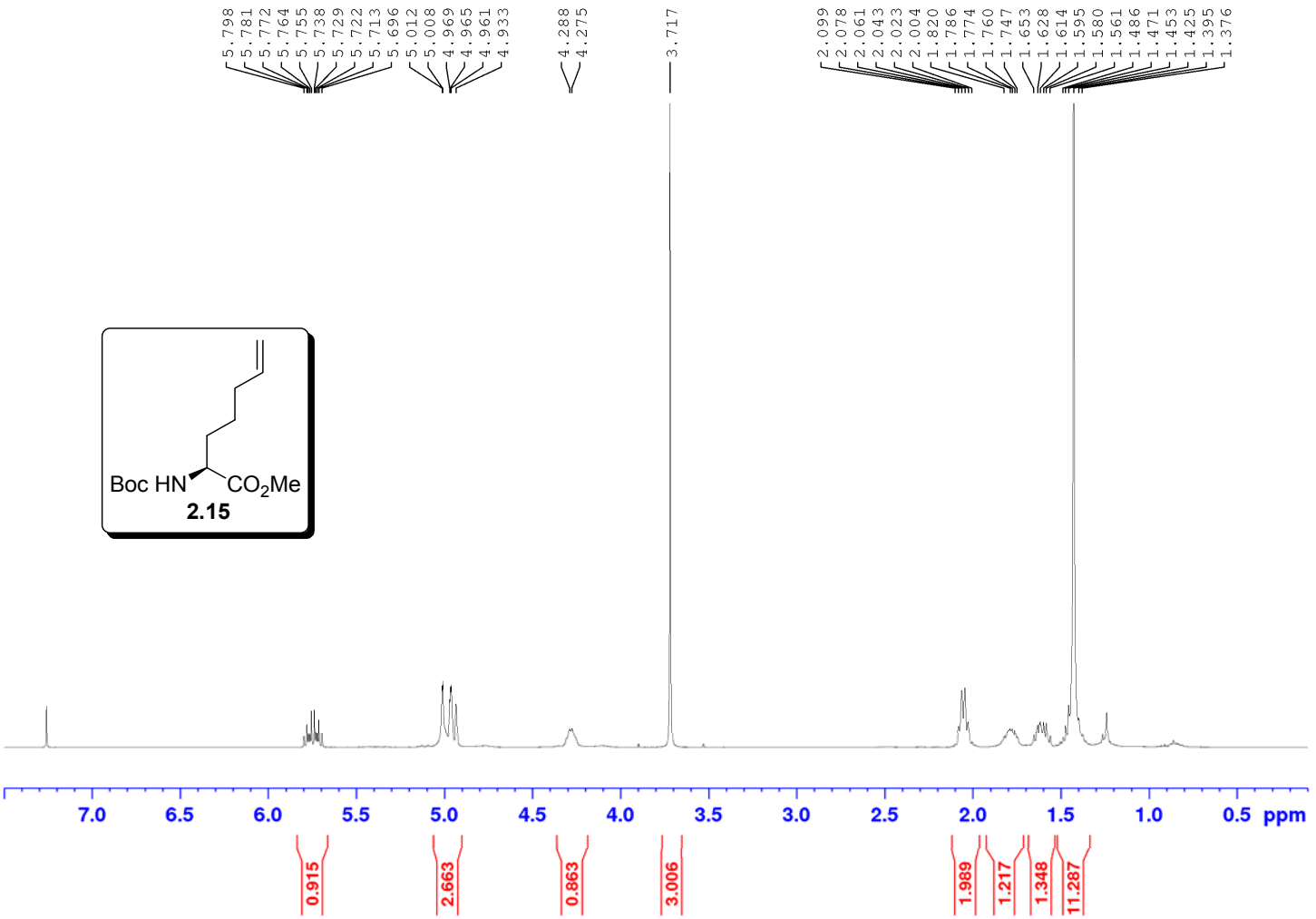

^{13}C NMR 400 MHz
Solvent: $CDCl_3$

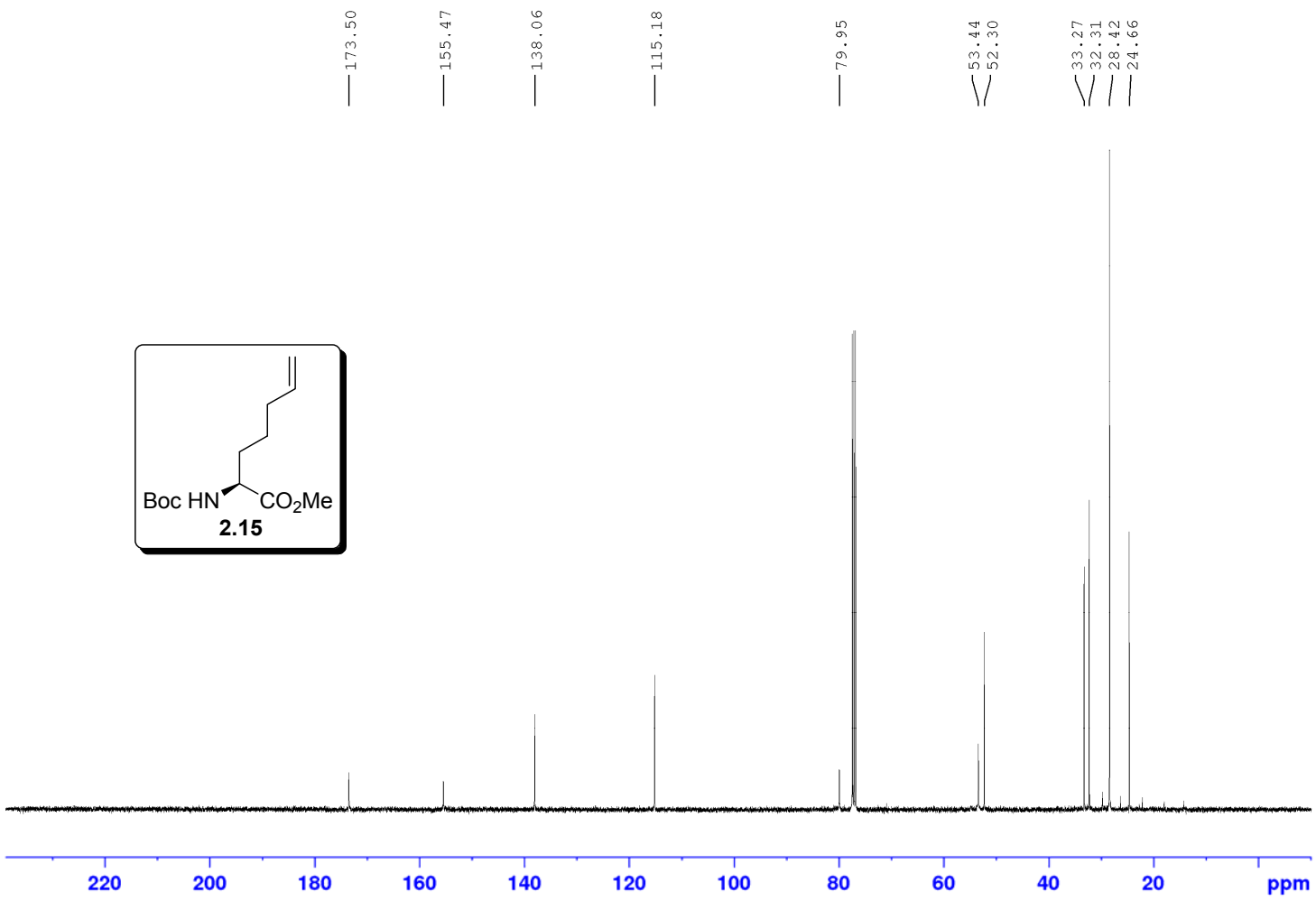

^{1}H NMR 700 MHz
Solvent: CD_3CN

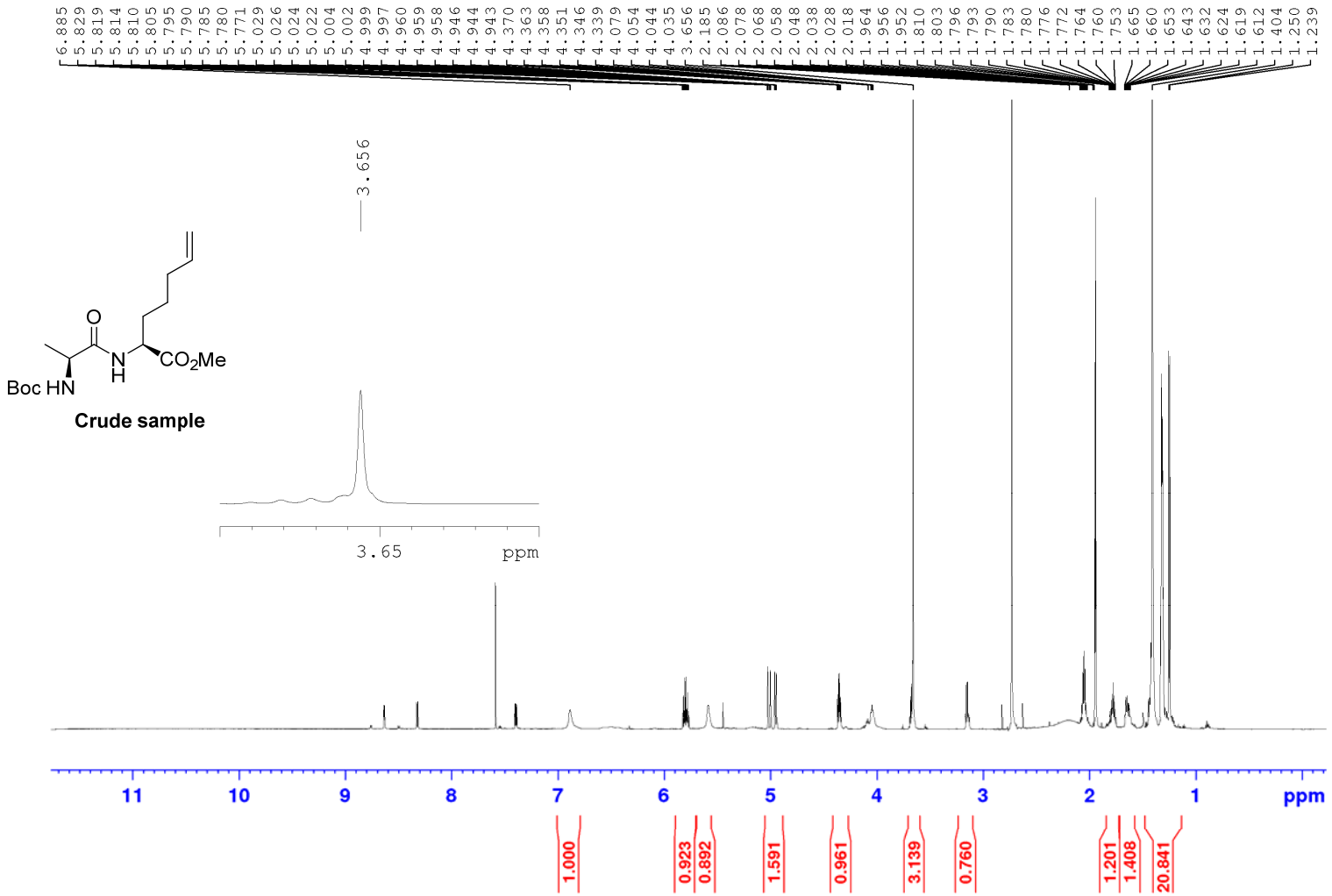

^{1}H NMR 700 MHz
Solvent: CD_3CN

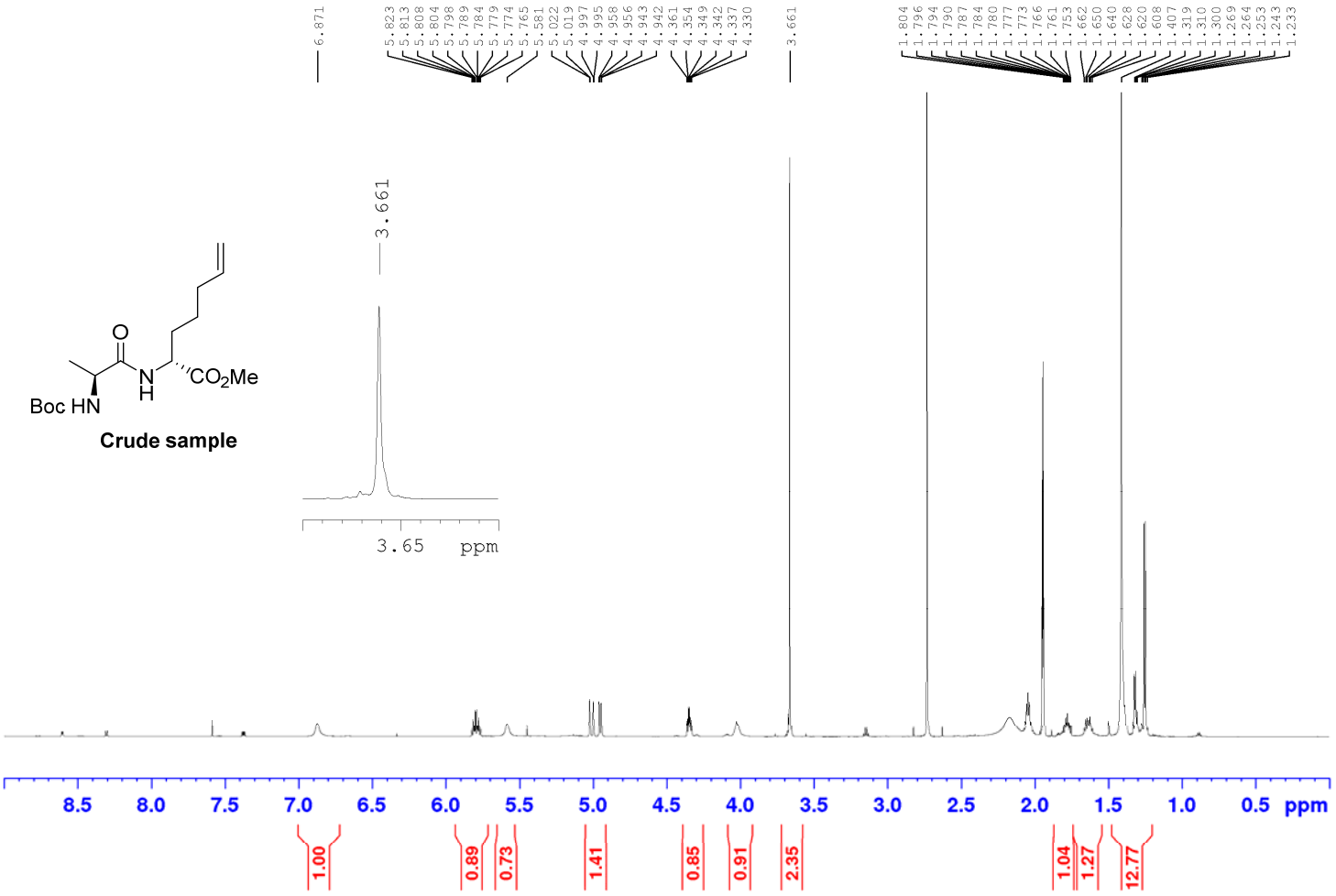

^{1}H NMR 700 MHz
Solvent: CD_3CN

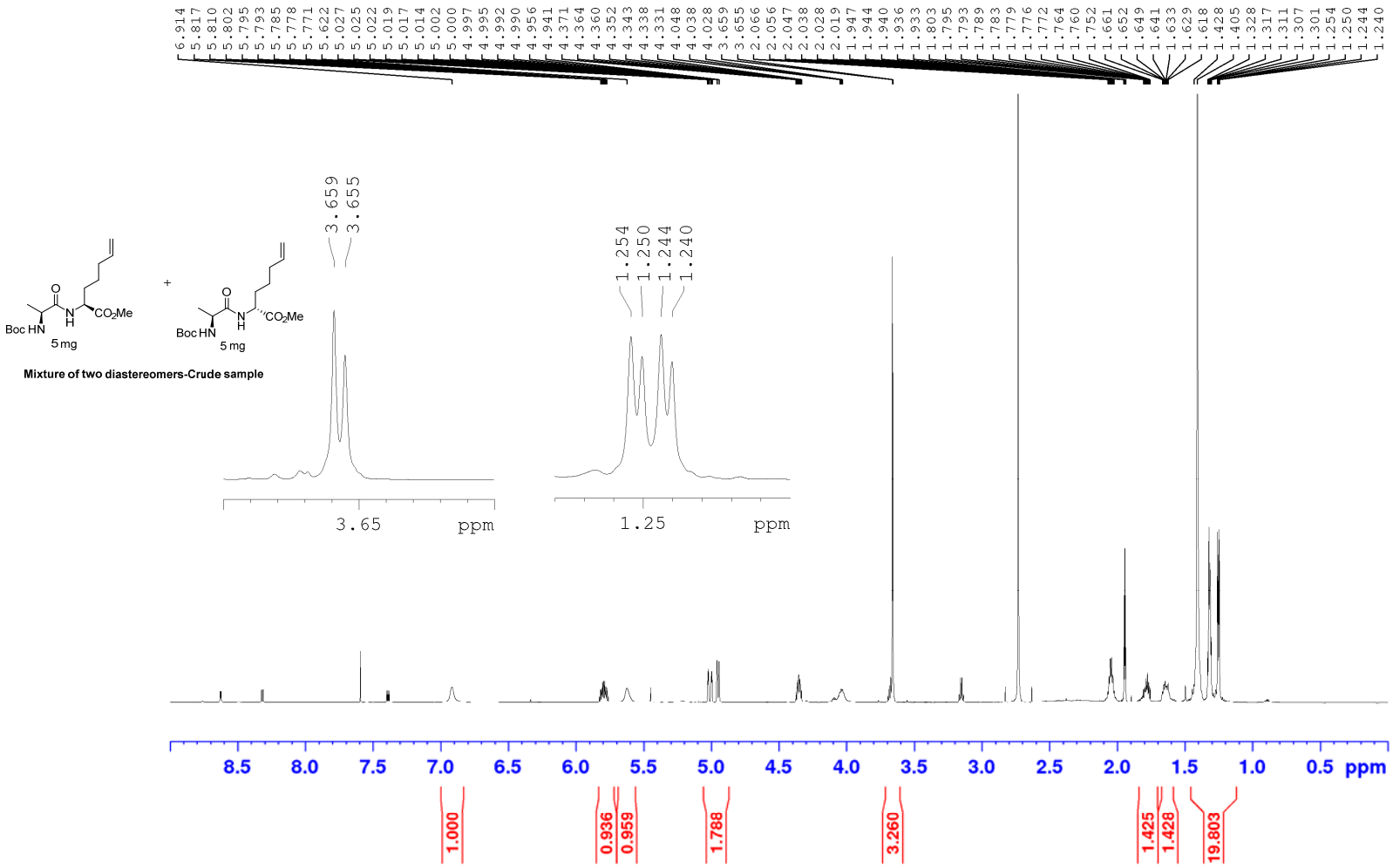

^{1}H NMR 700 MHz
Solvent: CD_3CN

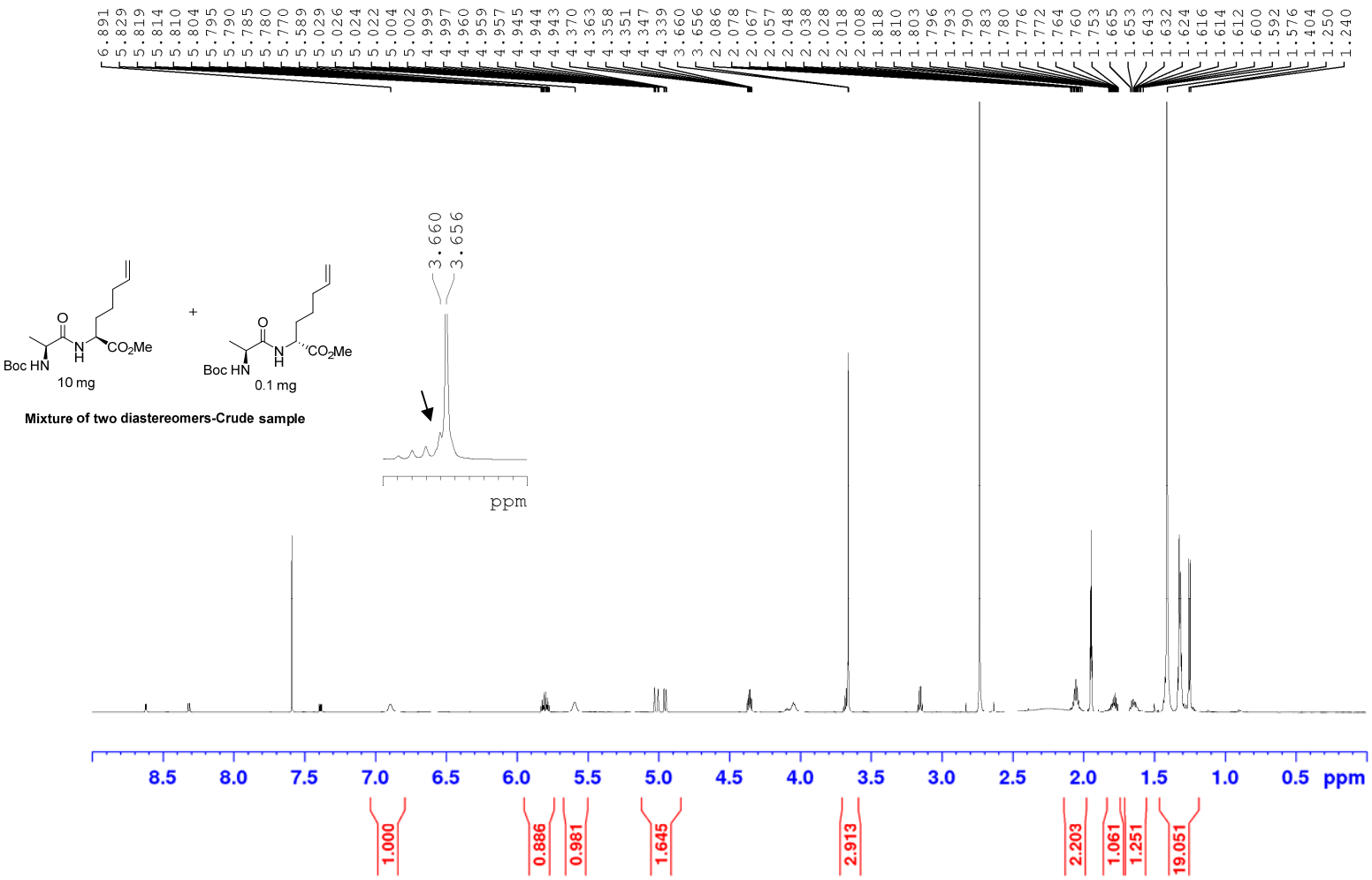

^{1}H NMR 700 MHz
Solvent: CD_3CN

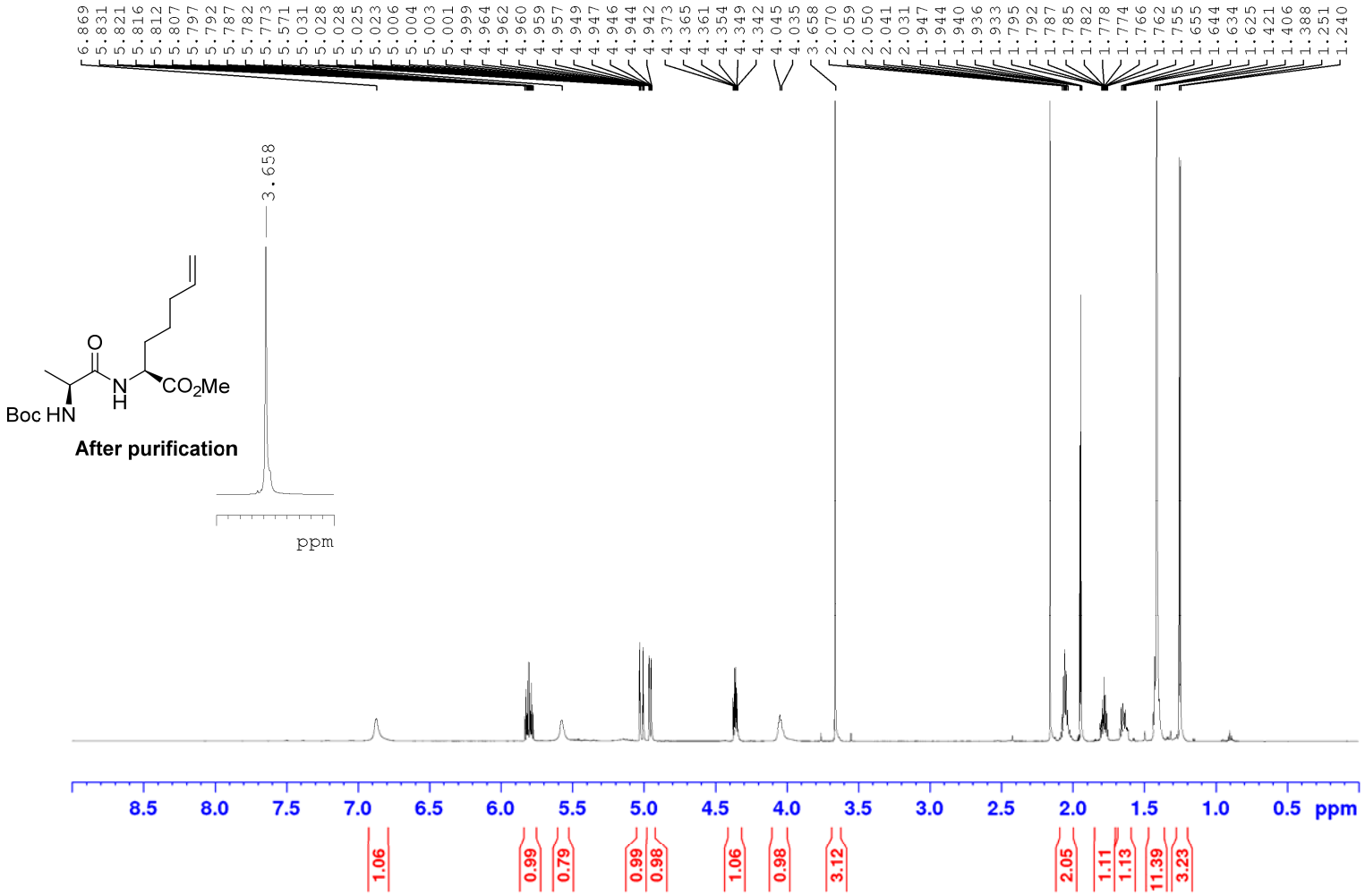

^{1}H NMR 700 MHz
Solvent: CD_3CN

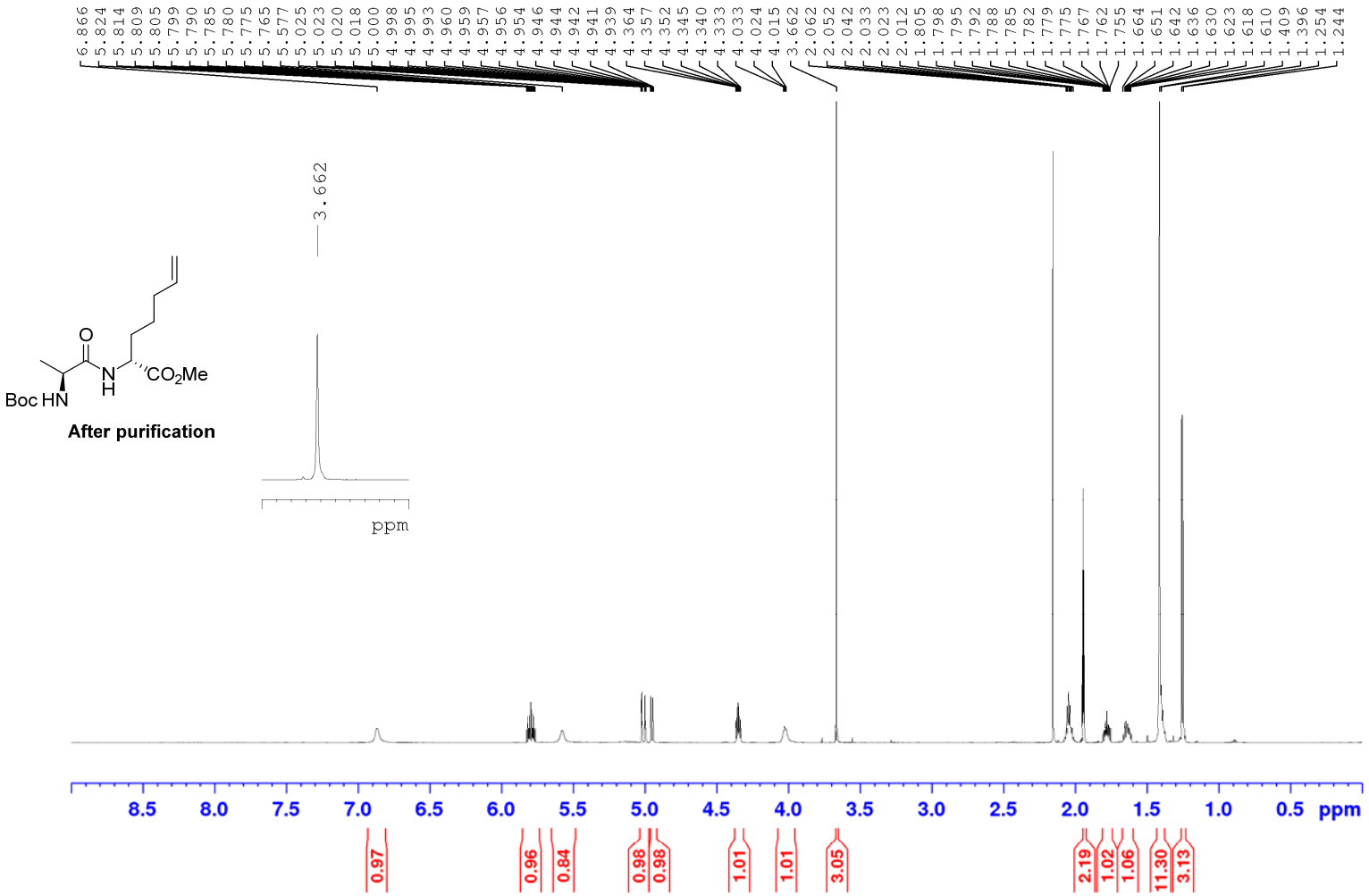

^{1}H NMR 700 MHz
Solvent: CD_3CN

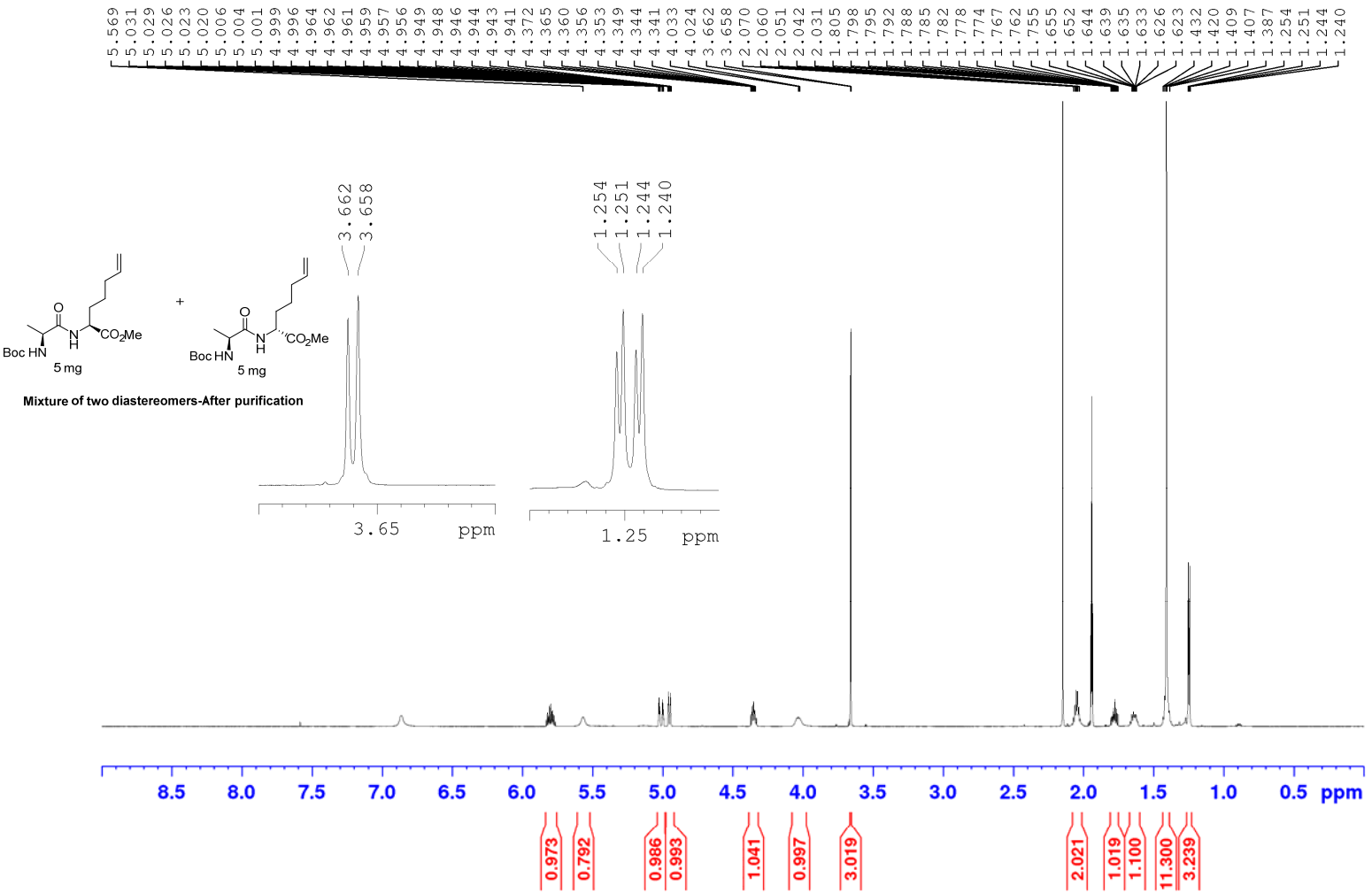

^{1}H NMR 400 MHz
Solvent: CD_3OD

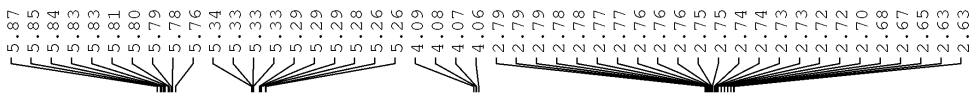

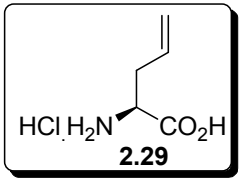

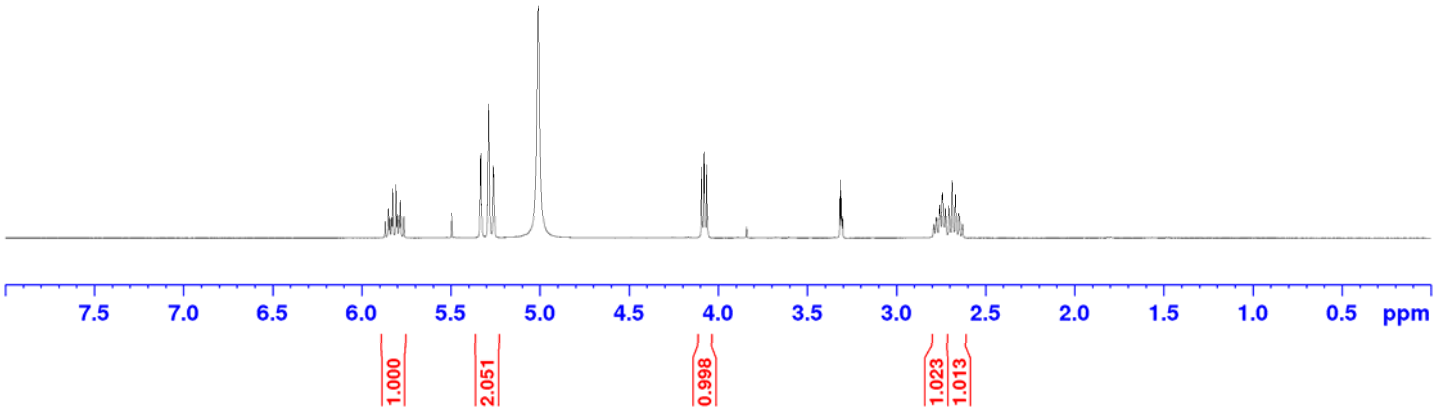

^{13}C NMR 400 MHz
Solvent: CD_3OD

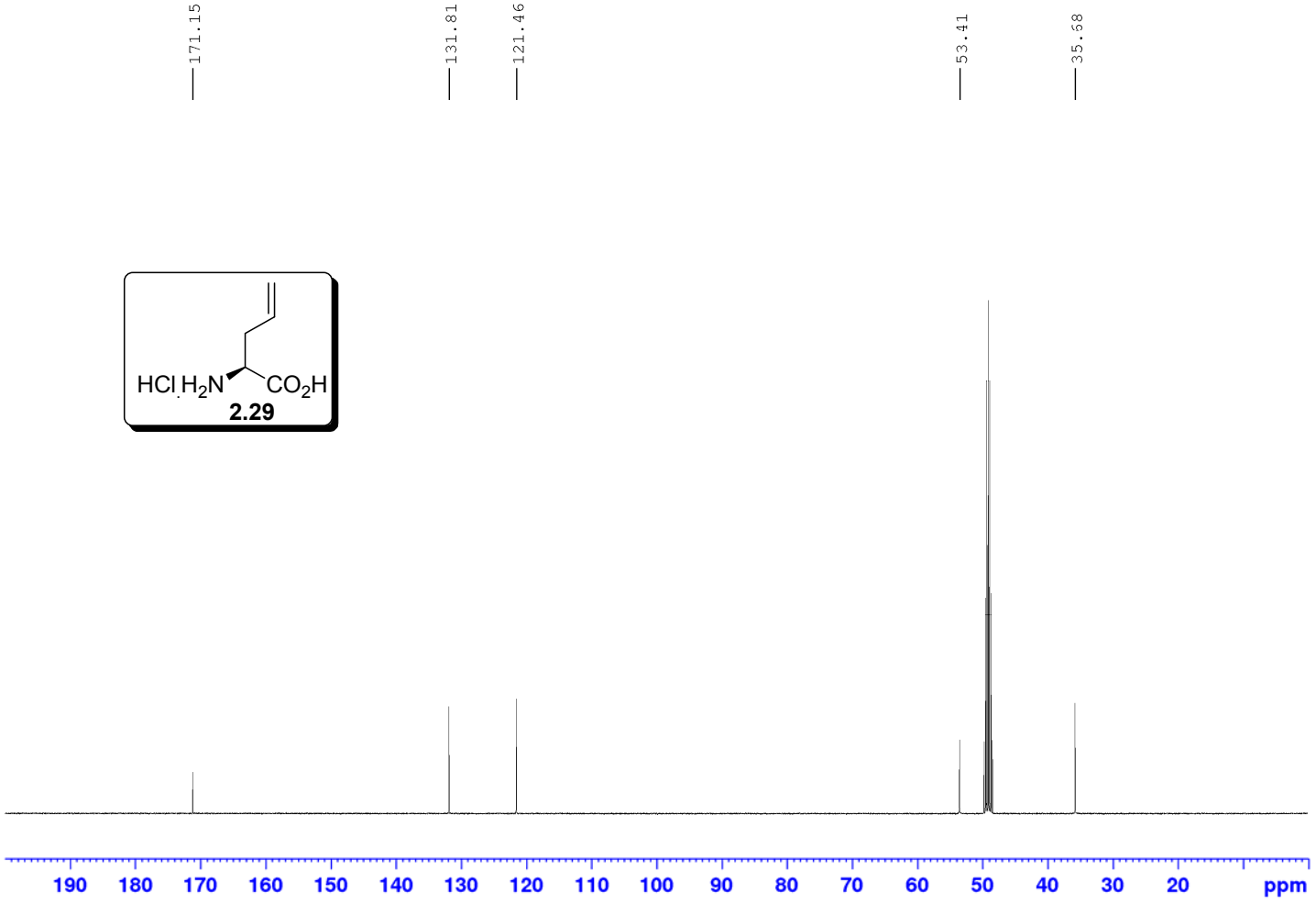

^{1}H NMR 500 MHz
Solvent: CD_3OD

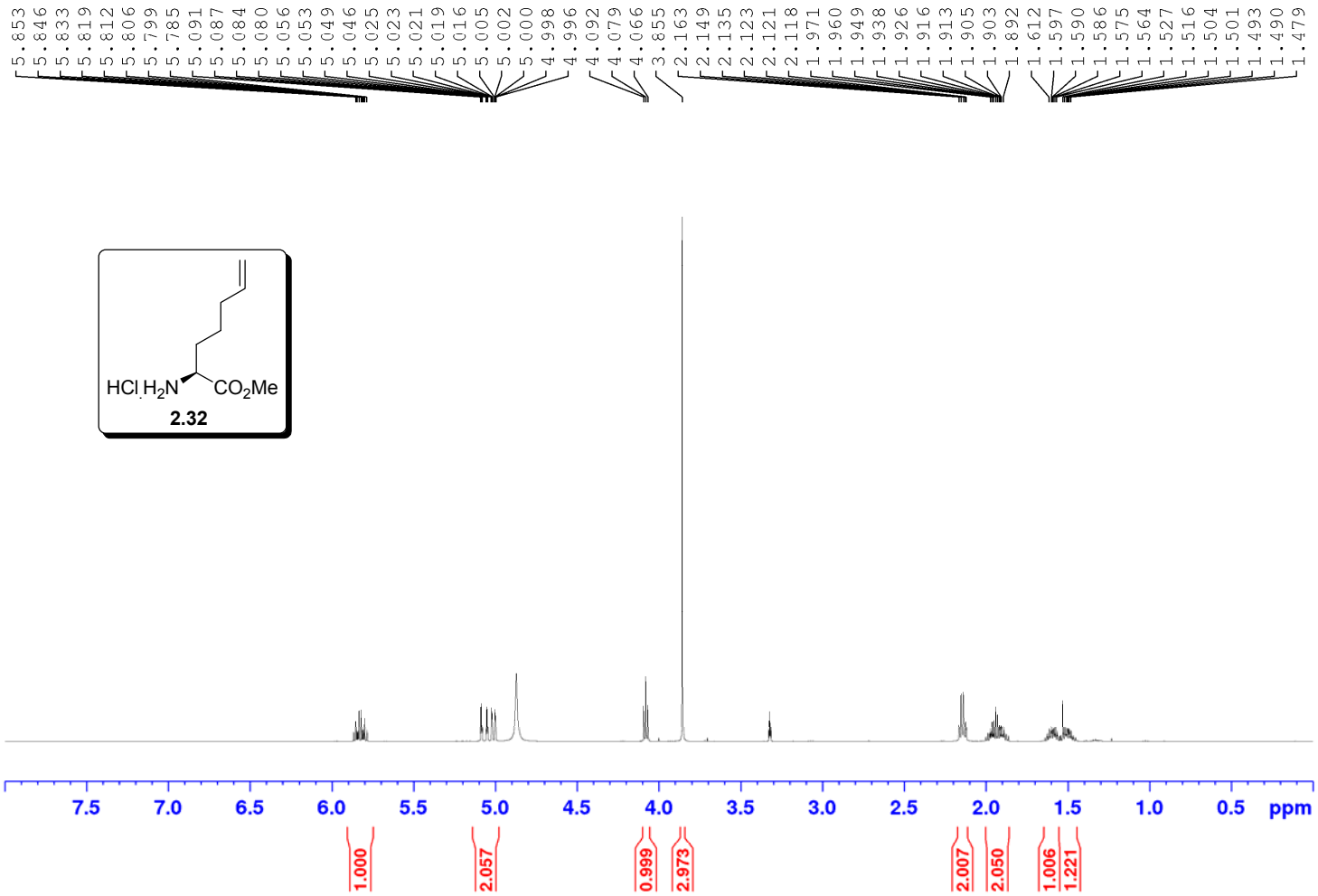

^{13}C NMR 500 MHz
Solvent: CD_3OD

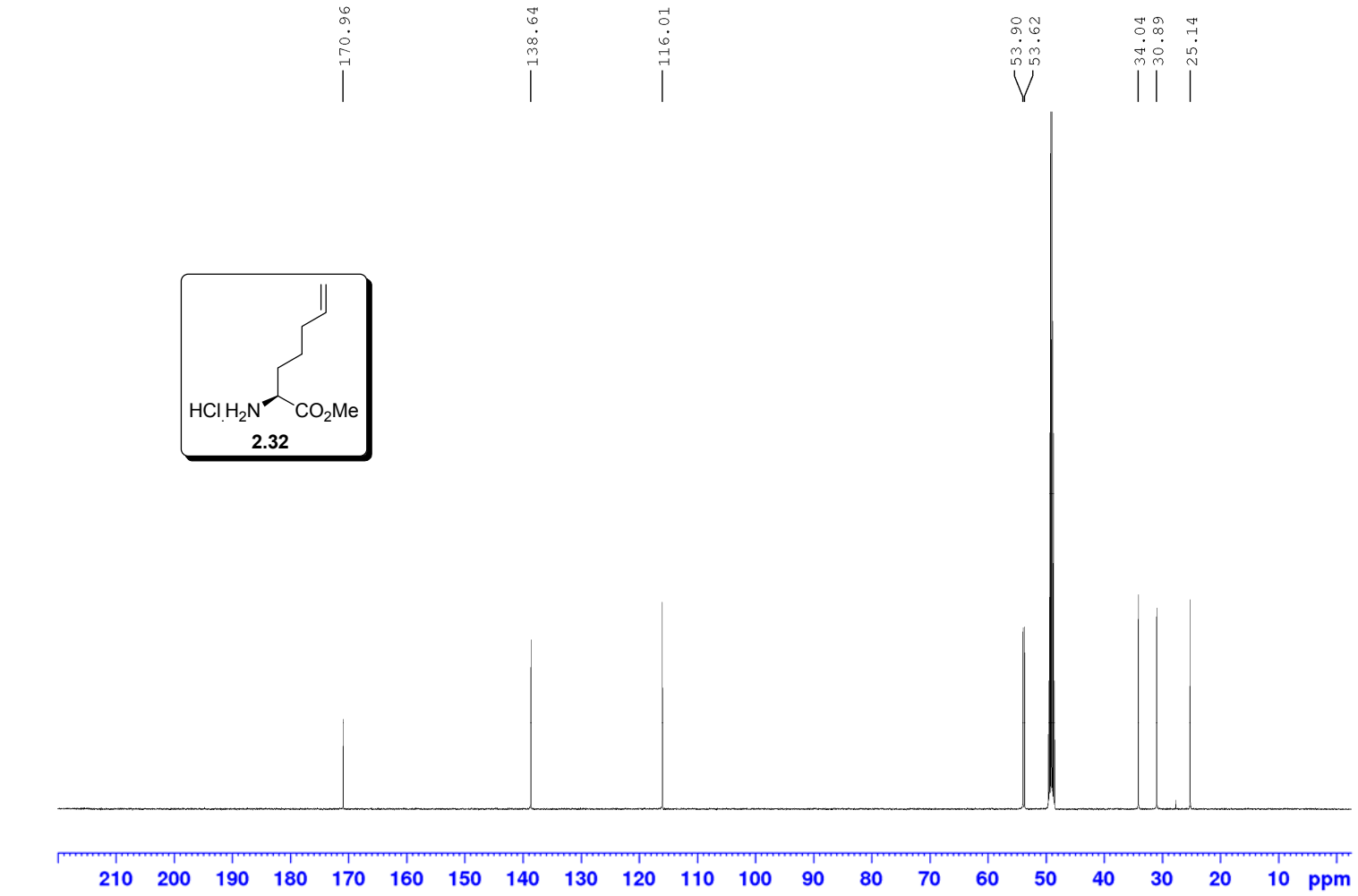

^{1}H NMR 500 MHz
Solvent: $CDCl_3$

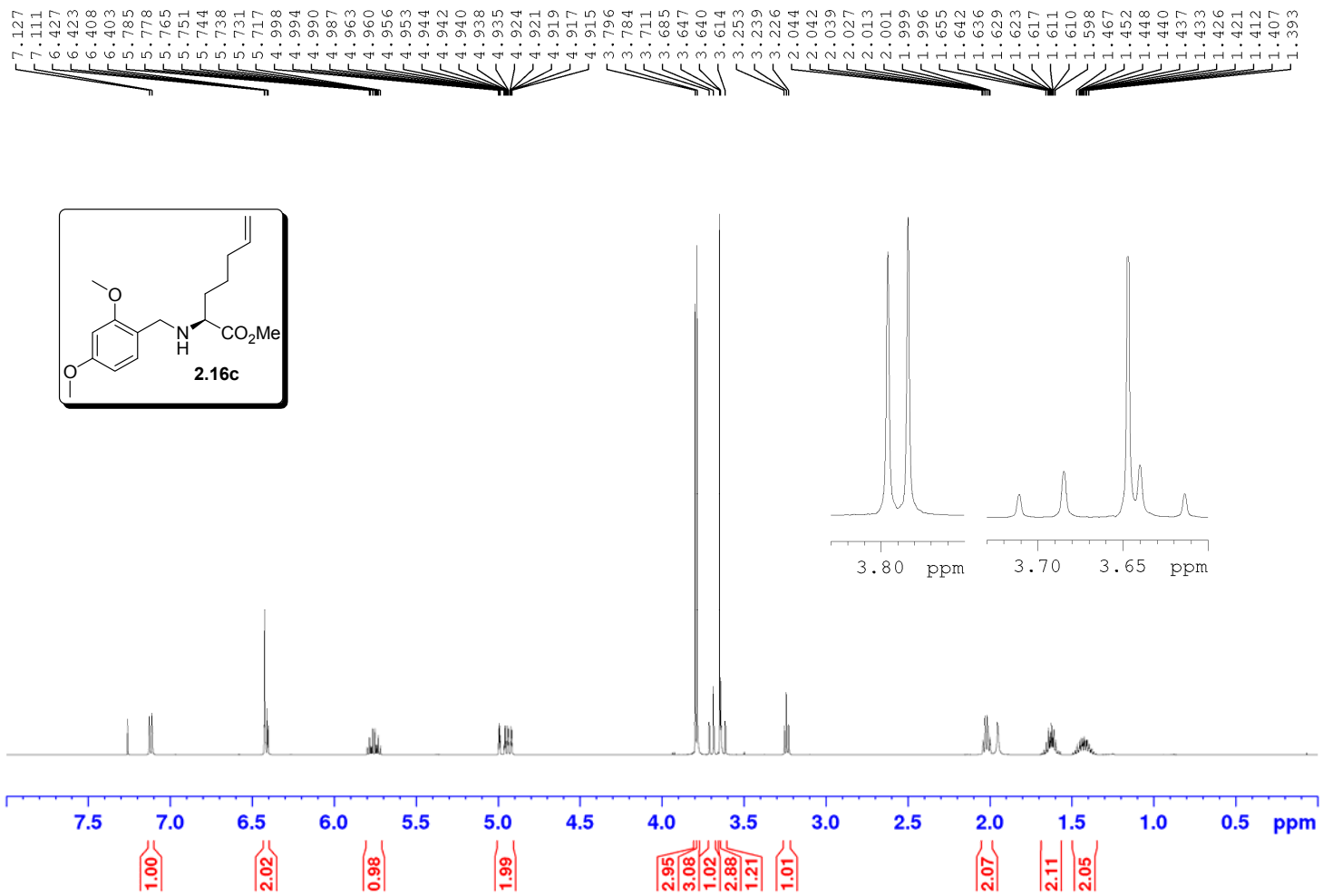

^{13}C NMR 500 MHz
Solvent: $CDCl_3$

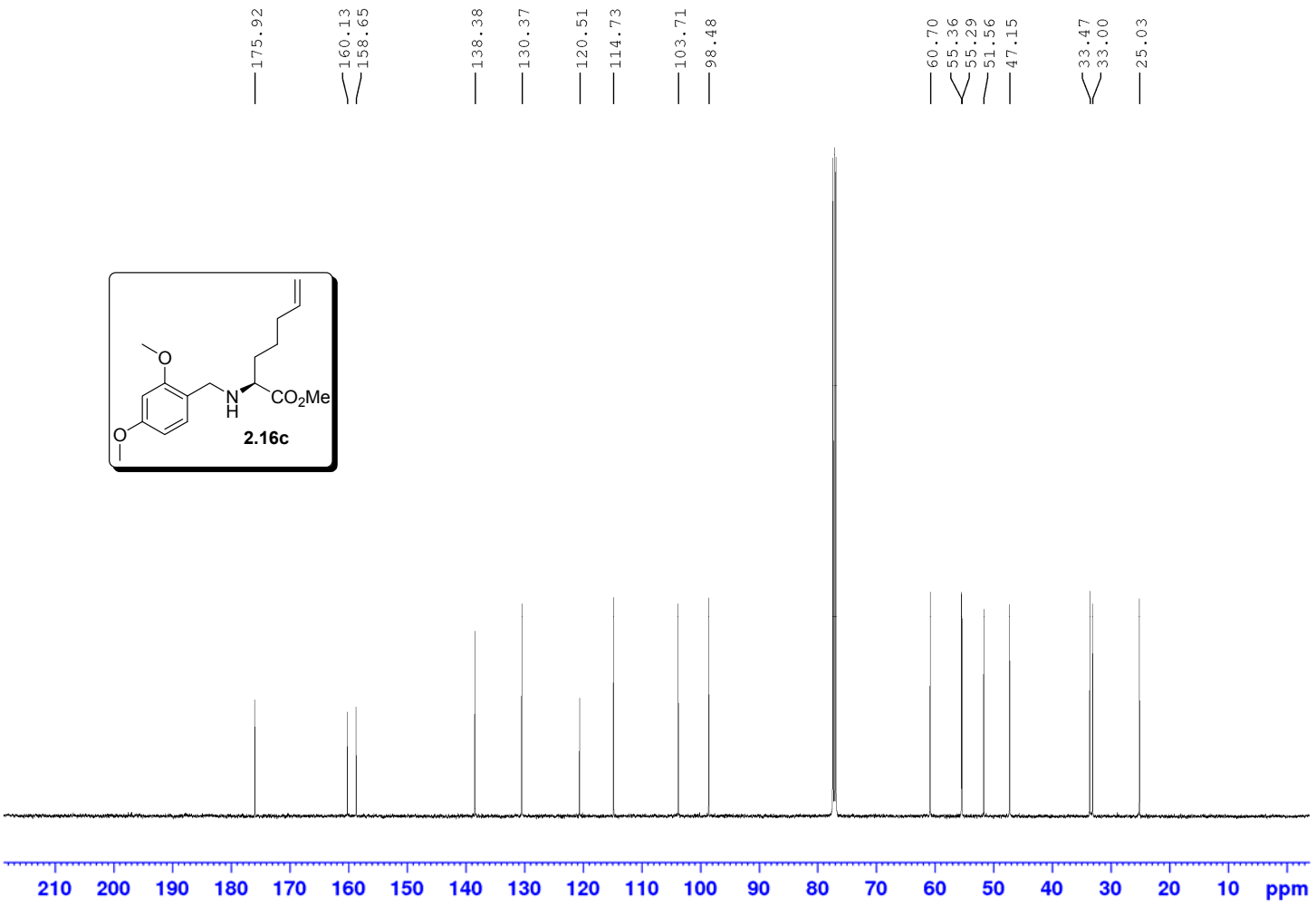

^{1}H NMR 500 MHz
Solvent: CD_3OD

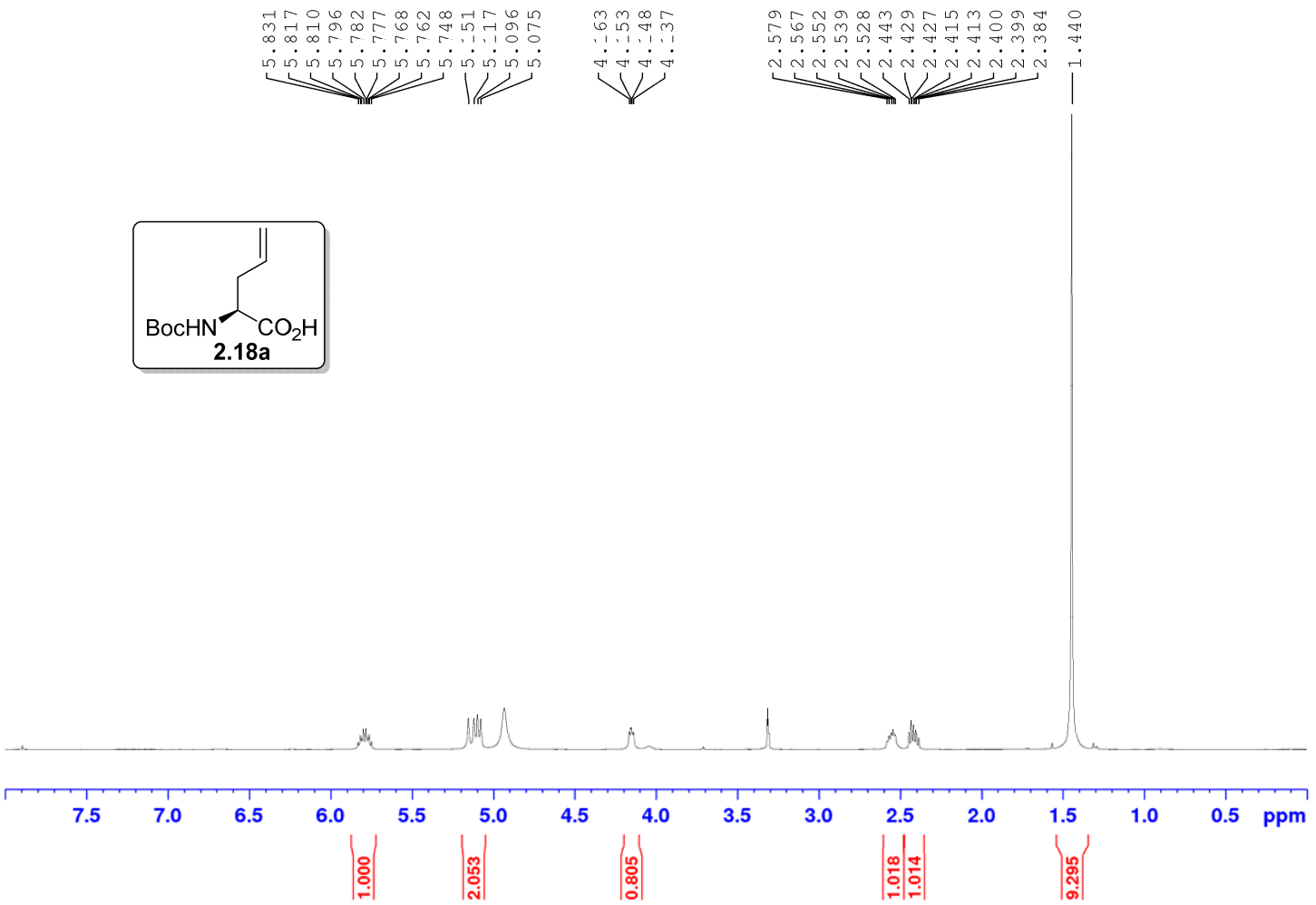

^{13}C NMR 500 MHz
Solvent: CD_3OD

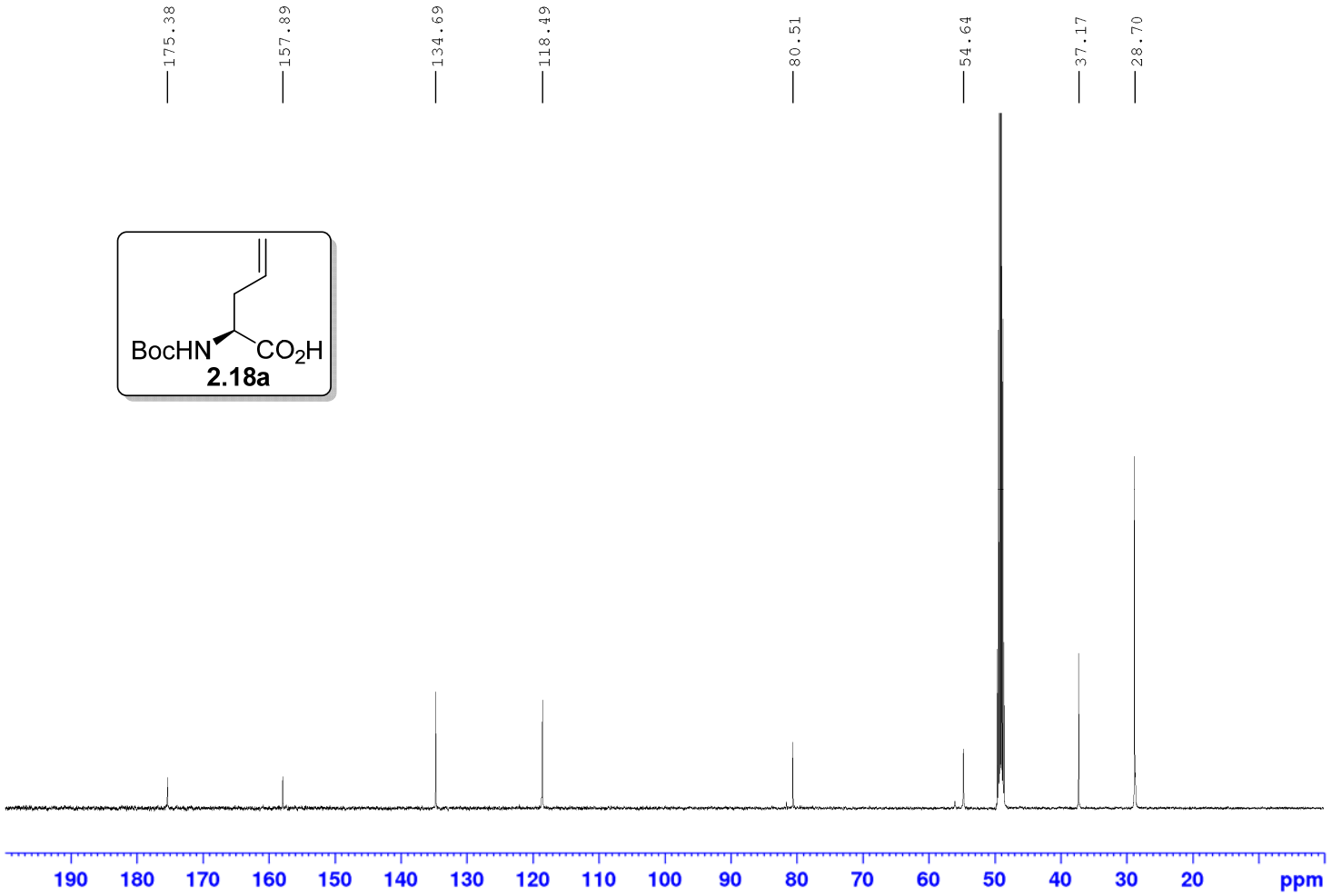

^{1}H NMR 500 MHz
Solvent: CD_3OD

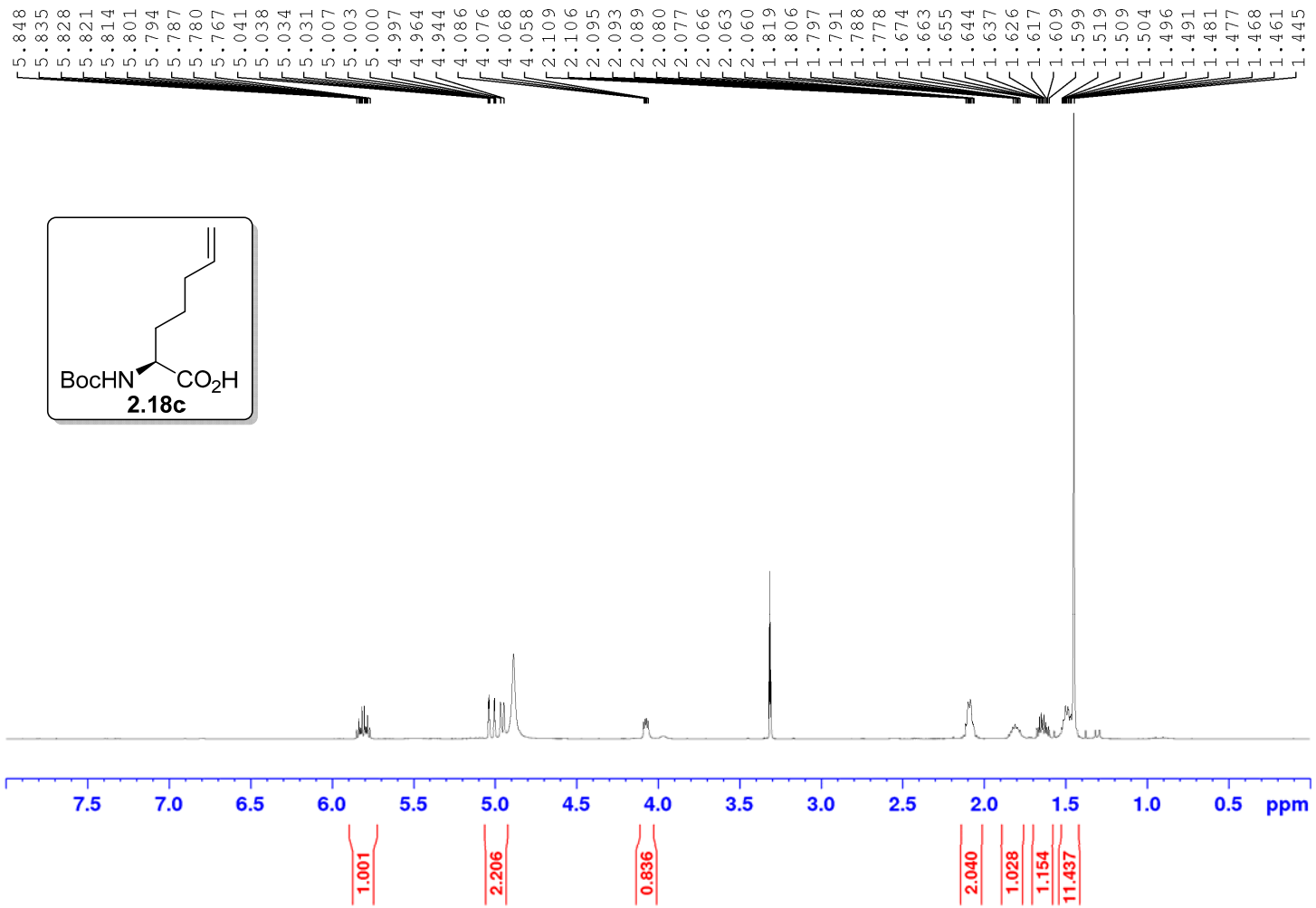

^{13}C NMR 500 MHz
Solvent: CD_3OD

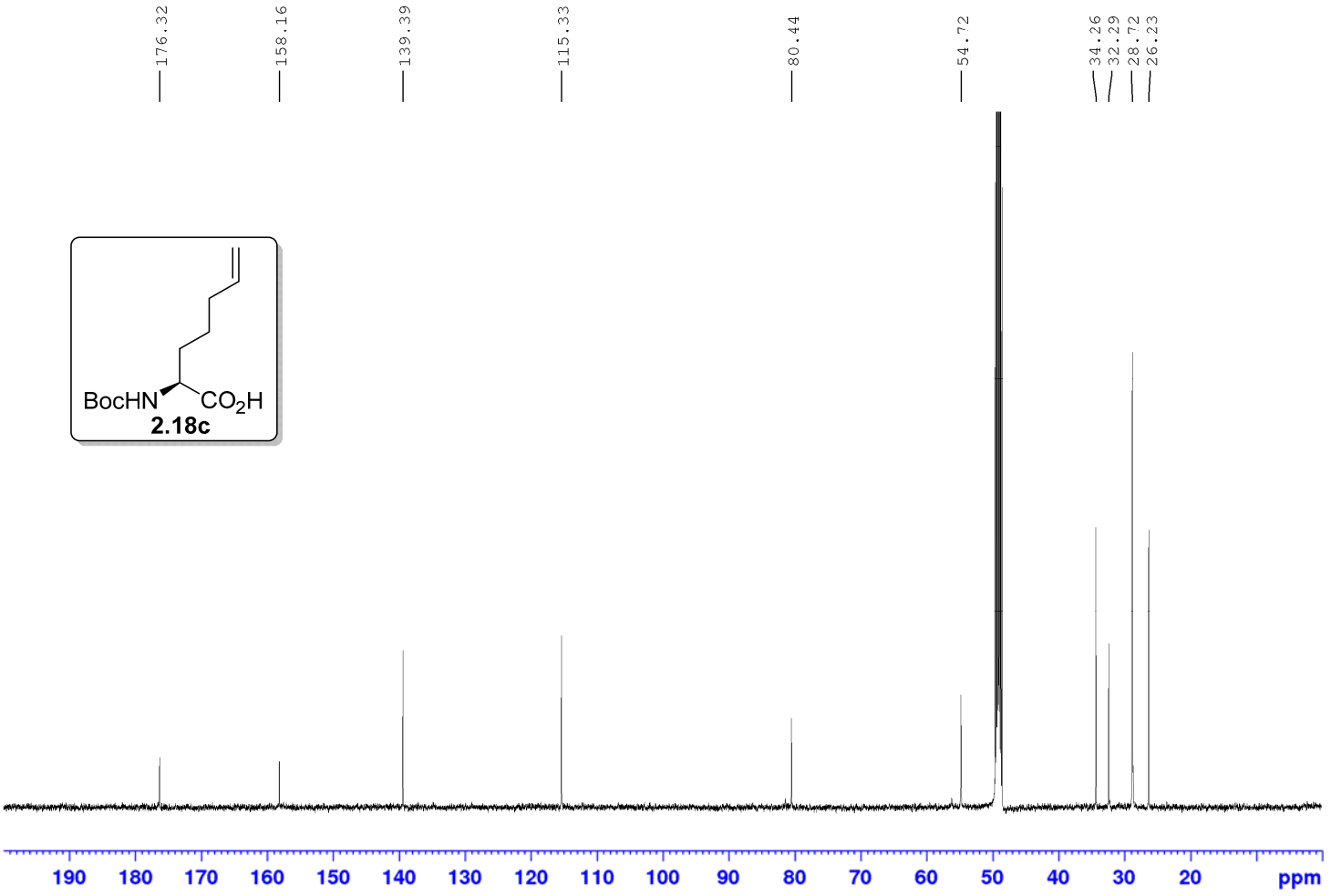

^{1}H NMR 500 MHz
Solvent: DMSO-d_6
**Spectrum was recorded at 100 ^{o}C*

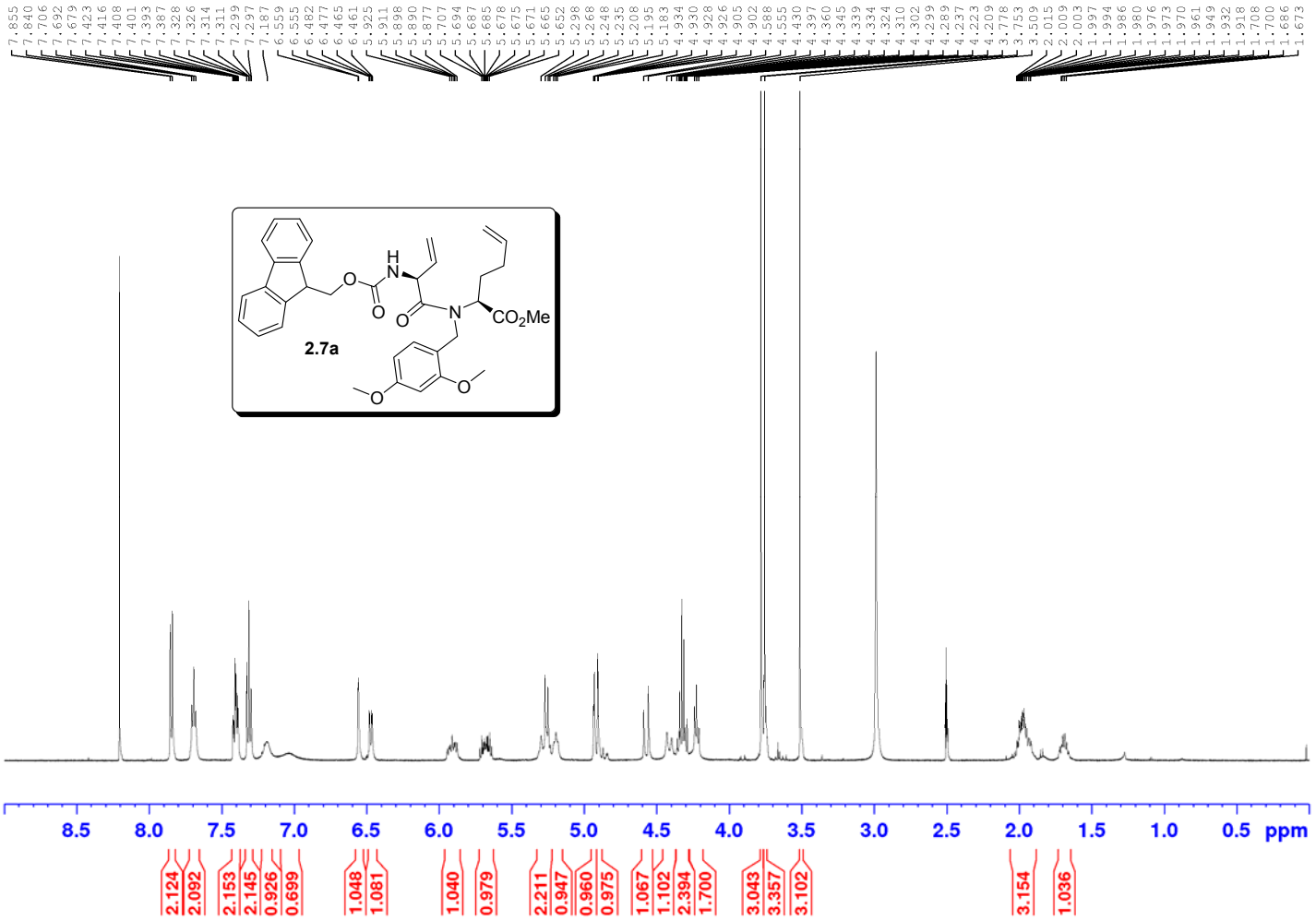

^{13}C NMR 500 MHz
Solvent: DMSO-d_6
**Spectrum was recorded at 100 ^{o}C*

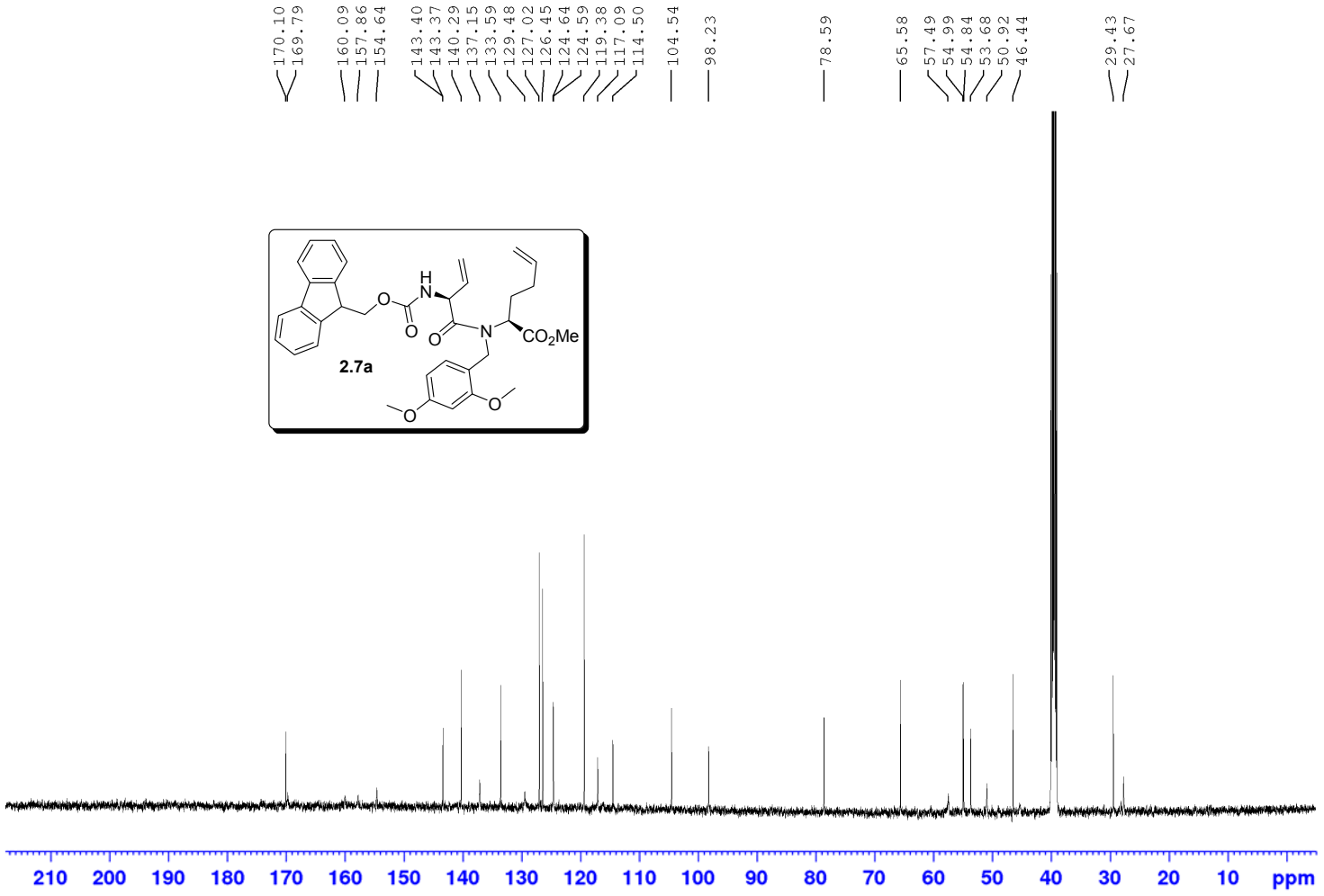

^{1}H NMR 500 MHz
Solvent: DMSO-d_6
**Spectrum was recorded at 100 °C*

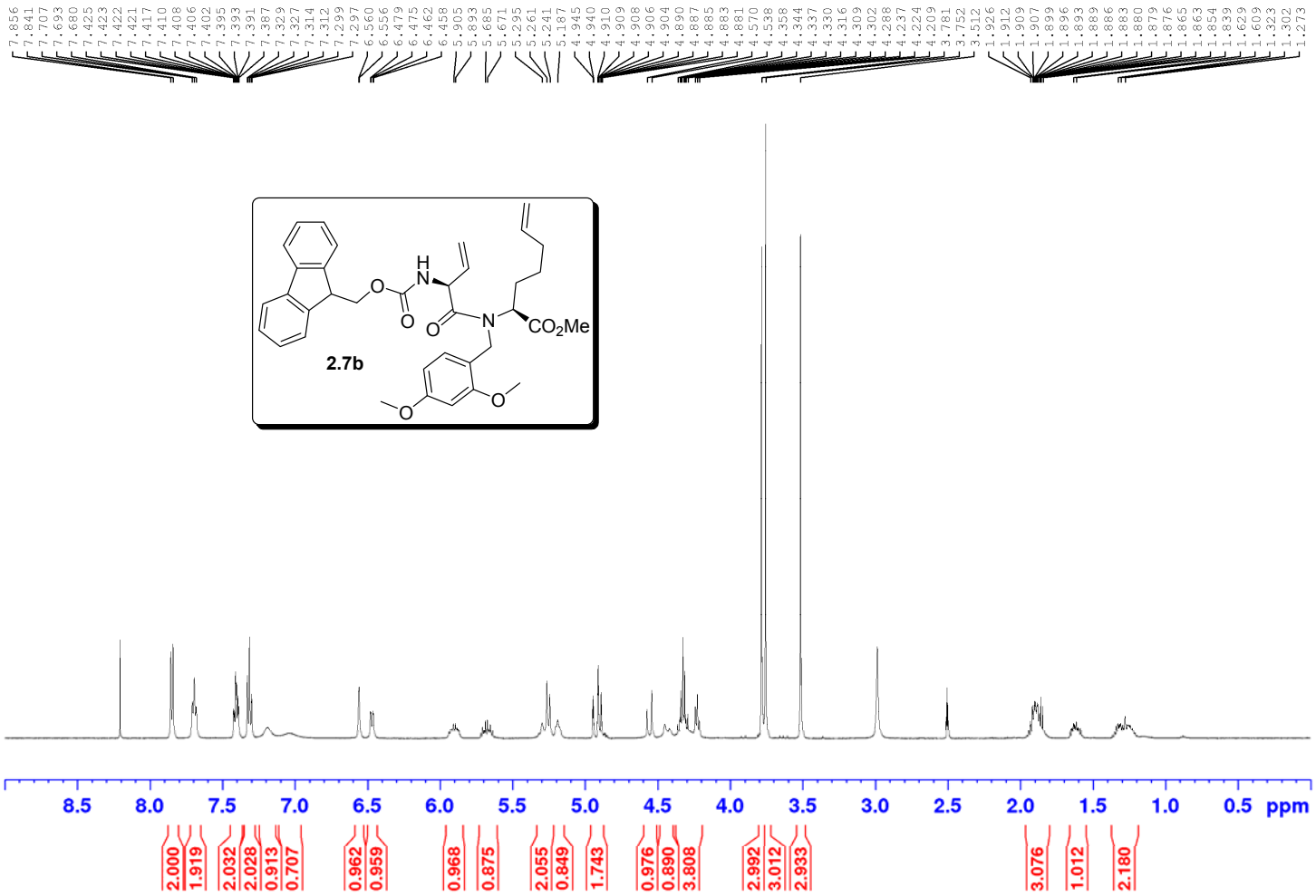

^{13}C NMR 500 MHz
Solvent: DMSO-d_6
**Spectrum was recorded at 100 °C*

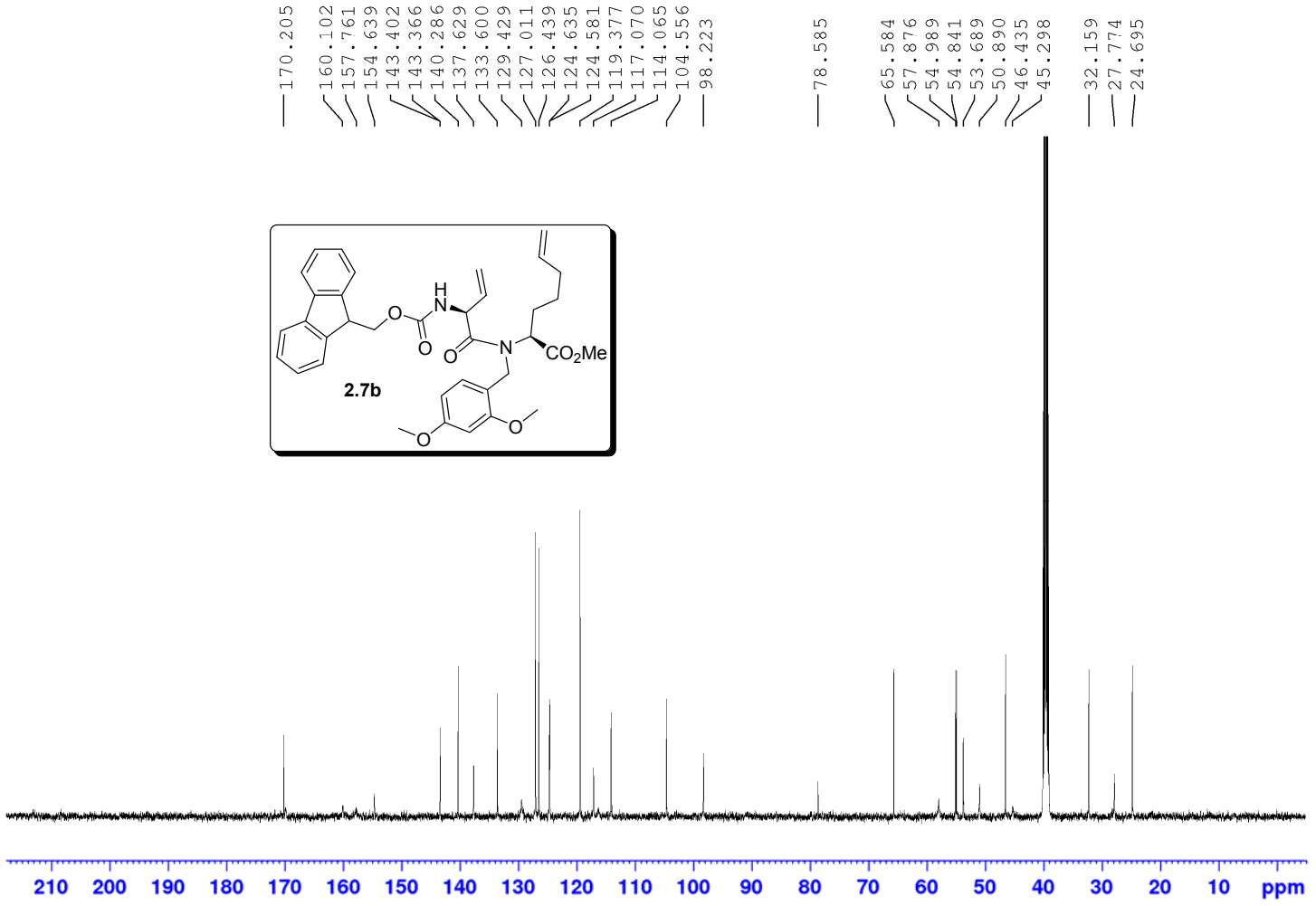

^{1}H NMR 500 MHz
Solvent: DMSO-d_6
**Spectrum was recorded at 100 ^{o}C*

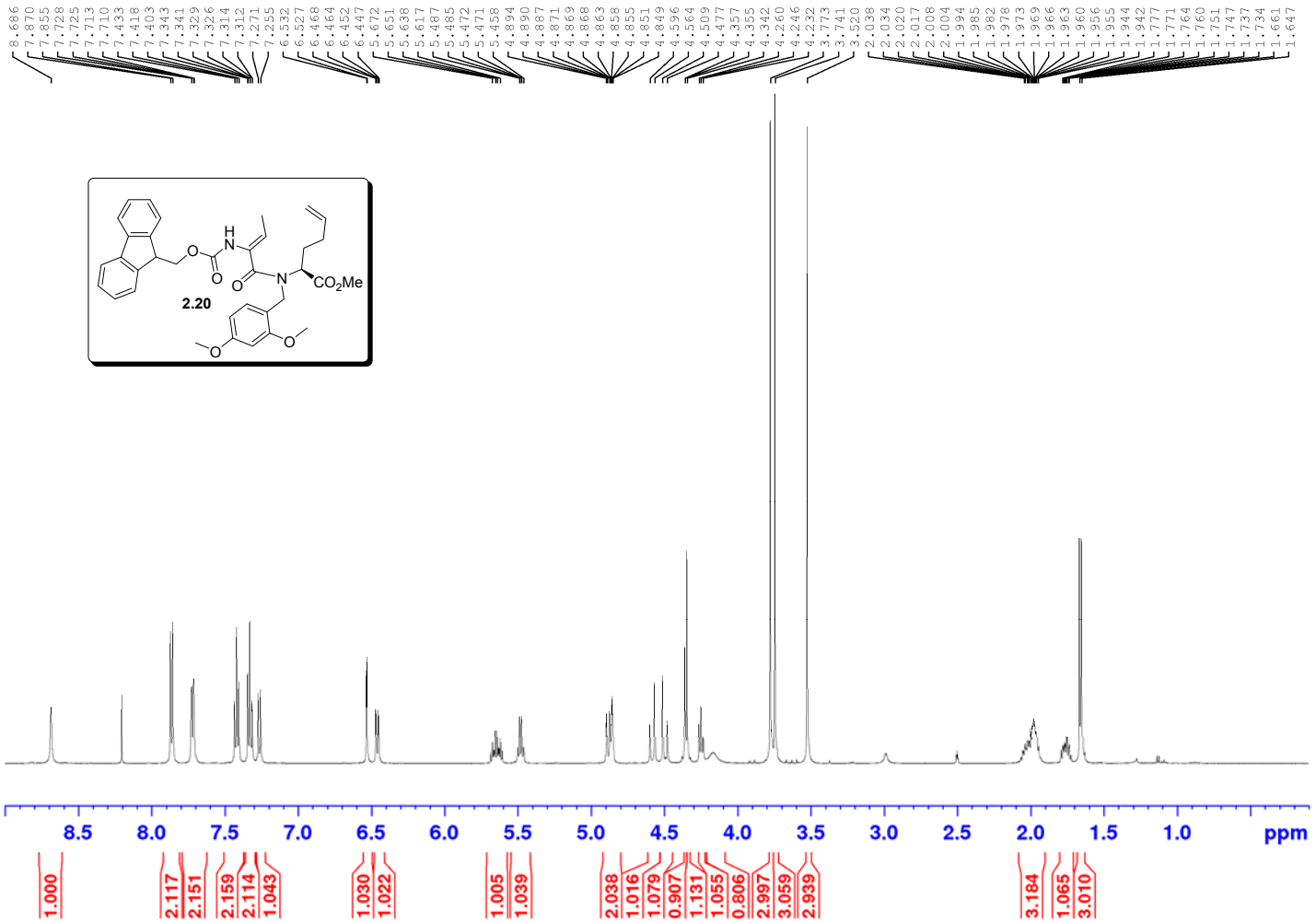

^{13}C NMR 500 MHz
Solvent: DMSO-d_6
**Spectrum was recorded at 100 ^oC*

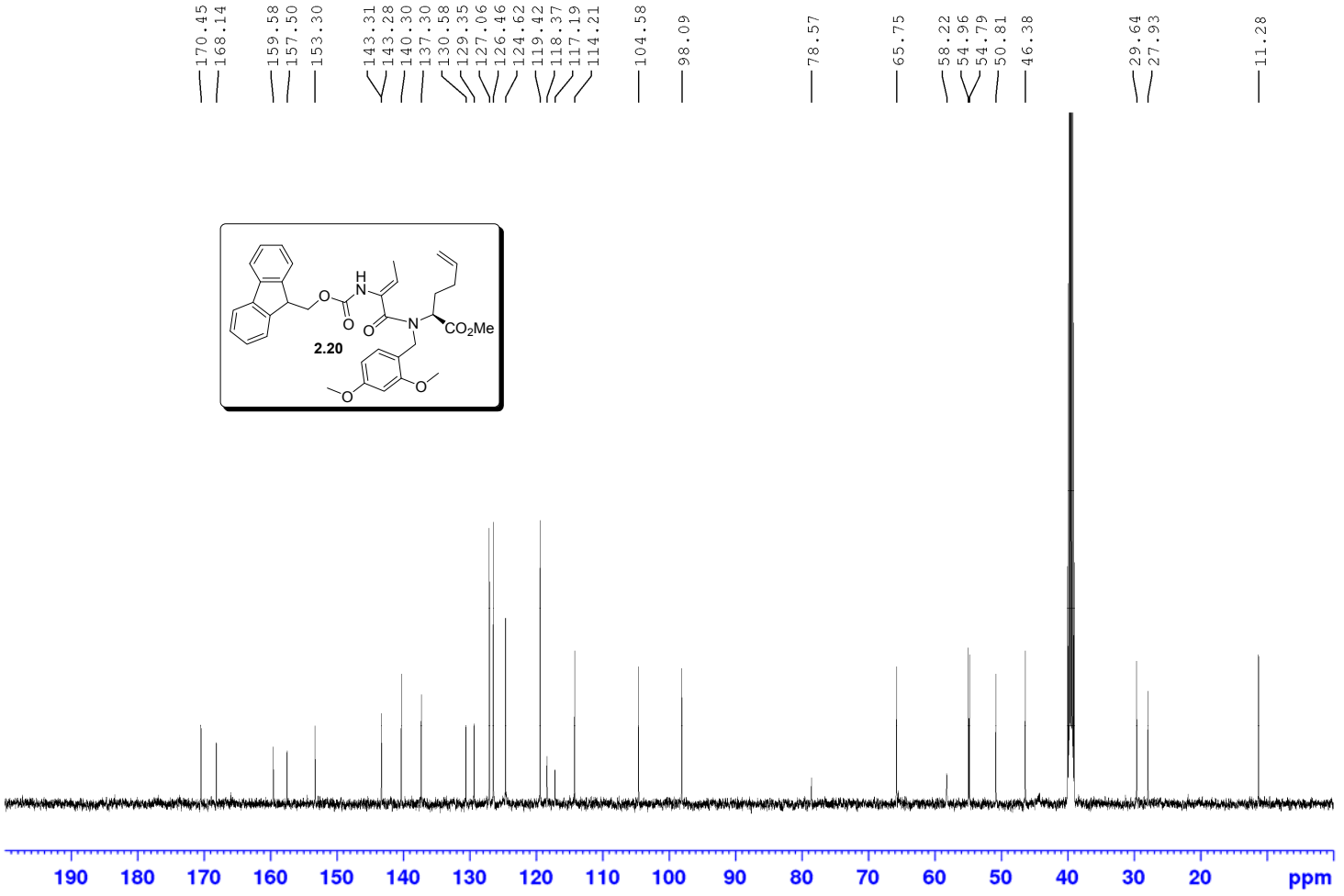

^{1}H NMR 500 MHz
Solvent: DMSO-d_6
**Spectrum was recorded at 100 °C*

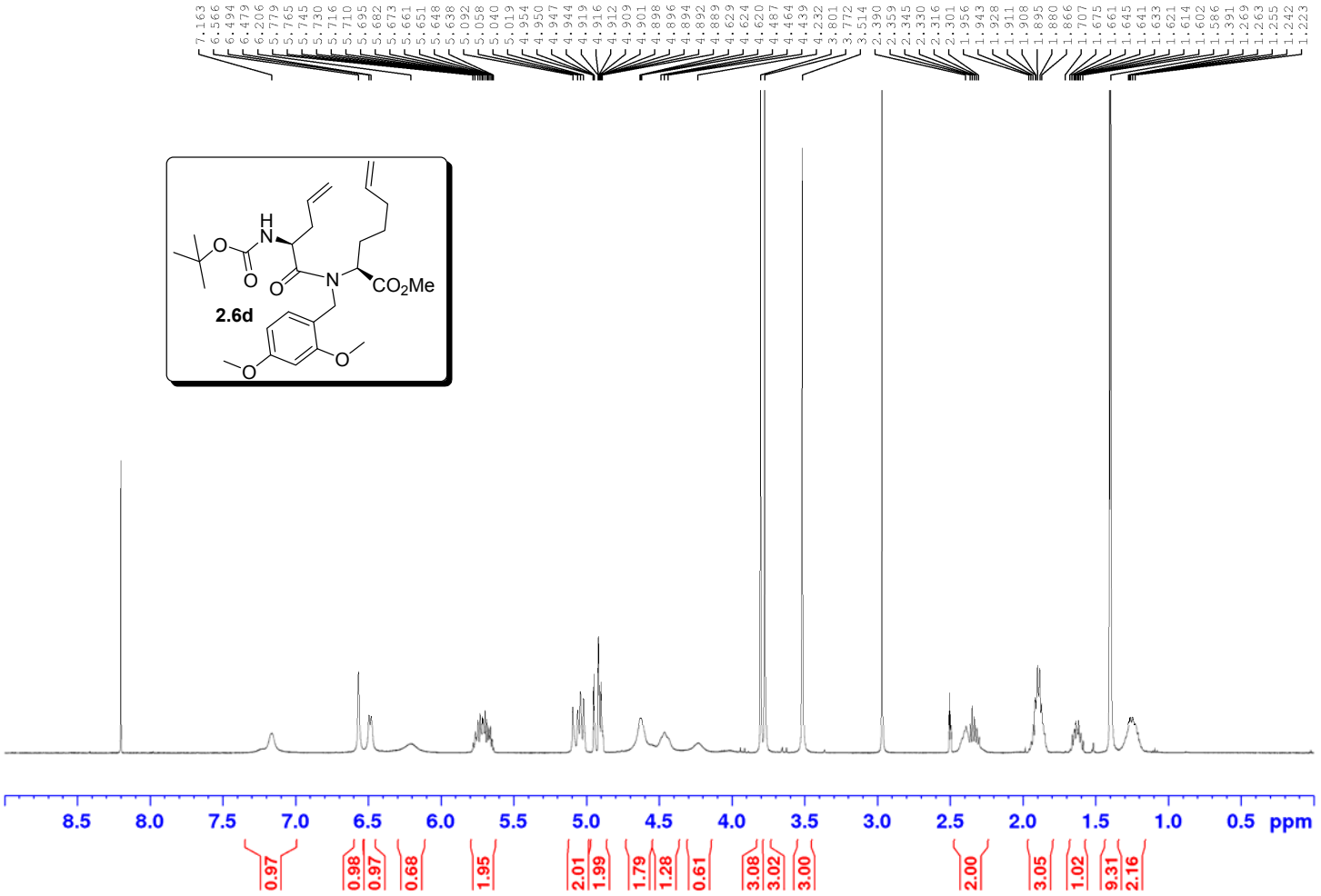

^{13}C NMR 500 MHz
Solvent: DMSO-d_6
**Spectrum was recorded at 100 ^{o}C*

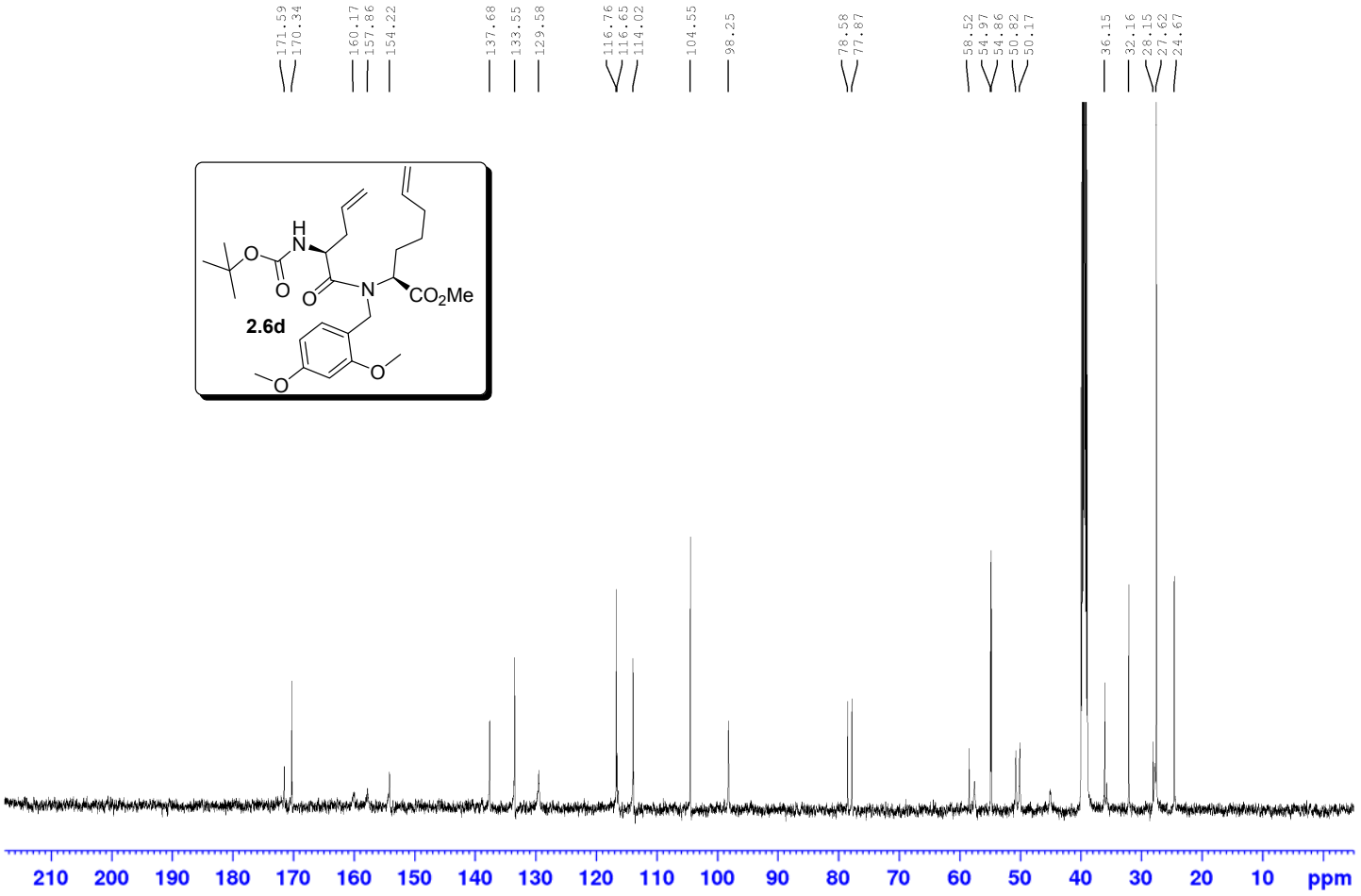

^{1}H NMR 500 MHz
Solvent: DMSO-d_6
**Spectrum was recorded at 100 ^{o}C*

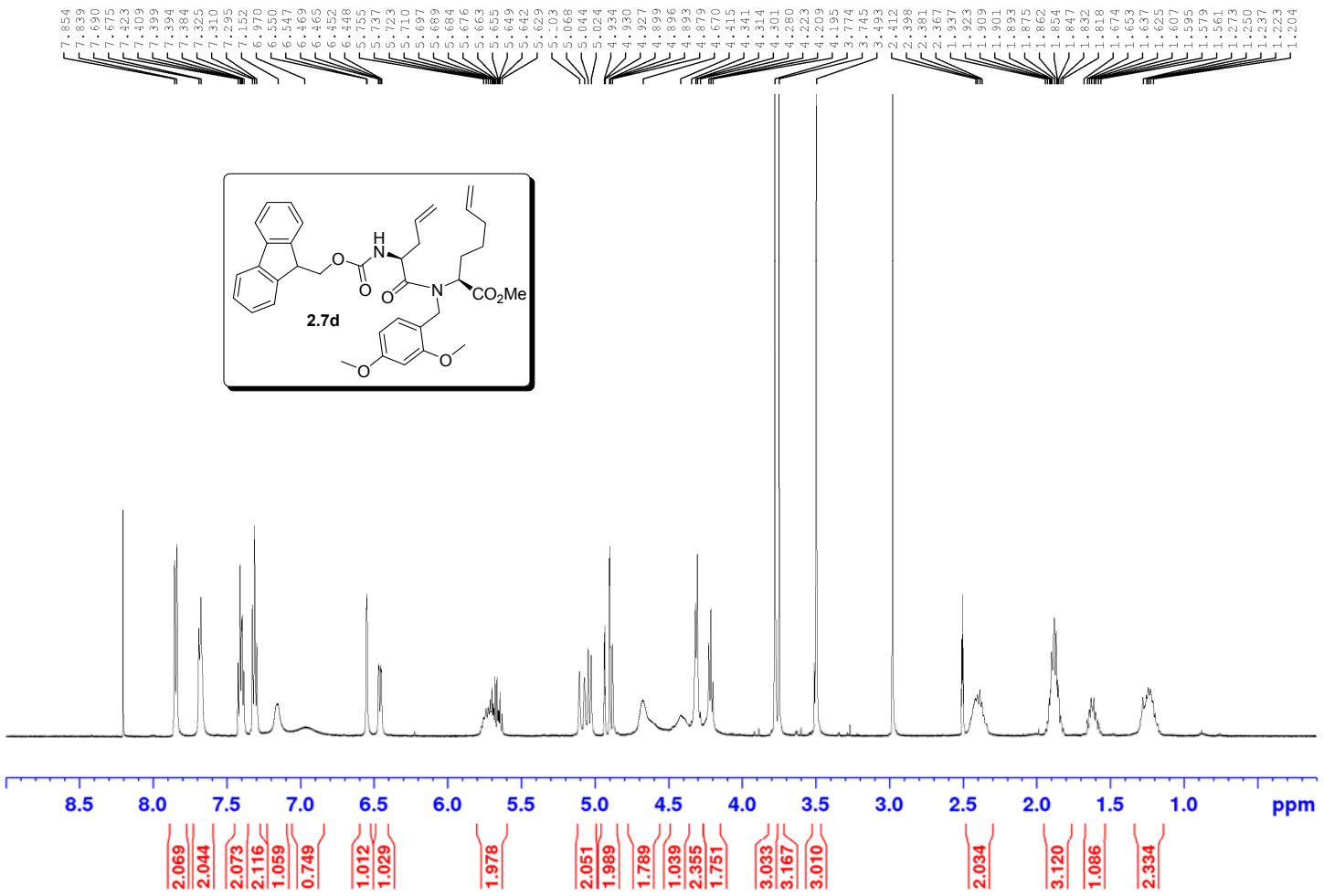

^{13}C NMR 500 MHz
Solvent: DMSO-d_6
**Spectrum was recorded at 100 ^oC*

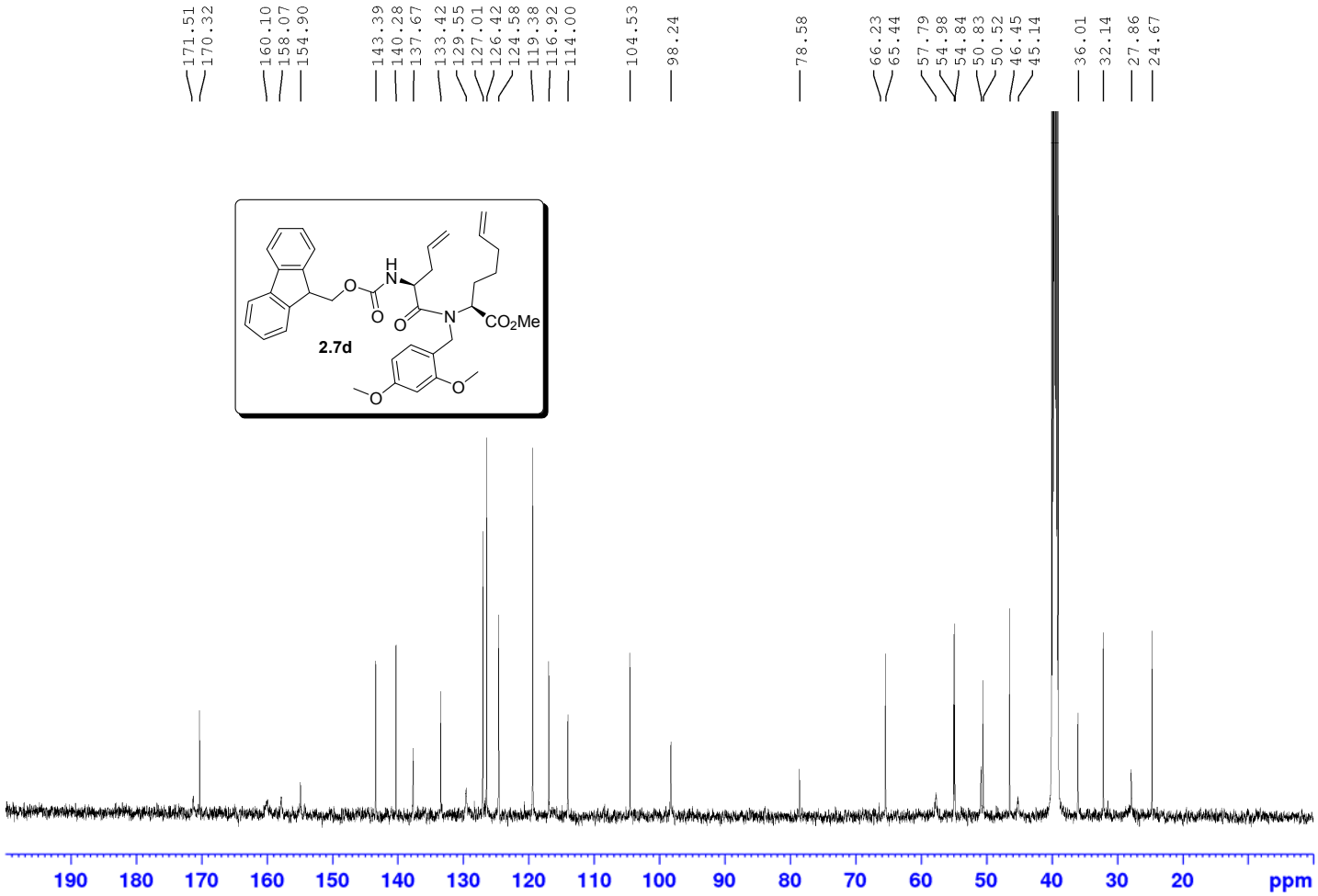

^{1}H NMR 500 MHz
Solvent: DMSO-d_6
**Spectrum was recorded at 100 °C*

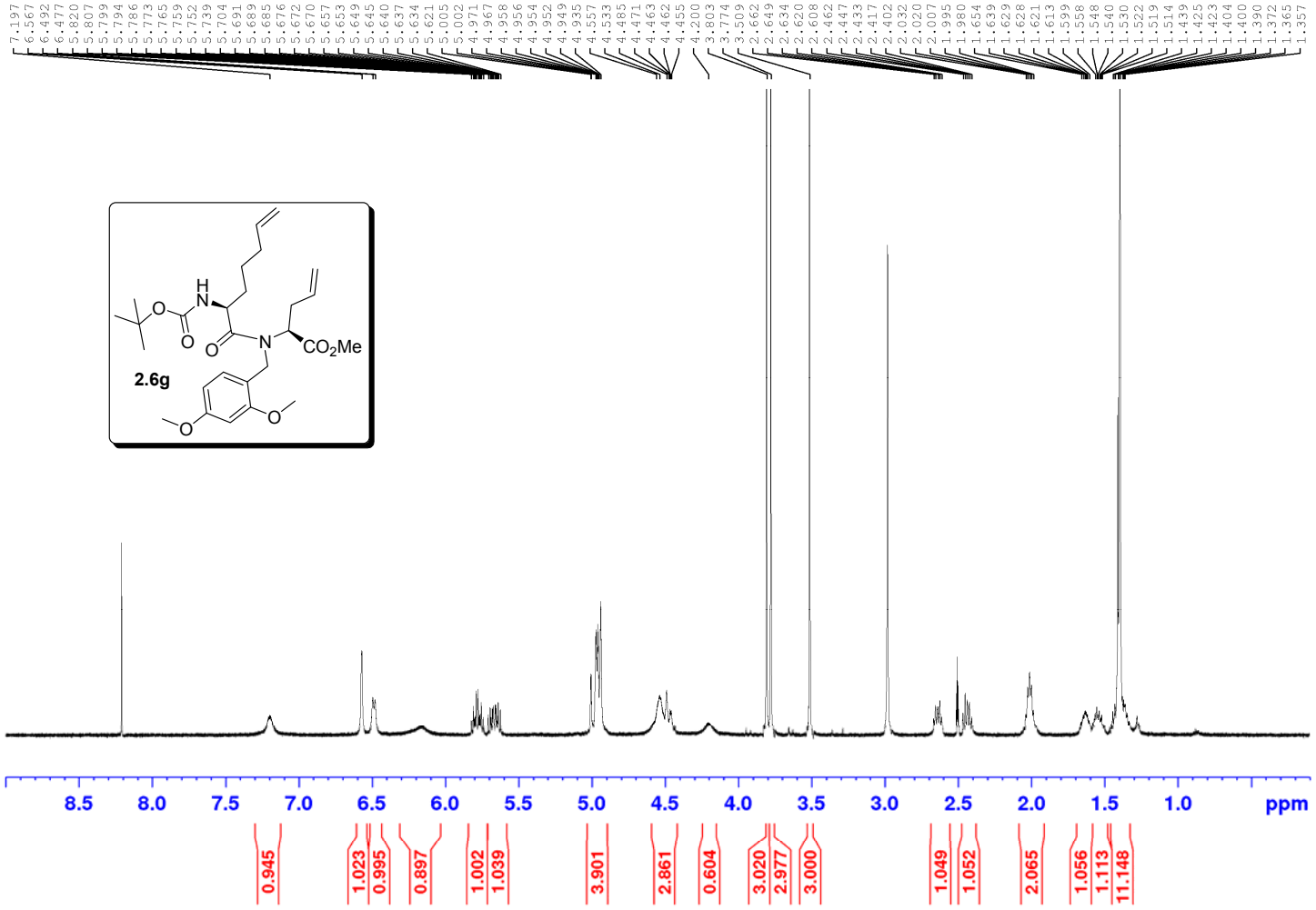

^{13}C NMR 500 MHz
Solvent: DMSO-d_6
**Spectrum was recorded at 100 ^{o}C*

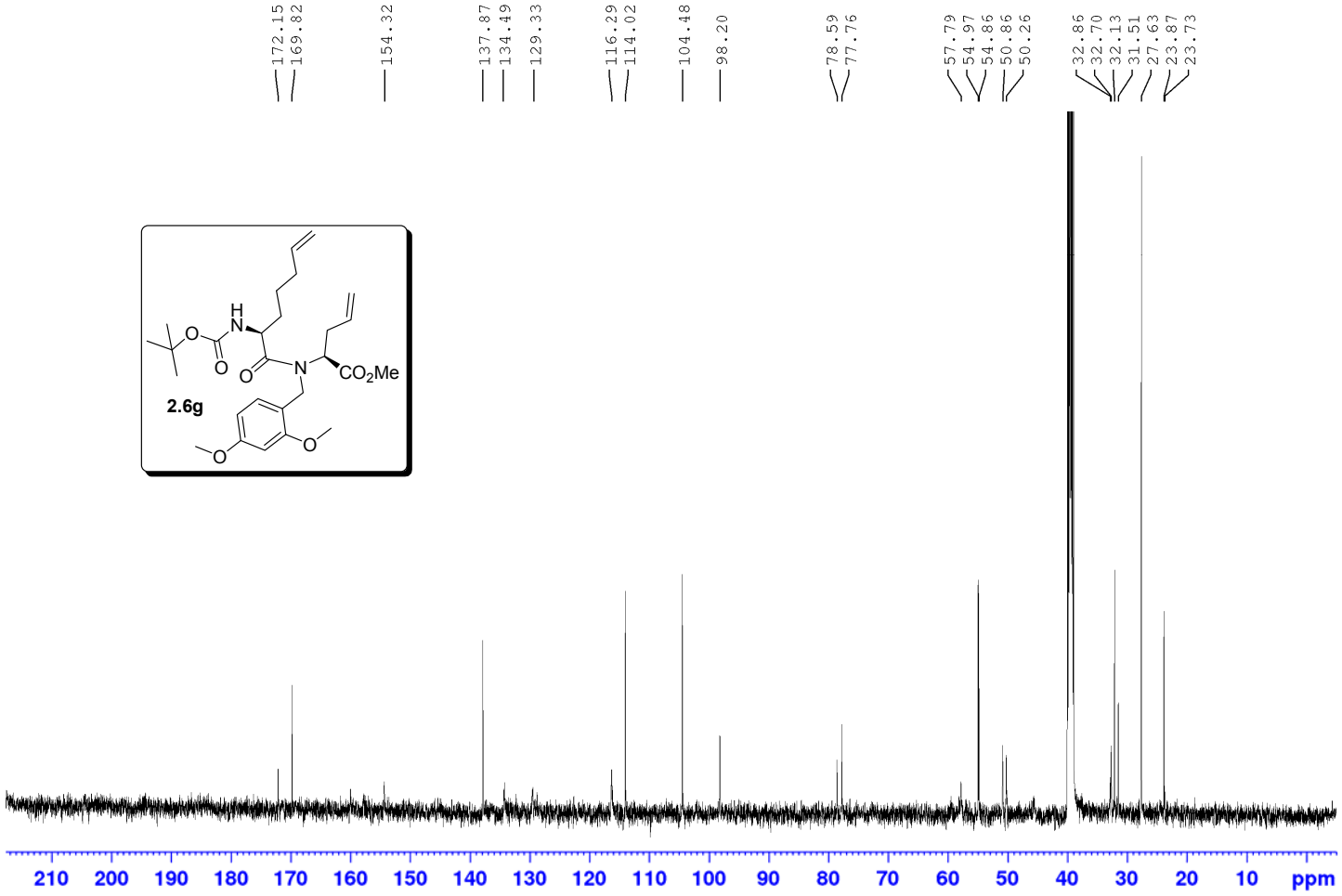

^{1}H NMR 300 MHz
Solvent: $CDCl_3$

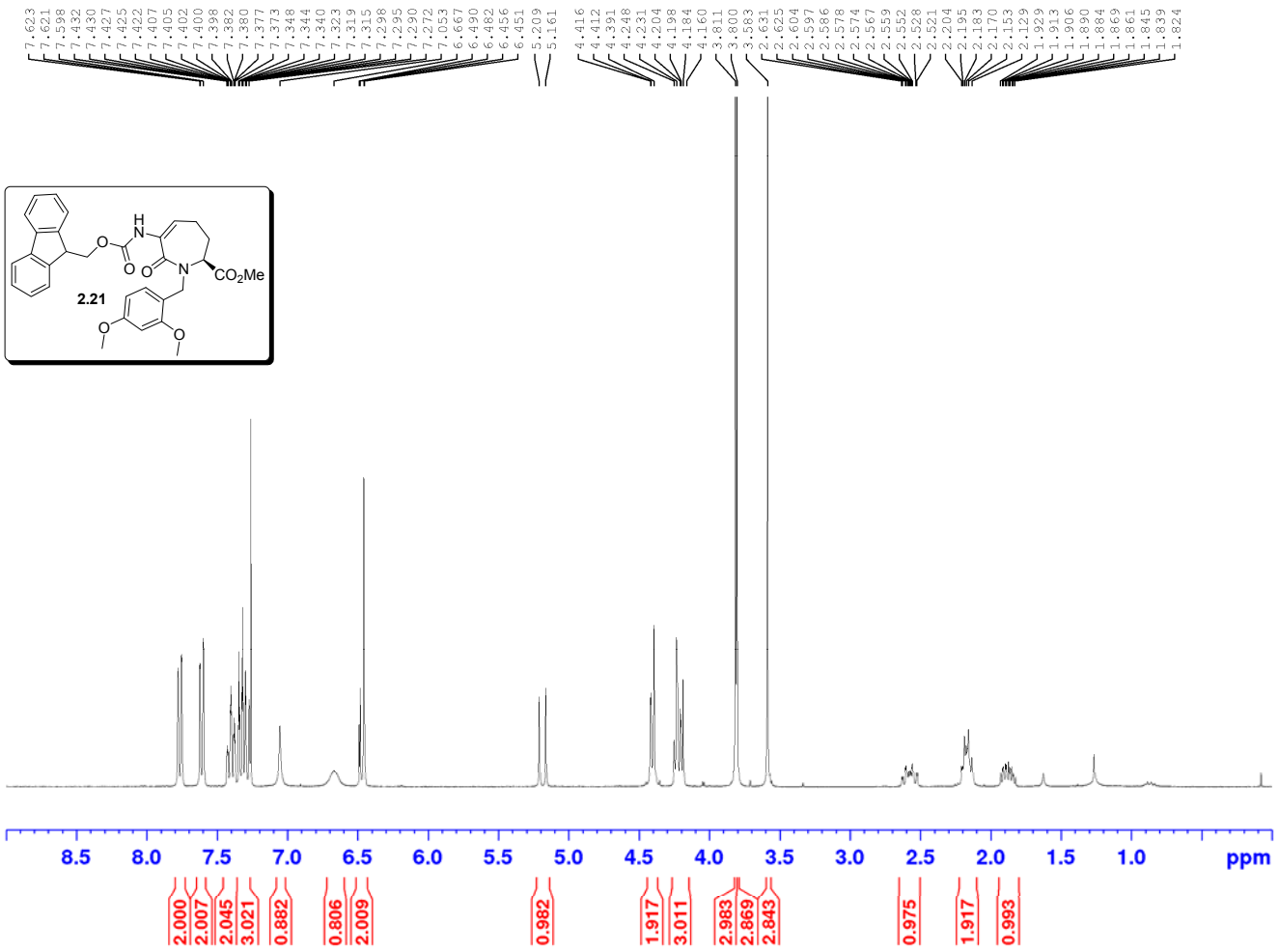

^{13}C NMR 300 MHz
Solvent: $CDCl_3$

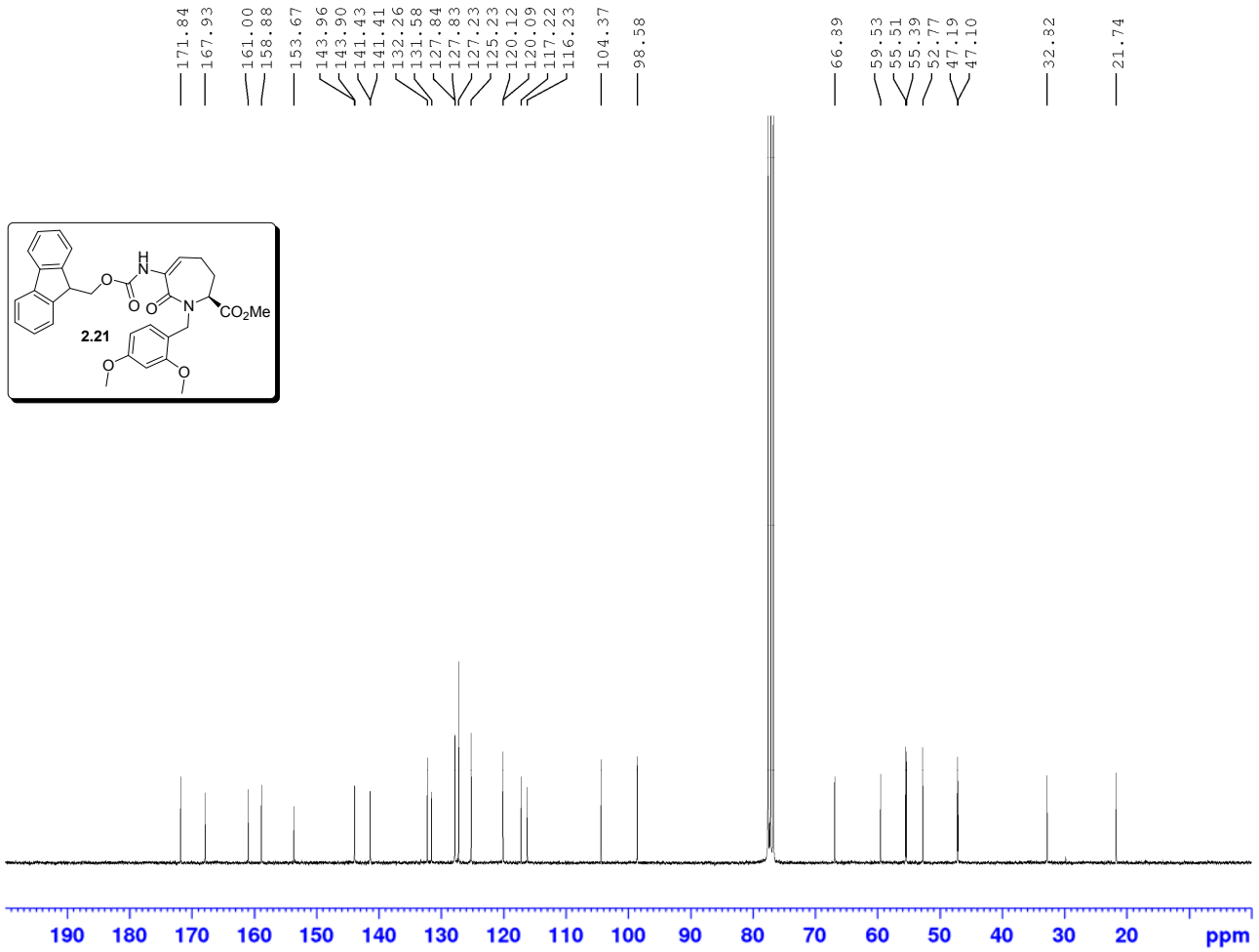

^{1}H NMR 300 MHz
Solvent: $CDCl_3$

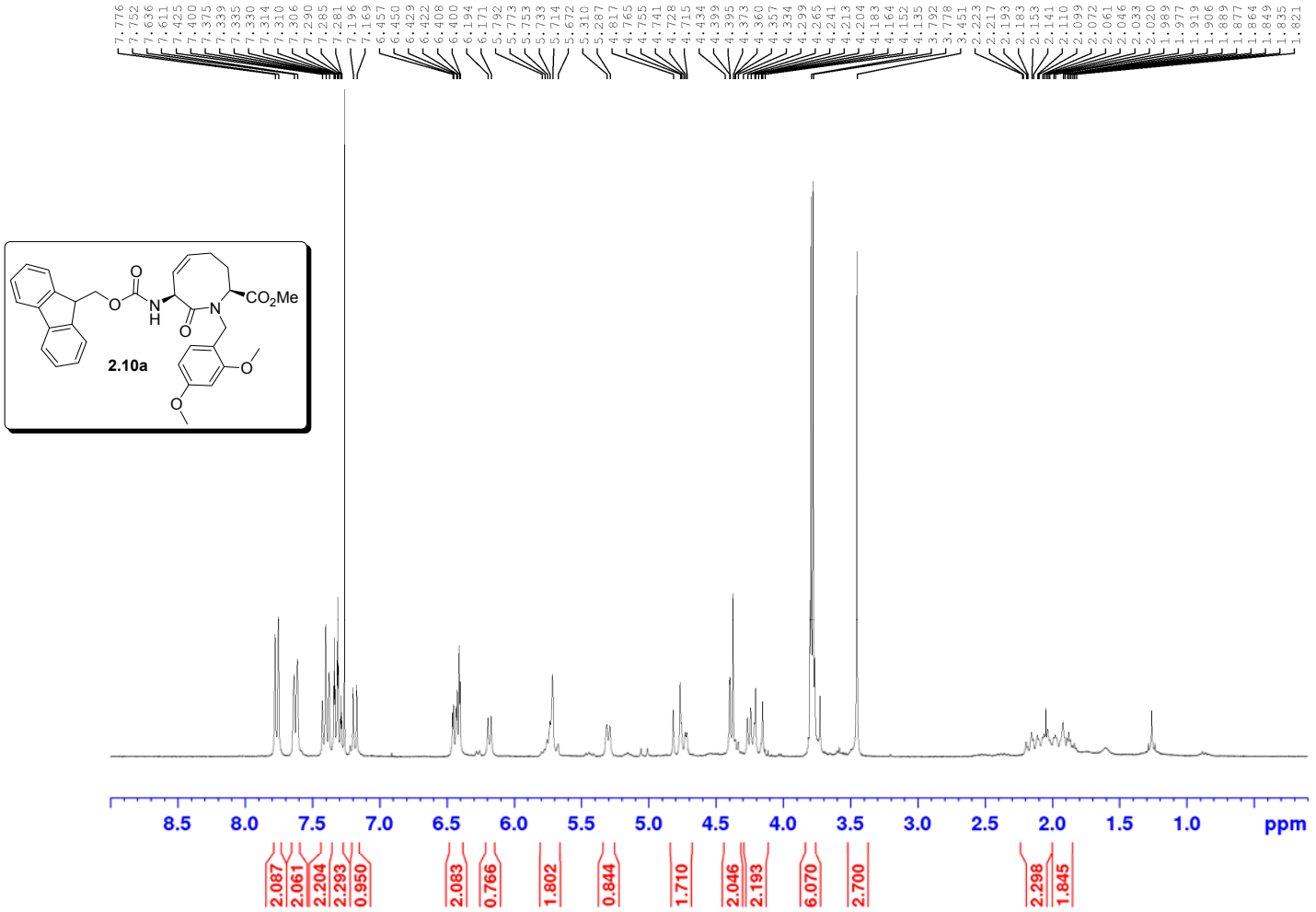

^{13}C NMR 300 MHz
Solvent: $CDCl_3$

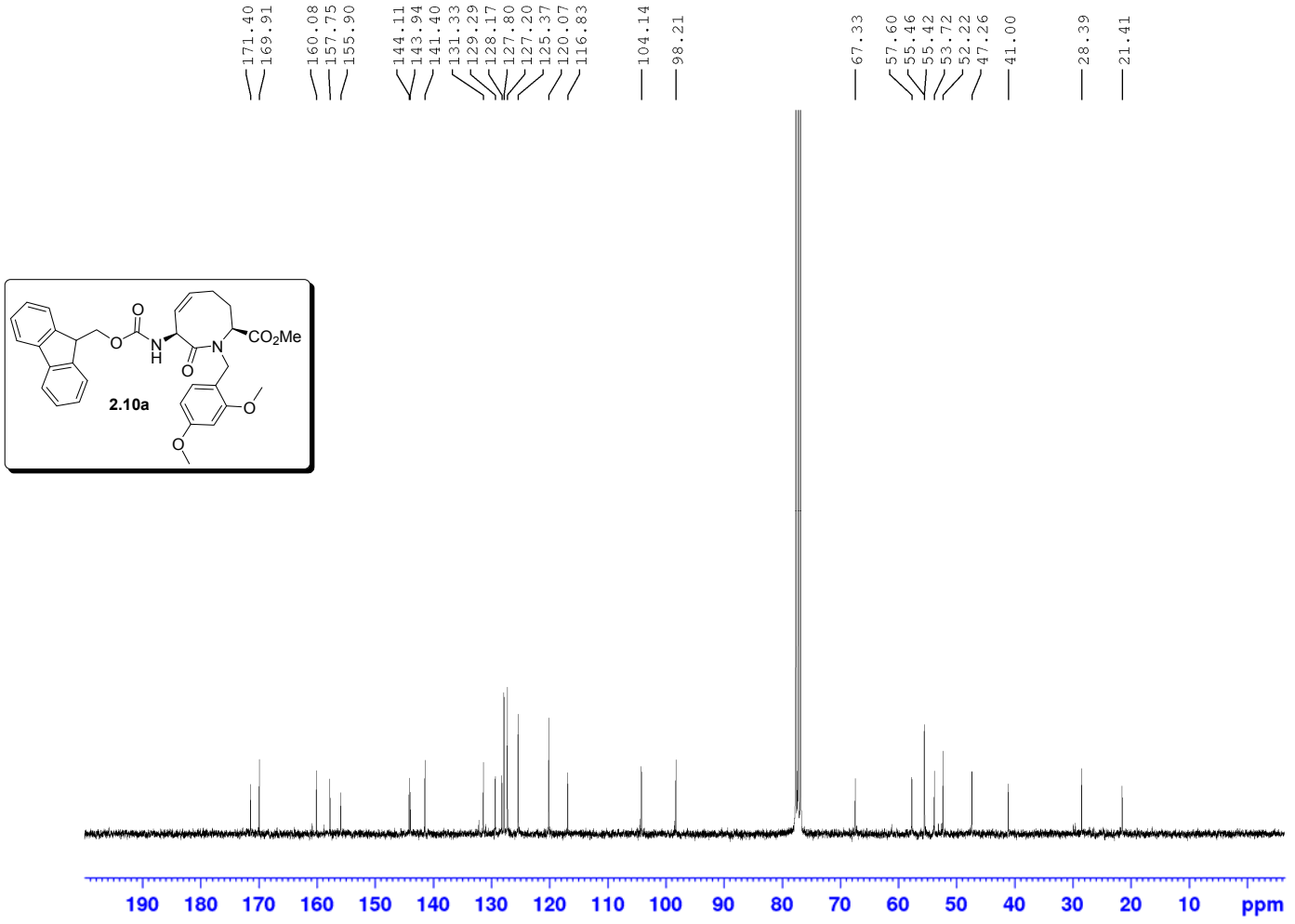

^{1}H NMR 400 MHz
Solvent: $CDCl_3$

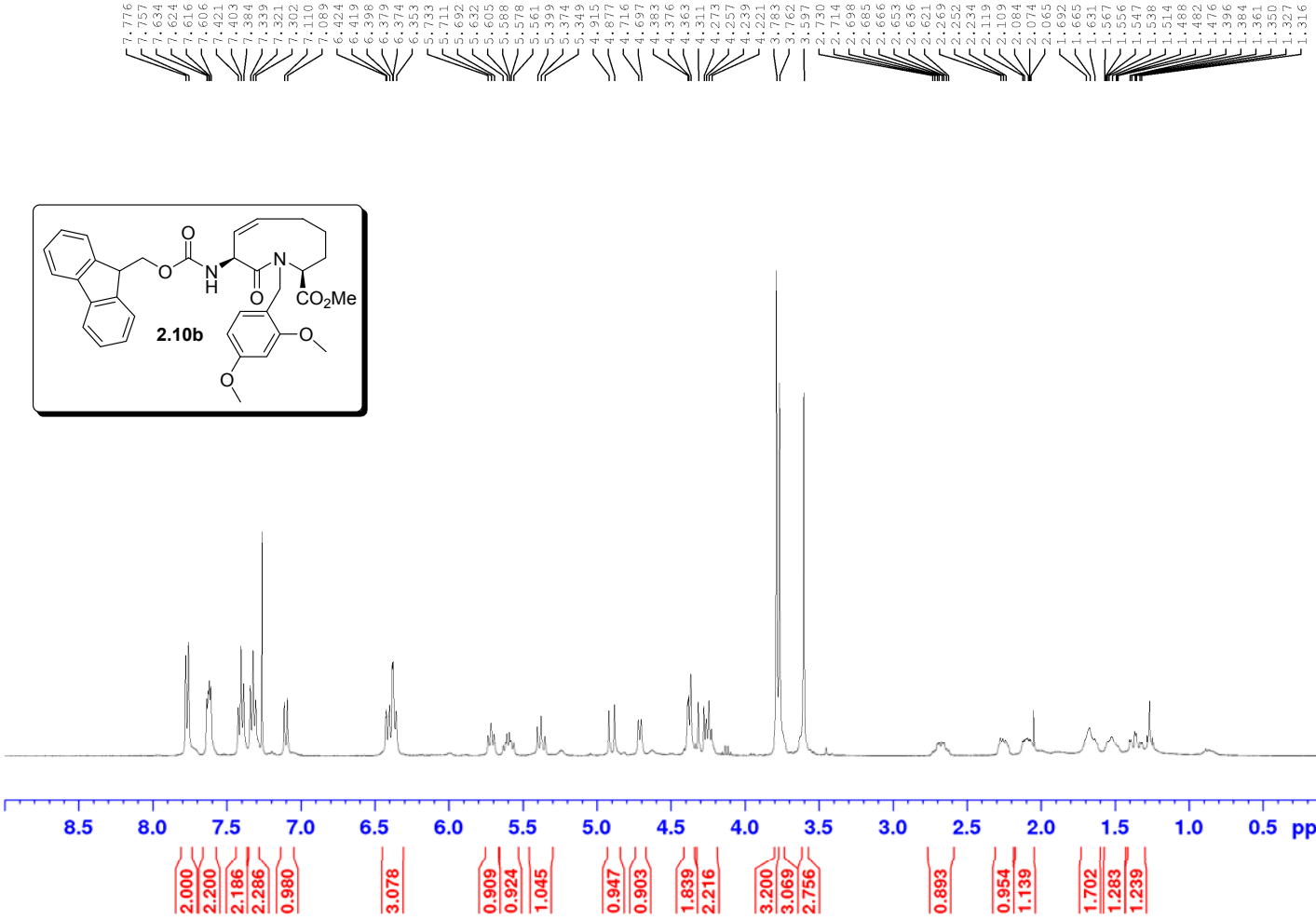

^{13}C NMR 400 MHz
Solvent: $CDCl_3$

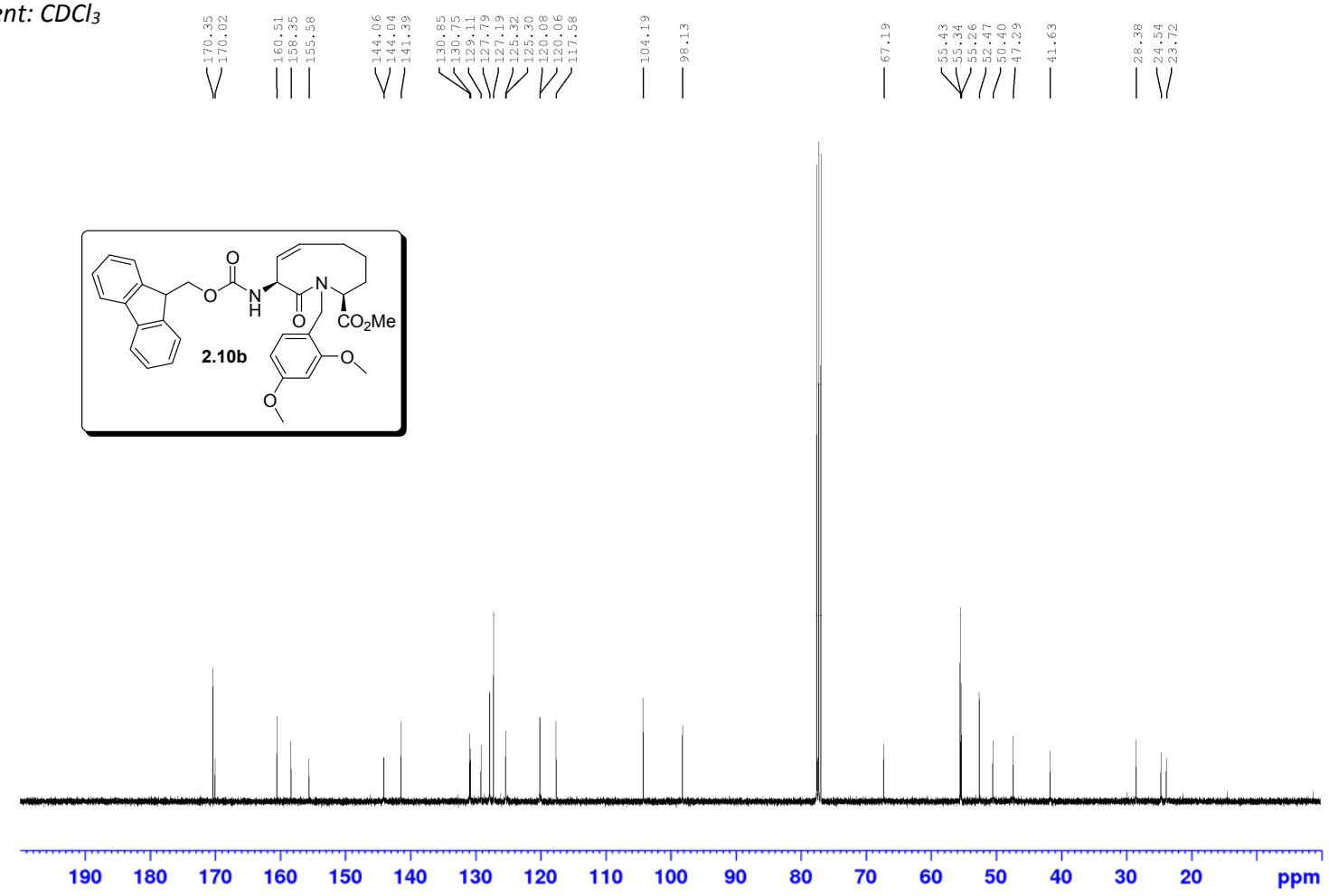

^{1}H NMR 500 MHz
Solvent: $CDCl_3$

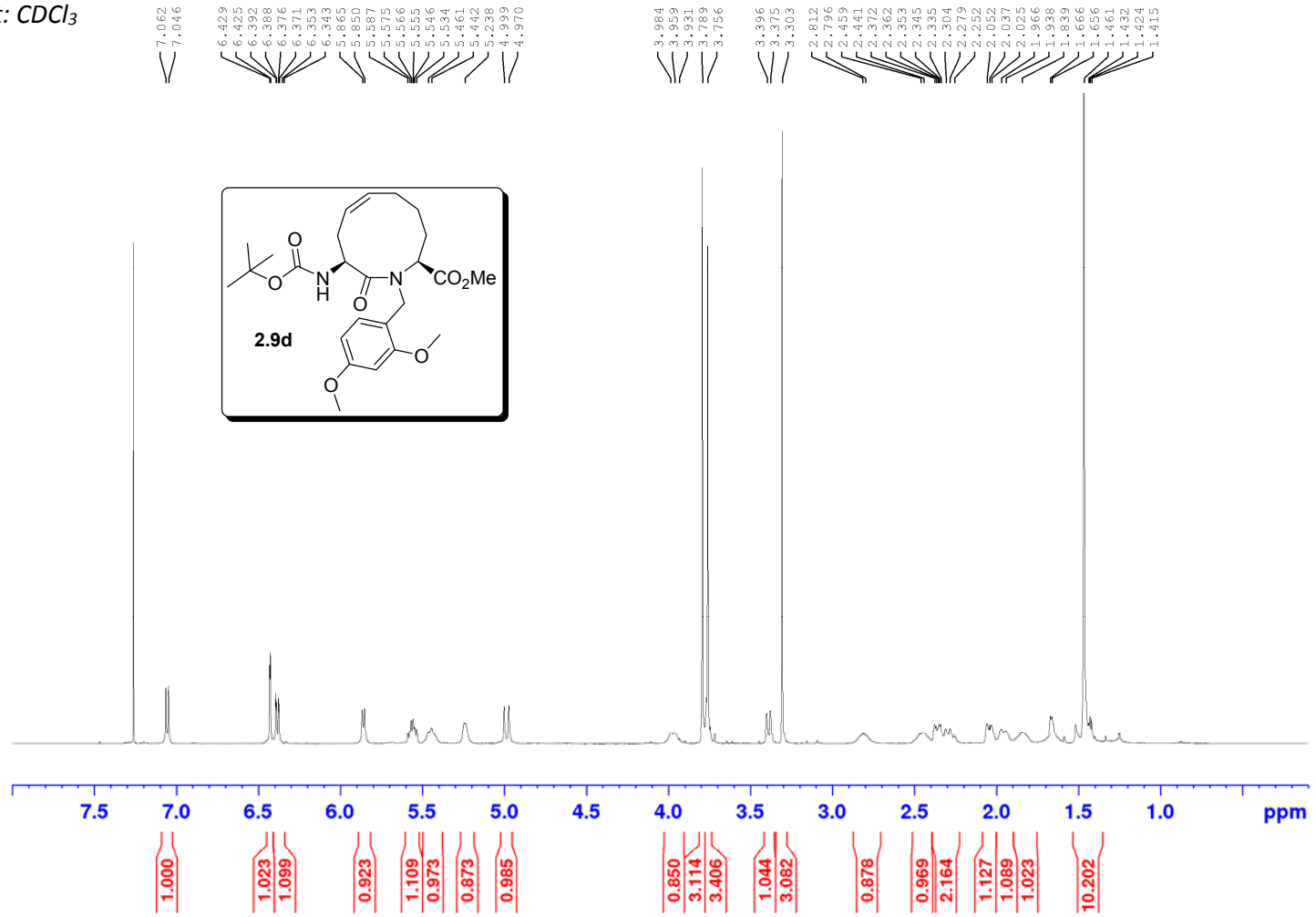

^{13}C NMR 500 MHz
Solvent: $CDCl_3$

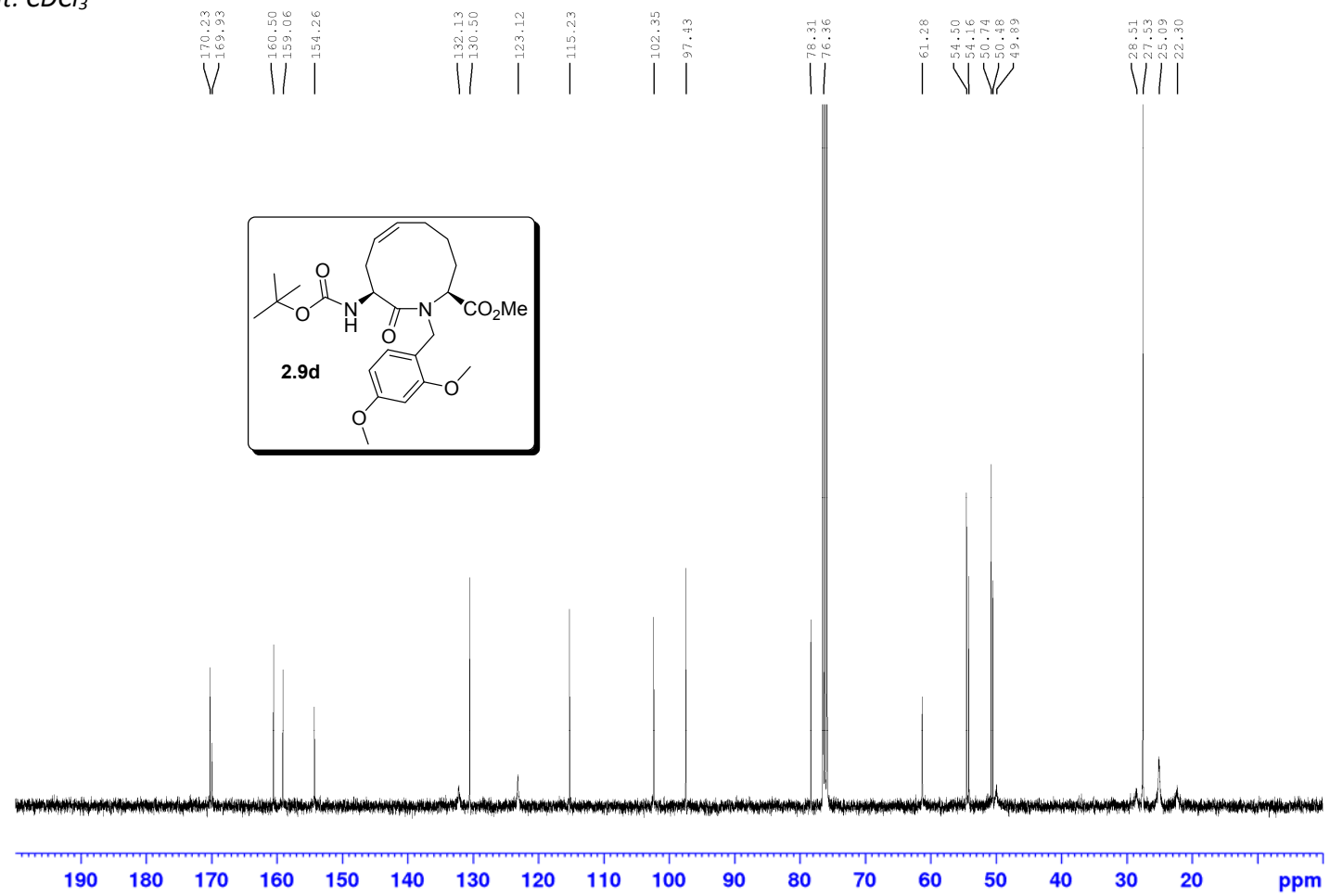

^{1}H NMR 400 MHz
Solvent: $CDCl_3$

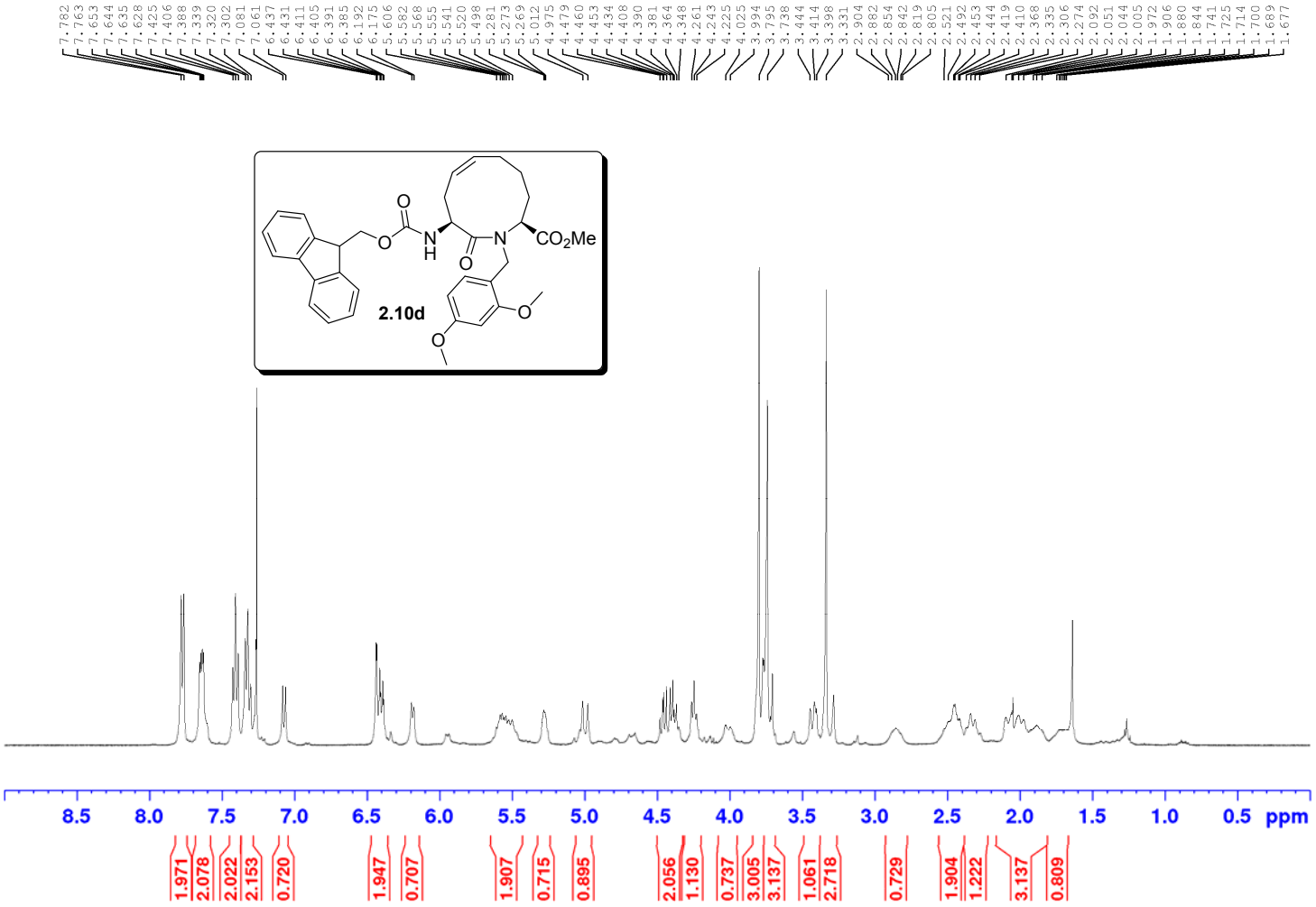

^{13}C NMR 400 MHz
Solvent: $CDCl_3$

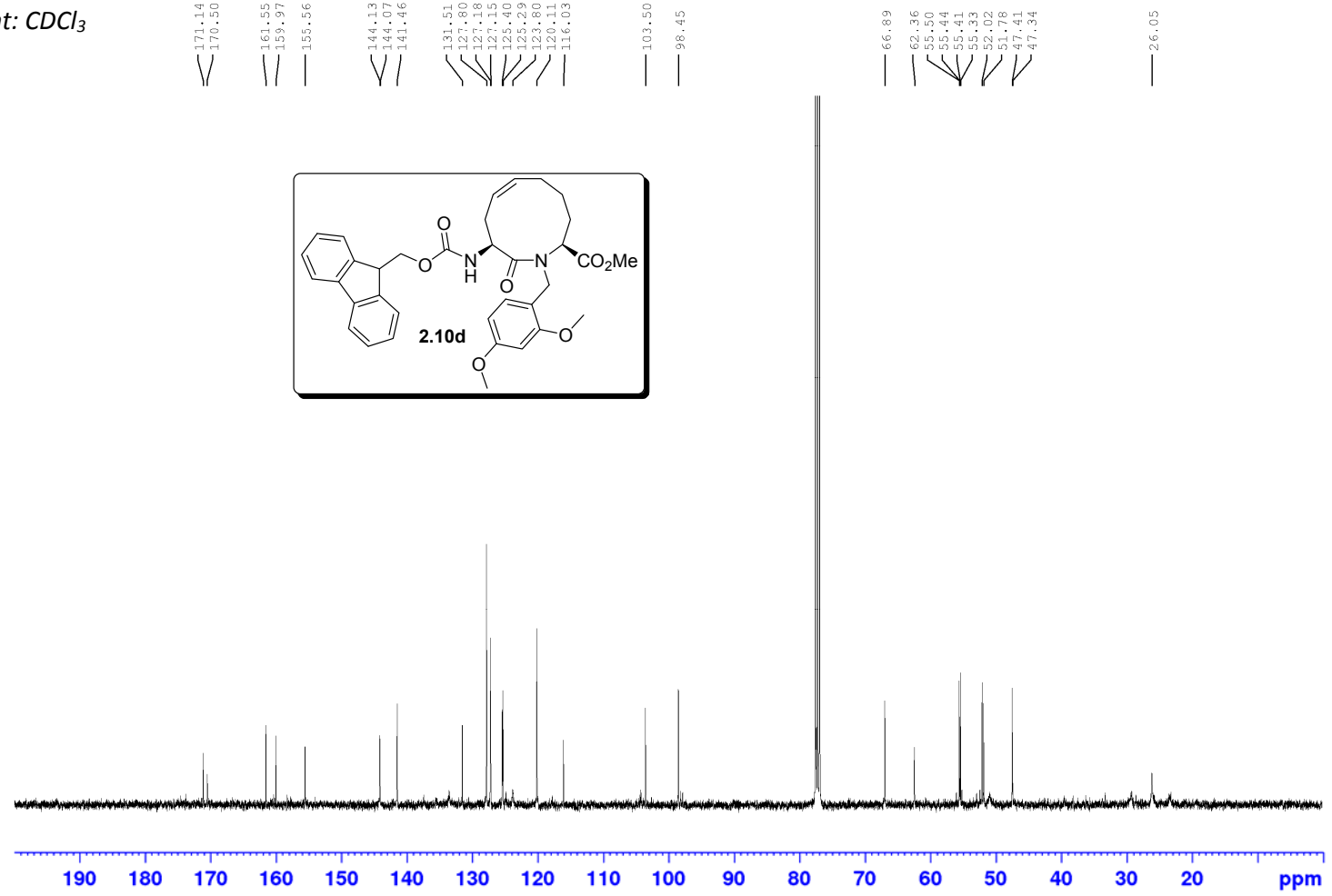

^{1}H NMR 400 MHz
Solvent: $CDCl_3$

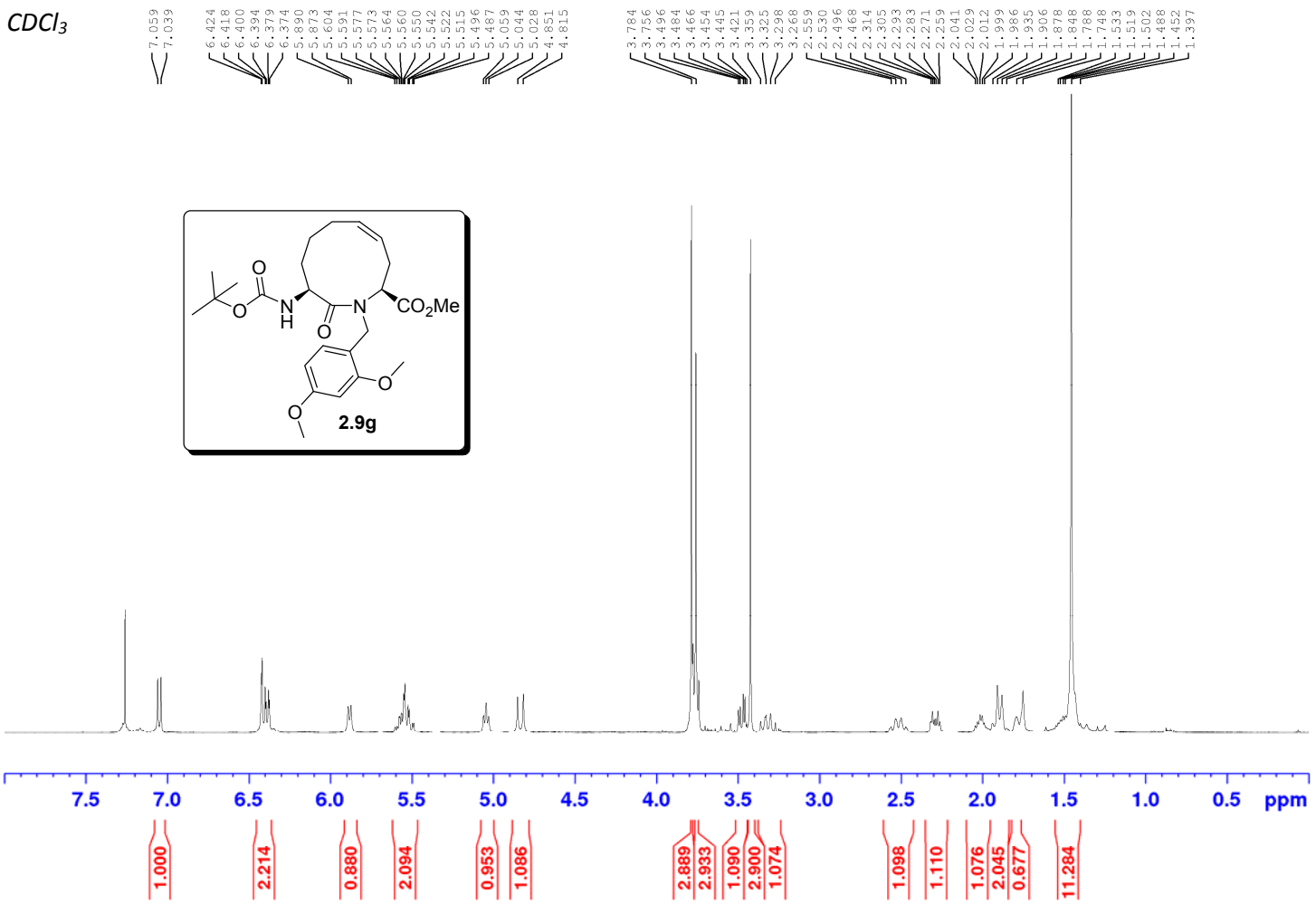

^{13}C NMR 400 MHz
Solvent: $CDCl_3$

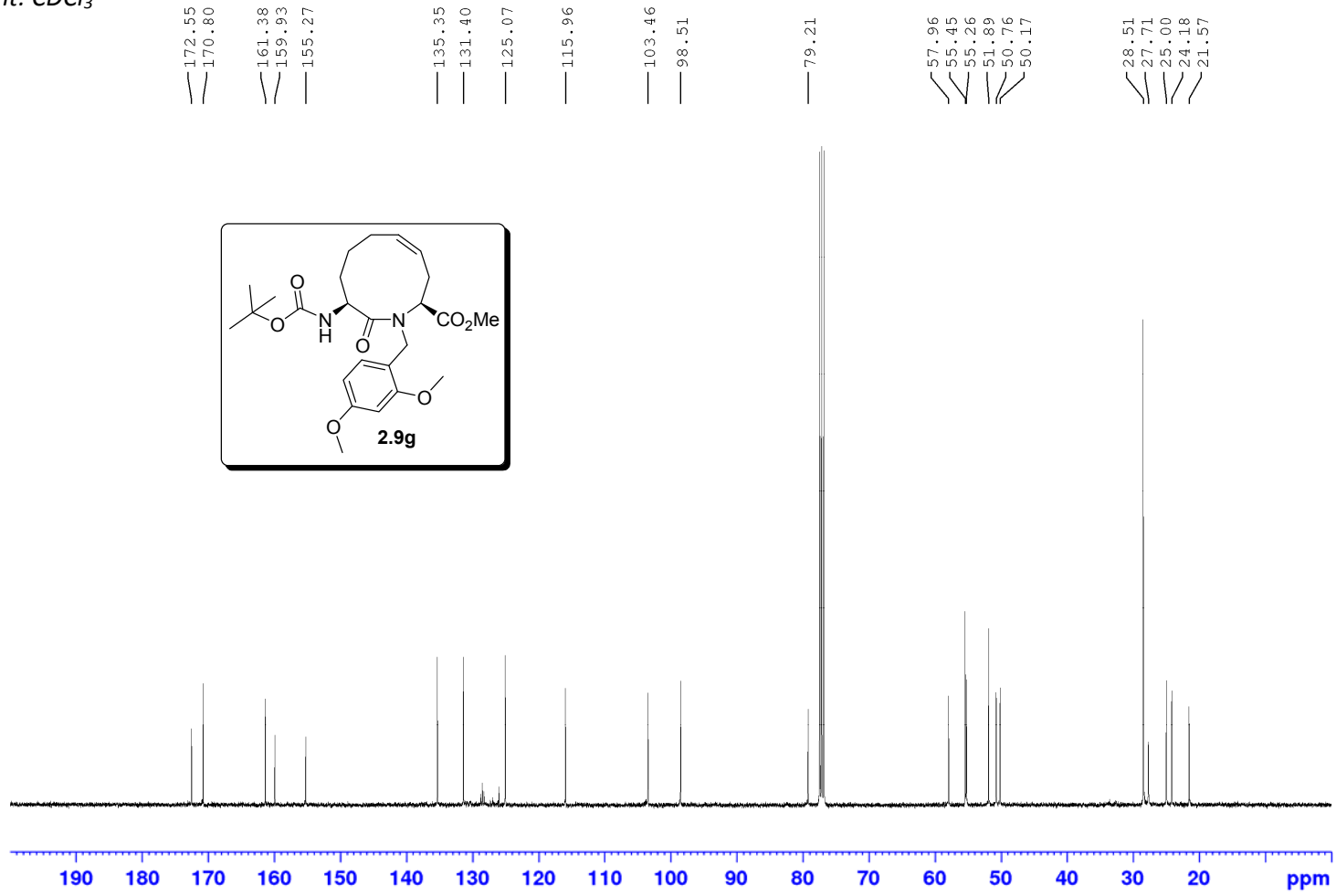

^{1}H NMR 400 MHz
Solvent: $CDCl_3$

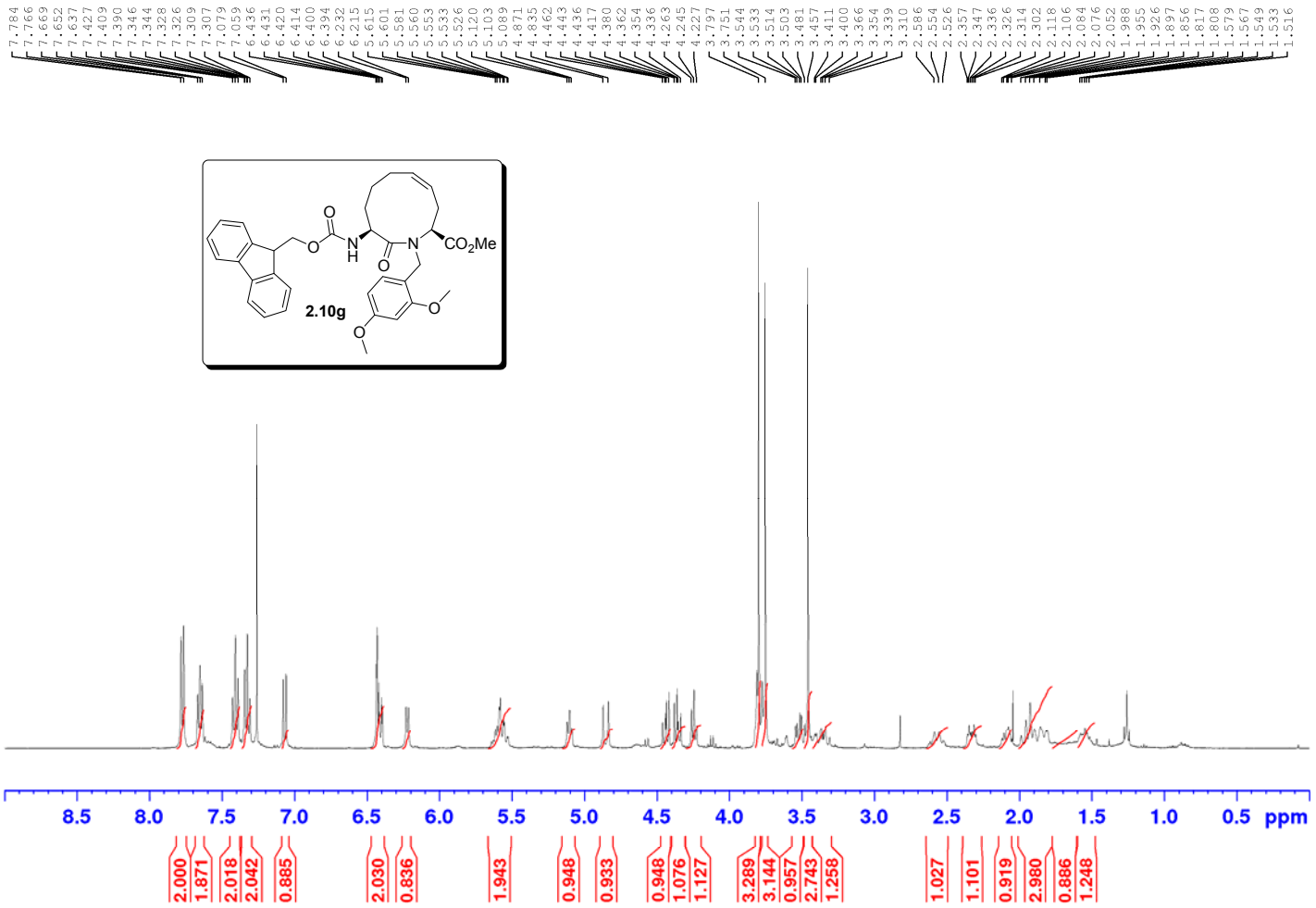

^{13}C NMR 400 MHz
Solvent: $CDCl_3$

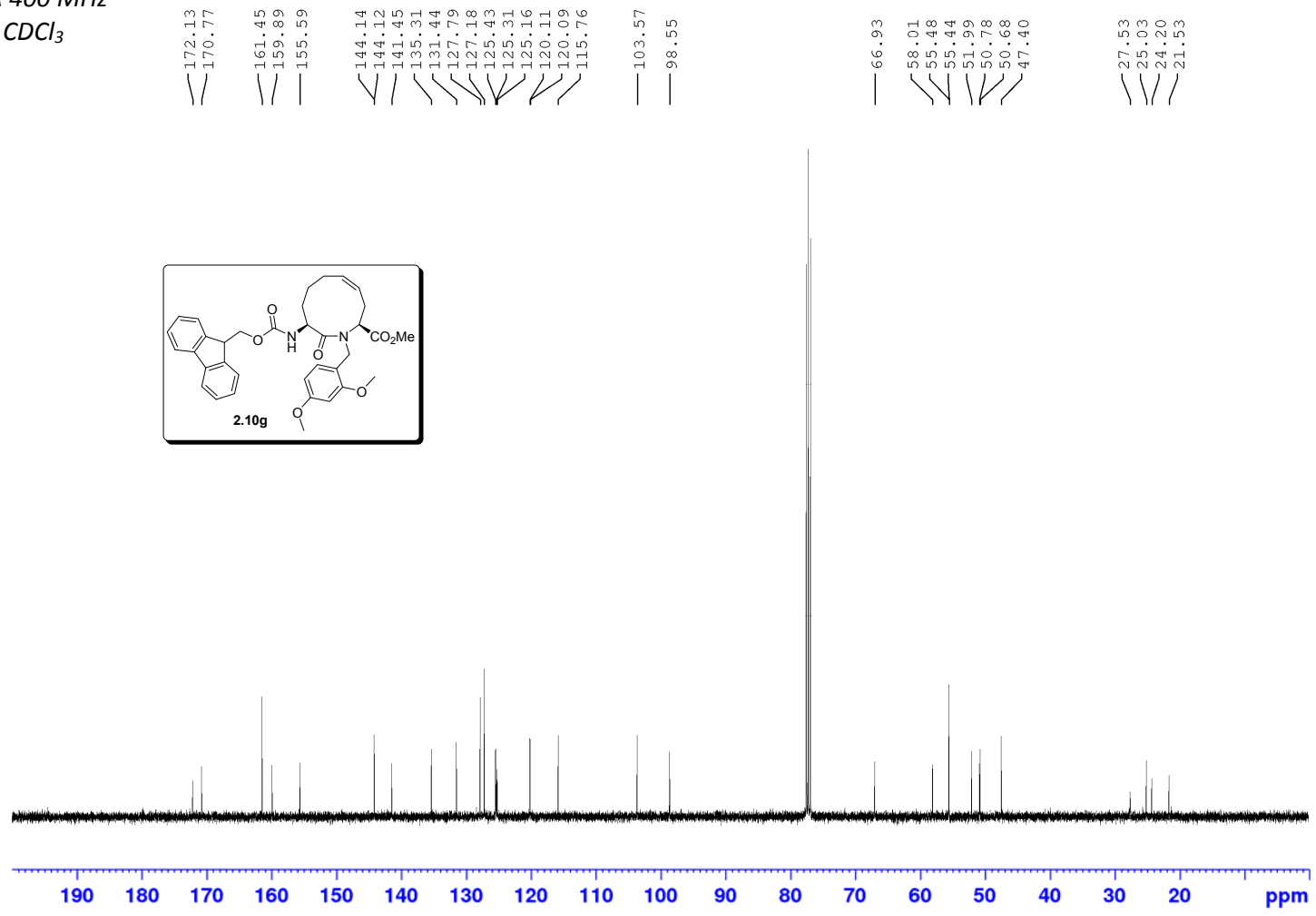

^{1}H NMR 400 MHz
Solvent: $CDCl_3$

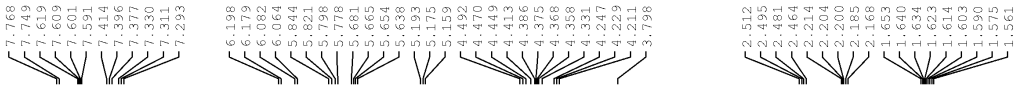

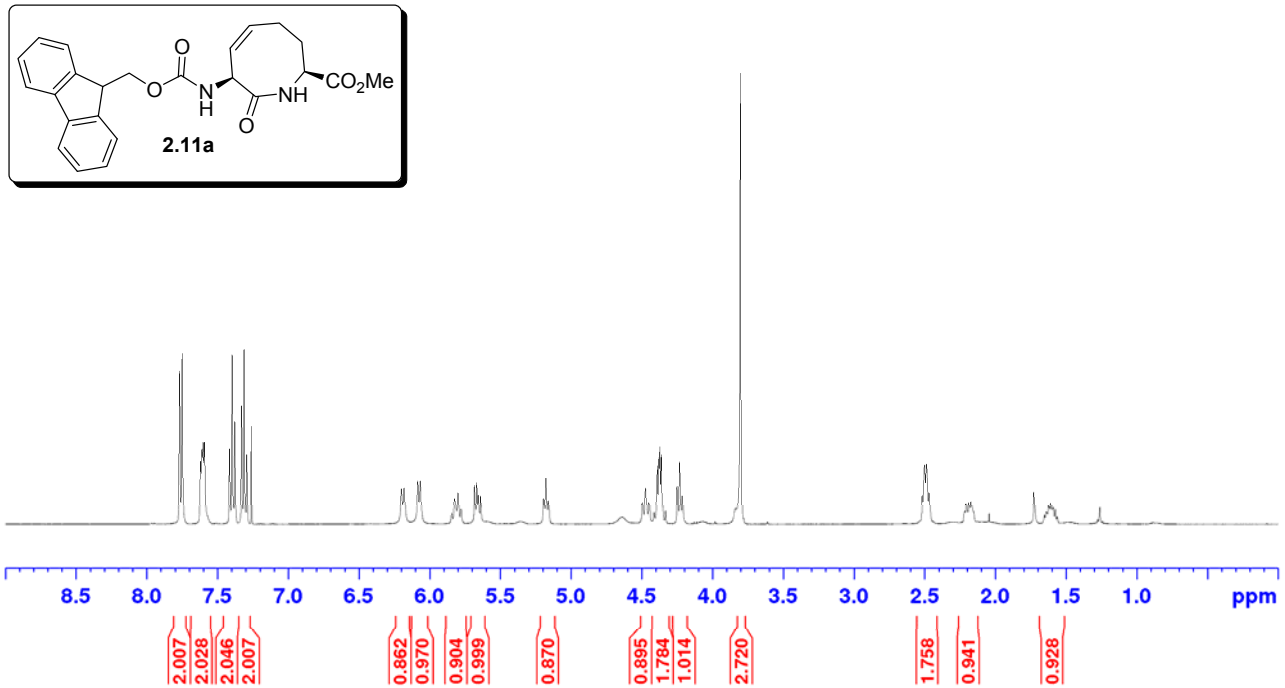

^{13}C NMR 400 MHz
Solvent: $CDCl_3$

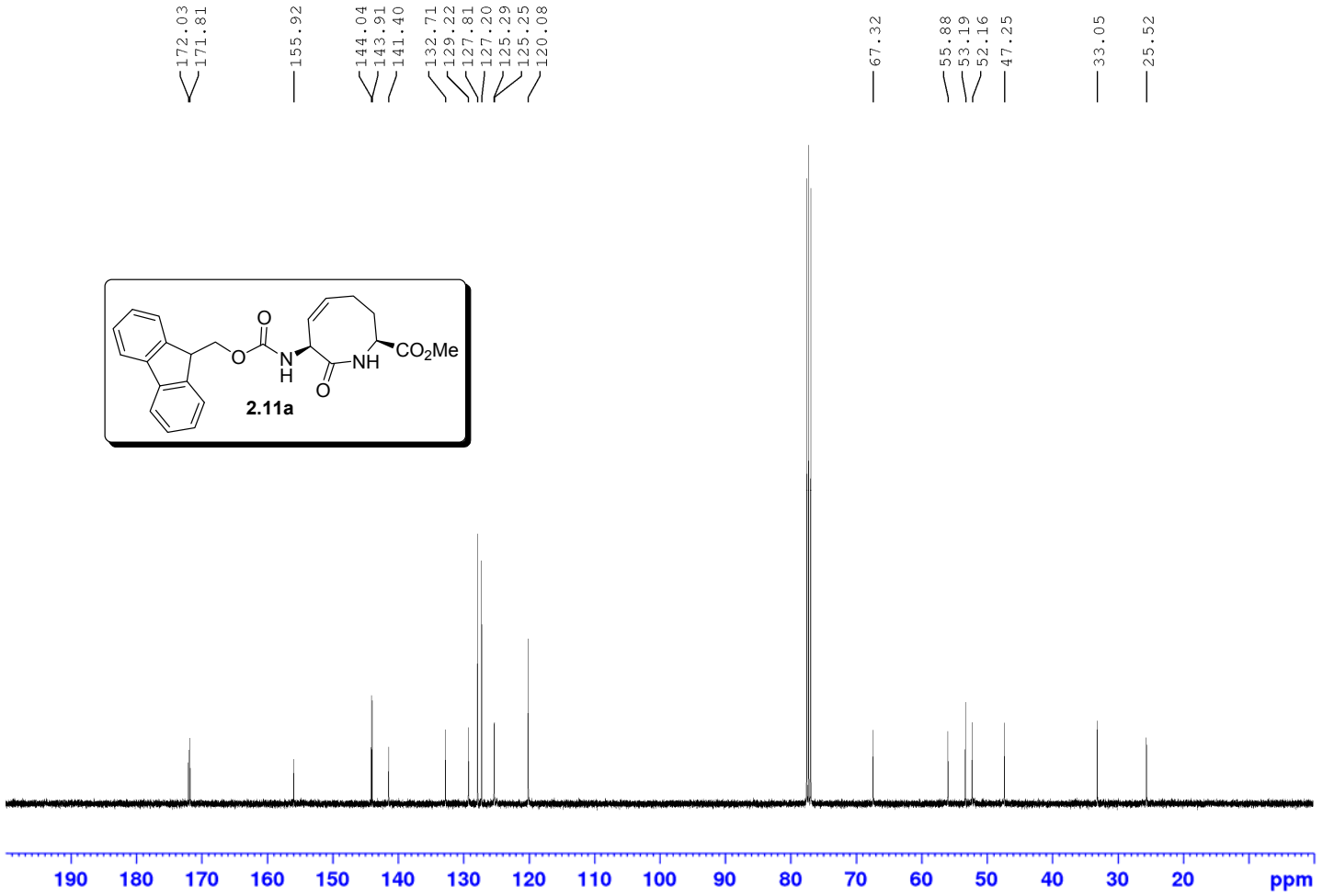

^{1}H NMR 500 MHz
Solvent: $CDCl_3$

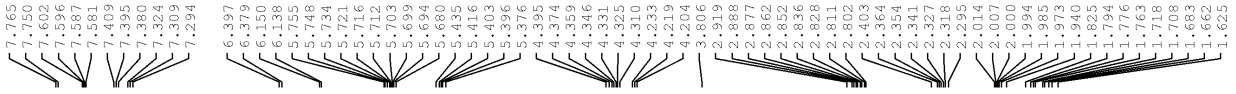

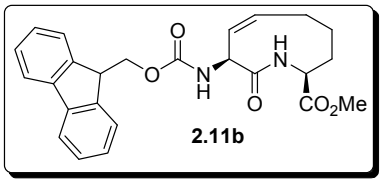

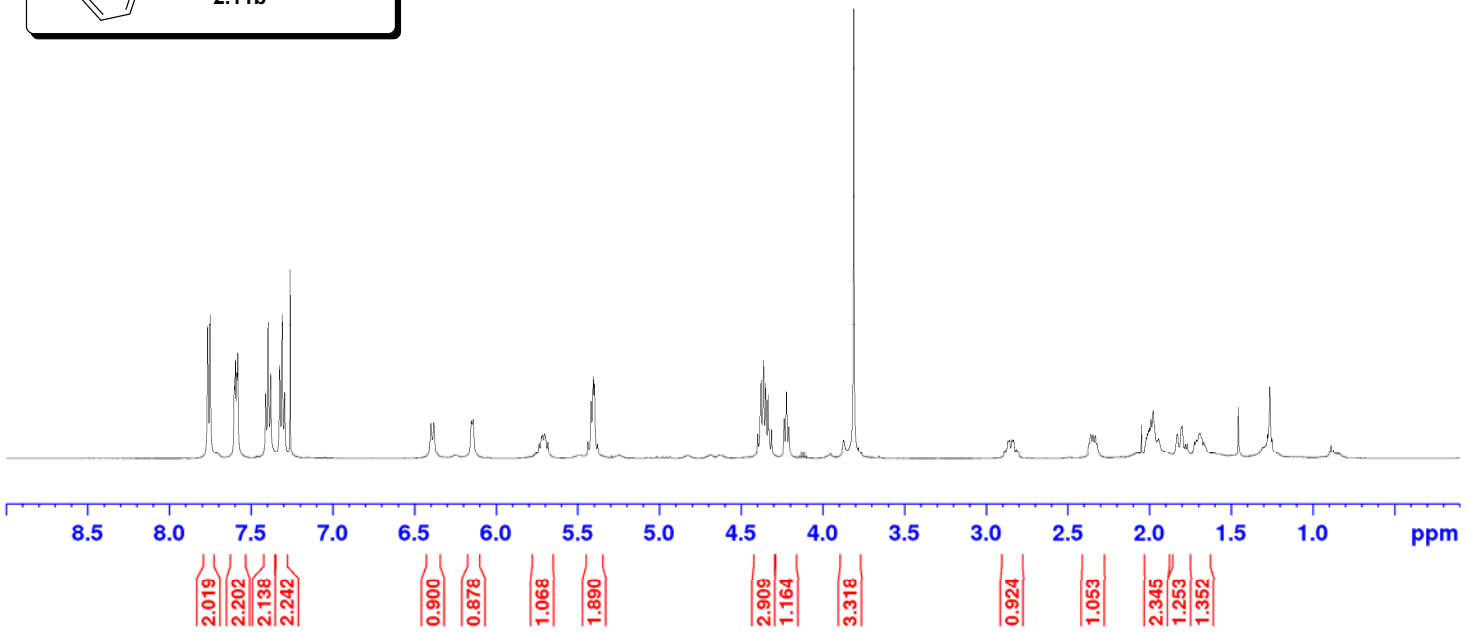

^{13}C NMR 500 MHz
Solvent: $CDCl_3$

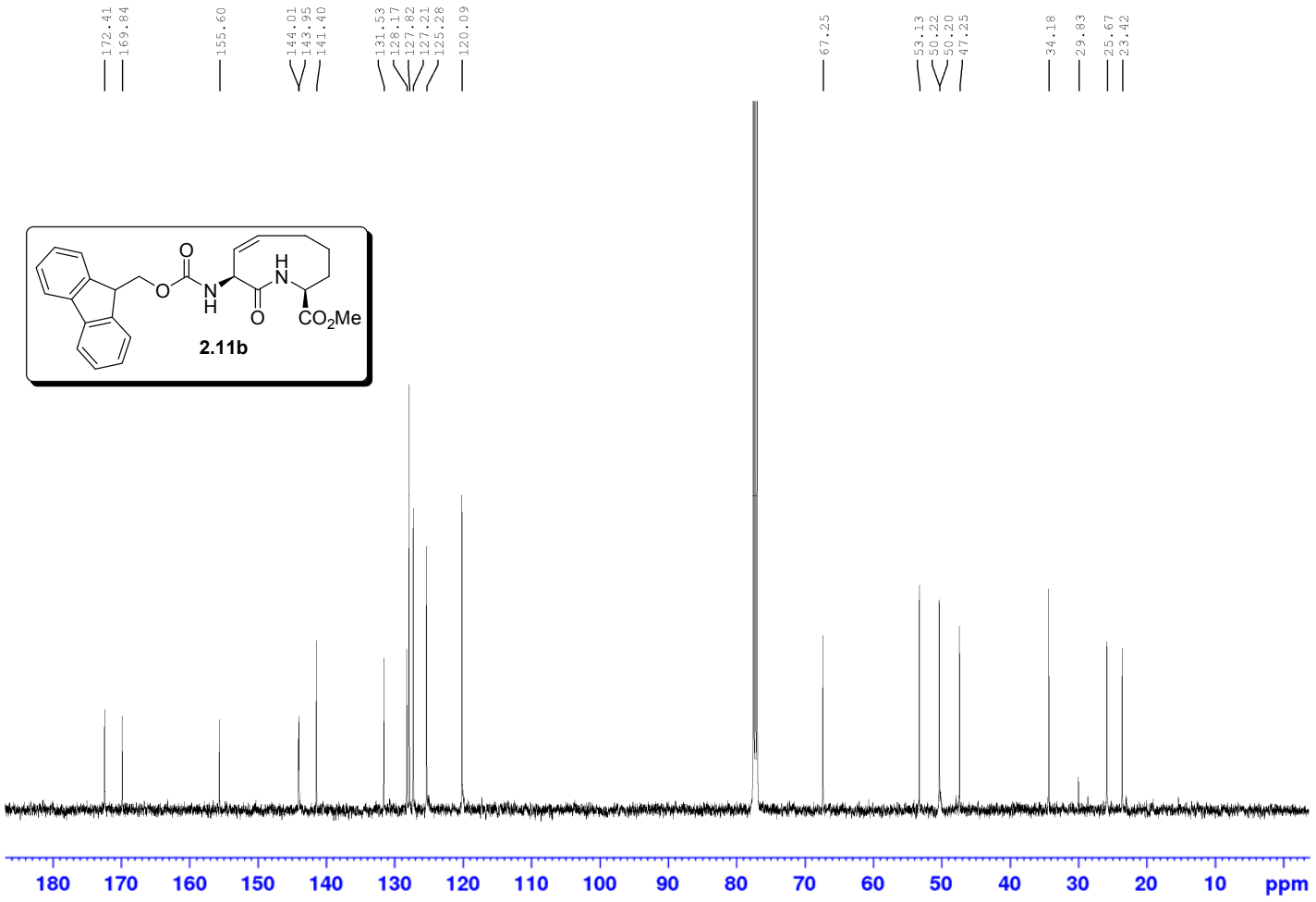

^{1}H NMR 500 MHz
Solvent: DMSO-d_6
**Spectrum was recorded at 100 °C*

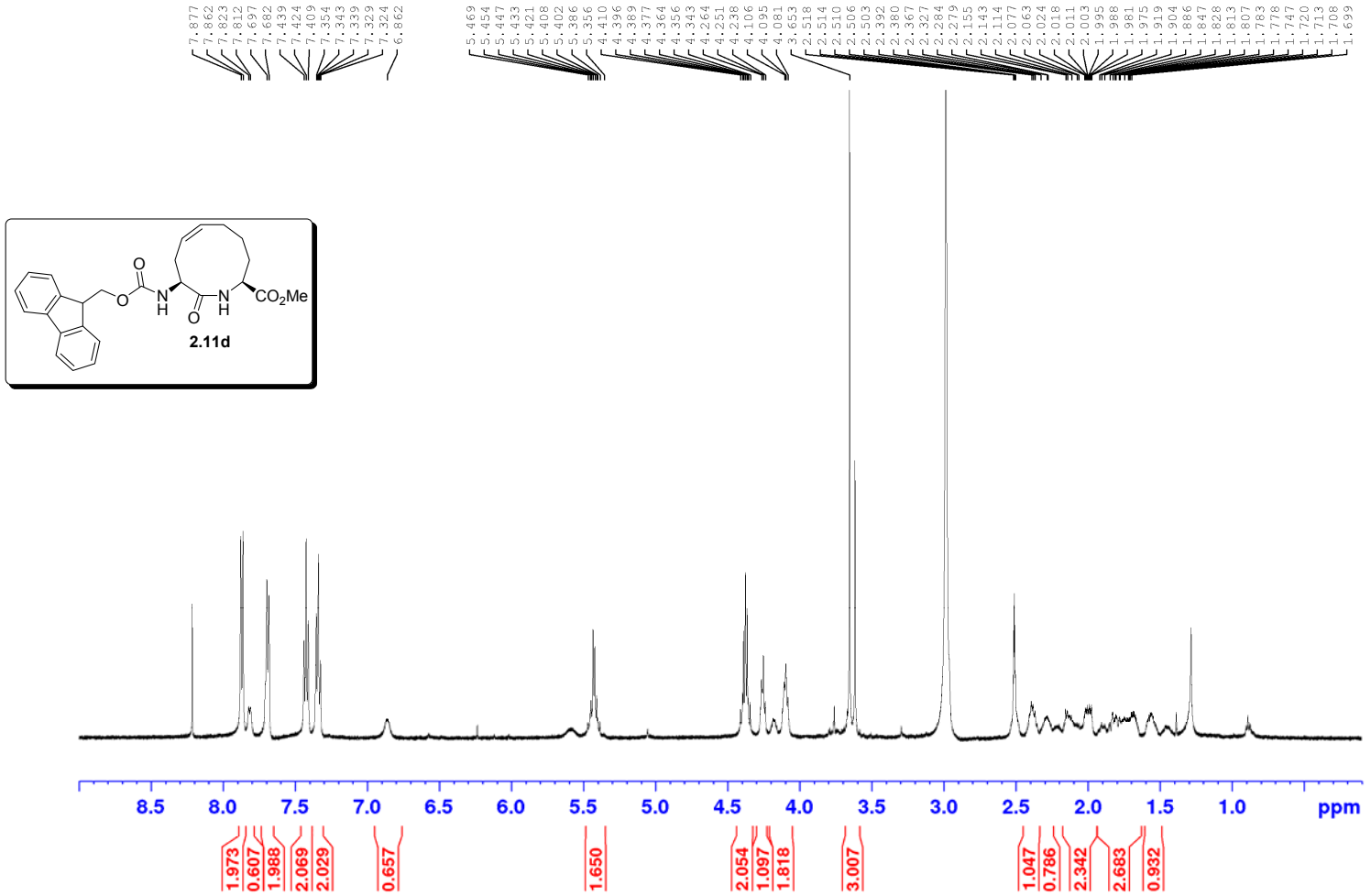

^{13}C NMR 500 MHz
Solvent: DMSO-d_6
**Spectrum was recorded at 100 ^{o}C*

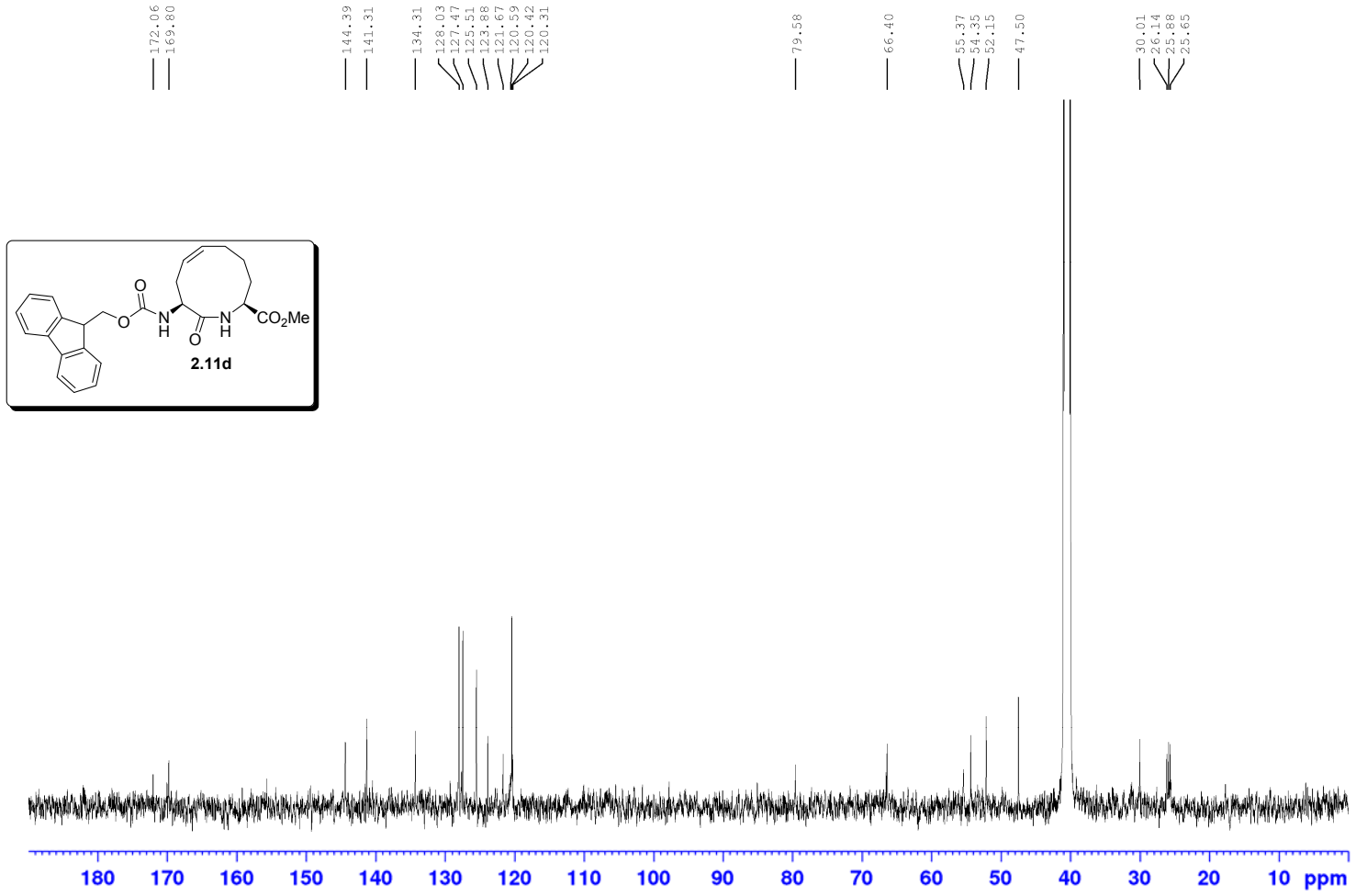

^{1}H NMR 500 MHz
Solvent: DMSO-d_6
**Spectrum was recorded at 100 ^{o}C*

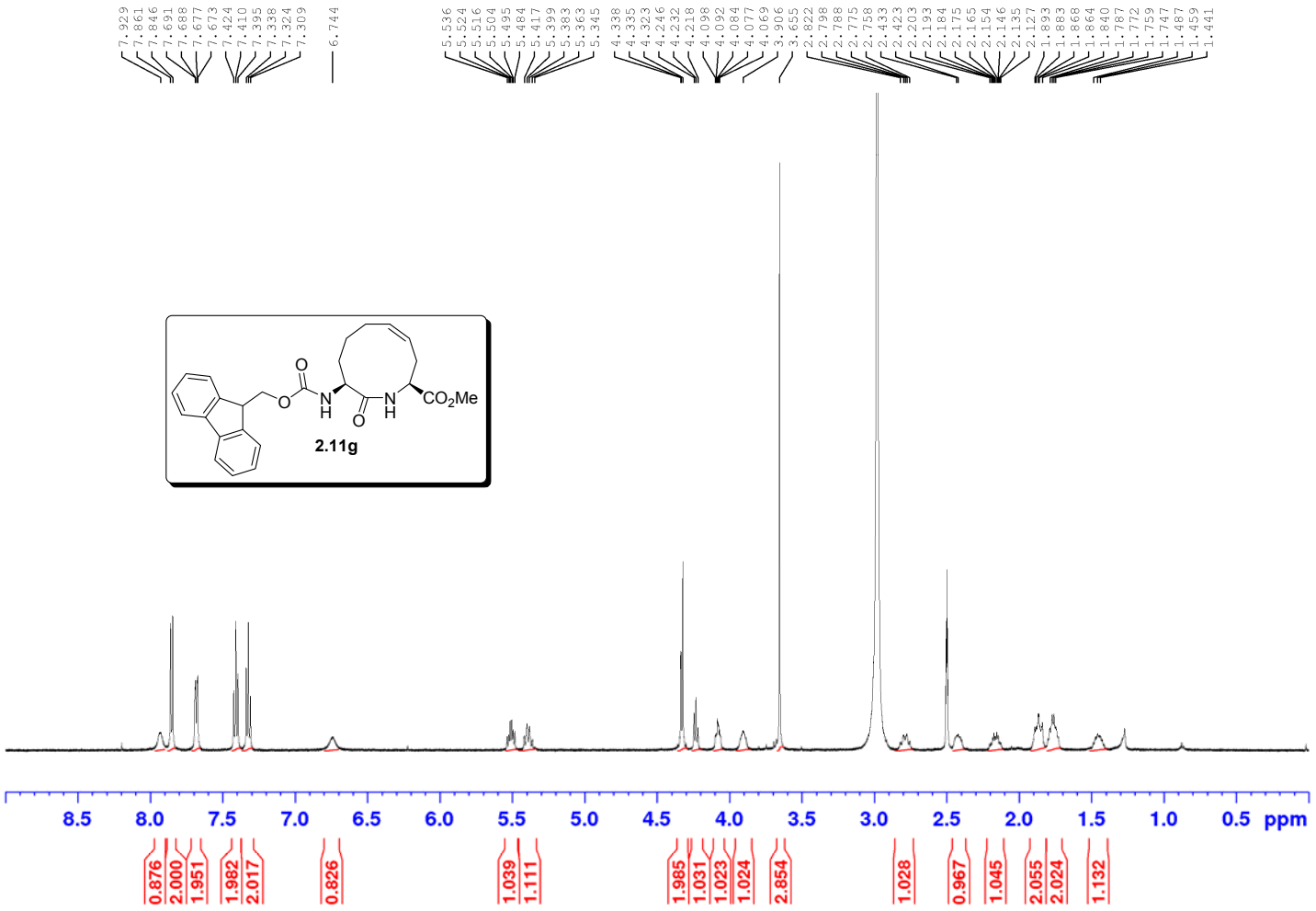

^{13}C NMR 500 MHz
Solvent: DMSO-d_6
**Spectrum was recorded at 100 ^{o}C*

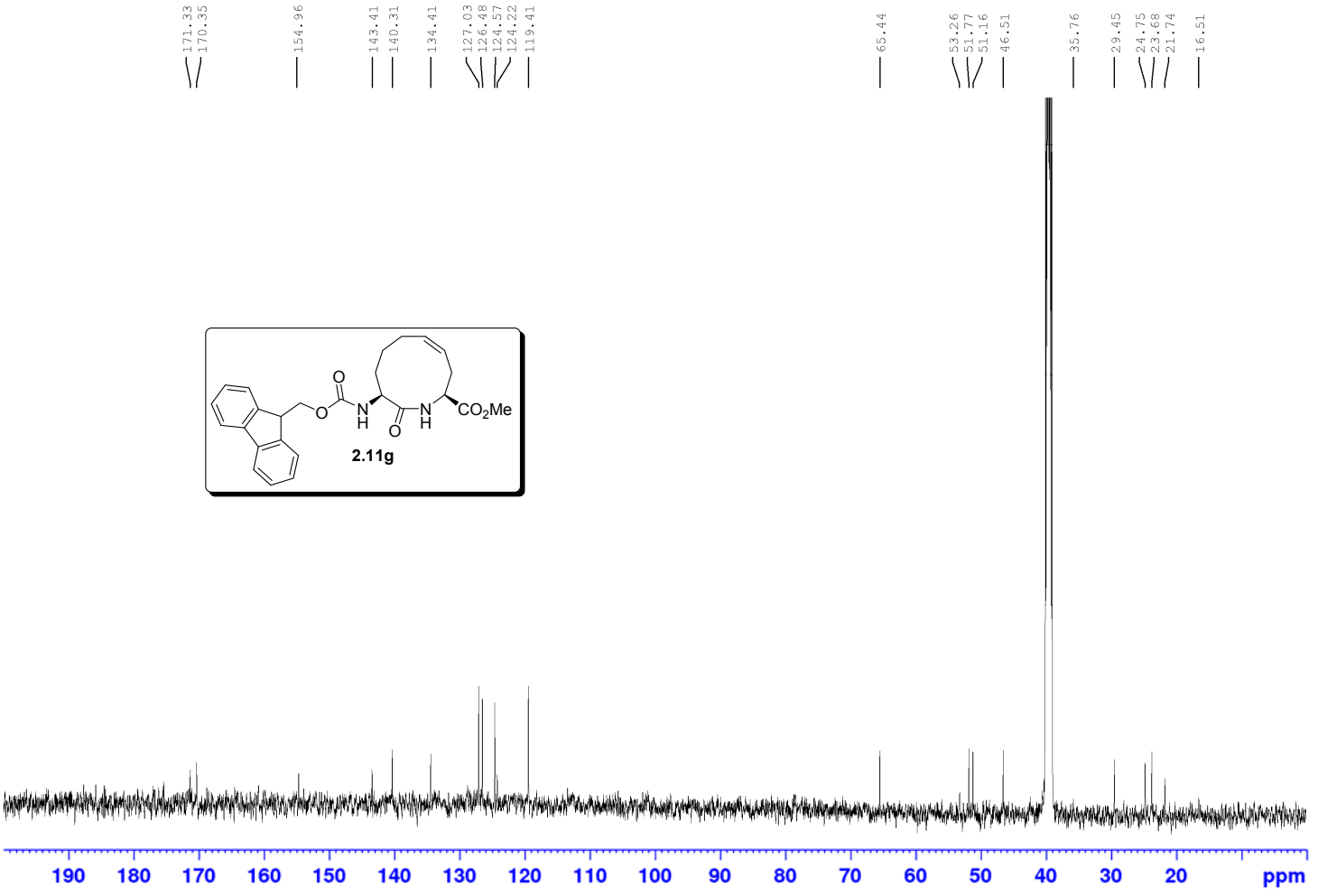

^{1}H NMR 700 MHz
Solvent: C_6D_6

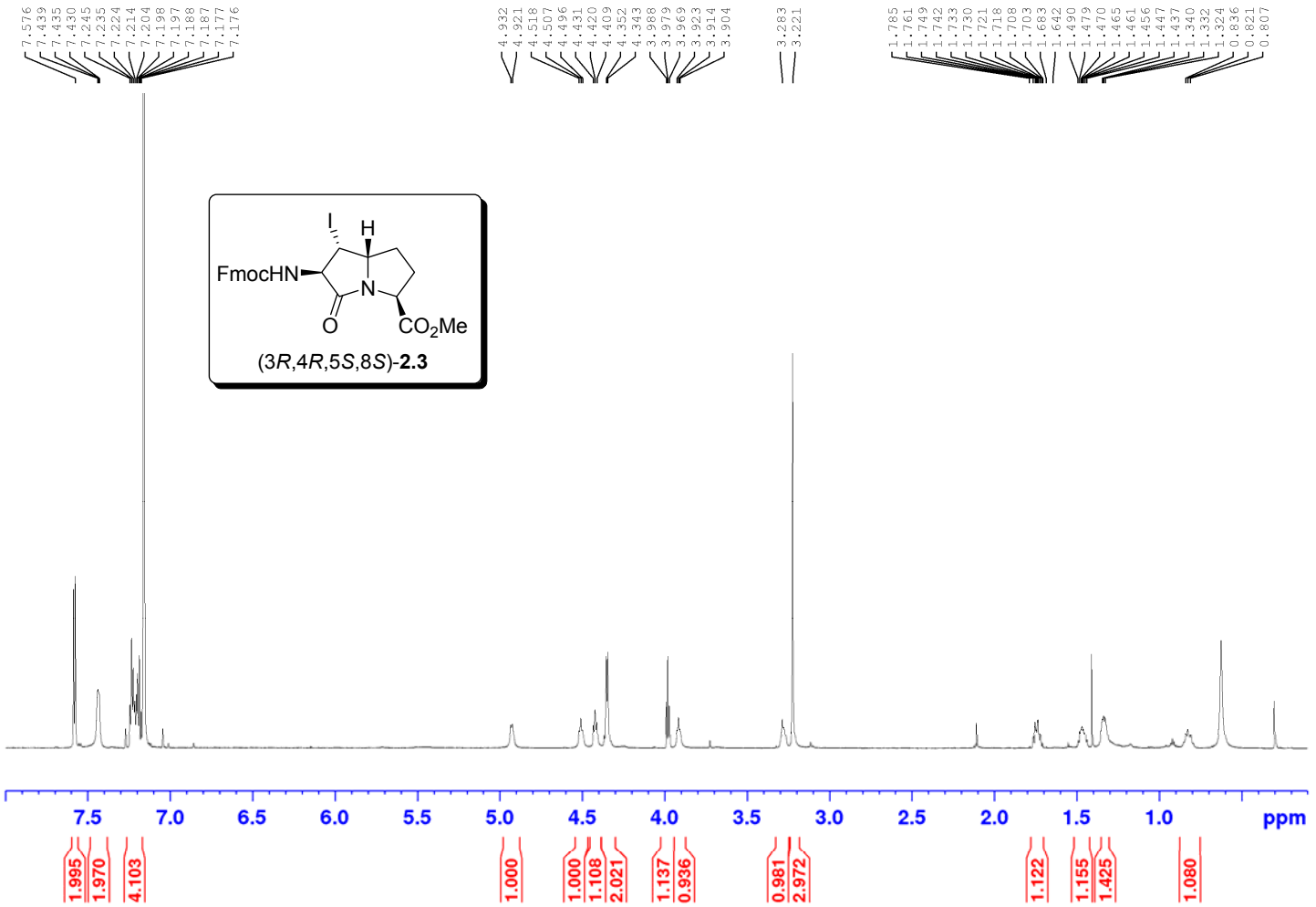

^{13}C NMR 700 MHz
Solvent: C_6D_6

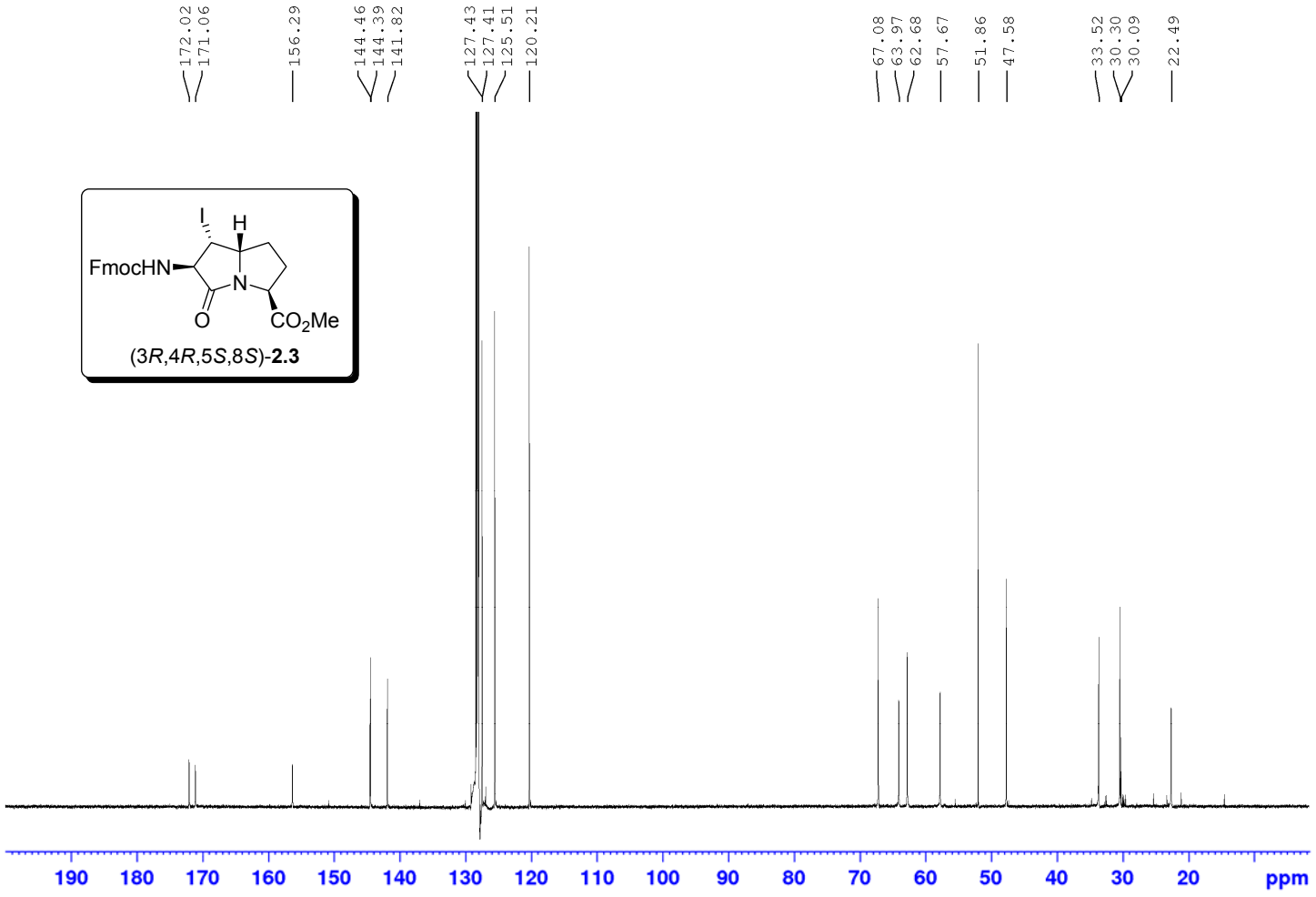

COSY 700 MHz
Solvent: C_6D_6

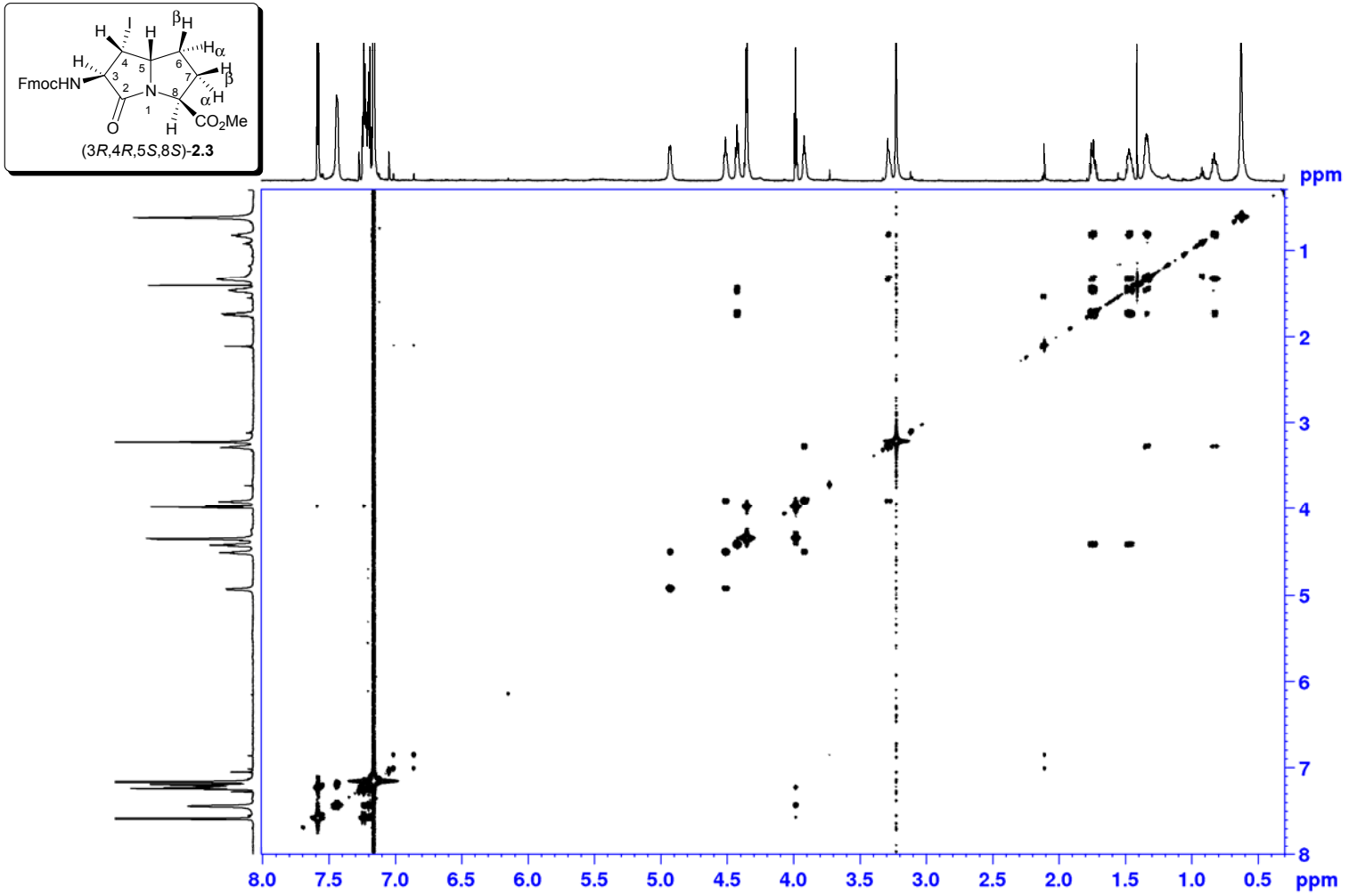

HSQC 700 MHz
Solvent: C_6D_6

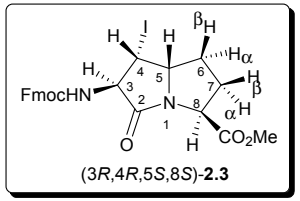

(3*R*,4*R*,5*S*,8*S*)-**2.3**

NOSY 700 MHz
Solvent: C_6D_6

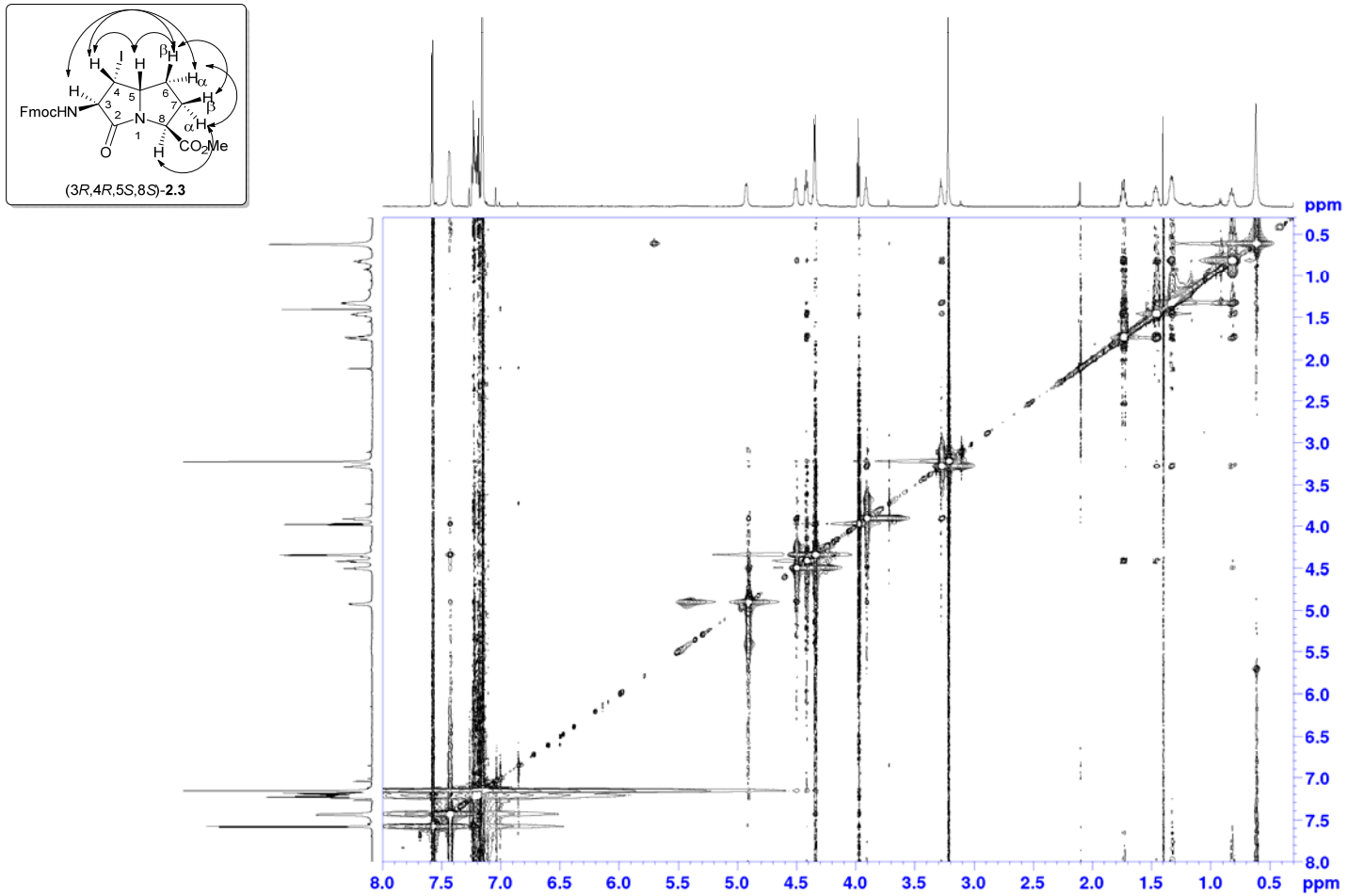

^{1}H NMR 700 MHz
Solvent: $CDCl_3$

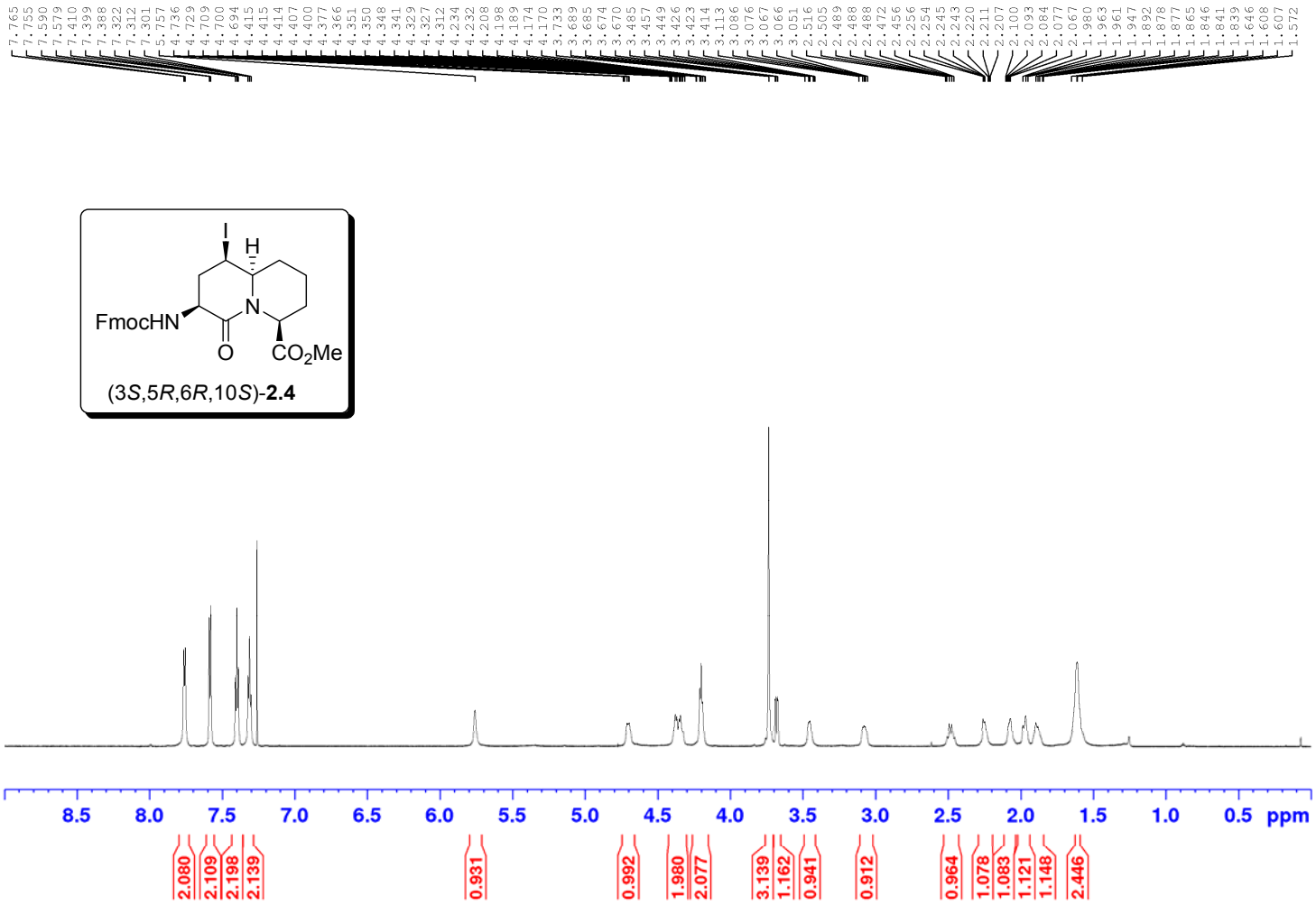

^{13}C NMR 700 MHz
Solvent: $CDCl_3$

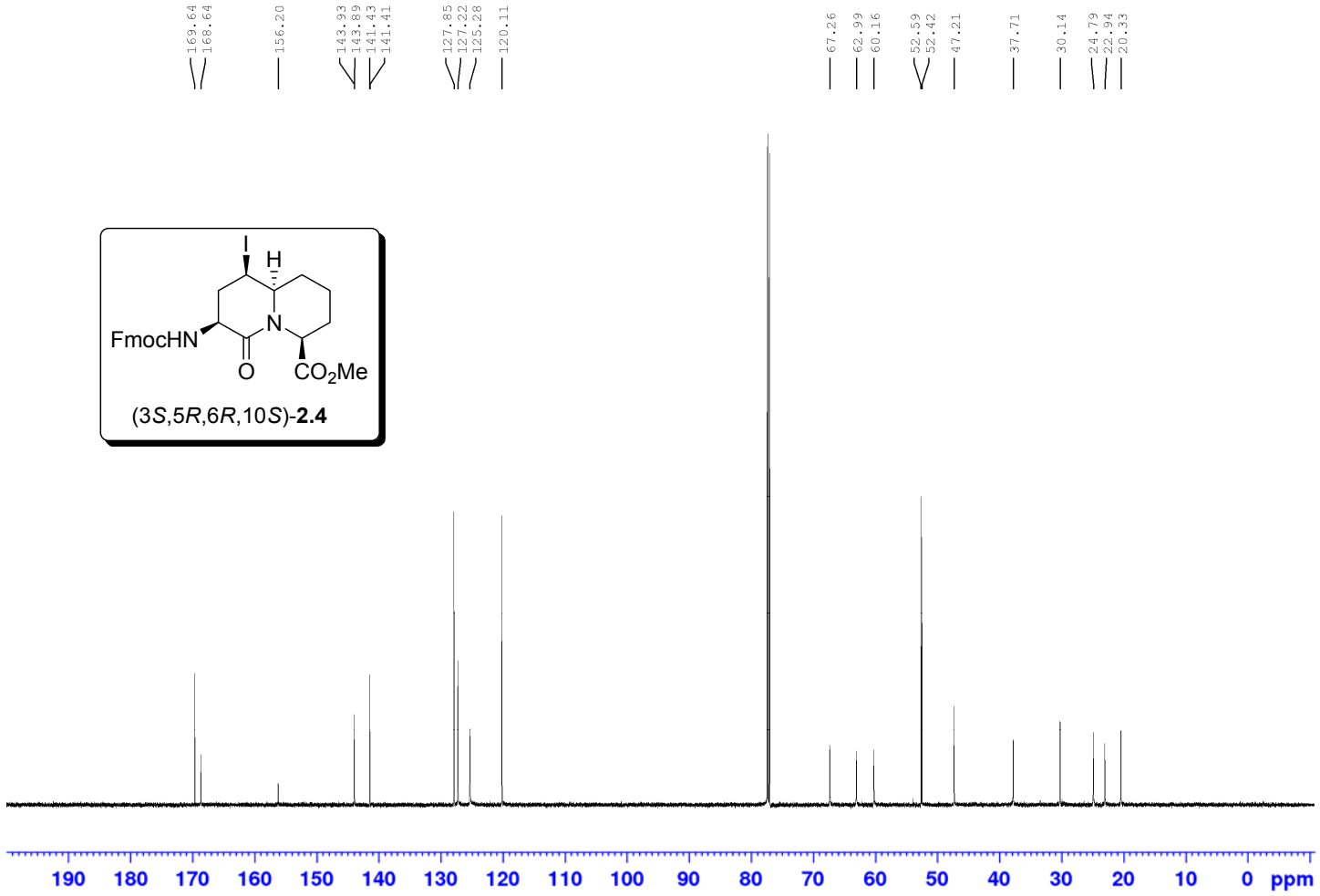

COSY 700 MHz
Solvent: $CDCl_3$

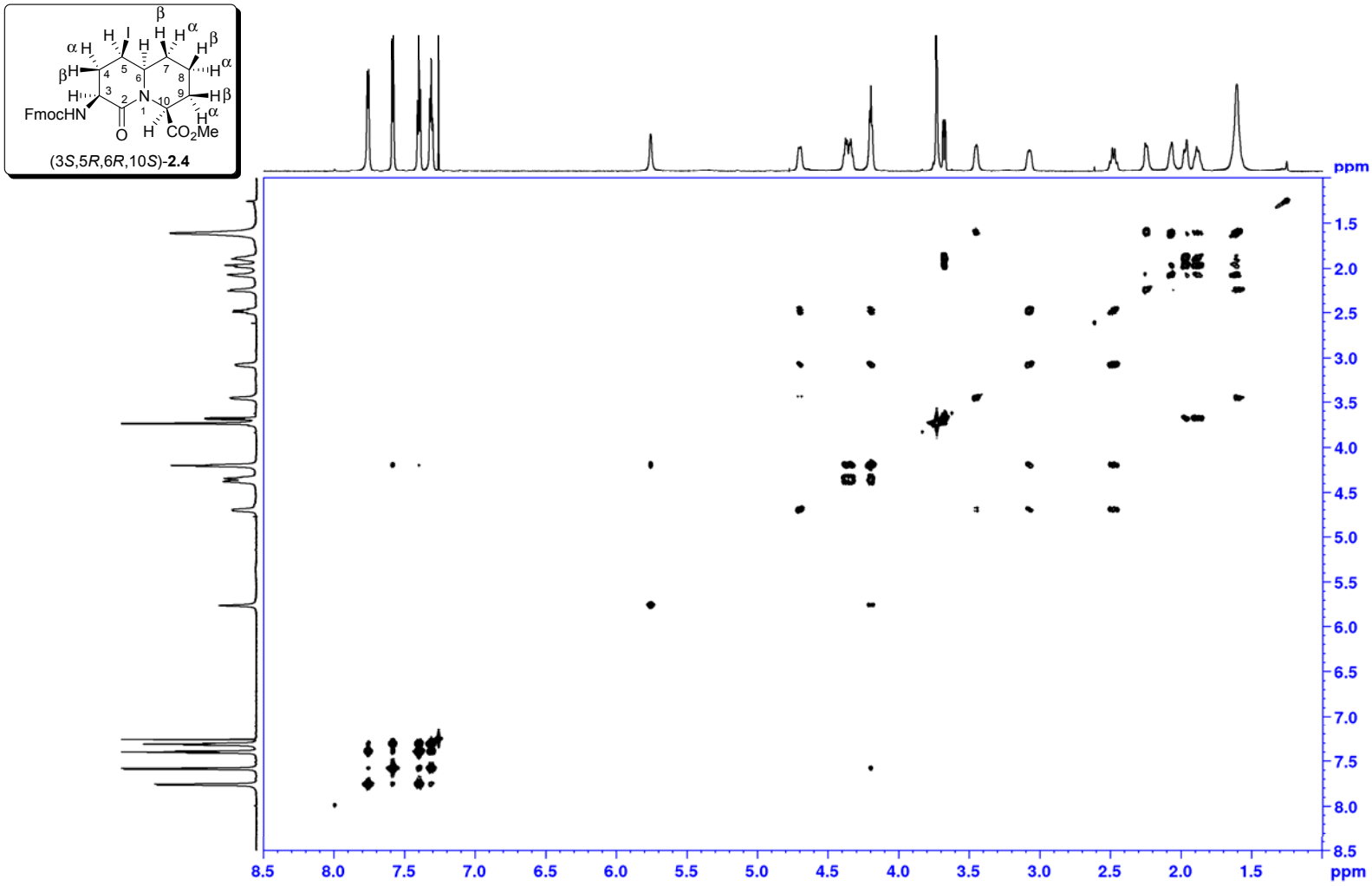

ROSY 700 MHz
Solvent: $CDCl_3$

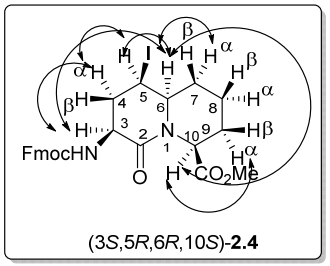

(3*S*,5*R*,6*R*,10*S*)-**2.4**

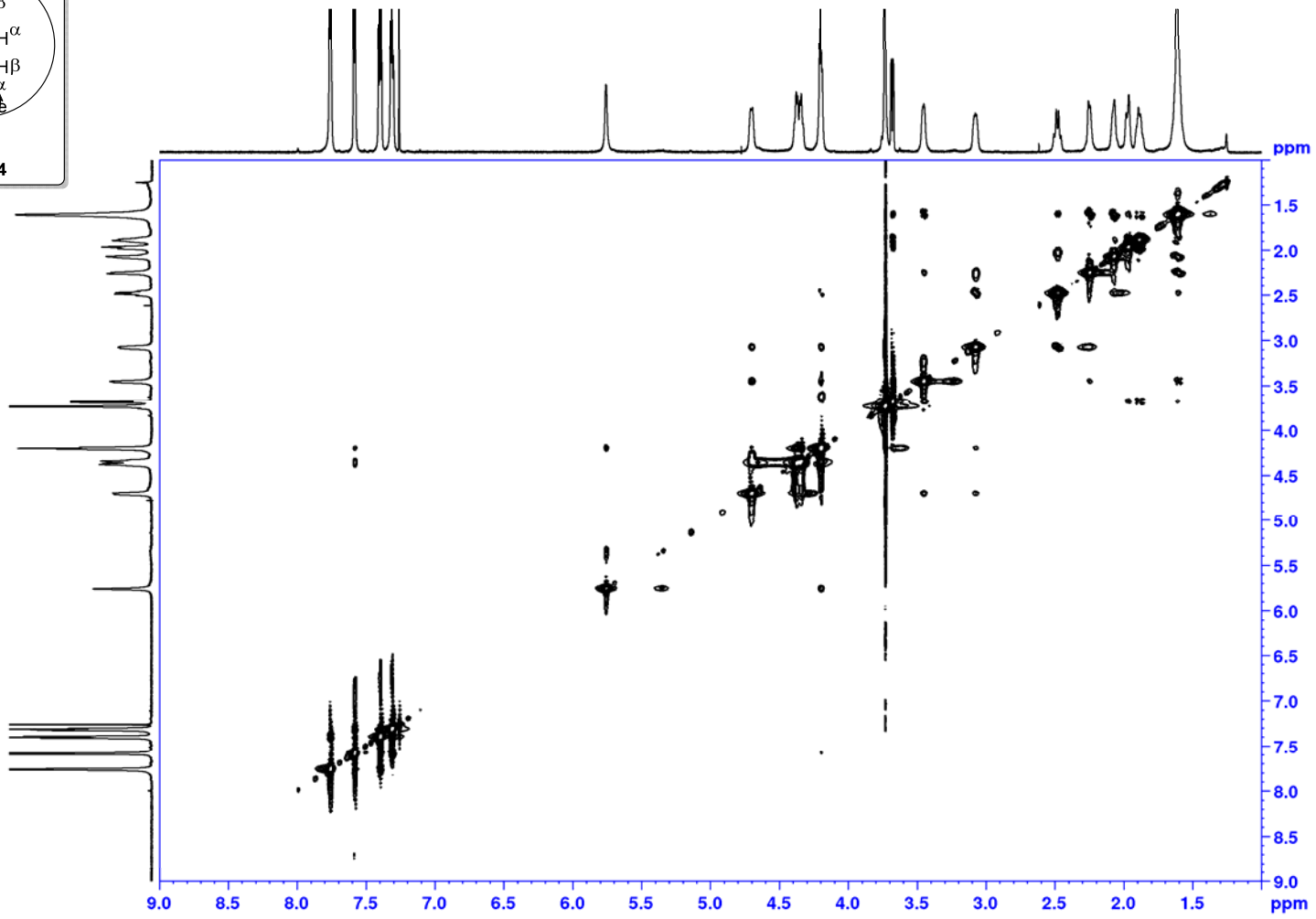

HSQC 700 MHz
Solvent: $CDCl_3$

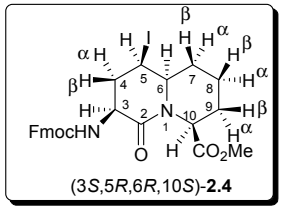

(3*S*,5*R*,6*R*,10*S*)-**2.4**

^{1}H NMR 700 MHz
Solvent: $CDCl_3$

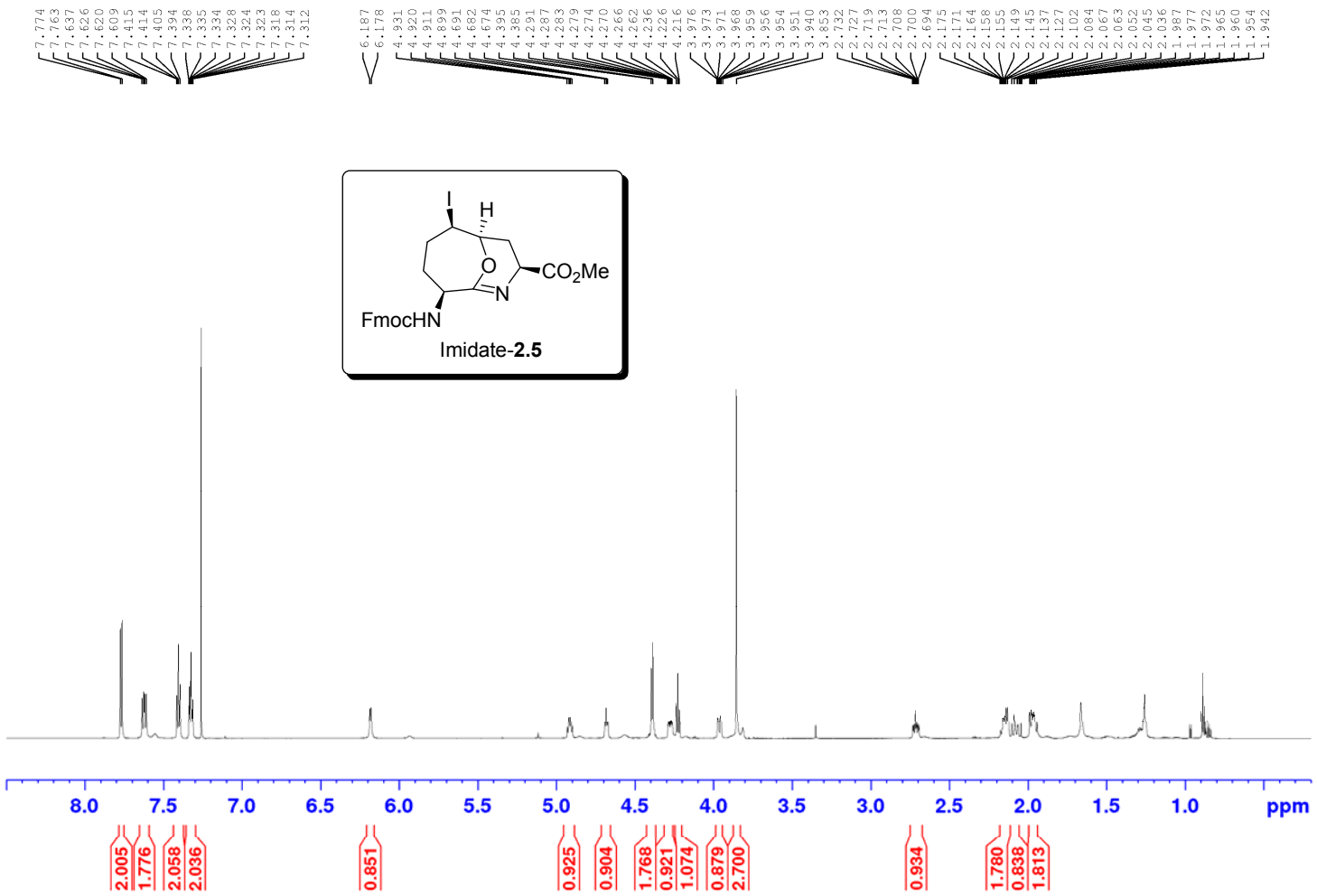

^{1}H NMR 700 MHz
Solvent: C_6D_6

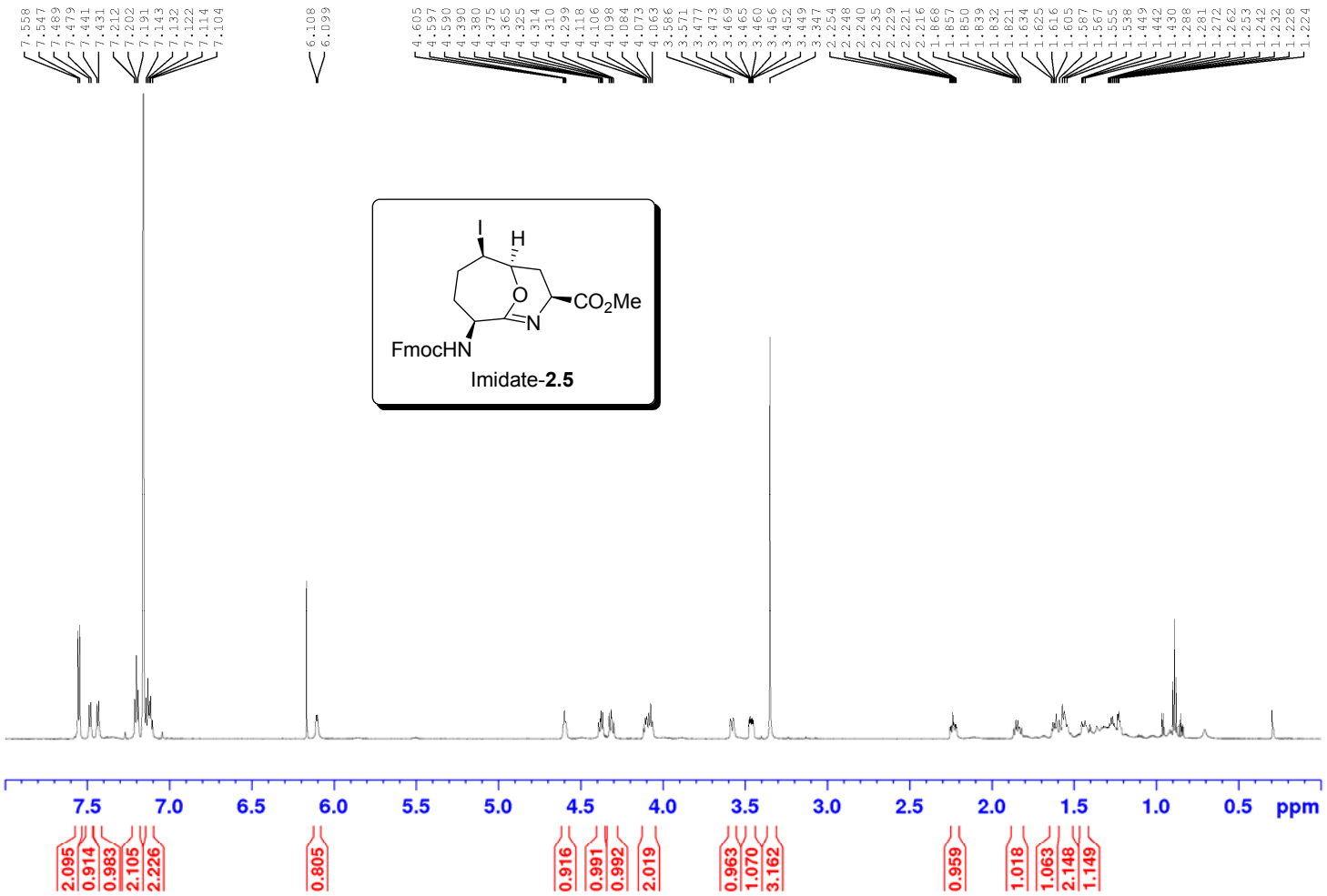

^{13}C NMR 700 MHz
Solvent: $CDCl_3$

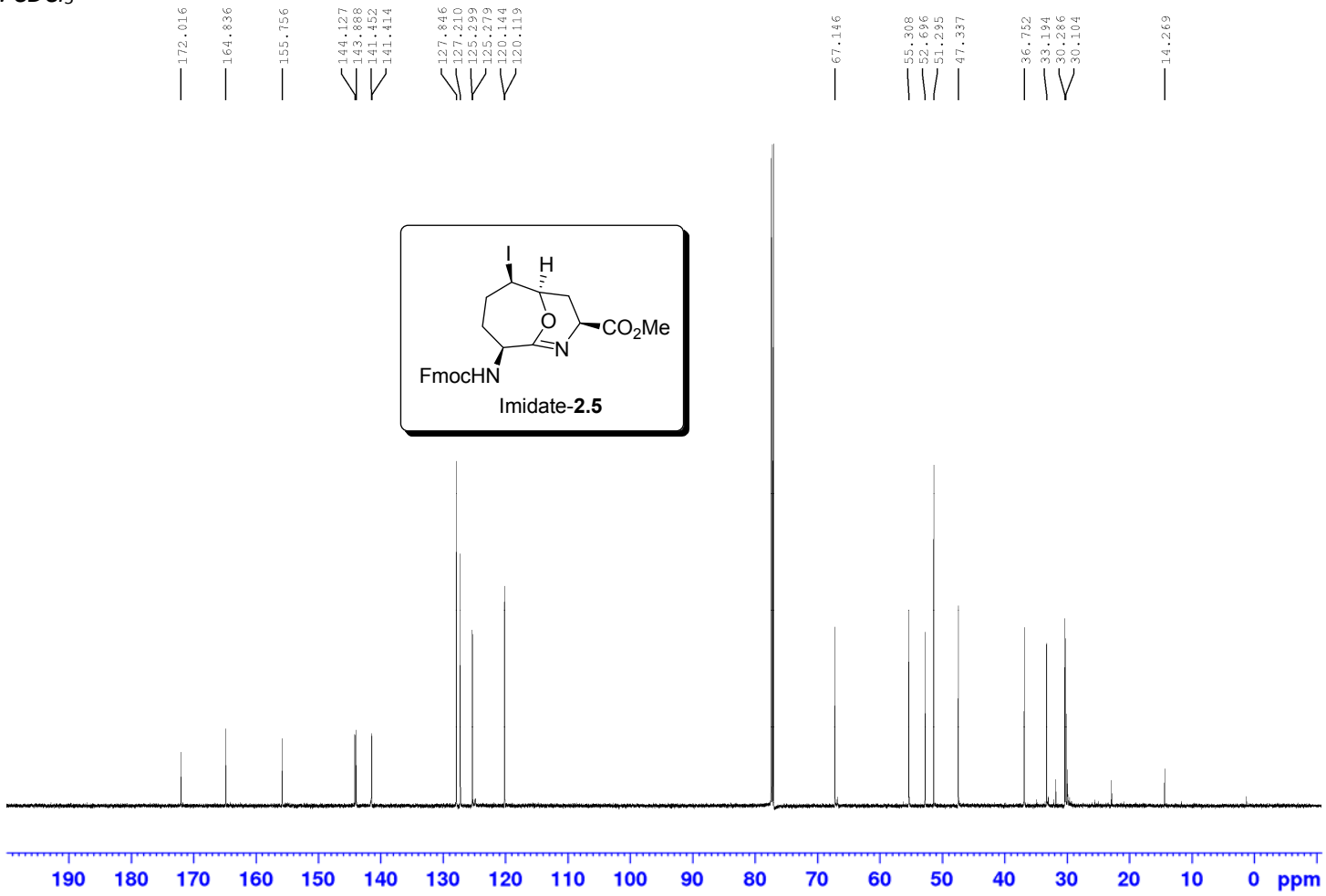

COSY 700 MHz
Solvent: C_6D_6

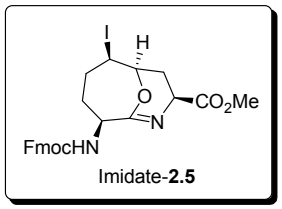

Imidate-**2.5**

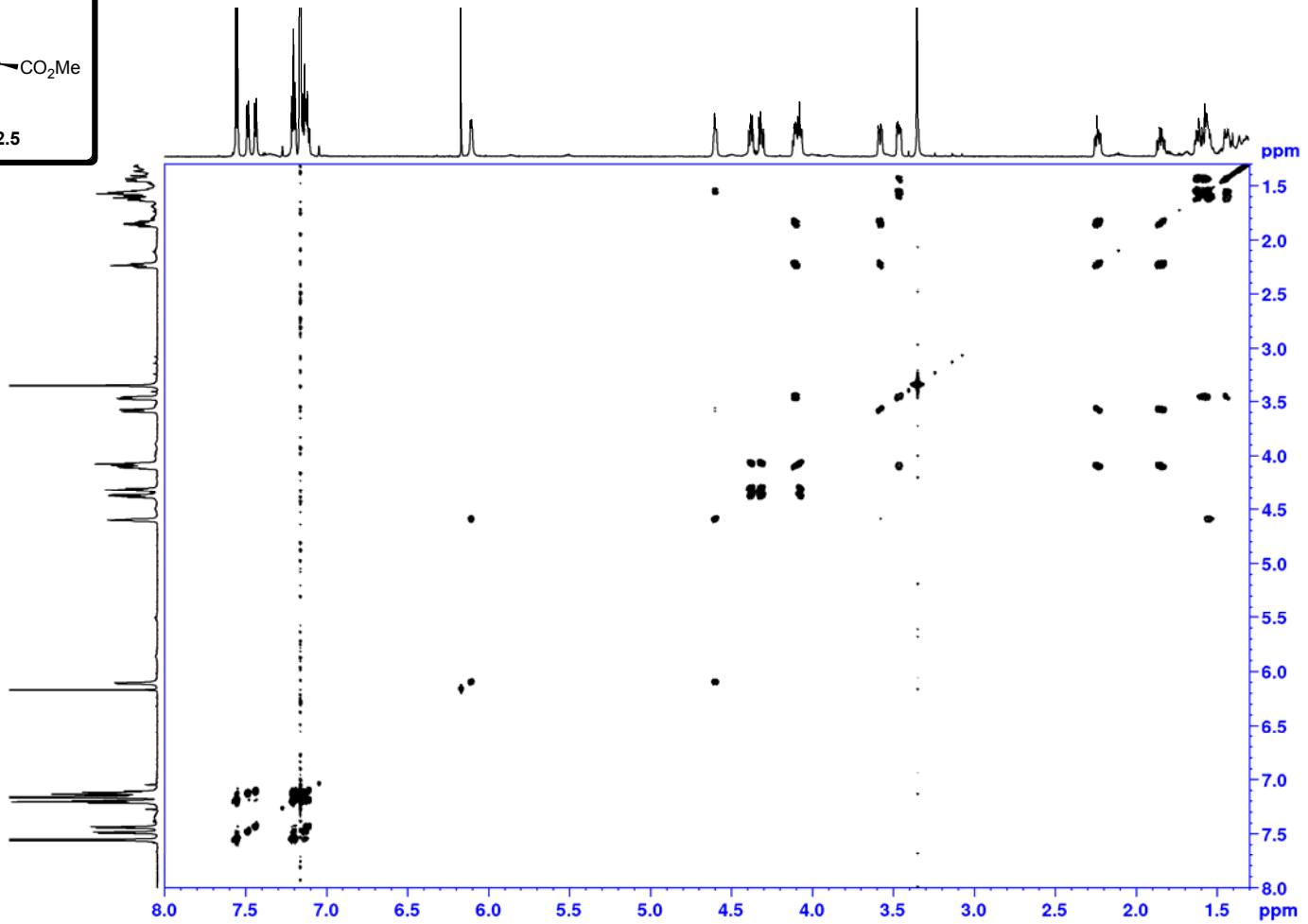

COSY 700 MHz
Solvent: C_6D_6

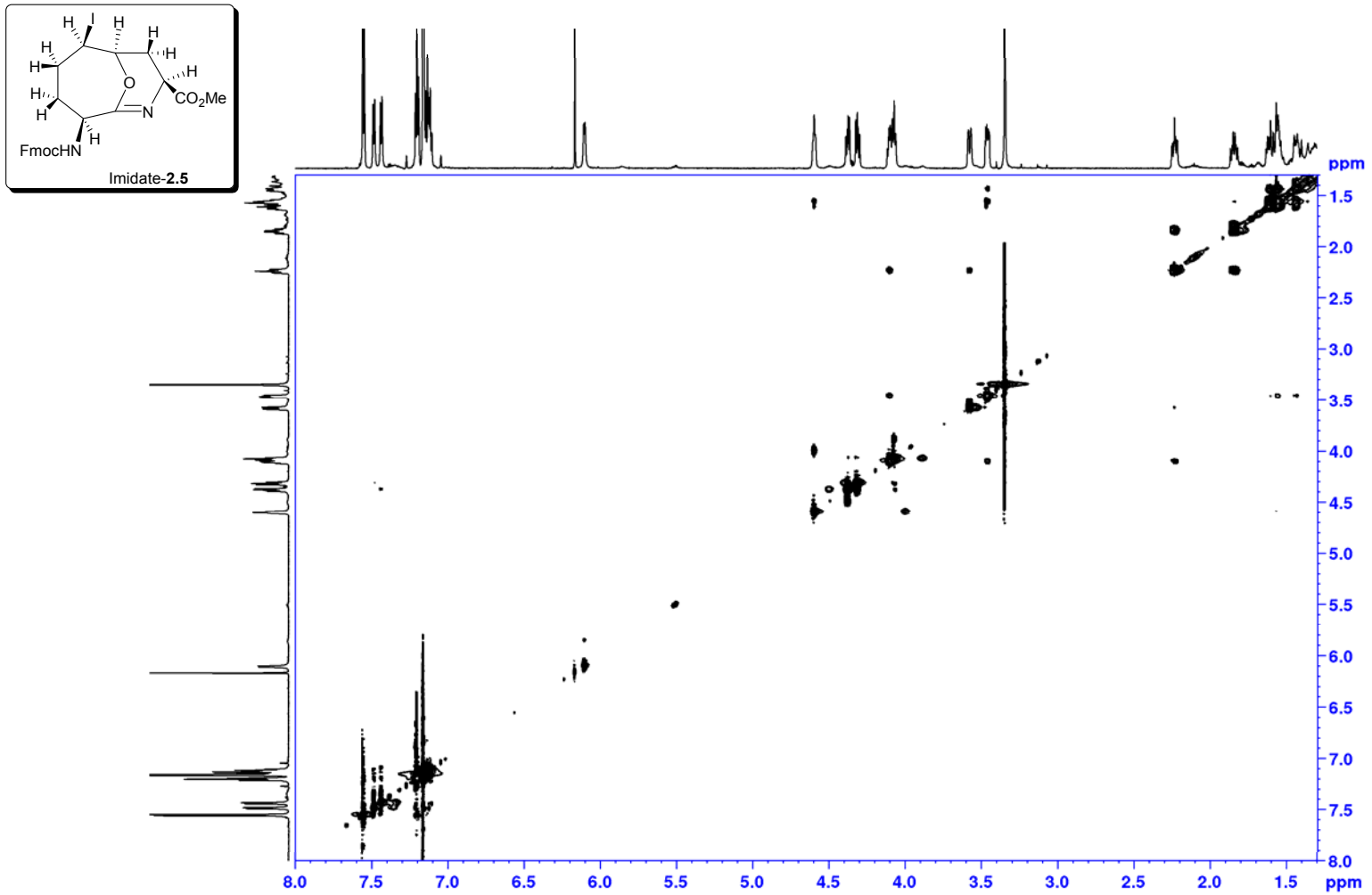

HSQC 700 MHz
Solvent: C_6D_6

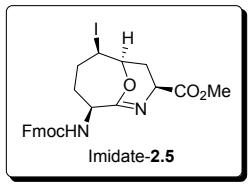

Imidate-**2.5**

1D NOE 700 MHz
Solvent: C_6D_6

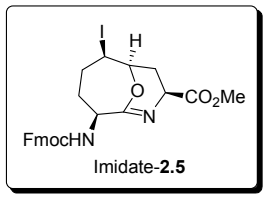

Imidate-**2.5**

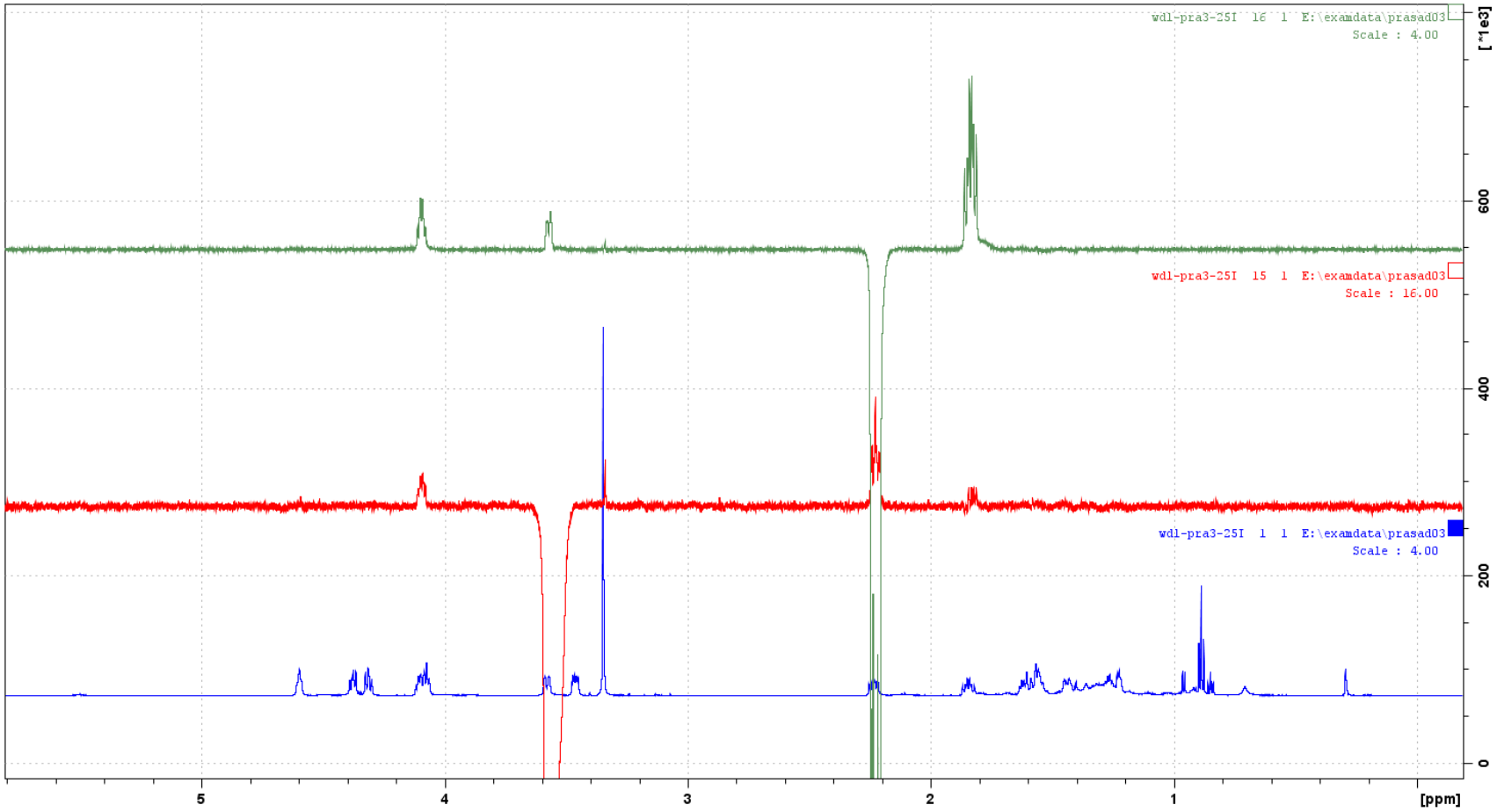

HOMO-DECOUPING700 MHz
Solvent: C_6D_6

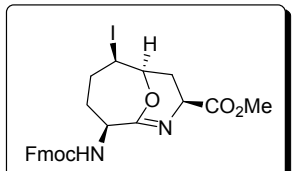

Imidate-**2.5**

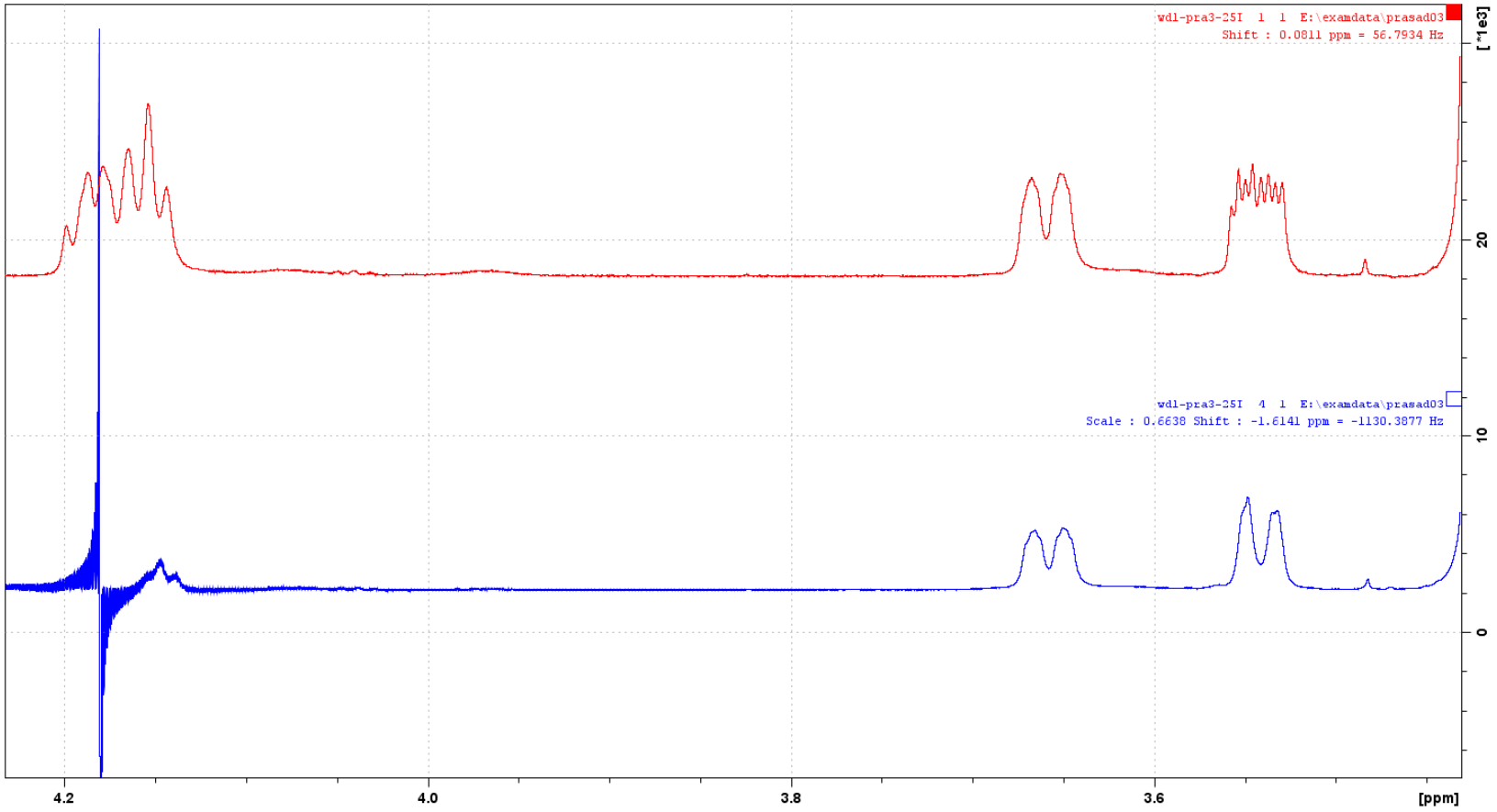

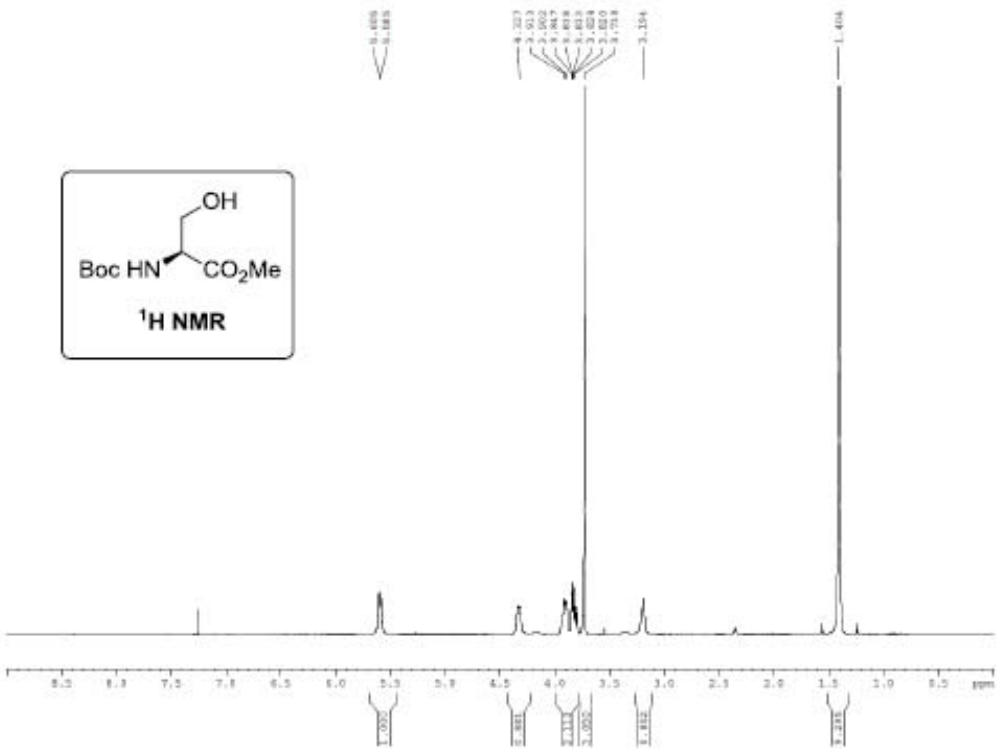
OH
Boc HN
CO2Me
1H NMR

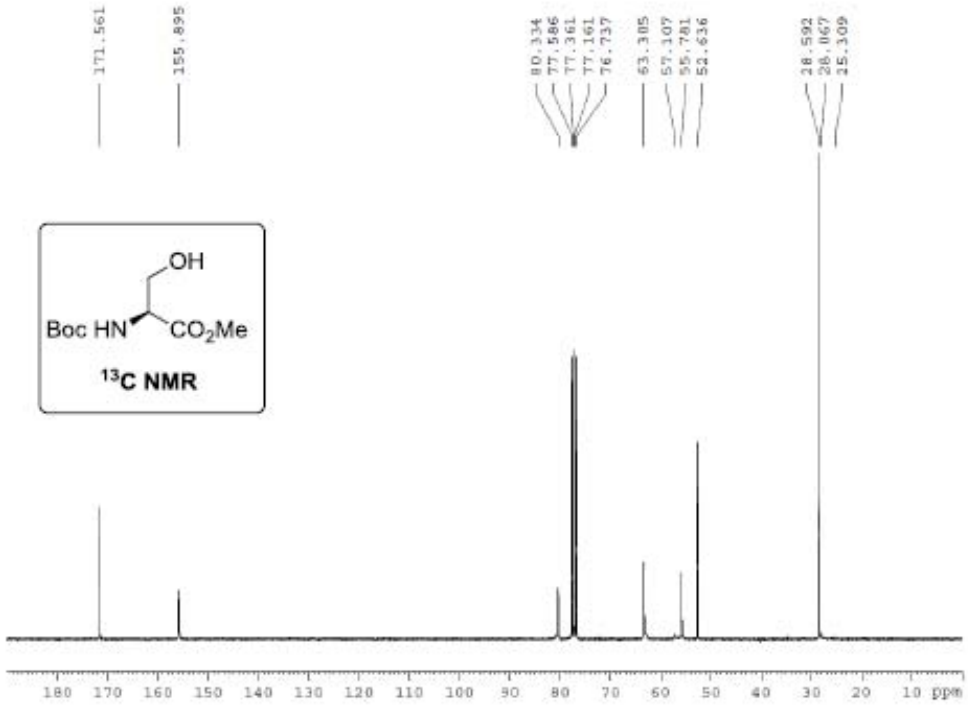
171.561
155.895
80.334
77.586
77.361
77.161
76.737
63.385
57.107
55.781
52.636
28.592
28.067
25.309
OH
Boc HN
CO2Me
13C NMR

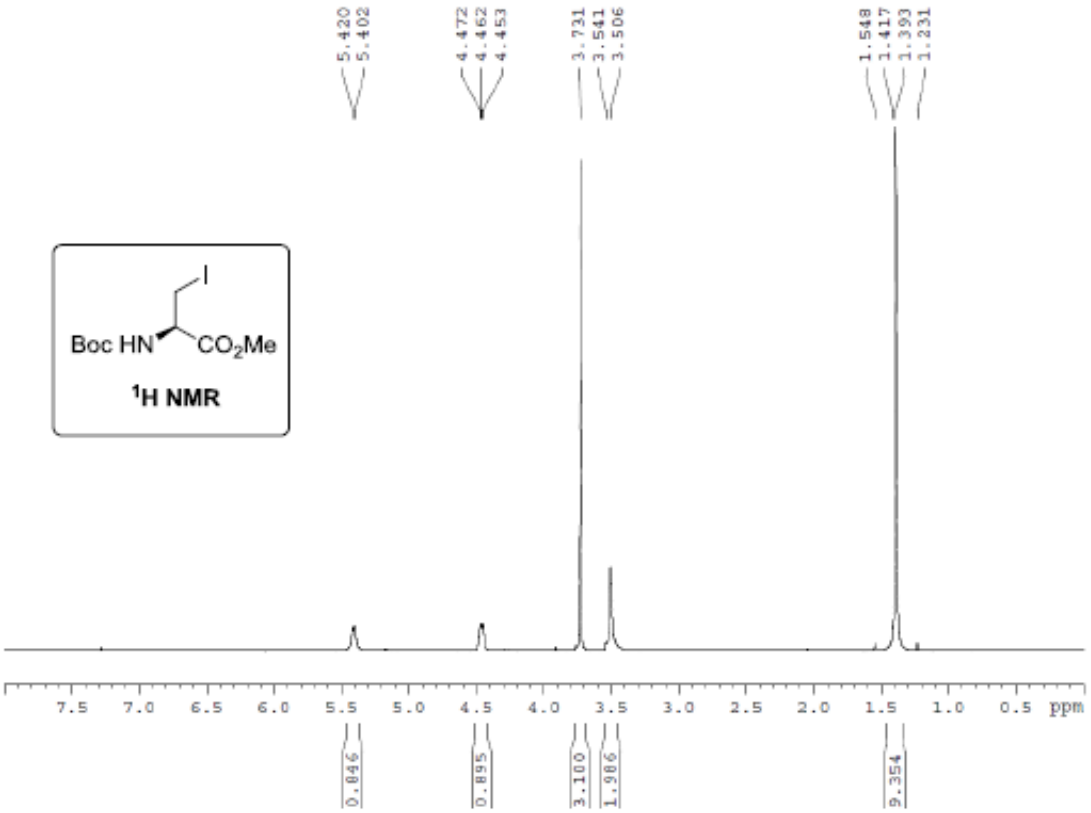
5.420
5.402
4.472
4.462
4.453
3.731
3.541
3.506
1.548
1.417
1.393
1.231
Boc HN
CO2Me
I
1H NMR
7.5 7.0 6.5 6.0 5.5 5.0 4.5 4.0 3.5 3.0 2.5 2.0 1.5 1.0 0.5 ppm
0.846
0.895
3.100
1.986
9.354

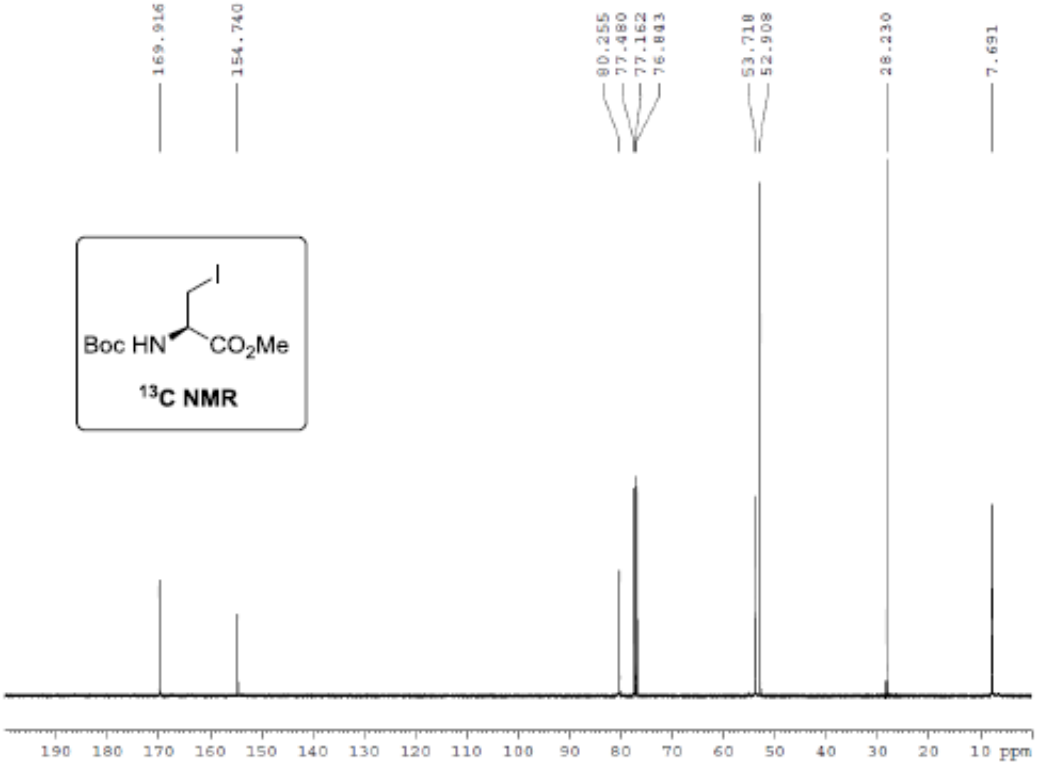
169.916
154.740
80.255
77.480
77.162
76.843
53.718
52.908
28.230
7.691
Boc HN
CO2Me
I
13C NMR
190 180 170 160 150 140 130 120 110 100 90 80 70 60 50 40 30 20 10 ppm

Data File D:\RESULTS\2014JAN14\2013NOV14 2014-01-14 09-27-12\PRA-L-D-12-18-PU-5.D
Sample Name: PRA-L-D-12-18-PU

Sample ID : PRA-L-D-12-18-PU	Operator : Christophe
Location : Vial 3	BPR Press : 150 bar
Solvent : 1 (MeOH), start @ 10%	Column : AD-H, 25cm, 5um (1)
Col Temp : 35deg C 35deg C	Inj Vol : 25uL into 20uL loop

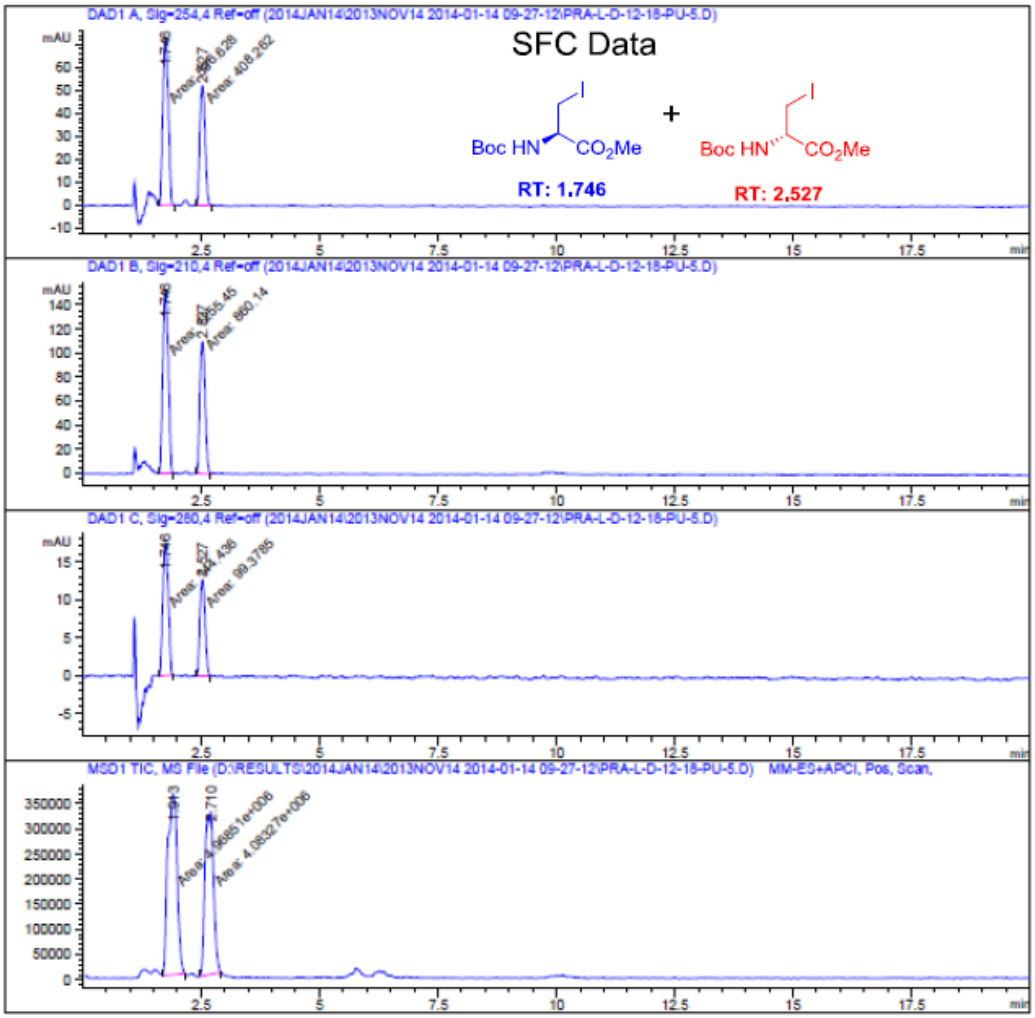

Data File D:\RESULTS\2014JAN14\2013NOV14 2014-01-14 09-27-12\PRA-L-D-12-18-PU-5.D
Sample Name: PRA-L-D-12-18-PU

Area Percent Report

Sorted By : Signal
Multiplier: : 1.0000
Dilution: : 1.0000
Use Multiplier & Dilution Factor with ISTDs

Signal 1: DAD1 A, Sig=254,4 Ref=off

Peak #	RetTime [min]	Type	Width [min]	Area [mAU*s]	Height [mAU]	Area %
1	1.746	MM	0.1379	596.62830	72.10466	59.3725
2	2.527	MM	0.1309	408.26178	51.99735	40.6275
Totals :				1004.89008	124.10201	

Signal 2: DAD1 B, Sig=210,4 Ref=off

Peak #	RetTime [min]	Type	Width [min]	Area [mAU*s]	Height [mAU]	Area %
1	1.746	MM	0.1381	1255.45166	151.47560	59.3428
2	2.527	MM	0.1310	860.13989	109.41715	40.6572
Totals :				2115.59155	260.89275	

Signal 3: DAD1 C, Sig=280,4 Ref=off

Peak #	RetTime [min]	Type	Width [min]	Area [mAU*s]	Height [mAU]	Area %
1	1.746	MM	0.1380	144.43571	17.43937	59.2401
2	2.527	MM	0.1311	99.37851	12.63045	40.7599
Totals :				243.81422	30.06982	

Signal 4: MSD1 TIC, MS File

Peak #	RetTime [min]	Type	Width [min]	Area	Height	Area %
1	1.913	MM	0.2308	4.96851e6	3.58739e5	54.8898
2	2.710	MM	0.2074	4.08327e6	3.28087e5	45.1102
Totals :				9.05178e6	6.86826e5	

Data File D:\RESULTS\2014JAN14\2013NOV14 2014-01-14 09-27-12\PRA-L-D-12-18-PU-5.D
Sample Name: PRA-L-D-12-18-PU

Signal DAD1 B, Sig=210,4 Ref=off (2014JAN14\2013NOV14 2014-01-14 09-27-12\PRA-L-D-12-18-PU-5.D)

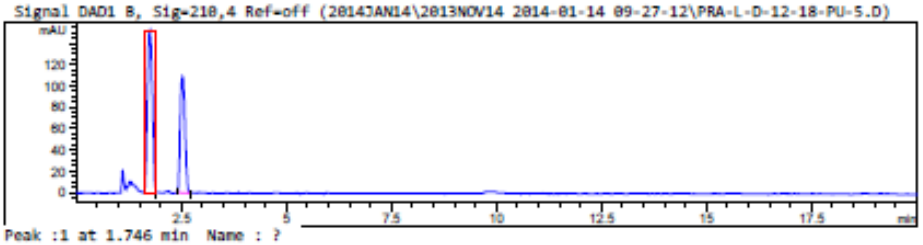

Peak :1 at 1.746 min Name : ?

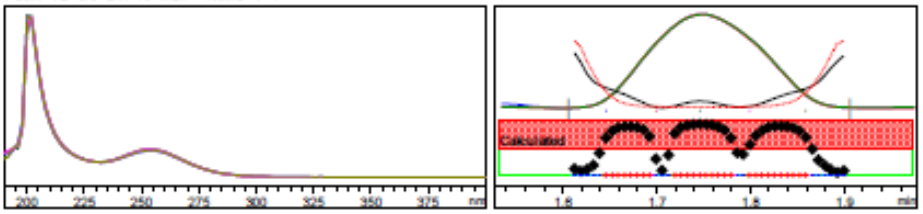

-> The purity factor exceeds the calculated threshold limit. <-

Purity factor : 998.759 (28 of 44 spectra exceed the calculated threshold limit.)
Threshold : 999.579 (Calculated with 28 of 44 spectra)
Reference : Peak start and end spectra (integrated) (1.606 / 1.906)
Spectra : 5 (Selection automatic, 5)
Noise Threshol: 0.420 (12 spectra, St.Dev 0.2012 + 3 * 0.073)

Data File D:\RESULTS\2014JAN14\2013NOV14 2014-01-14 09-27-12\PRA-L-D-12-18-PU-5.D
Sample Name: PRA-L-D-12-18-PU

Signal DAD1 B, Sig=210,4 Ref=off (2014JAN14\2013NOV14 2014-01-14 09-27-12\PRA-L-D-12-18-PU-5.D)

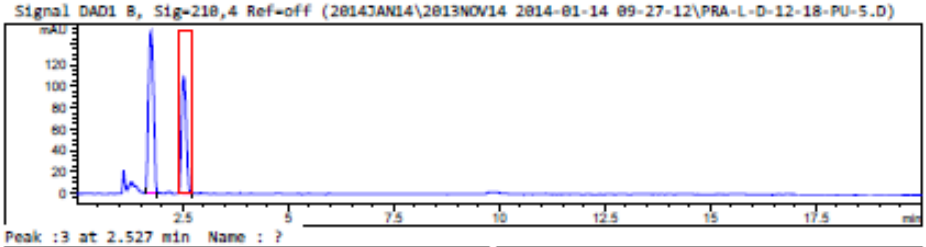

Peak :3 at 2.527 min Name : ?

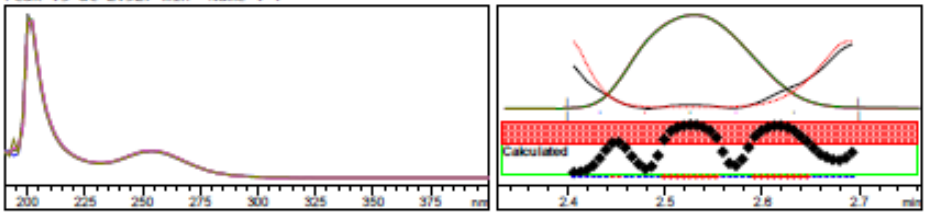

-> The purity factor exceeds the calculated threshold limit. <-

Purity factor : 997.660 (18 of 44 spectra exceed the calculated threshold limit.)
Threshold : 998.450 (Calculated with 18 of 44 spectra)
Reference : Peak start and end spectra (integrated) (2.399 / 2.699)
Spectra : 5 (Selection automatic, 5)
Noise Threshol: 0.420 (12 spectra, St.Dev 0.2012 + 3 * 0.073)

Data File D:\RESULTS\2014JAN14\2013NOV14 2014-01-14 09-27-12\PRA-L-D-12-18-PU-5.D
Sample Name: PRA-L-D-12-18-PU

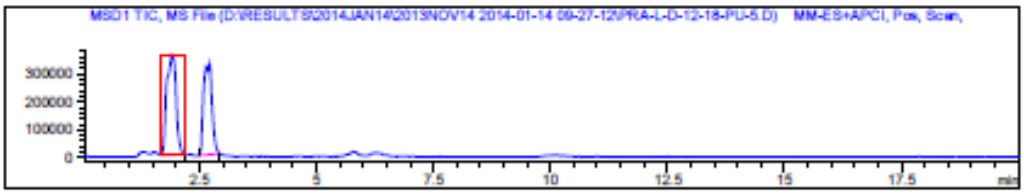

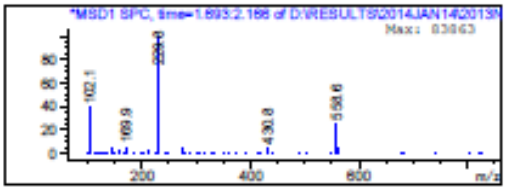

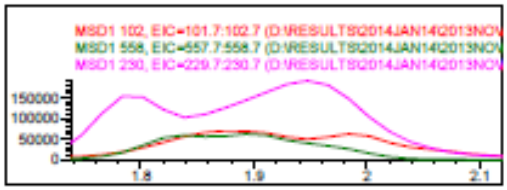

Peak #1 at 1.913 min (1.690 to 2.168 min)
-> The analysis found 3 components, indicating an impure peak. <-

Component 1: Peak at Scan 181.4. Top ions are 102
Component 2: Peak at Scan 182.1. Top ions are 558
Component 3: Peak at Scan 184.9. Top ions are 230

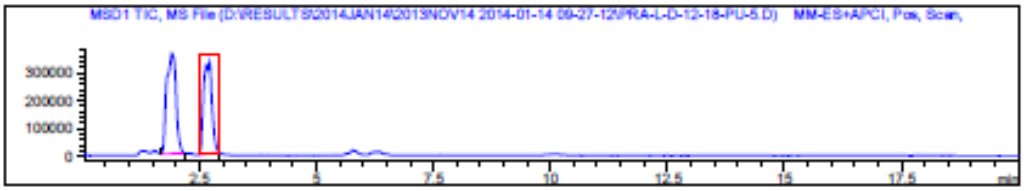

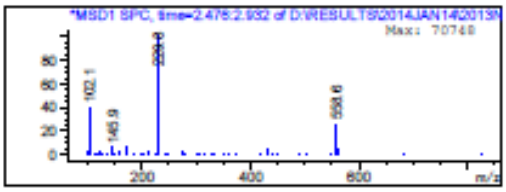

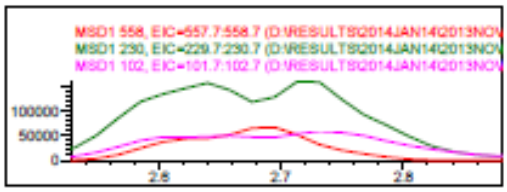

Peak #2 at 2.710 min (2.484 to 2.925 min)
-> The analysis found 3 components, indicating an impure peak. <-

Component 1: Peak at Scan 145.6. Top ions are 558
Component 2: Peak at Scan 147.5. Top ions are 230
Component 3: Peak at Scan 148.2. Top ions are 102

*** End of Report ***

Data File D:\RESULTS\2014JAN15\2013NOV14 2014-01-15 09-04-17\PRA-L-D-18-PU.D
Sample Name: PRA-L-D-18-PU

Sample ID	: PRA-L-D-18-PU	Operator	: Christophe
Location	: Vial 6	BPR Press	: 150 bar
Solvent	: 1 (MeOH), start @ 10%	Column	: AD-H, 25cm, Sun (1)
Col Temp	: 35deg C 35deg C	Inj Vol	: 25uL into 20uL loop

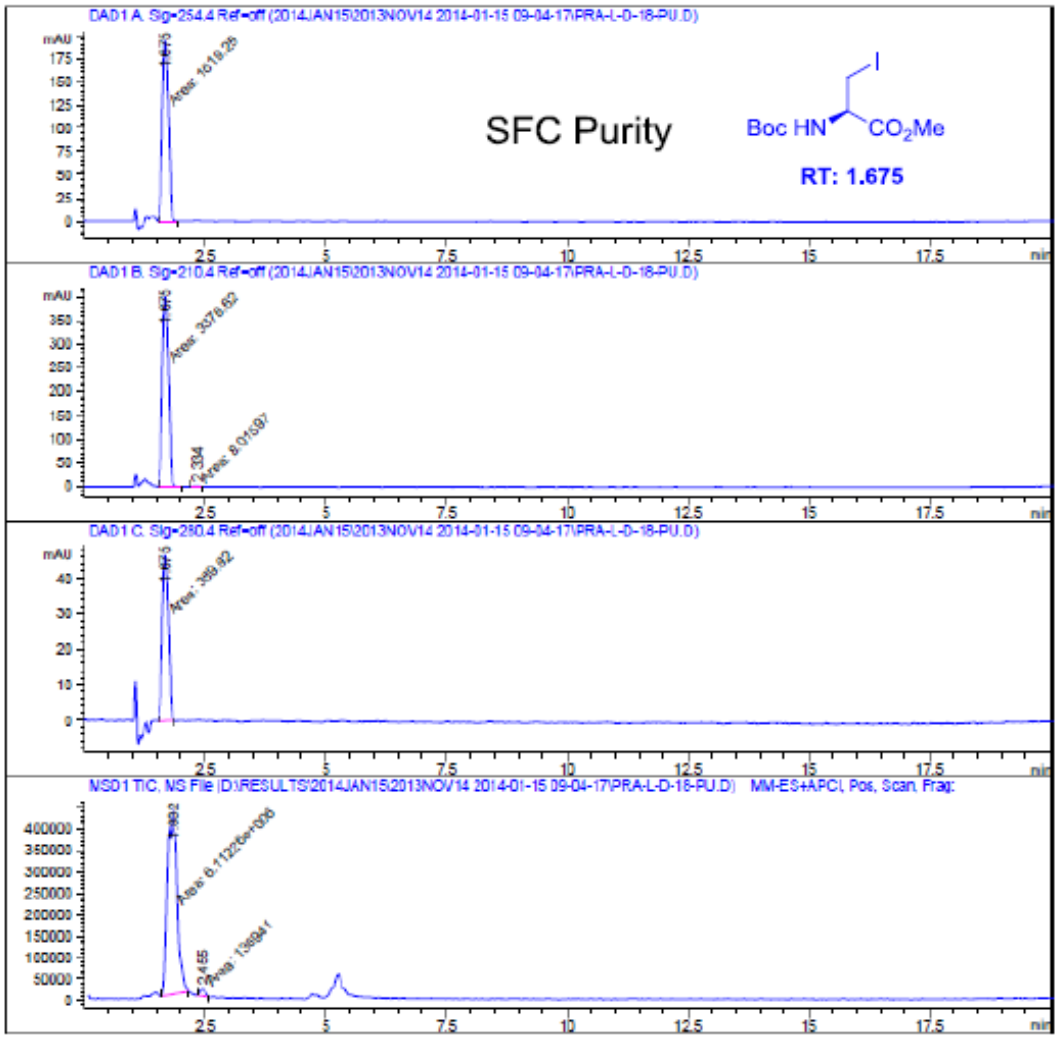

Data File D:\RESULTS\2014JAN15\2013NOV14 2014-01-15 09-04-17\PRA-L-D-12-PU.D
Sample Name: PRA-L-D-12-PU

Sample ID : PRA-L-D-12-PU	Operator : Christophe
Location : Vial 5	BPR Press : 150 bar
Solvent : 1 (MeOH), start @ 10%	Column : AD-H, 25cm, 5um (1)
Col Temp : 35deg C 35deg C	Inj Vol : 25uL into 20uL loop

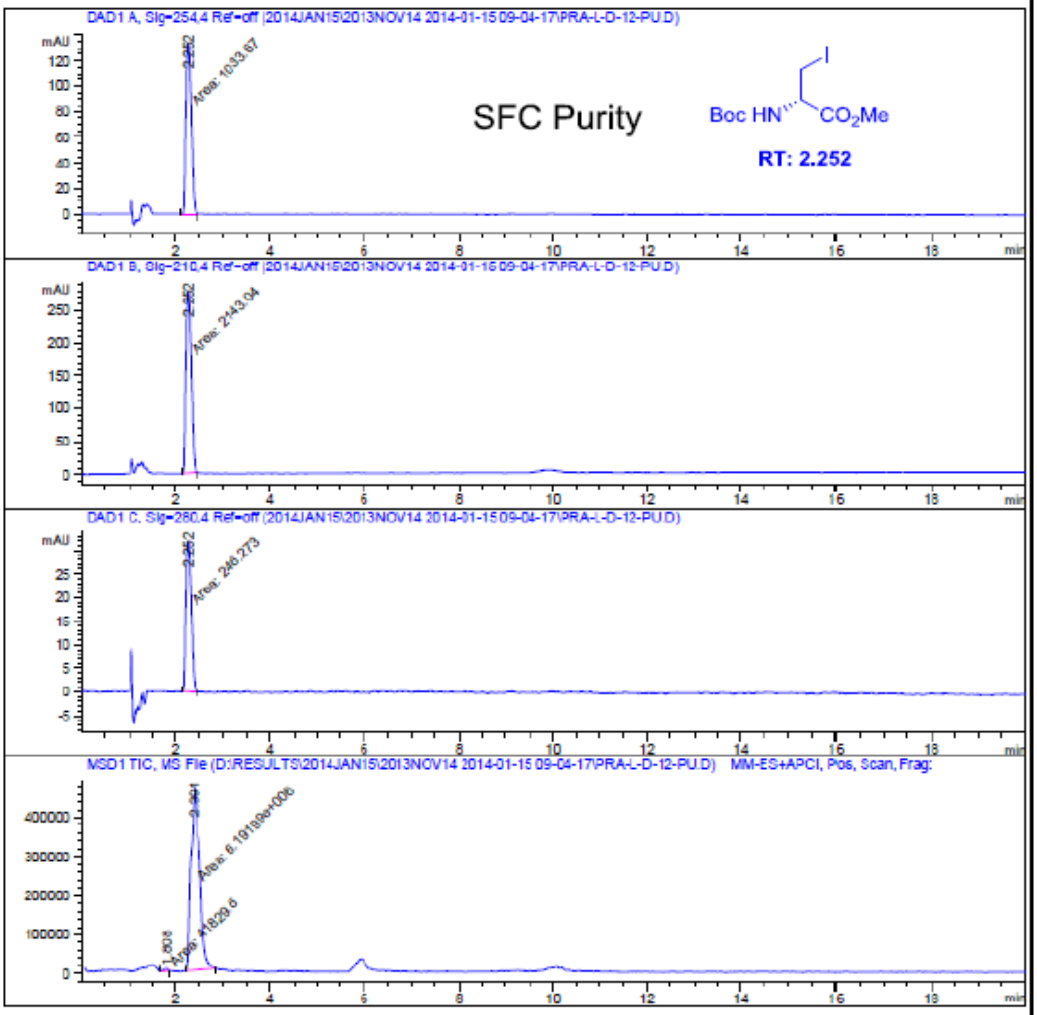

LUBE81: **(2.11a)**

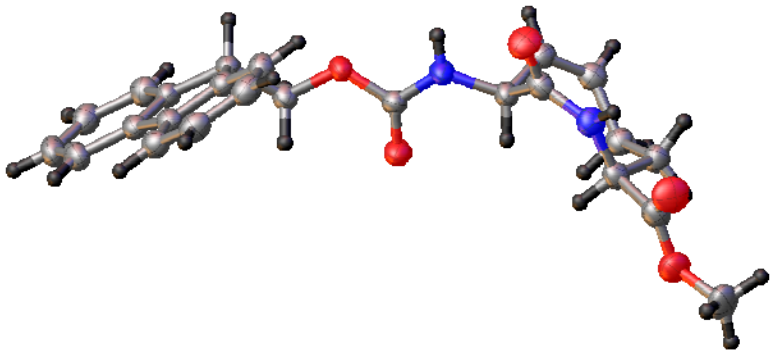

Table 1 Crystal data and structure refinement for LUBE81.

Identification code	LUBE81
Empirical formula	$C_{24}H_{24}N_2O_5$
Formula weight	420.45
Temperature/K	150
Crystal system	monoclinic
Space group	$P2_1$
a/Å	4.8504(4)
b/Å	11.6933(9)
c/Å	18.5551(15)
α/°	90
β/°	96.390(4)
γ/°	90
Volume/Å^3	1045.85(15)
Z	2
ρ_{calc}g/cm^3	1.335
μ/mm^{-1}	0.772
F(000)	444.0
Crystal size/mm^3	0.2 × 0.03 × 0.02
Radiation	CuKα (λ = 1.54178)
2Θ range for data collection/°	4.792 to 140.862
Index ranges	$-5 \leq h \leq 5$, $-14 \leq k \leq 13$, $-22 \leq l \leq 22$
Reflections collected	22284
Independent reflections	3776 [R_{int} = 0.0669, R_{sigma} = 0.0471]
Data/restraints/parameters	3776/1/289
Goodness-of-fit on F^2	1.046
Final R indexes [I>=2σ (I)]	R_1 = 0.0357, wR_2 = 0.0851
Final R indexes [all data]	R_1 = 0.0465, wR_2 = 0.0906
Largest diff. peak/hole / e Å^{-3}	0.12/-0.16
Flack parameter	-0.18(14)

Table 2 Fractional Atomic Coordinates ($\times 10^4$) and Equivalent Isotropic Displacement Parameters ($Å^2 \times 10^3$) for LUBE81. U_{eq} is defined as 1/3 of of the trace of the orthogonalised U_{IJ} tensor.

Atom	*x*	*y*	*z*	U(eq)
O1	12721(4)	4253.6(18)	3929.0(12)	44.3(5)
O2	4749(3)	3778.9(17)	2216.5(11)	37.7(5)
O3	7693(3)	4907.8(16)	1675.6(11)	32.4(5)
O4	9155(5)	3018(2)	5946.7(12)	55.8(6)
O5	5380(4)	1926(2)	5683.4(12)	46.9(6)
N1	9242(5)	3996(2)	2685.3(14)	35.5(6)
N2	10189(5)	3118(2)	4576.3(14)	35.4(6)
C1	9198(5)	3140(2)	3247.4(15)	30.1(6)
C2	10800(5)	3575(2)	3946.3(16)	32.9(7)
C3	7972(5)	2350(2)	4720.6(15)	33.0(6)
C4	8493(6)	1077(3)	4573.9(16)	35.3(6)
C5	7907(5)	724(2)	3780.8(16)	34.0(6)
C6	10093(5)	1014(3)	3306.2(15)	33.2(6)
C7	10629(5)	2052(2)	3056.2(15)	31.7(6)
C8	7041(5)	4182(2)	2197.1(15)	28.0(6)
C9	5461(5)	5194(2)	1121.1(16)	30.9(6)
C10	6238(5)	6302(2)	768.2(15)	28.7(6)
C11	6353(5)	7305(2)	1285.2(15)	28.9(6)
C12	8145(6)	7505(3)	1902.3(16)	35.6(7)
C13	7812(6)	8504(3)	2298.9(17)	39.6(7)
C14	5726(6)	9270(3)	2083.4(17)	40.7(7)
C15	3899(6)	9070(2)	1466.6(17)	35.7(6)
C16	4256(5)	8097(2)	1060.9(16)	30.2(6)
C17	2798(5)	7703(2)	370.7(15)	29.0(6)
C18	679(5)	8210(3)	-93.5(17)	37.0(7)
C19	-216(6)	7678(3)	-743.3(17)	40.0(8)
C20	949(6)	6653(3)	-927.5(17)	38.6(7)
C21	3016(6)	6128(3)	-461.0(16)	34.9(6)
C22	3956(5)	6665(2)	183.5(15)	28.7(6)
C23	7599(6)	2496(3)	5519.6(18)	38.3(7)
C24	5083(8)	1814(4)	6450.5(18)	56.6(9)

Table 3 Anisotropic Displacement Parameters ($Å^2 \times 10^3$) for LUBE81. The Anisotropic displacement factor exponent takes the form: $-2\pi^2[h^2a^{*2}U_{11}+2hka^*b^*U_{12}+\ldots]$.

Atom	U_{11}	U_{22}	U_{33}	U_{23}	U_{13}	U_{12}
O1	42.3(11)	45.0(12)	44.4(14)	-4.7(10)	-0.2(10)	-14.8(9)
O2	25.4(9)	47.4(12)	39.4(12)	10.1(10)	-0.2(8)	-4.6(8)
O3	23.7(8)	34.4(10)	38.2(11)	10.4(9)	-0.4(8)	0.1(7)

O4	61.3(13)	70.7(16)	35.0(13)	-13.4(12)	3.7(11)	-7.3(12)
O5	46.7(12)	61.9(15)	33.2(12)	3.7(11)	8.9(10)	4.8(10)
N1	22.8(11)	41.7(14)	41.2(15)	12.2(12)	-0.5(10)	-2.2(9)
N2	36.1(12)	40.4(14)	28.3(14)	-2.3(11)	-2.9(10)	-3(1)
C1	25.2(12)	33.6(14)	30.7(15)	5.7(13)	-0.5(11)	-1.8(10)
C2	30.1(13)	30.7(14)	36.9(17)	-2.5(13)	-1.4(12)	2.2(11)
C3	31.0(13)	38.3(16)	28.8(16)	-1.7(13)	-0.4(11)	2.6(11)
C4	36.8(14)	36.9(15)	32.0(16)	2.3(13)	3.1(12)	1.7(12)
C5	33.3(14)	31.2(15)	37.4(17)	0.0(13)	3.5(12)	-4.2(11)
C6	31.9(13)	33.9(15)	32.9(16)	-5.7(13)	-0.6(11)	-1.4(11)
C7	28.6(13)	37.0(16)	28.9(15)	0.2(12)	0.9(11)	-2.9(11)
C8	24.0(12)	28.9(13)	31.3(15)	1.3(12)	3.7(10)	0.5(10)
C9	25.5(12)	32.7(15)	33.5(16)	4.2(12)	-1.3(11)	-1.4(10)
C10	25.3(12)	29.9(14)	30.8(15)	3.6(12)	3.1(11)	-1.2(10)
C11	28.8(12)	28.3(14)	29.9(15)	2.1(12)	4.5(11)	-3.2(10)
C12	35.4(14)	37.1(16)	33.3(16)	4.4(13)	-1.0(12)	-3.3(11)
C13	42.5(15)	42.7(17)	33.0(16)	0.1(14)	1.9(13)	-11.5(13)
C14	49.9(16)	39.0(16)	34.7(17)	-5.3(14)	11.6(14)	-8.1(13)
C15	38.0(14)	32.6(15)	37.4(17)	0.4(13)	8.7(12)	0.0(11)
C16	27.7(12)	29.6(14)	33.6(15)	2.4(12)	4.6(11)	-3.5(10)
C17	26.7(12)	27.9(15)	32.5(16)	3.7(12)	3.9(11)	-2.4(10)
C18	31.6(13)	34.2(15)	44.7(18)	6.4(14)	1.3(13)	2.6(11)
C19	32.7(14)	43.5(18)	41.6(19)	12.7(14)	-5.0(13)	-2.3(12)
C20	40.0(15)	42.8(17)	31.6(17)	4.5(14)	-2.5(13)	-10.2(13)
C21	38.0(14)	31.4(14)	34.8(16)	0.0(13)	1.2(12)	-3.3(12)
C22	26.3(12)	31.2(14)	28.5(15)	3.9(12)	3.0(11)	-1.4(10)
C23	37.6(15)	42.4(17)	34.6(16)	-0.8(14)	2.3(13)	8.1(13)
C24	67(2)	72(3)	32.8(18)	10.9(17)	15.1(16)	17.8(19)

Table 4 Bond Lengths for LUBE81.

Atom	Atom	Length/Å	Atom	Atom	Length/Å
O1	C2	1.227(3)	C6	C7	1.335(4)
O2	C8	1.212(3)	C9	C10	1.518(4)
O3	C8	1.351(3)	C10	C11	1.512(4)
O3	C9	1.448(3)	C10	C22	1.521(4)
O4	C23	1.198(4)	C11	C12	1.378(4)
O5	C23	1.330(4)	C11	C16	1.404(4)
O5	C24	1.452(4)	C12	C13	1.399(5)
N1	C1	1.447(4)	C13	C14	1.376(5)
N1	C8	1.339(3)	C14	C15	1.387(4)
N2	C2	1.348(4)	C15	C16	1.386(4)
N2	C3	1.448(4)	C16	C17	1.466(4)
C1	C2	1.523(4)	C17	C18	1.397(4)

C1	C7	1.510(4)	C17	C22	1.398(4)
C3	C4	1.539(4)	C18	C19	1.383(5)
C3	C23	1.523(4)	C19	C20	1.383(5)
C4	C5	1.524(4)	C20	C21	1.392(4)
C5	C6	1.491(4)	C21	C22	1.382(4)

Table 5 Bond Angles for LUBE81.

Atom	Atom	Atom	Angle/°	Atom	Atom	Atom	Angle/°
C8	O3	C9	116.01(19)	C12	C11	C10	129.3(3)
C23	O5	C24	116.1(3)	C12	C11	C16	120.2(3)
C8	N1	C1	121.7(2)	C16	C11	C10	110.4(2)
C2	N2	C3	130.2(2)	C11	C12	C13	118.6(3)
N1	C1	C2	109.6(2)	C14	C13	C12	121.0(3)
N1	C1	C7	111.6(2)	C13	C14	C15	120.8(3)
C7	C1	C2	106.1(2)	C16	C15	C14	118.6(3)
O1	C2	N2	121.3(3)	C11	C16	C17	108.4(2)
O1	C2	C1	120.7(3)	C15	C16	C11	120.7(2)
N2	C2	C1	117.7(2)	C15	C16	C17	130.9(2)
N2	C3	C4	115.3(2)	C18	C17	C16	130.9(3)
N2	C3	C23	106.3(2)	C18	C17	C22	120.2(3)
C23	C3	C4	108.7(2)	C22	C17	C16	108.7(2)
C5	C4	C3	114.6(2)	C19	C18	C17	118.9(3)
C6	C5	C4	116.1(2)	C18	C19	C20	120.5(3)
C7	C6	C5	126.2(3)	C19	C20	C21	120.9(3)
C6	C7	C1	124.9(3)	C22	C21	C20	118.9(3)
O2	C8	O3	123.7(2)	C17	C22	C10	110.2(2)
O2	C8	N1	125.6(3)	C21	C22	C10	129.4(3)
N1	C8	O3	110.8(2)	C21	C22	C17	120.4(2)
O3	C9	C10	107.6(2)	O4	C23	O5	124.8(3)
C9	C10	C22	110.5(2)	O4	C23	C3	124.5(3)
C11	C10	C9	112.4(2)	O5	C23	C3	110.7(2)
C11	C10	C22	102.1(2)				

Table 6 Hydrogen Bonds for LUBE81.

D	H	A	d(D-H)/Å	d(H-A)/Å	d(D-A)/Å	D-H-A/°
N1	H1	O2[1]	0.81(4)	2.18(4)	2.911(3)	149(3)

[1]1+X,+Y,+Z

Table 7 Torsion Angles for LUBE81.

A	B	C	D	Angle/°	A	B	C	D	Angle/°
O3	C9	C10	C11	-66.0(3)	C10	C11	C16	C15	177.8(3)
O3	C9	C10	C22	-179.3(2)	C10	C11	C16	C17	-3.8(3)
N1	C1	C2	O1	-28.8(3)	C11	C10	C22	C17	-3.6(3)
N1	C1	C2	N2	156.6(2)	C11	C10	C22	C21	175.5(3)
N1	C1	C7	C6	-154.3(3)	C11	C12	C13	C14	0.5(5)
N2	C3	C4	C5	-81.2(3)	C11	C16	C17	C18	-175.9(3)
N2	C3	C23	O4	-10.1(4)	C11	C16	C17	C22	1.4(3)
N2	C3	C23	O5	172.5(2)	C12	C11	C16	C15	-2.0(4)
C1	N1	C8	O2	9.1(5)	C12	C11	C16	C17	176.4(3)
C1	N1	C8	O3	-172.0(2)	C12	C13	C14	C15	0.0(5)
C2	N2	C3	C4	81.5(4)	C13	C14	C15	C16	-1.6(4)
C2	N2	C3	C23	-158.0(3)	C14	C15	C16	C11	2.6(4)
C2	C1	C7	C6	86.4(3)	C14	C15	C16	C17	-175.5(3)
C3	N2	C2	O1	177.1(3)	C15	C16	C17	C18	2.3(5)
C3	N2	C2	C1	-8.4(4)	C15	C16	C17	C22	179.6(3)
C3	C4	C5	C6	78.9(3)	C16	C11	C12	C13	0.4(4)
C4	C3	C23	O4	114.5(3)	C16	C17	C18	C19	175.9(3)
C4	C3	C23	O5	-62.8(3)	C16	C17	C22	C10	1.6(3)
C4	C5	C6	C7	-74.5(4)	C16	C17	C22	C21	-177.7(3)
C5	C6	C7	C1	3.6(4)	C17	C18	C19	C20	0.7(4)
C7	C1	C2	O1	91.9(3)	C18	C17	C22	C10	179.1(2)
C7	C1	C2	N2	-82.7(3)	C18	C17	C22	C21	-0.1(4)
C8	O3	C9	C10	159.4(2)	C18	C19	C20	C21	0.8(5)
C8	N1	C1	C2	-142.7(3)	C19	C20	C21	C22	-1.9(5)
C8	N1	C1	C7	100.0(3)	C20	C21	C22	C10	-177.5(3)
C9	O3	C8	O2	0.0(4)	C20	C21	C22	C17	1.6(4)
C9	O3	C8	N1	-178.9(2)	C22	C10	C11	C12	-175.7(3)
C9	C10	C11	C12	65.9(4)	C22	C10	C11	C16	4.5(3)
C9	C10	C11	C16	-113.9(2)	C22	C17	C18	C19	-1.0(4)
C9	C10	C22	C17	116.2(3)	C23	C3	C4	C5	159.6(2)
C9	C10	C22	C21	-64.7(4)	C24	O5	C23	O4	-8.6(4)
C10	C11	C12	C13	-179.4(3)	C24	O5	C23	C3	168.8(3)

Table 8 Hydrogen Atom Coordinates (Å×10^4) and Isotropic Displacement Parameters (Å^2×10^3) for LUBE81.

Atom	*x*	*y*	*z*	U(eq)
H1	10770(80)	4200(30)	2592(18)	41(9)
H2	11290(70)	3330(30)	4970(20)	49(9)
H1A	7237	2970	3330	36
H3	6226	2593	4422	40
H4A	10453	898	4744	42
H4B	7316	612	4864	42

H5A	7612	-114	3762	41
H5B	6151	1090	3576	41
H6	11211	402	3168	40
H7	12014	2111	2734	38
H9A	3705	5291	1340	37
H9B	5206	4576	755	37
H10	8041	6216	560	34
H12	9577	6976	2055	43
H13	9042	8655	2723	48
H14	5537	9943	2360	49
H15	2432	9589	1325	43
H18	-134	8910	35	44
H19	-1641	8018	-1066	48
H20	329	6303	-1379	46
H21	3769	5413	-584	42
H24A	3348	1413	6510	85
H24B	5047	2575	6670	85
H24C	6652	1378	6689	85

Experimental

Crystals of $C_{24}H_{24}N_2O_5$ LUBE81 (**2.11a**) were grown in acetone-hexane, a suitable crystal was selected and mounted on a **Bruker Microstar X8** diffractometer. The crystal was kept at 150 K during data collection. Using Olex2 [1], the structure was solved with the ShelXT [2] structure solution program using Direct Methods and refined with the XL [3] refinement package using Least Squares minimisation.

1. Dolomanov, O.V., Bourhis, L.J., Gildea, R.J, Howard, J.A.K. & Puschmann, H. (2009), J. Appl. Cryst. 42, 339-341.
2. Sheldrick, G.M. (2008). Acta Cryst. A64, 112-122.
3. Sheldrick, G.M. (2008). Acta Cryst. A64, 112-122.

Crystal structure determination of [LUBE81]

Crystal Data for $C_{24}H_{24}N_2O_5$ (M =420.45 g/mol): monoclinic, space group $P2_1$ (no. 4), a = 4.8504(4) Å, b = 11.6933(9) Å, c = 18.5551(15) Å, β = 96.390(4)°, V = 1045.85(15) Å^3, Z = 2, T = 150 K, μ(CuKα) = 0.772 mm^{-1}, *Dcalc* = 1.335 g/cm^3, 22284 reflections measured (4.792° ≤ 2Θ ≤ 140.862°), 3776 unique (R_{int} = 0.0669, R_{sigma} = 0.0471) which were used in all calculations. The final R_1 was 0.0357 (I > 2σ(I)) and wR_2 was 0.0906 (all data).

Refinement model description

Number of restraints - 1, number of constraints - unknown.

Details:

```
1. Fixed Uiso
 At 1.2 times of:
  All C(H) groups, All C(H,H) groups
 At 1.5 times of:
  All C(H,H,H) groups
2.a Ternary CH refined with riding coordinates:
 C1(H1A), C3(H3), C10(H10)
2.b Secondary CH2 refined with riding coordinates:
 C4(H4A,H4B), C5(H5A,H5B), C9(H9A,H9B)
2.c Aromatic/amide H refined with riding coordinates:
 C6(H6), C7(H7), C12(H12), C13(H13), C14(H14), C15(H15), C18(H18), C19(H19),
 C20(H20), C21(H21)
2.d Idealised Me refined as rotating group:
 C24(H24A,H24B,H24C)
```

This report has been created with Olex2, compiled on 2014.09.19 svn.r3010 for OlexSys. Please let us know if there are any errors or if you would like to have additional features.

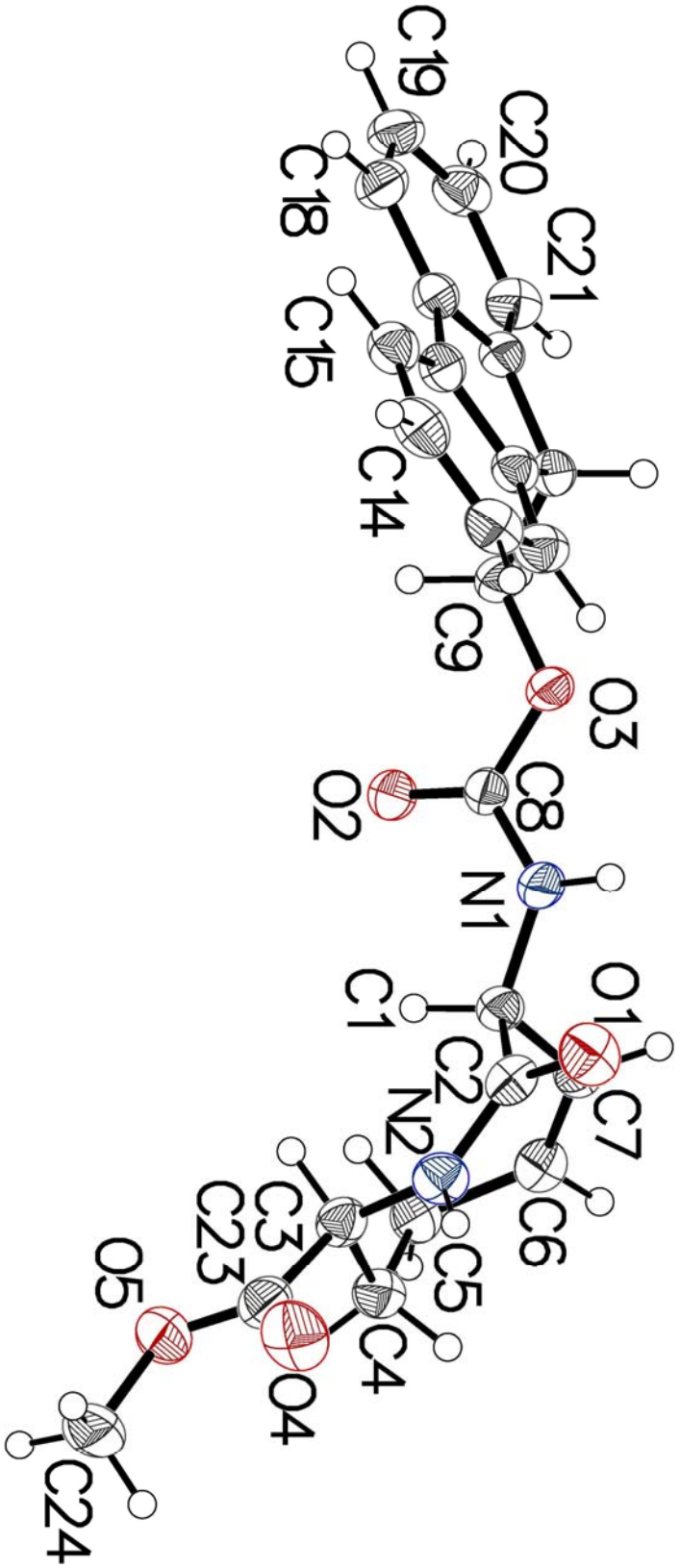
C19
C20
C21
C18
C15
C14
C9
O3
O2
C8
N1
C1
O1
C2
C7
N2
C6
C3
C5
C23
O5
C4
O4
C24

lube86: **(2.11e)**

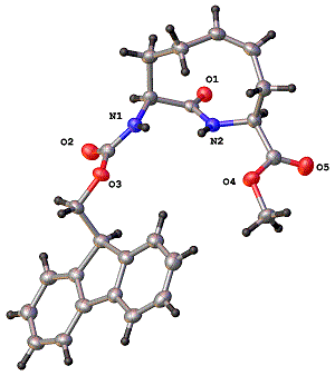

Table 1 Crystal data and structure refinement for lube86.

Identification code	lube86
Empirical formula	$C_{25}H_{26}N_2O_5$
Formula weight	434.48
Temperature/K	100
Crystal system	orthorhombic
Space group	$P2_12_12_1$
a/Å	5.1384(3)
b/Å	15.0009(9)
c/Å	28.0218(16)
α/°	90
β/°	90
γ/°	90
Volume/Å^3	2159.9(2)
Z	4
ρ_{calc}g/cm^3	1.336
μ/mm^{-1}	0.491
F(000)	920.0
Crystal size/mm^3	0.22 × 0.02 × 0.02
Radiation	GaKα (λ = 1.34139)
2Θ range for data collection/°	5.488 to 110.196
Index ranges	$-6 \leq h \leq 6$, $-18 \leq k \leq 18$, $-34 \leq l \leq 32$
Reflections collected	20748
Independent reflections	4125 [R_{int} = 0.1312, R_{sigma} = 0.0899]
Data/restraints/parameters	4125/0/298
Goodness-of-fit on F^2	1.072
Final R indexes [I>=2σ (I)]	R_1 = 0.0540, wR_2 = 0.1053
Final R indexes [all data]	R_1 = 0.0886, wR_2 = 0.1172
Largest diff. peak/hole / e Å^{-3}	0.25/-0.24
Flack parameter	0.2(3)

Table 2 Fractional Atomic Coordinates (×10^4) and Equivalent Isotropic Displacement Parameters (Å^2×10^3) for lube86. U_{eq} is defined as 1/3 of of the trace of the orthogonalised U_{IJ} tensor.

Atom	*x*	*y*	*z*	U(eq)
O1	6557(5)	6201.6(17)	2862.8(9)	30.0(7)
O2	2081(5)	3924(2)	3576.7(9)	36.3(7)
O3	-2047(5)	4450.9(19)	3601.6(9)	30.4(6)
O4	-368(5)	7885.4(19)	3453.6(9)	35.7(7)
O5	2566(6)	8965(2)	3350.9(11)	45.7(8)
N1	602(6)	4977(2)	3051.4(12)	28.4(8)
N2	2441(6)	6695(2)	2998.5(10)	27.3(7)
C1	3078(7)	5128(3)	2814.3(14)	28.7(9)
C2	4187(7)	6050(3)	2904.7(13)	24.8(9)
C3	2934(8)	7626(3)	2887.2(13)	29.6(9)
C4	1848(8)	7824(3)	2385.0(14)	34.4(10)
C5	3425(8)	7362(3)	1999.7(14)	34.9(10)
C6	3205(8)	6520(3)	1856.3(14)	34.2(10)
C7	1386(7)	5790(3)	2008.9(14)	33.4(10)
C8	2807(8)	5020(3)	2266.4(13)	32.4(10)
C9	397(7)	4409(3)	3427.0(13)	27.3(9)
C10	-2476(7)	3986(3)	4050.6(13)	29.4(9)
C11	-2040(7)	4626(3)	4466.3(13)	29.2(9)
C12	-4072(7)	5354(3)	4509.5(14)	31.5(10)
C13	-4701(8)	6032(3)	4192.9(15)	36.6(10)
C14	-6696(9)	6617(3)	4307.7(16)	40.9(11)
C15	-8071(9)	6533(3)	4733.4(15)	39.0(11)
C16	-7473(7)	5851(3)	5048.7(14)	34.9(10)
C17	-5456(7)	5265(3)	4936.4(14)	30.6(9)
C18	-4372(8)	4506(3)	5202.9(14)	32(1)
C19	-5043(8)	4158(3)	5649.7(14)	35.1(10)
C20	-3604(8)	3441(3)	5823.5(14)	37.2(11)
C21	-1550(8)	3092(3)	5566.8(15)	38.6(11)
C22	-903(8)	3430(3)	5116.4(15)	34.9(10)
C23	-2337(7)	4140(3)	4940.5(13)	29.8(9)
C24	1733(7)	8243(3)	3254.0(14)	29.0(9)
C25	-1567(8)	8412(3)	3832.6(15)	40.1(10)

Table 3 Anisotropic Displacement Parameters (Å^2×10^3) for lube86. The Anisotropic displacement factor exponent takes the form: $-2\pi^2[h^2a^{*2}U_{11}+2hka^*b^*U_{12}+\ldots]$.

Atom	U_{11}	U_{22}	U_{33}	U_{23}	U_{13}	U_{12}
O1	25.1(14)	32.6(16)	32.3(15)	2.4(13)	0.1(11)	0.0(11)
O2	28.7(14)	45.2(17)	35.1(16)	7.4(14)	-1.5(13)	3.2(14)

O3	25.9(13)	40.3(16)	25.1(14)	4.9(13)	1.5(11)	0.0(12)
O4	31.8(15)	37.3(18)	37.9(17)	-8.2(14)	8.3(12)	-2.6(13)
O5	46.1(18)	34.9(18)	56(2)	-5.6(15)	11.4(15)	-3.7(15)
N1	23.9(16)	31(2)	29.9(19)	2.1(16)	1.9(13)	-1.0(14)
N2	26.2(17)	30.1(19)	25.6(17)	0.6(14)	0.0(13)	-0.6(14)
C1	23.4(17)	29(2)	33(2)	1.7(19)	6.0(17)	4.6(17)
C2	23.5(18)	32(2)	19(2)	4.8(18)	-1.7(15)	3.5(17)
C3	27.8(18)	30(2)	31(2)	3.6(19)	2.0(17)	0.4(17)
C4	36(2)	34(2)	33(2)	3.9(19)	-2.4(18)	3(2)
C5	34(2)	45(3)	26(2)	9(2)	1.0(17)	0.1(19)
C6	36(2)	42(3)	24(2)	2(2)	3.3(18)	2(2)
C7	32(2)	42(3)	26(2)	0.1(19)	1.0(16)	-4.7(18)
C8	32(2)	36(2)	29(2)	-4.0(19)	5.3(17)	0.7(18)
C9	24.1(19)	31(2)	27(2)	-1(2)	-1.8(16)	-1.9(17)
C10	31(2)	33(2)	24(2)	5.9(18)	0.9(17)	-1.1(18)
C11	25.4(18)	37(2)	25(2)	1.2(18)	-1.9(16)	-2.9(17)
C12	32(2)	36(3)	26(2)	0(2)	-3.4(17)	-4.5(18)
C13	41(2)	39(3)	30(2)	1(2)	-2.0(19)	0(2)
C14	44(2)	38(3)	41(3)	1(2)	-10(2)	4(2)
C15	39(2)	38(3)	40(3)	-11(2)	-9(2)	6(2)
C16	34(2)	42(3)	29(2)	-7(2)	-4.6(18)	-1.4(19)
C17	30(2)	32(2)	30(2)	-2.8(19)	-5.0(17)	-1.8(18)
C18	28.8(19)	42(3)	25(2)	-1(2)	-4.6(16)	-6(2)
C19	36(2)	42(3)	27(2)	-3(2)	0.6(18)	-1.2(19)
C20	43(3)	43(3)	26(2)	3(2)	-1.0(18)	-5(2)
C21	46(2)	37(3)	32(2)	3(2)	-9(2)	2(2)
C22	33(2)	41(3)	30(2)	-5(2)	-2.0(17)	2(2)
C23	26.7(19)	36(2)	27(2)	-1.0(18)	-5.2(17)	-3.0(17)
C24	23.8(18)	32(2)	31(2)	3.1(19)	-1.2(17)	2.8(18)
C25	40(2)	42(3)	39(2)	-8(2)	11(2)	3(2)

Table 4 Bond Lengths for lube86.

Atom	Atom	Length/Å	Atom	Atom	Length/Å
O1	C2	1.244(4)	C7	C8	1.545(6)
O2	C9	1.206(5)	C10	C11	1.526(6)
O3	C9	1.349(4)	C11	C12	1.515(6)
O3	C10	1.456(4)	C11	C23	1.524(5)
O4	C24	1.329(5)	C12	C13	1.388(6)
O4	C25	1.460(5)	C12	C17	1.398(6)
O5	C24	1.196(5)	C13	C14	1.387(6)
N1	C1	1.454(5)	C14	C15	1.392(6)
N1	C9	1.358(5)	C15	C16	1.387(6)
N2	C2	1.345(5)	C16	C17	1.394(6)

N2	C3	1.454(5)	C17	C18	1.472(6)
C1	C2	1.517(5)	C18	C19	1.400(6)
C1	C8	1.550(6)	C18	C23	1.392(6)
C3	C4	1.543(5)	C19	C20	1.392(6)
C3	C24	1.515(6)	C20	C21	1.381(6)
C4	C5	1.518(6)	C21	C22	1.400(6)
C5	C6	1.331(6)	C22	C23	1.385(6)
C6	C7	1.501(6)			

Table 5 Bond Angles for lube86.

Atom	Atom	Atom	Angle/°	Atom	Atom	Atom	Angle/°
C9	O3	C10	115.6(3)	C23	C11	C10	110.4(3)
C24	O4	C25	115.5(3)	C13	C12	C11	129.6(4)
C9	N1	C1	121.3(3)	C13	C12	C17	119.8(4)
C2	N2	C3	122.2(3)	C17	C12	C11	110.5(3)
N1	C1	C2	113.3(3)	C14	C13	C12	119.2(4)
N1	C1	C8	111.0(3)	C13	C14	C15	121.1(4)
C2	C1	C8	107.1(3)	C16	C15	C14	120.0(4)
O1	C2	N2	122.7(4)	C15	C16	C17	119.0(4)
O1	C2	C1	121.2(3)	C12	C17	C18	108.4(3)
N2	C2	C1	116.0(3)	C16	C17	C12	120.8(4)
N2	C3	C4	108.5(3)	C16	C17	C18	130.8(4)
N2	C3	C24	111.8(3)	C19	C18	C17	130.5(4)
C24	C3	C4	110.7(3)	C23	C18	C17	108.8(3)
C5	C4	C3	111.6(3)	C23	C18	C19	120.7(4)
C6	C5	C4	127.1(4)	C20	C19	C18	118.0(4)
C5	C6	C7	131.2(4)	C21	C20	C19	121.1(4)
C6	C7	C8	112.6(3)	C20	C21	C22	120.9(4)
C7	C8	C1	115.3(3)	C23	C22	C21	118.2(4)
O2	C9	O3	124.7(4)	C18	C23	C11	110.3(3)
O2	C9	N1	126.3(3)	C22	C23	C11	128.7(4)
O3	C9	N1	108.9(3)	C22	C23	C18	121.0(4)
O3	C10	C11	109.6(3)	O4	C24	C3	111.7(3)
C12	C11	C10	114.4(3)	O5	C24	O4	124.1(4)
C12	C11	C23	101.9(3)	O5	C24	C3	124.2(4)

Table 6 Hydrogen Bonds for lube86.

D	H	A	d(D-H)/Å	d(H-A)/Å	d(D-A)/Å	D-H-A/°
N1	H1	O1[1]	1.06(5)	1.80(6)	2.824(4)	161(5)
N2	H2	O1[1]	0.96(4)	2.20(4)	3.136(4)	165(3)

[1]-1+X,+Y,+Z

Table 7 Torsion Angles for lube86.

A	B	C	D	Angle/°	A	B	C	D	Angle/°
O3	C10	C11	C12	68.8(4)	C11	C12	C17	C16	-178.5(3)
O3	C10	C11	C23	-177.0(3)	C11	C12	C17	C18	1.9(4)
N1	C1	C2	O1	157.1(3)	C12	C11	C23	C18	3.4(4)
N1	C1	C2	N2	-27.4(5)	C12	C11	C23	C22	-176.8(4)
N1	C1	C8	C7	73.8(4)	C12	C13	C14	C15	0.0(6)
N2	C3	C4	C5	-69.4(4)	C12	C17	C18	C19	178.8(4)
N2	C3	C24	O4	-28.6(4)	C12	C17	C18	C23	0.3(4)
N2	C3	C24	O5	151.6(4)	C13	C12	C17	C16	0.2(6)
C1	N1	C9	O2	-6.9(6)	C13	C12	C17	C18	-179.4(4)
C1	N1	C9	O3	175.0(3)	C13	C14	C15	C16	-0.7(6)
C2	N2	C3	C4	92.3(4)	C14	C15	C16	C17	1.2(6)
C2	N2	C3	C24	-145.3(3)	C15	C16	C17	C12	-0.9(6)
C2	C1	C8	C7	-50.3(4)	C15	C16	C17	C18	178.5(4)
C3	N2	C2	O1	23.3(5)	C16	C17	C18	C19	-0.7(7)
C3	N2	C2	C1	-152.1(3)	C16	C17	C18	C23	-179.2(4)
C3	C4	C5	C6	82.4(5)	C17	C12	C13	C14	0.3(6)
C4	C3	C24	O4	92.5(4)	C17	C18	C19	C20	-177.8(4)
C4	C3	C24	O5	-87.3(5)	C17	C18	C23	C11	-2.4(4)
C4	C5	C6	C7	1.7(7)	C17	C18	C23	C22	177.8(3)
C5	C6	C7	C8	-113.4(5)	C18	C19	C20	C21	1.0(6)
C6	C7	C8	C1	89.1(4)	C19	C18	C23	C11	179.0(4)
C8	C1	C2	O1	-80.2(4)	C19	C18	C23	C22	-0.8(6)
C8	C1	C2	N2	95.3(4)	C19	C20	C21	C22	-2.1(6)
C9	O3	C10	C11	91.6(4)	C20	C21	C22	C23	1.6(6)
C9	N1	C1	C2	-109.8(4)	C21	C22	C23	C11	-180.0(4)
C9	N1	C1	C8	129.7(4)	C21	C22	C23	C18	-0.2(6)
C10	O3	C9	O2	11.0(5)	C23	C11	C12	C13	178.3(4)
C10	O3	C9	N1	-170.9(3)	C23	C11	C12	C17	-3.2(4)
C10	C11	C12	C13	-62.5(5)	C23	C18	C19	C20	0.5(6)
C10	C11	C12	C17	116.0(4)	C24	C3	C4	C5	167.6(4)
C10	C11	C23	C18	-118.6(4)	C25	O4	C24	O5	-3.7(5)
C10	C11	C23	C22	61.2(5)	C25	O4	C24	C3	176.5(3)
C11	C12	C13	C14	178.7(4)					

Table 8 Hydrogen Atom Coordinates (Å×10^4) and Isotropic Displacement Parameters (Å^2×10^3) for lube86.

Atom	*x*	*y*	*z*	U(eq)
H1	-1130(100)	5320(40)	2959(19)	71(16)
H2	620(80)	6550(30)	3017(12)	24(10)
H1A	4355	4676	2933	34

H3	4858	7726	2883	36
H4A	17	7621	2367	41
H4B	1873	8476	2329	41
H5	4710	7712	1844	42
H6	4409	6351	1615	41
H7A	482	5551	1724	40
H7B	52	6043	2225	40
H8A	4570	4960	2127	39
H8B	1858	4459	2201	39
H10A	-1259	3476	4076	35
H10B	-4275	3751	4061	35
H11	-266	4897	4444	35
H13	-3776	6095	3901	44
H14	-7132	7082	4092	49
H15	-9419	6944	4808	47
H16	-8424	5783	5337	42
H19	-6440	4403	5829	42
H20	-4044	3189	6124	45
H21	-561	2616	5698	46
H22	482	3179	4936	42
H25A	-2518	8914	3692	60
H25B	-212	8639	4047	60
H25C	-2777	8037	4014	60

Experimental

Crystals of $C_{25}H_{26}N_2O_5$ lube86 (**2.11e**) were grown in acetone-hexane, a suitable crystal was selected and mounted on the **Bruker Venture Metaljet** diffractometer. The crystal was kept at 100 K during data collection. Using Olex2 [1], the structure was solved with the XM [2] structure solution program using Dual Space and refined with the XL [3] refinement package using Least Squares minimisation.

1. Dolomanov, O.V., Bourhis, L.J., Gildea, R.J, Howard, J.A.K. & Puschmann, H. (2009), J. Appl. Cryst. 42, 339-341.
2. Sheldrick, G.M. (2008). Acta Cryst. A64, 112-122.
3. Sheldrick, G.M. (2008). Acta Cryst. A64, 112-122.

Crystal structure determination of [lube86]

Crystal Data for $C_{25}H_{26}N_2O_5$ (M =434.48 g/mol): orthorhombic, space group $P2_12_12_1$ (no. 19), a = 5.1384(3) Å, b = 15.0009(9) Å, c = 28.0218(16) Å, V = 2159.9(2) Å^3, Z = 4, T = 100 K, μ(GaKα) = 0.491 mm^{-1}, *Dcalc* = 1.336 g/cm^3, 20748 reflections measured (5.488° ≤ 2Θ ≤ 110.196°), 4125 unique (R_{int} = 0.1312, R_{sigma} = 0.0899) which were used in all calculations. The final R_1 was 0.0540 (I > 2σ(I)) and wR_2 was 0.1172 (all data).

Refinement model description

Number of restraints - 0, number of constraints - unknown.

Details:

```
1. Fixed Uiso
 At 1.2 times of:
  All C(H) groups, All C(H,H) groups
 At 1.5 times of:
  All C(H,H,H) groups
2.a Ternary CH refined with riding coordinates:
 C1(H1A), C3(H3), C11(H11)
2.b Secondary CH2 refined with riding coordinates:
 C4(H4A,H4B), C7(H7A,H7B), C8(H8A,H8B), C10(H10A,H10B)
```

```
2.c Aromatic/amide H refined with riding coordinates:
 C5(H5), C6(H6), C13(H13), C14(H14), C15(H15), C16(H16), C19(H19), C20(H20),
 C21(H21), C22(H22)
2.d Idealised Me refined as rotating group:
 C25(H25A,H25B,H25C)
```

This report has been created with Olex2, compiled on 2014.09.19 svn.r3010 for OlexSys. Please let us know if there are any errors or if you would like to have additional features.

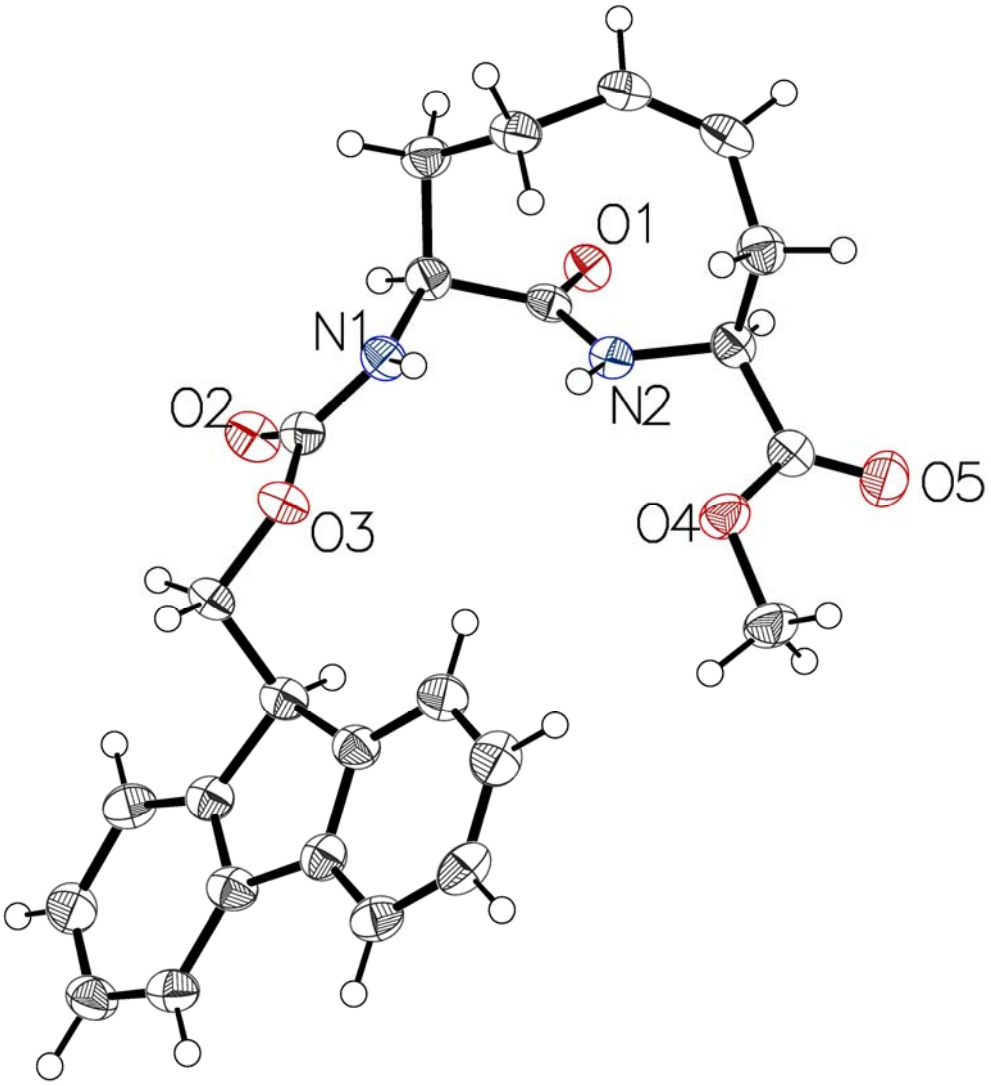
O1
N1
N2
O2
O3
O4
O5

lube87: **(2.10d)**

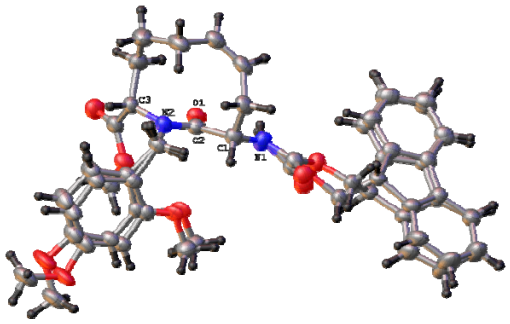

Table 1 Crystal data and structure refinement for lube87.

Identification code	lube87
Empirical formula	$C_{35}H_{38}N_2O_7$
Formula weight	598.67
Temperature/K	100
Crystal system	orthorhombic
Space group	$P2_12_12_1$
a/Å	9.4075(8)
b/Å	12.1987(10)
c/Å	27.339(2)
α/°	90
β/°	90
γ/°	90
Volume/Å^3	3137.4(5)
Z	4
ρ_{calc}g/cm^3	1.267
μ/mm^{-1}	0.462
F(000)	1272.0
Crystal size/mm^3	0.12 × 0.12 × 0.02
Radiation	GaKα (λ = 1.34139)
2Θ range for data collection/°	5.624 to 121.52
Index ranges	$-11 \leq h \leq 11$, $-15 \leq k \leq 13$, $-34 \leq l \leq 35$
Reflections collected	28548
Independent reflections	7022 [R_{int} = 0.0988, R_{sigma} = 0.0916]
Data/restraints/parameters	7022/69/413
Goodness-of-fit on F^2	1.012
Final R indexes [I>=2σ (I)]	R_1 = 0.0547, wR_2 = 0.1057
Final R indexes [all data]	R_1 = 0.1170, wR_2 = 0.1246
Largest diff. peak/hole / e Å^{-3}	0.22/-0.18
Flack parameter	0.3(2)

Table 2 Fractional Atomic Coordinates ($\times 10^4$) and Equivalent Isotropic Displacement Parameters ($Å^2 \times 10^3$) for lube87. U_{eq} is defined as 1/3 of of the trace of the orthogonalised U_{IJ} tensor.

Atom	*x*	*y*	*z*	U(eq)
O1	8823(2)	4323.5(19)	2219.5(9)	40.6(6)
O2	12065(3)	3755(2)	1556.8(10)	53.3(7)
O3	10705(2)	2489(2)	1920.4(9)	45.0(6)
N1	6417(3)	4086(2)	2671.3(11)	45.5(8)
N2	8286(3)	3298(2)	1559.8(11)	34.4(7)
C1	6438(4)	3654(3)	2181.7(14)	39.4(9)
C2	7960(4)	3743(3)	1995.1(14)	35.9(8)
C3	9607(4)	3641(3)	1326.0(14)	38.1(9)
C4	9622(4)	4857(3)	1187.2(15)	49.7(10)
C5	8601(5)	5184(4)	777.6(17)	62.8(13)
C6	7018(5)	5162(4)	896.9(15)	55.4(11)
C7	6627(4)	5801(3)	1347.6(16)	50.7(11)
C8	5953(4)	5444(3)	1740.2(16)	47(1)
C9	5447(4)	4289(3)	1831.7(15)	45.7(10)
C10	10929(4)	3328(3)	1618.0(14)	39.4(9)
C11	11921(4)	2100(3)	2198.1(15)	49.2(10)
C12	7506(4)	2380(3)	1326.8(14)	40.0(9)
C13A	8410(30)	1345(13)	1302(6)	40(2)
C14A	8580(20)	725(13)	1725(4)	35.7(19)
C15A	9347(17)	-247(9)	1710(3)	38(2)
C16A	9946(15)	-599(8)	1272(3)	49(3)
C17A	9775(19)	21(10)	850(3)	57(3)
C18A	9010(20)	993(12)	865(4)	49(3)
O4A	7844(19)	1079(10)	2123(5)	34.8(18)
C19A	7930(40)	470(14)	2568(6)	55(4)
O5A	10752(7)	-1513(4)	1223(2)	64.3(16)
C20A	10756(9)	-2275(6)	1619(3)	65.0(19)
C13B	8250(40)	1260(20)	1372(9)	40(2)
C14B	8390(40)	750(20)	1825(7)	35.7(19)
C15B	9150(30)	-217(16)	1866(5)	38(2)
C16B	9780(20)	-680(13)	1454(5)	49(3)
C17B	9640(30)	-172(16)	1002(5)	57(3)
C18B	8880(40)	800(20)	961(7)	49(3)
O4B	7850(30)	1322(16)	2214(8)	34.8(18)
C19B	7950(60)	760(30)	2671(9)	55(4)
O5B	10418(12)	-1679(8)	1525(4)	64.3(16)
C20B	11048(13)	-2194(9)	1107(4)	65.0(19)
O6A	4331(4)	3262(4)	2872.7(15)	44.8(11)
O7A	5541(4)	4300(3)	3416.9(12)	41.7(8)
C21A	5336(5)	3833(5)	2973.0(18)	38.9(14)
C22A	4452(5)	4055(4)	3770.4(16)	41.5(12)

C23A	4985(5)	4361(4)	4272.5(16)	40.4(11)
C24A	5125(3)	5577(3)	4370.9(14)	35.9(11)
C25A	5955(4)	6355(4)	4132.7(16)	43.7(13)
C26A	5922(7)	7443(3)	4284(3)	44.6(11)
C27A	5061(9)	7753(3)	4673(3)	44.1(14)
C28A	4231(8)	6976(4)	4911(2)	41.5(10)
C29A	4263(4)	5888(3)	4760.0(15)	35.3(12)
C30A	3513(4)	4925(3)	4939.5(15)	35.6(13)
C31A	2514(6)	4794(4)	5309.7(18)	43.8(10)
C32A	1920(6)	3769(5)	5397.0(18)	61.8(16)
C33A	2325(5)	2875(4)	5114.2(17)	77(2)
C34A	3324(5)	3006(2)	4744.0(15)	62.7(16)
C35A	3917(4)	4031(3)	4656.7(12)	43.0(12)
O6B	4640(30)	3170(30)	3035(11)	44.8(11)
O7B	6170(20)	4107(17)	3523(7)	41.7(8)
C21B	5680(30)	3750(40)	3078(8)	38.9(14)
C22B	5380(20)	3781(19)	3950(8)	41.5(12)
C23B	4190(20)	4567(16)	4075(9)	40.4(11)
C24B	4610(20)	5690(15)	4268(8)	35.9(11)
C25B	5530(30)	6440(20)	4055(10)	43.7(13)
C26B	5790(40)	7440(20)	4284(15)	44.6(11)
C27B	5130(60)	7680(20)	4727(17)	44.1(14)
C28B	4220(50)	6930(30)	4940(14)	41.5(10)
C29B	3960(30)	5930(20)	4711(10)	35.3(12)
C30B	3190(30)	4963(16)	4864(9)	35.6(13)
C31B	2430(40)	4750(30)	5289(10)	43.8(10)
C32B	1730(40)	3750(30)	5344(10)	61.8(16)
C33B	1790(30)	2970(20)	4973(11)	77(2)
C34B	2540(30)	3190(15)	4547(9)	62.7(16)
C35B	3250(20)	4185(15)	4493(7)	43.0(12)

Table 3 Anisotropic Displacement Parameters ($Å^2×10^3$) for lube87. The Anisotropic displacement factor exponent takes the form: $-2\pi^2[h^2a^{*2}U_{11}+2hka^*b^*U_{12}+\ldots]$.

Atom	U_{11}	U_{22}	U_{33}	U_{23}	U_{13}	U_{12}
O1	33.3(13)	32.9(13)	55.5(16)	-3.8(13)	-1.5(12)	-4.5(11)
O2	36.4(15)	50.0(16)	73(2)	-2.5(15)	5.6(14)	-6.3(14)
O3	35.0(14)	36.3(14)	63.8(17)	0.8(14)	-6.0(12)	1.8(12)
N1	43.4(18)	41.7(19)	51(2)	-7.1(16)	10.4(16)	-11.9(15)
N2	30.5(16)	28.6(16)	44.3(19)	-0.8(14)	0.6(14)	-0.3(12)
C1	34.4(19)	33(2)	51(2)	-3.7(18)	3.6(18)	-2.5(16)
C2	34.8(19)	30.8(19)	42(2)	3.4(18)	0.1(17)	0.3(17)
C3	34.8(19)	36(2)	44(2)	-2.2(18)	4.7(18)	3.1(16)
C4	45(2)	36(2)	68(3)	9(2)	13(2)	0.0(18)

C5	69(3)	52(3)	67(3)	14(2)	14(2)	17(2)
C6	68(3)	40(2)	57(3)	4(2)	-6(2)	18(2)
C7	45(2)	36(2)	71(3)	-1(2)	-5(2)	8.5(18)
C8	40(2)	35(2)	66(3)	-6.2(19)	-2(2)	11.6(17)
C9	30.4(19)	41(2)	66(3)	-3(2)	-1.0(19)	4.2(17)
C10	37(2)	31(2)	50(2)	-5.2(19)	6.0(18)	3.1(17)
C11	39(2)	45(2)	64(3)	-2(2)	-10(2)	8.9(17)
C12	42(2)	32(2)	46(2)	-2.9(18)	-6.9(18)	2.8(16)
C13A	39(5)	32(3)	48(5)	-2(3)	-5(4)	1(4)
C14A	32(6)	31(2)	44(5)	-4(4)	0(4)	-3(2)
C15A	43(5)	27(2)	43(6)	-3(4)	-5(5)	1(2)
C16A	57(5)	40(3)	49(8)	-11(5)	-7(6)	11(3)
C17A	71(4)	57(6)	43(6)	-10(5)	-6(6)	25(5)
C18A	59(5)	43(6)	46(5)	-2(3)	-5(5)	13(5)
O4A	46.3(15)	17(6)	42(5)	-12(3)	-6(4)	-4(4)
C19A	55(3)	56(10)	53(7)	12(6)	2(7)	2(9)
O5A	86(4)	38(3)	69(4)	-6(3)	-8(4)	35(3)
C20A	69(4)	35(3)	92(5)	-4(4)	-9(4)	18(3)
C13B	39(5)	32(3)	48(5)	-2(3)	-5(4)	1(4)
C14B	32(6)	31(2)	44(5)	-4(4)	0(4)	-3(2)
C15B	43(5)	27(2)	43(6)	-3(4)	-5(5)	1(2)
C16B	57(5)	40(3)	49(8)	-11(5)	-7(6)	11(3)
C17B	71(4)	57(6)	43(6)	-10(5)	-6(6)	25(5)
C18B	59(5)	43(6)	46(5)	-2(3)	-5(5)	13(5)
O4B	46.3(15)	17(6)	42(5)	-12(3)	-6(4)	-4(4)
C19B	55(3)	56(10)	53(7)	12(6)	2(7)	2(9)
O5B	86(4)	38(3)	69(4)	-6(3)	-8(4)	35(3)
C20B	69(4)	35(3)	92(5)	-4(4)	-9(4)	18(3)
O6A	36(2)	44.5(18)	53(3)	-2(2)	-1.0(17)	-10.3(17)
O7A	38(2)	41.6(18)	45.7(19)	-5.6(15)	4.8(16)	-5.7(17)
C21A	34(3)	36(2)	47(3)	1(2)	-1(2)	3(3)
C22A	34(3)	37(3)	53(3)	2(2)	8(2)	-3(2)
C23A	42(3)	33(2)	47(3)	8(2)	2(2)	6(2)
C24A	25(3)	35(2)	47(3)	2(2)	-5(2)	-1(2)
C25A	35(3)	46(3)	51(3)	3(2)	-4(2)	-5(3)
C26A	42(3)	36(2)	56(3)	2(2)	-5(2)	-11(2)
C27A	44(3)	36(2)	53(3)	1(2)	-9(2)	-4(2)
C28A	39(2)	37(2)	49(2)	-0.2(19)	-4(2)	-0.6(18)
C29A	27(3)	35(2)	44(2)	1.3(19)	-4(2)	1.4(19)
C30A	33(3)	32(2)	42(3)	1.5(19)	-1(2)	0.3(19)
C31A	44(2)	36(2)	51(3)	4.0(19)	3(2)	2.6(18)
C32A	75(4)	45(3)	65(3)	3(2)	26(3)	-7(3)
C33A	109(6)	39(3)	84(5)	5(3)	37(4)	-19(3)
C34A	94(5)	30(3)	64(4)	2(3)	17(3)	-1(3)
C35A	49(3)	31(2)	49(3)	8(2)	1(2)	0(2)

O6B	36(2)	44.5(18)	53(3)	-2(2)	-1.0(17)	-10.3(17)
O7B	38(2)	41.6(18)	45.7(19)	-5.6(15)	4.8(16)	-5.7(17)
C21B	34(3)	36(2)	47(3)	1(2)	-1(2)	3(3)
C22B	34(3)	37(3)	53(3)	2(2)	8(2)	-3(2)
C23B	42(3)	33(2)	47(3)	8(2)	2(2)	6(2)
C24B	25(3)	35(2)	47(3)	2(2)	-5(2)	-1(2)
C25B	35(3)	46(3)	51(3)	3(2)	-4(2)	-5(3)
C26B	42(3)	36(2)	56(3)	2(2)	-5(2)	-11(2)
C27B	44(3)	36(2)	53(3)	1(2)	-9(2)	-4(2)
C28B	39(2)	37(2)	49(2)	-0.2(19)	-4(2)	-0.6(18)
C29B	27(3)	35(2)	44(2)	1.3(19)	-4(2)	1.4(19)
C30B	33(3)	32(2)	42(3)	1.5(19)	-1(2)	0.3(19)
C31B	44(2)	36(2)	51(3)	4.0(19)	3(2)	2.6(18)
C32B	75(4)	45(3)	65(3)	3(2)	26(3)	-7(3)
C33B	109(6)	39(3)	84(5)	5(3)	37(4)	-19(3)
C34B	94(5)	30(3)	64(4)	2(3)	17(3)	-1(3)
C35B	49(3)	31(2)	49(3)	8(2)	1(2)	0(2)

Table 4 Bond Lengths for lube87.

Atom	Atom	Length/Å	Atom	Atom	Length/Å
O1	C2	1.240(4)	O5B	C20B	1.434(14)
O2	C10	1.201(4)	O6A	C21A	1.205(6)
O3	C10	1.332(4)	O7A	C21A	1.354(6)
O3	C11	1.453(4)	O7A	C22A	1.440(5)
N1	C1	1.439(5)	C22A	C23A	1.508(6)
N1	C21A	1.346(5)	C23A	C24A	1.514(5)
N1	C21B	1.37(2)	C23A	C35A	1.508(5)
N2	C2	1.343(4)	C24A	C25A	1.3900
N2	C3	1.458(4)	C24A	C29A	1.3900
N2	C12	1.483(4)	C25A	C26A	1.3900
C1	C2	1.524(5)	C26A	C27A	1.3900
C1	C9	1.544(5)	C27A	C28A	1.3900
C3	C4	1.532(5)	C28A	C29A	1.3900
C3	C10	1.527(5)	C29A	C30A	1.456(4)
C4	C5	1.528(6)	C30A	C31A	1.3900
C5	C6	1.525(6)	C30A	C35A	1.3900
C6	C7	1.504(6)	C31A	C32A	1.3900
C7	C8	1.321(6)	C32A	C33A	1.3900
C8	C9	1.508(6)	C33A	C34A	1.3900
C12	C13A	1.521(7)	C34A	C35A	1.3900
C12	C13B	1.538(11)	O6B	C21B	1.21(2)
C13A	C14A	1.3900	O7B	C21B	1.37(2)
C13A	C18A	1.3900	O7B	C22B	1.44(2)

C14A	C15A	1.3900	C22B	C23B	1.51(2)
C14A	O4A	1.360(10)	C23B	C24B	1.520(19)
C15A	C16A	1.3900	C23B	C35B	1.519(18)
C16A	C17A	1.3900	C24B	C25B	1.3900
C16A	O5A	1.355(7)	C24B	C29B	1.3900
C17A	C18A	1.3900	C25B	C26B	1.3900
O4A	C19A	1.426(11)	C26B	C27B	1.3900
O5A	C20A	1.428(10)	C27B	C28B	1.3900
C13B	C14B	1.3900	C28B	C29B	1.3900
C13B	C18B	1.3900	C29B	C30B	1.446(17)
C14B	C15B	1.3900	C30B	C31B	1.3900
C14B	O4B	1.369(14)	C30B	C35B	1.3900
C15B	C16B	1.3900	C31B	C32B	1.3900
C16B	C17B	1.3900	C32B	C33B	1.3900
C16B	O5B	1.373(11)	C33B	C34B	1.3900
C17B	C18B	1.3900	C34B	C35B	1.3900
O4B	C19B	1.430(17)			

Table 5 Bond Angles for lube87.

Atom	Atom	Atom	Angle/°	Atom	Atom	Atom	Angle/°
C10	O3	C11	116.8(3)	N1	C21A	O7A	110.2(4)
C21A	N1	C1	119.7(4)	O6A	C21A	N1	125.9(5)
C21B	N1	C1	130.7(13)	O6A	C21A	O7A	123.9(4)
C2	N2	C3	117.9(3)	O7A	C22A	C23A	108.8(3)
C2	N2	C12	124.9(3)	C22A	C23A	C24A	115.7(4)
C3	N2	C12	116.7(3)	C35A	C23A	C22A	110.3(4)
N1	C1	C2	107.3(3)	C35A	C23A	C24A	101.3(3)
N1	C1	C9	112.7(3)	C25A	C24A	C23A	129.3(3)
C2	C1	C9	108.9(3)	C25A	C24A	C29A	120.0
O1	C2	N2	121.3(3)	C29A	C24A	C23A	110.7(3)
O1	C2	C1	119.4(3)	C24A	C25A	C26A	120.0
N2	C2	C1	118.8(3)	C25A	C26A	C27A	120.0
N2	C3	C4	113.2(3)	C28A	C27A	C26A	120.0
N2	C3	C10	113.2(3)	C27A	C28A	C29A	120.0
C10	C3	C4	111.4(3)	C24A	C29A	C30A	108.7(3)
C5	C4	C3	115.4(3)	C28A	C29A	C24A	120.0
C6	C5	C4	116.9(4)	C28A	C29A	C30A	131.3(3)
C7	C6	C5	113.9(4)	C31A	C30A	C29A	131.8(3)
C8	C7	C6	127.7(4)	C31A	C30A	C35A	120.0
C7	C8	C9	126.5(4)	C35A	C30A	C29A	108.2(3)
C8	C9	C1	112.4(3)	C32A	C31A	C30A	120.0
O2	C10	O3	124.1(3)	C31A	C32A	C33A	120.0
O2	C10	C3	122.9(4)	C34A	C33A	C32A	120.0

O3	C10	C3	112.8(3)	C33A	C34A	C35A	120.0
N2	C12	C13A	111.7(12)	C30A	C35A	C23A	111.1(3)
N2	C12	C13B	114.1(18)	C34A	C35A	C23A	128.8(3)
C14A	C13A	C12	118.6(8)	C34A	C35A	C30A	120.0
C14A	C13A	C18A	120.0	C21B	O7B	C22B	117.5(18)
C18A	C13A	C12	121.3(8)	O6B	C21B	N1	120(2)
C13A	C14A	C15A	120.0	O6B	C21B	O7B	123(2)
O4A	C14A	C13A	115.7(8)	O7B	C21B	N1	117.2(19)
O4A	C14A	C15A	124.0(8)	O7B	C22B	C23B	112.9(18)
C16A	C15A	C14A	120.0	C22B	C23B	C24B	117.2(19)
C15A	C16A	C17A	120.0	C22B	C23B	C35B	114.0(17)
O5A	C16A	C15A	124.5(6)	C35B	C23B	C24B	99.7(15)
O5A	C16A	C17A	115.4(6)	C25B	C24B	C23B	127.8(14)
C16A	C17A	C18A	120.0	C25B	C24B	C29B	120.0
C17A	C18A	C13A	120.0	C29B	C24B	C23B	112.2(14)
C14A	O4A	C19A	119.2(13)	C24B	C25B	C26B	120.0
C16A	O5A	C20A	117.5(6)	C27B	C26B	C25B	120.0
C14B	C13B	C12	120.6(14)	C26B	C27B	C28B	120.0
C14B	C13B	C18B	120.0	C29B	C28B	C27B	120.0
C18B	C13B	C12	119.3(13)	C24B	C29B	C30B	107.4(15)
C15B	C14B	C13B	120.0	C28B	C29B	C24B	120.0
O4B	C14B	C13B	115.7(13)	C28B	C29B	C30B	132.3(15)
O4B	C14B	C15B	124.0(14)	C31B	C30B	C29B	130.8(14)
C14B	C15B	C16B	120.0	C31B	C30B	C35B	120.0
C15B	C16B	C17B	120.0	C35B	C30B	C29B	109.2(14)
O5B	C16B	C15B	115.6(10)	C30B	C31B	C32B	120.0
O5B	C16B	C17B	124.2(10)	C33B	C32B	C31B	120.0
C18B	C17B	C16B	120.0	C32B	C33B	C34B	120.0
C17B	C18B	C13B	120.0	C35B	C34B	C33B	120.0
C14B	O4B	C19B	114.4(19)	C30B	C35B	C23B	111.2(13)
C16B	O5B	C20B	117.2(10)	C34B	C35B	C23B	128.8(13)
C21A	O7A	C22A	114.4(3)	C34B	C35B	C30B	120.0

Table 6 Torsion Angles for lube87.

A	B	C	D	Angle/°	A	B	C	D	Angle/°
N1	C1	C2	O1	-14.1(4)	C22A	O7A	C21A	N1	-178.7(4)
N1	C1	C2	N2	173.9(3)	C22A	O7A	C21A	O6A	0.4(7)
N1	C1	C9	C8	67.2(4)	C22A	C23A	C24A	C25A	-60.3(5)
N2	C3	C4	C5	-68.2(4)	C22A	C23A	C24A	C29A	119.6(4)
N2	C3	C10	O2	-161.0(3)	C22A	C23A	C35A	C30A	-123.6(4)
N2	C3	C10	O3	23.1(4)	C22A	C23A	C35A	C34A	55.2(5)
N2	C12	C13A	C14A	77.2(13)	C23A	C24A	C25A	C26A	179.9(5)
N2	C12	C13A	C18A	-105.4(13)	C23A	C24A	C29A	C28A	-179.9(4)

N2	C12	C13B	C14B	68(2)	C23A	C24A	C29A	C30A	-0.1(4)
N2	C12	C13B	C18B	-108(2)	C24A	C23A	C35A	C30A	-0.6(4)
C1	N1	C21A	O6A	-0.5(8)	C24A	C23A	C35A	C34A	178.2(2)
C1	N1	C21A	O7A	178.6(4)	C24A	C25A	C26A	C27A	0.0
C1	N1	C21B	O6B	-18(6)	C24A	C29A	C30A	C31A	-178.3(3)
C1	N1	C21B	O7B	161(2)	C24A	C29A	C30A	C35A	-0.3(4)
C2	N2	C3	C4	-64.2(4)	C25A	C24A	C29A	C28A	0.0
C2	N2	C3	C10	63.7(4)	C25A	C24A	C29A	C30A	179.8(3)
C2	N2	C12	C13A	-112.3(7)	C25A	C26A	C27A	C28A	0.0
C2	N2	C12	C13B	-102.1(11)	C26A	C27A	C28A	C29A	0.0
C2	C1	C9	C8	-51.7(4)	C27A	C28A	C29A	C24A	0.0
C3	N2	C2	O1	-8.4(5)	C27A	C28A	C29A	C30A	-179.7(4)
C3	N2	C2	C1	163.4(3)	C28A	C29A	C30A	C31A	1.4(5)
C3	N2	C12	C13A	59.4(7)	C28A	C29A	C30A	C35A	179.5(3)
C3	N2	C12	C13B	69.6(11)	C29A	C24A	C25A	C26A	0.0
C3	C4	C5	C6	70.2(5)	C29A	C30A	C31A	C32A	177.9(4)
C4	C3	C10	O2	-32.2(5)	C29A	C30A	C35A	C23A	0.6(4)
C4	C3	C10	O3	152.0(3)	C29A	C30A	C35A	C34A	-178.3(3)
C4	C5	C6	C7	52.7(5)	C30A	C31A	C32A	C33A	0.0
C5	C6	C7	C8	-123.7(4)	C31A	C30A	C35A	C23A	178.9(4)
C6	C7	C8	C9	1.7(6)	C31A	C30A	C35A	C34A	0.0
C7	C8	C9	C1	101.8(5)	C31A	C32A	C33A	C34A	0.0
C9	C1	C2	O1	108.1(4)	C32A	C33A	C34A	C35A	0.0
C9	C1	C2	N2	-63.9(4)	C33A	C34A	C35A	C23A	-178.7(4)
C10	C3	C4	C5	162.9(3)	C33A	C34A	C35A	C30A	0.0
C11	O3	C10	O2	1.5(5)	C35A	C23A	C24A	C25A	-179.5(3)
C11	O3	C10	C3	177.3(3)	C35A	C23A	C24A	C29A	0.5(4)
C12	N2	C2	O1	163.2(3)	C35A	C30A	C31A	C32A	0.0
C12	N2	C2	C1	-25.0(5)	O7B	C22B	C23B	C24B	-70(3)
C12	N2	C3	C4	123.5(3)	O7B	C22B	C23B	C35B	174.1(19)
C12	N2	C3	C10	-108.6(3)	C21B	N1	C1	C2	-143(3)
C12	C13A	C14A	C15A	177(2)	C21B	N1	C1	C9	98(3)
C12	C13A	C14A	O4A	3.4(16)	C21B	O7B	C22B	C23B	-88(3)
C12	C13A	C18A	C17A	-177(2)	C22B	O7B	C21B	N1	179(3)
C12	C13B	C14B	C15B	-176(3)	C22B	O7B	C21B	O6B	-1(6)
C12	C13B	C14B	O4B	-1(3)	C22B	C23B	C24B	C25B	54(3)
C12	C13B	C18B	C17B	176(3)	C22B	C23B	C24B	C29B	-126(2)
C13A	C14A	C15A	C16A	0.0	C22B	C23B	C35B	C30B	124(2)
C13A	C14A	O4A	C19A	178.3(17)	C22B	C23B	C35B	C34B	-52(3)
C14A	C13A	C18A	C17A	0.0	C23B	C24B	C25B	C26B	180(3)
C14A	C15A	C16A	C17A	0.0	C23B	C24B	C29B	C28B	-180(2)
C14A	C15A	C16A	O5A	177.7(16)	C23B	C24B	C29B	C30B	6(3)
C15A	C14A	O4A	C19A	5(3)	C24B	C23B	C35B	C30B	-1(2)
C15A	C16A	C17A	C18A	0.0	C24B	C23B	C35B	C34B	-178.2(17)
C15A	C16A	O5A	C20A	13.0(16)	C24B	C25B	C26B	C27B	0.0

C16A	C17A	C18A	C13A	0.0	C24B	C29B	C30B	C31B	175.7(17)
C17A	C16A	O5A	C20A	-169.3(9)	C24B	C29B	C30B	C35B	-7(3)
C18A	C13A	C14A	C15A	0.0	C25B	C24B	C29B	C28B	0.0
C18A	C13A	C14A	O4A	-174(2)	C25B	C24B	C29B	C30B	-174(2)
O4A	C14A	C15A	C16A	173(2)	C25B	C26B	C27B	C28B	0.0
O5A	C16A	C17A	C18A	-177.9(15)	C26B	C27B	C28B	C29B	0.0
C13B	C14B	C15B	C16B	0.0	C27B	C28B	C29B	C24B	0.0
C13B	C14B	O4B	C19B	177(3)	C27B	C28B	C29B	C30B	173(3)
C14B	C13B	C18B	C17B	0.0	C28B	C29B	C30B	C31B	2(3)
C14B	C15B	C16B	C17B	0.0	C28B	C29B	C30B	C35B	179.9(19)
C14B	C15B	C16B	O5B	-175(2)	C29B	C24B	C25B	C26B	0.0
C15B	C14B	O4B	C19B	-9(5)	C29B	C30B	C31B	C32B	177(3)
C15B	C16B	C17B	C18B	0.0	C29B	C30B	C35B	C23B	5(3)
C15B	C16B	O5B	C20B	178.6(15)	C29B	C30B	C35B	C34B	-178(2)
C16B	C17B	C18B	C13B	0.0	C30B	C31B	C32B	C33B	0.0
C17B	C16B	O5B	C20B	3(2)	C31B	C30B	C35B	C23B	-177(2)
C18B	C13B	C14B	C15B	0.0	C31B	C30B	C35B	C34B	0.0
C18B	C13B	C14B	O4B	174(4)	C31B	C32B	C33B	C34B	0.0
O4B	C14B	C15B	C16B	-174(4)	C32B	C33B	C34B	C35B	0.0
O5B	C16B	C17B	C18B	175(3)	C33B	C34B	C35B	C23B	176(2)
O7A	C22A	C23A	C24A	70.5(5)	C33B	C34B	C35B	C30B	0.0
O7A	C22A	C23A	C35A	-175.4(3)	C35B	C23B	C24B	C25B	177.5(18)
C21A	N1	C1	C2	-161.1(4)	C35B	C23B	C24B	C29B	-3(2)
C21A	N1	C1	C9	79.0(5)	C35B	C30B	C31B	C32B	0.0
C21A	O7A	C22A	C23A	165.2(4)					

Table 7 Hydrogen Atom Coordinates (Å×10^4) and Isotropic Displacement Parameters (Å^2×10^3) for lube87.

Atom	*x*	*y*	*z*	U(eq)
H1A	7110	4514	2773	55
H1	6972	4658	2718	55
H1B	6149	2866	2189	47
H3	9665	3225	1011	46
H4A	9387	5293	1482	60
H4B	10599	5058	1087	60
H5A	8849	5936	671	75
H5B	8768	4690	496	75
H6A	6484	5462	615	66
H6B	6718	4390	942	66
H7	6898	6552	1350	61
H8	5768	5967	1990	56
H9A	5391	3893	1516	55
H9B	4479	4313	1973	55

H11A	12689	1900	1973	74
H11B	11645	1457	2391	74
H11C	12251	2681	2418	74
H12A	7222	2595	992	48
H12B	6630	2227	1516	48
H12C	7372	2549	976	48
H12D	6552	2325	1478	48
H15A	9464	-671	1998	45
H17A	10183	-219	551	68
H18A	8888	1417	576	59
H19A	7620	-286	2509	82
H19B	7318	809	2815	82
H19C	8917	468	2684	82
H20A	11360	-2902	1536	98
H20B	9784	-2529	1680	98
H20C	11126	-1916	1913	98
H15B	9243	-565	2175	45
H17B	10073	-488	721	68
H18B	8789	1148	651	59
H19D	7521	28	2640	82
H19E	7442	1174	2924	82
H19F	8950	684	2764	82
H20D	10303	-2386	871	98
H20E	11548	-2860	1209	98
H20F	11724	-1688	954	98
H22A	4218	3264	3760	50
H22B	3579	4475	3694	50
H23A	5914	3989	4337	48
H25A	6544	6142	3867	52
H26A	6489	7974	4121	54
H27A	5039	8497	4776	53
H28A	3642	7188	5177	50
H31A	2237	5405	5503	53
H32A	1238	3680	5650	74
H33A	1920	2175	5174	93
H34A	3600	2396	4551	75
H22C	6035	3730	4231	50
H22D	4969	3043	3894	50
H23B	3583	4671	3778	48
H25B	5975	6280	3752	52
H26B	6414	7958	4138	54
H27B	5311	8365	4883	53
H28B	3768	7094	5243	50
H31B	2394	5277	5543	53
H32B	1213	3601	5635	74

H33B	1307	2292	5010	93
H34B	2582	2658	4294	75

Table 8 Atomic Occupancy for lube87.

Atom	*Occupancy*	Atom	*Occupancy*	Atom	*Occupancy*
H1A	0.848(4)	H1	0.152(4)	H12A	0.601(5)
H12B	0.601(5)	H12C	0.399(5)	H12D	0.399(5)
C13A	0.601(5)	C14A	0.601(5)	C15A	0.601(5)
H15A	0.601(5)	C16A	0.601(5)	C17A	0.601(5)
H17A	0.601(5)	C18A	0.601(5)	H18A	0.601(5)
O4A	0.601(5)	C19A	0.601(5)	H19A	0.601(5)
H19B	0.601(5)	H19C	0.601(5)	O5A	0.601(5)
C20A	0.601(5)	H20A	0.601(5)	H20B	0.601(5)
H20C	0.601(5)	C13B	0.399(5)	C14B	0.399(5)
C15B	0.399(5)	H15B	0.399(5)	C16B	0.399(5)
C17B	0.399(5)	H17B	0.399(5)	C18B	0.399(5)
H18B	0.399(5)	O4B	0.399(5)	C19B	0.399(5)
H19D	0.399(5)	H19E	0.399(5)	H19F	0.399(5)
O5B	0.399(5)	C20B	0.399(5)	H20D	0.399(5)
H20E	0.399(5)	H20F	0.399(5)	O6A	0.848(4)
O7A	0.848(4)	C21A	0.848(4)	C22A	0.848(4)
H22A	0.848(4)	H22B	0.848(4)	C23A	0.848(4)
H23A	0.848(4)	C24A	0.848(4)	C25A	0.848(4)
H25A	0.848(4)	C26A	0.848(4)	H26A	0.848(4)
C27A	0.848(4)	H27A	0.848(4)	C28A	0.848(4)
H28A	0.848(4)	C29A	0.848(4)	C30A	0.848(4)
C31A	0.848(4)	H31A	0.848(4)	C32A	0.848(4)
H32A	0.848(4)	C33A	0.848(4)	H33A	0.848(4)
C34A	0.848(4)	H34A	0.848(4)	C35A	0.848(4)
O6B	0.152(4)	O7B	0.152(4)	C21B	0.152(4)
C22B	0.152(4)	H22C	0.152(4)	H22D	0.152(4)
C23B	0.152(4)	H23B	0.152(4)	C24B	0.152(4)
C25B	0.152(4)	H25B	0.152(4)	C26B	0.152(4)
H26B	0.152(4)	C27B	0.152(4)	H27B	0.152(4)
C28B	0.152(4)	H28B	0.152(4)	C29B	0.152(4)
C30B	0.152(4)	C31B	0.152(4)	H31B	0.152(4)
C32B	0.152(4)	H32B	0.152(4)	C33B	0.152(4)
H33B	0.152(4)	C34B	0.152(4)	H34B	0.152(4)
C35B	0.152(4)				

Experimental

Crystals of $C_{35}H_{38}N_2O_7$ lube87 (**2.10d**) were grown in acetone-hexane, a suitable crystal was selected and mounted on the **Bruker Venture Metaljet** diffractometer. The crystal was kept at 100 K during data collection. Using Olex2 [1], the structure was solved with the XT [2] structure solution program using Direct Methods and refined with the XL [3] refinement package using Least Squares minimisation.

1. Dolomanov, O.V., Bourhis, L.J., Gildea, R.J, Howard, J.A.K. & Puschmann, H. (2009), J. Appl. Cryst. 42, 339-341.
2. Sheldrick, G.M. (2008). Acta Cryst. A64, 112-122.
3. Sheldrick, G.M. (2008). Acta Cryst. A64, 112-122.

Crystal structure determination of [lube87]

Crystal Data for $C_{35}H_{38}N_2O_7$ (M =598.67 g/mol): orthorhombic, space group $P2_12_12_1$ (no. 19), a = 9.4075(8) Å, b = 12.1987(10) Å, c = 27.339(2) Å, V = 3137.4(5) Å^3, Z = 4, T = 100 K, μ(GaKα) = 0.462 mm^{-1}, *Dcalc* = 1.267 g/cm^3, 28548 reflections measured (5.624° ≤ 2Θ ≤ 121.52°), 7022 unique (R_{int} = 0.0988, R_{sigma} = 0.0916) which were used in all calculations. The final R_1 was 0.0547 (I > 2σ(I)) and wR_2 was 0.1246 (all data).

Refinement model description

Number of restraints - 69, number of constraints - unknown.

Details:

```
1. Fixed Uiso
 At 1.2 times of:
  All C(H) groups, All C(H,H) groups, All C(H,H,H,H) groups, All N(H,H) groups
 At 1.5 times of:
  All C(H,H,H) groups
2. Restrained distances
 N1-C21A ≈ N1-C21B
 with sigma of 0.02
 C12-C13A ≈ C12-C13B
 with sigma of 0.02
3. Uiso/Uaniso restraints and constraints
Uanis(C13A) = Uanis(C13B)
Uanis(C14A) = Uanis(C14B)
Uanis(C15A) = Uanis(C15B)
Uanis(C16A) = Uanis(C16B)
Uanis(C17A) = Uanis(C17B)
Uanis(C18A) = Uanis(C18B)
Uanis(C19A) = Uanis(C19B)
Uanis(C20A) = Uanis(C20B)
Uanis(C21A) = Uanis(C21B)
Uanis(O4A) = Uanis(O4B)
Uanis(O5A) = Uanis(O5B)
Uanis(O6A) = Uanis(O6B)
Uanis(O7A) = Uanis(O7B)
Uanis(C22A) = Uanis(C22B)
Uanis(C23A) = Uanis(C23B)
Uanis(C24A) = Uanis(C24B)
Uanis(C25A) = Uanis(C25B)
Uanis(C26A) = Uanis(C26B)
Uanis(C27A) = Uanis(C27B)
Uanis(C28A) = Uanis(C28B)
Uanis(C29A) = Uanis(C29B)
Uanis(C35A) = Uanis(C35B)
Uanis(C34A) = Uanis(C34B)
Uanis(C30A) = Uanis(C30B)
Uanis(C31A) = Uanis(C31B)
Uanis(C32A) = Uanis(C32B)
Uanis(C33A) = Uanis(C33B)
Uanis(C34A) = Uanis(C34B)
Uanis(C35A) = Uanis(C35B)
4. Same fragment restrains
{C13A, C14A, C15A, C16A, C17A, C18A, O4A, C19A, O5A, C20A}
as
{C13B, C14B, C15B, C16B, C17B, C18B, O4B, C19B, O5B, C20B}
{O6A, O7A, C21A, C22A, C23A, C24A, C25A, C26A, C27A, C28A, C29A, C30A, C31A,
C32A, C33A, C34A, C35A}
as
{O6B, O7B, C21B, C22B, C23B, C24B, C25B, C26B, C27B, C28B, C29B, C30B, C31B,
C32B, C33B, C34B, C35B}
5. Others
```

```
 Sof(H12C)=Sof(H12D)=Sof(C13B)=Sof(C14B)=Sof(C15B)=Sof(H15B)=Sof(C16B)=
 Sof(C17B)=Sof(H17B)=Sof(C18B)=Sof(H18B)=Sof(O4B)=Sof(C19B)=Sof(H19D)=Sof(H19E)=
 Sof(H19F)=Sof(O5B)=Sof(C20B)=Sof(H20D)=Sof(H20E)=Sof(H20F)=1-FVAR(1)
 Sof(H12A)=Sof(H12B)=Sof(C13A)=Sof(C14A)=Sof(C15A)=Sof(H15A)=Sof(C16A)=
 Sof(C17A)=Sof(H17A)=Sof(C18A)=Sof(H18A)=Sof(O4A)=Sof(C19A)=Sof(H19A)=Sof(H19B)=
 Sof(H19C)=Sof(O5A)=Sof(C20A)=Sof(H20A)=Sof(H20B)=Sof(H20C)=FVAR(1)
 Sof(H1)=Sof(O6B)=Sof(O7B)=Sof(C21B)=Sof(C22B)=Sof(H22C)=Sof(H22D)=Sof(C23B)=
 Sof(H23B)=Sof(C24B)=Sof(C25B)=Sof(H25B)=Sof(C26B)=Sof(H26B)=Sof(C27B)=
 Sof(H27B)=Sof(C28B)=Sof(H28B)=Sof(C29B)=Sof(C30B)=Sof(C31B)=Sof(H31B)=
 Sof(C32B)=Sof(H32B)=Sof(C33B)=Sof(H33B)=Sof(C34B)=Sof(H34B)=Sof(C35B)=1-FVAR(2)
 Sof(H1A)=Sof(O6A)=Sof(O7A)=Sof(C21A)=Sof(C22A)=Sof(H22A)=Sof(H22B)=Sof(C23A)=
 Sof(H23A)=Sof(C24A)=Sof(C25A)=Sof(H25A)=Sof(C26A)=Sof(H26A)=Sof(C27A)=
 Sof(H27A)=Sof(C28A)=Sof(H28A)=Sof(C29A)=Sof(C30A)=Sof(C31A)=Sof(H31A)=
 Sof(C32A)=Sof(H32A)=Sof(C33A)=Sof(H33A)=Sof(C34A)=Sof(H34A)=Sof(C35A)=FVAR(2)
6.a Ternary CH refined with riding coordinates:
 C1(H1B), C3(H3), C23A(H23A), C23B(H23B)
6.b Secondary CH2 refined with riding coordinates:
 C4(H4A,H4B), C5(H5A,H5B), C6(H6A,H6B), C9(H9A,H9B), C12(H12A,H12B), C12(H12C,
 H12D), C22A(H22A,H22B), C22B(H22C,H22D)
6.c Aromatic/amide H refined with riding coordinates:
 N1(H1A), N1(H1), C7(H7), C8(H8), C15A(H15A), C17A(H17A), C18A(H18A),
 C15B(H15B), C17B(H17B), C18B(H18B), C25A(H25A), C26A(H26A), C27A(H27A),
 C28A(H28A), C31A(H31A), C32A(H32A), C33A(H33A), C34A(H34A), C25B(H25B),
 C26B(H26B), C27B(H27B), C28B(H28B), C31B(H31B), C32B(H32B), C33B(H33B),
 C34B(H34B)
6.d Fitted hexagon refined as free rotating group:
 C13A(C14A,C15A,C16A,C17A,C18A), C13B(C14B,C15B,C16B,C17B,C18B), C24A(C25A,
 C26A,C27A,C28A,C29A), C30A(C31A,C32A,C33A,C34A,C35A), C24B(C25B,C26B,C27B,C28B,
 C29B), C30B(C31B,C32B,C33B,C34B,C35B)
6.e Idealised Me refined as rotating group:
 C11(H11A,H11B,H11C), C19A(H19A,H19B,H19C), C20A(H20A,H20B,H20C), C19B(H19D,
 H19E,H19F), C20B(H20D,H20E,H20F)
```

This report has been created with Olex2, compiled on 2014.09.19 svn.r3010 for OlexSys. Please let us know if there are any errors or if you would like to have additional features.

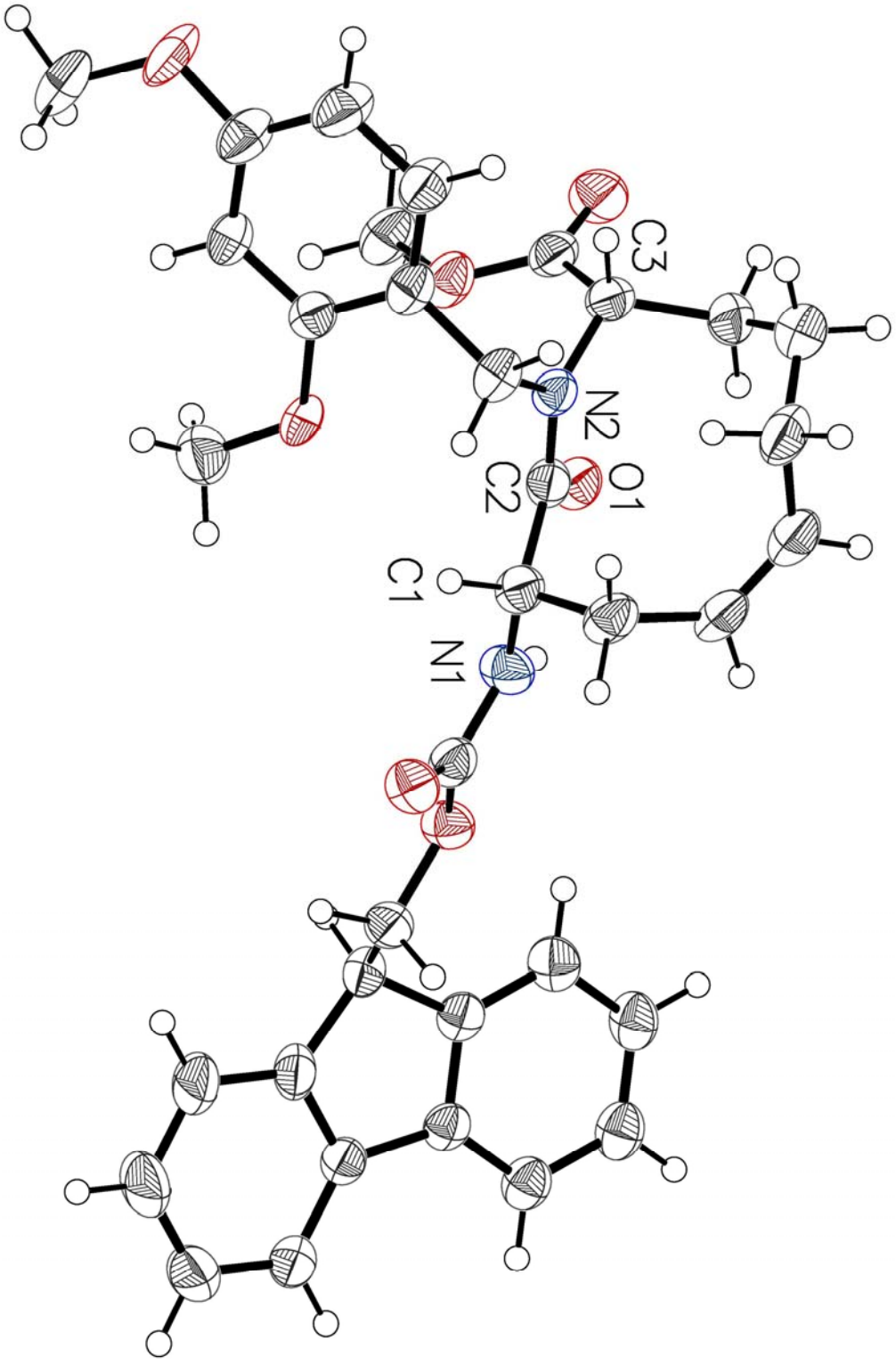
C3
N2
O1
C2
C1
N1

LUBE80: **(2.3)**

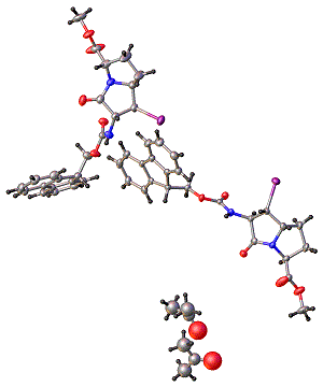

Table 1 Crystal data and structure refinement for LUBE80.

Identification code	LUBE80
Empirical formula	$C_{51}H_{52}I_2N_4O_{11}$
Formula weight	1150.76
Temperature/K	150
Crystal system	orthorhombic
Space group	$P2_12_12_1$
a/Å	5.2638(2)
b/Å	19.7530(8)
c/Å	46.4372(18)
α/°	90
β/°	90
γ/°	90
Volume/Å^3	4828.3(3)
Z	4
ρ_{calc}g/cm^3	1.583
μ/mm^{-1}	10.774
F(000)	2320.0
Crystal size/mm^3	0.2 × 0.03 × 0.02
Radiation	CuKα (λ = 1.54178)
2Θ range for data collection/°	3.806 to 141.26
Index ranges	$-5 \leq h \leq 6$, $-24 \leq k \leq 24$, $-56 \leq l \leq 56$
Reflections collected	90175
Independent reflections	9214 [R_{int} = 0.0737, R_{sigma} = 0.0441]
Data/restraints/parameters	9214/14/620
Goodness-of-fit on F^2	1.047
Final R indexes [I>=2σ (I)]	R_1 = 0.0301, wR_2 = 0.0734
Final R indexes [all data]	R_1 = 0.0347, wR_2 = 0.0752
Largest diff. peak/hole / e Å^{-3}	0.66/-0.46
Flack parameter	0.020(3)

Table 2 Fractional Atomic Coordinates ($\times 10^4$) and Equivalent Isotropic Displacement Parameters ($Å^2 \times 10^3$) for LUBE80. U_{eq} is defined as 1/3 of of the trace of the orthogonalised U_{IJ} tensor.

Atom	*x*	*y*	*z*	U(eq)
I1	7441.3(6)	1935.9(2)	5295.8(2)	37.04(10)
O1	10078(7)	3921.1(17)	6052.7(8)	34.0(8)
O2	15988(7)	2916(3)	6334.2(9)	57.6(13)
O3	13857(7)	2599(2)	6726.0(8)	48.3(10)
O4	4231(6)	3858.3(17)	5425.1(7)	26.8(7)
O5	6777(5)	4513.3(15)	5145.5(6)	24.3(6)
N1	11531(7)	2834.3(19)	5999.3(8)	25.0(8)
N2	8552(8)	3761(2)	5435.0(9)	26.0(9)
C1	10164(9)	3401(2)	5919.6(10)	25.8(10)
C2	8669(8)	3230(2)	5646.0(9)	22.0(9)
C3	9952(9)	2581(2)	5540.2(10)	24.7(10)
C4	11044(9)	2249(2)	5809.6(10)	27.2(10)
C5	9473(10)	1783(3)	5998.5(11)	33.7(12)
C6	10806(11)	1871(3)	6292.4(12)	41.4(13)
C7	11575(9)	2629(3)	6301.4(10)	29.0(11)
C8	14082(9)	2738(3)	6445.0(11)	29.7(11)
C9	16097(12)	2680(4)	6900.3(13)	54.1(17)
C10	6334(8)	4027(2)	5346.2(10)	22.3(9)
C11	4563(8)	4887(2)	5051.5(10)	24.7(10)
C12	5524(8)	5447(2)	4857.3(10)	23.3(10)
C13	3452(9)	5958(2)	4790.2(10)	23.4(10)
C14	2048(9)	6354(2)	4977.3(11)	29.4(10)
C15	211(10)	6785(2)	4865.3(12)	33.3(12)
C16	-226(9)	6810(3)	4568.4(12)	35.8(12)
C17	1170(9)	6419(3)	4381.0(12)	33.0(12)
C18	3024(9)	5996(2)	4491.1(10)	25.6(10)
C19	4840(9)	5543(3)	4347.8(10)	26.1(10)
C20	5261(11)	5419(3)	4056.8(11)	36.7(12)
C21	7198(12)	4977(3)	3981.0(11)	42.6(13)
C22	8676(10)	4664(3)	4187.3(12)	36.4(12)
C23	8225(9)	4776(2)	4479.7(10)	30(1)
C24	6326(9)	5221(2)	4557.6(10)	26.1(10)
I31	11891.3(6)	4425.2(2)	3338.6(2)	40.54(10)
O31	9385(8)	6648(2)	2711.8(9)	45.7(10)
O32	3475(8)	5715(4)	2377.2(9)	87(2)
O33	5586(7)	5622(2)	1965.2(7)	44.5(10)
O34	6617(6)	6430.2(18)	3356.9(8)	35.1(8)
O35	9407(6)	7057.5(18)	3616.1(8)	34.0(8)
N31	7891(8)	5559(2)	2697.7(8)	32.6(9)

N32	10887(8)	6288(2)	3310.9(10)	31.0(9)
C31	9249(10)	6089(3)	2810.9(11)	32.7(12)
C32	10706(9)	5826(2)	3073.5(10)	28.8(10)
C33	9419(9)	5153(2)	3137.8(10)	26.9(10)
C34	8277(11)	4914(3)	2851.0(11)	35.8(12)
C35	9844(15)	4507(4)	2639.1(12)	57.4(18)
C36	8623(17)	4703(4)	2350.2(13)	72(2)
C37	7879(10)	5453(3)	2386.1(10)	39.4(13)
C38	5385(9)	5617(3)	2252.2(11)	35.4(12)
C39	3317(12)	5747(4)	1803.5(13)	60.0(19)
C40	8780(9)	6582(2)	3421.5(10)	28.1(11)
C41	7259(10)	7407(3)	3748.3(11)	34.9(11)
C42	8375(9)	7967(2)	3931.3(10)	29.9(10)
C43	6353(9)	8304(2)	4117.1(10)	28(1)
C44	4561(9)	8014(3)	4296.6(11)	29.5(10)
C45	2844(10)	8440(2)	4435(1)	30.9(10)
C46	2966(10)	9130(3)	4396.4(10)	32.7(11)
C47	4766(9)	9424(3)	4220.7(10)	32.2(11)
C48	6451(9)	9006(2)	4078.7(10)	27.4(10)
C49	8463(9)	9165(2)	3868.9(10)	28(1)
C50	9347(11)	9785(3)	3772.8(12)	36.9(12)
C51	11318(11)	9800(3)	3575.1(12)	42.7(14)
C52	12320(11)	9202(3)	3467.5(11)	42.5(13)
C53	11466(10)	8573(3)	3571.0(12)	38.9(13)
C54	9540(9)	8560(3)	3774.7(11)	31.5(11)
O61A	10520(40)	6462(8)	7509(4)	170(6)
C61A	10200(30)	7009(7)	7391(2)	74(3)
C62A	9210(30)	7524(7)	7573(3)	102(4)
C63A	10540(40)	7102(9)	7083(3)	104(4)
O61B	1560(60)	6810(17)	7542(6)	170(6)
C61B	850(40)	6882(13)	7291(5)	74(3)
C62B	-1070(50)	7357(14)	7200(7)	102(4)
C63B	2710(60)	6780(16)	7070(5)	104(4)

Table 3 Anisotropic Displacement Parameters ($Å^2×10^3$) for LUBE80. The Anisotropic displacement factor exponent takes the form: $-2\pi^2[h^2a^{*2}U_{11}+2hka^*b^*U_{12}+\ldots]$.

Atom	U_{11}	U_{22}	U_{33}	U_{23}	U_{13}	U_{12}
I1	46.10(19)	31.76(16)	33.27(16)	-6.67(13)	-4.78(16)	-3.73(15)
O1	41.2(19)	26.6(19)	34.1(19)	-1.7(16)	-7.2(17)	-1.9(16)
O2	25.3(19)	105(4)	43(2)	21(2)	-2.0(17)	-6(2)
O3	37(2)	78(3)	30(2)	9.1(19)	-7.2(16)	0(2)
O4	19.8(15)	30.1(18)	30.5(18)	4.6(14)	-0.1(14)	0.5(14)
O5	21.2(14)	23.9(16)	28.0(16)	7.3(13)	-1.3(13)	2.7(13)

N1	25.7(19)	27(2)	22.8(19)	5.4(15)	-2.7(16)	0.3(16)
N2	18.0(19)	28(2)	32(2)	8.1(17)	-0.5(18)	-2.2(17)
C1	25(2)	27(3)	25(2)	5(2)	2(2)	-4(2)
C2	24(2)	20(2)	22(2)	1.9(17)	-1.6(18)	-1.4(18)
C3	28(2)	23(2)	24(2)	0.4(19)	-0.2(19)	-2.2(19)
C4	26(2)	22(2)	33(3)	2(2)	1(2)	4.3(19)
C5	42(3)	26(3)	32(3)	10(2)	-4(2)	-5(2)
C6	50(3)	36(3)	38(3)	18(3)	-10(3)	-7(3)
C7	24(2)	36(3)	27(2)	8(2)	-4(2)	0(2)
C8	24(2)	36(3)	29(3)	6(2)	-2(2)	1(2)
C9	45(3)	79(5)	38(3)	2(3)	-18(3)	3(3)
C10	26(2)	18(2)	22(2)	-2.3(18)	-4.5(19)	-2.5(18)
C11	20(2)	26(2)	28(2)	2.6(19)	-3.8(19)	3.6(19)
C12	23(2)	23(2)	24(2)	1.1(19)	-3.5(18)	0.6(18)
C13	25(2)	20(2)	26(2)	4.6(18)	-0.4(19)	-5.2(18)
C14	29(2)	24(2)	34(3)	5.1(19)	4(2)	-3(2)
C15	31(2)	24(3)	45(3)	6(2)	7(2)	6(2)
C16	25(2)	32(3)	50(3)	15(2)	-2(2)	1(2)
C17	30(2)	34(3)	35(3)	13(2)	-6(2)	-4(2)
C18	27(2)	21(2)	29(2)	7.2(18)	-6(2)	-2.7(19)
C19	26(2)	26(2)	26(2)	4(2)	-2.6(19)	-3(2)
C20	46(3)	39(3)	26(3)	8(2)	-5(2)	-1(2)
C21	55(3)	44(3)	29(3)	-1(2)	7(3)	-1(3)
C22	36(3)	34(3)	39(3)	-5(2)	6(2)	1(2)
C23	31(2)	28(2)	32(2)	1(2)	3(2)	1(2)
C24	27(2)	24(2)	27(2)	3.5(19)	-4(2)	-5.7(19)
I31	44.8(2)	41.03(19)	35.75(17)	9.21(15)	1.00(16)	11.64(16)
O31	49(2)	41(2)	47(2)	14.1(19)	2.7(19)	7.5(19)
O32	32(2)	193(7)	36(2)	-25(3)	-2.4(19)	27(3)
O33	37.9(19)	72(3)	23.2(18)	0.3(19)	-3.4(15)	12(2)
O34	24.3(16)	42(2)	39(2)	-11.3(17)	-1.3(16)	4.6(14)
O35	27.4(16)	35(2)	39(2)	-15.5(16)	-3.2(15)	8.8(16)
N31	34(2)	41(2)	22.6(19)	-2.5(17)	-0.5(17)	11(2)
N32	22(2)	34(2)	38(2)	-9(2)	1.2(19)	3.4(18)
C31	33(3)	36(3)	30(3)	3(2)	6(2)	8(2)
C32	28(2)	31(3)	27(2)	0(2)	2(2)	6(2)
C33	28(2)	28(3)	24(2)	1(2)	3(2)	8(2)
C34	41(3)	37(3)	29(3)	-1(2)	-2(2)	4(2)
C35	86(5)	54(4)	32(3)	-14(3)	-9(3)	35(4)
C36	106(6)	72(5)	37(3)	-21(3)	-17(4)	55(4)
C37	34(3)	61(4)	23(2)	-4(2)	5(2)	12(3)
C38	28(2)	50(3)	28(3)	-6(3)	3(2)	1(3)
C39	41(3)	103(6)	35(3)	-6(3)	-14(3)	14(4)
C40	31(3)	25(3)	29(3)	-4.0(19)	-3(2)	4(2)
C41	28(2)	37(3)	40(3)	-10(2)	1(2)	3(2)

C42	29(2)	32(3)	29(2)	-2(2)	-2(2)	6(2)
C43	28(2)	28(2)	28(2)	-4(2)	-4(2)	2(2)
C44	29(2)	26(2)	34(3)	-1(2)	-6(2)	1(2)
C45	28(2)	39(3)	25(2)	-3(2)	0(2)	-2(2)
C46	36(3)	35(3)	27(2)	-5(2)	1(2)	6(2)
C47	40(3)	27(2)	30(3)	-4(2)	-3(2)	3(2)
C48	30(2)	27(2)	25(2)	-0.8(19)	-1(2)	2(2)
C49	29(2)	30(2)	25(2)	1.7(19)	-5(2)	0(2)
C50	42(3)	31(3)	37(3)	9(2)	1(2)	3(2)
C51	41(3)	46(3)	42(3)	19(3)	2(3)	-1(3)
C52	33(3)	60(4)	34(3)	13(2)	6(2)	2(3)
C53	32(3)	48(3)	37(3)	-1(2)	5(2)	10(2)
C54	29(2)	36(3)	29(3)	2(2)	0(2)	2(2)

Table 4 Bond Lengths for LUBE80.

Atom	Atom	Length/Å	Atom	Atom	Length/Å
I1	C3	2.159(5)	O33	C38	1.337(6)
O1	C1	1.200(6)	O33	C39	1.432(7)
O2	C8	1.181(6)	O34	C40	1.215(6)
O3	C8	1.339(6)	O35	C40	1.344(6)
O3	C9	1.439(7)	O35	C41	1.460(6)
O4	C10	1.213(6)	N31	C31	1.372(7)
O5	C10	1.359(5)	N31	C34	1.473(7)
O5	C11	1.447(5)	N31	C37	1.462(6)
N1	C1	1.381(6)	N32	C32	1.435(6)
N1	C4	1.476(6)	N32	C40	1.353(6)
N1	C7	1.460(6)	C31	C32	1.532(7)
N2	C2	1.436(6)	C32	C33	1.521(7)
N2	C10	1.345(6)	C33	C34	1.535(7)
C1	C2	1.532(6)	C34	C35	1.515(8)
C2	C3	1.530(6)	C35	C36	1.537(8)
C3	C4	1.526(6)	C36	C37	1.541(9)
C4	C5	1.517(7)	C37	C38	1.488(7)
C5	C6	1.544(7)	C41	C42	1.514(7)
C6	C7	1.551(7)	C42	C43	1.524(7)
C7	C8	1.494(7)	C42	C54	1.509(7)
C11	C12	1.515(6)	C43	C44	1.383(7)
C12	C13	1.518(6)	C43	C48	1.398(7)
C12	C24	1.522(6)	C44	C45	1.392(7)
C13	C14	1.383(7)	C45	C46	1.377(7)
C13	C18	1.409(6)	C46	C47	1.378(7)
C14	C15	1.389(7)	C47	C48	1.379(7)
C15	C16	1.399(8)	C48	C49	1.473(7)

C16	C17	1.376(8)	C49	C50	1.385(7)
C17	C18	1.382(7)	C49	C54	1.393(7)
C18	C19	1.469(7)	C50	C51	1.386(8)
C19	C20	1.391(7)	C51	C52	1.388(8)
C19	C24	1.402(6)	C52	C53	1.405(8)
C20	C21	1.388(8)	C53	C54	1.387(7)
C21	C22	1.381(8)	O61A	C61A	1.223(15)
C22	C23	1.396(7)	C61A	C62A	1.422(12)
C23	C24	1.379(7)	C61A	C63A	1.454(12)
I31	C33	2.152(5)	O61B	C61B	1.231(18)
O31	C31	1.198(6)	C61B	C62B	1.443(14)
O32	C38	1.177(6)	C61B	C63B	1.436(14)

Table 5 Bond Angles for LUBE80.

Atom	Atom	Atom	Angle/°	Atom	Atom	Atom	Angle/°
C8	O3	C9	116.9(5)	C31	N31	C37	119.4(4)
C10	O5	C11	115.4(3)	C37	N31	C34	110.8(4)
C1	N1	C4	112.6(4)	C40	N32	C32	120.7(4)
C1	N1	C7	119.4(4)	O31	C31	N31	125.9(5)
C7	N1	C4	111.0(4)	O31	C31	C32	126.1(5)
C10	N2	C2	122.1(4)	N31	C31	C32	107.9(4)
O1	C1	N1	125.1(4)	N32	C32	C31	115.4(4)
O1	C1	C2	126.6(4)	N32	C32	C33	115.8(4)
N1	C1	C2	108.2(4)	C33	C32	C31	103.3(4)
N2	C2	C1	115.3(4)	C32	C33	I31	113.5(3)
N2	C2	C3	114.3(4)	C32	C33	C34	105.8(4)
C3	C2	C1	102.9(4)	C34	C33	I31	114.1(3)
C2	C3	I1	113.2(3)	N31	C34	C33	102.0(4)
C4	C3	I1	114.0(3)	N31	C34	C35	102.7(4)
C4	C3	C2	105.3(4)	C35	C34	C33	120.9(5)
N1	C4	C3	102.6(4)	C34	C35	C36	101.9(5)
N1	C4	C5	103.0(4)	C35	C36	C37	104.7(5)
C5	C4	C3	122.0(4)	N31	C37	C36	104.1(4)
C4	C5	C6	101.2(4)	N31	C37	C38	112.7(4)
C5	C6	C7	104.6(4)	C38	C37	C36	112.9(5)
N1	C7	C6	103.8(4)	O32	C38	O33	123.9(5)
N1	C7	C8	113.7(4)	O32	C38	C37	125.7(5)
C8	C7	C6	112.5(4)	O33	C38	C37	110.4(4)
O2	C8	O3	124.1(5)	O34	C40	O35	124.7(4)
O2	C8	C7	126.8(5)	O34	C40	N32	124.6(4)
O3	C8	C7	109.1(4)	O35	C40	N32	110.7(4)
O4	C10	O5	124.0(4)	O35	C41	C42	106.3(4)
O4	C10	N2	126.3(4)	C41	C42	C43	111.5(4)

N2	C10	O5	109.7(4)	C54	C42	C41	117.0(4)
O5	C11	C12	106.5(4)	C54	C42	C43	102.5(4)
C11	C12	C13	111.6(4)	C44	C43	C42	129.5(4)
C11	C12	C24	114.9(4)	C44	C43	C48	120.9(5)
C13	C12	C24	102.0(4)	C48	C43	C42	109.6(4)
C14	C13	C12	129.1(4)	C43	C44	C45	118.0(5)
C14	C13	C18	120.2(4)	C46	C45	C44	120.6(5)
C18	C13	C12	110.6(4)	C45	C46	C47	121.7(5)
C13	C14	C15	118.9(5)	C46	C47	C48	118.3(5)
C14	C15	C16	120.3(5)	C43	C48	C49	108.8(4)
C17	C16	C15	121.1(5)	C47	C48	C43	120.5(5)
C16	C17	C18	118.8(5)	C47	C48	C49	130.7(5)
C13	C18	C19	108.1(4)	C50	C49	C48	130.0(5)
C17	C18	C13	120.6(5)	C50	C49	C54	121.4(5)
C17	C18	C19	131.3(4)	C54	C49	C48	108.5(4)
C20	C19	C18	130.6(4)	C49	C50	C51	118.9(5)
C20	C19	C24	120.4(5)	C50	C51	C52	120.3(5)
C24	C19	C18	108.9(4)	C51	C52	C53	120.5(5)
C21	C20	C19	118.3(5)	C54	C53	C52	119.0(5)
C22	C21	C20	121.4(5)	C49	C54	C42	110.4(4)
C21	C22	C23	120.5(5)	C53	C54	C42	129.8(5)
C24	C23	C22	118.7(5)	C53	C54	C49	119.7(5)
C19	C24	C12	110.3(4)	O61A	C61A	C62A	114.7(13)
C23	C24	C12	128.9(4)	O61A	C61A	C63A	122.4(14)
C23	C24	C19	120.7(4)	C62A	C61A	C63A	122.5(13)
C38	O33	C39	117.3(4)	O61B	C61B	C62B	124(2)
C40	O35	C41	115.0(4)	O61B	C61B	C63B	117(2)
C31	N31	C34	113.7(4)	C63B	C61B	C62B	111(2)

Table 6 Hydrogen Bonds for LUBE80.

D	H	A	d(D-H)/Å	d(H-A)/Å	d(D-A)/Å	D-H-A/°
N2	H2	O4[1]	0.74(5)	2.36(5)	2.996(5)	144(5)
N32	H32	O34[1]	0.82(8)	2.26(8)	3.037(5)	158(6)

[1]1+X,+Y,+Z

Table 7 Torsion Angles for LUBE80.

A	B	C	D	Angle/°	A	B	C	D	Angle/°
I1	C3	C4	N1	-153.0(3)	I31	C33	C34	N31	-151.6(3)
I1	C3	C4	C5	-38.7(6)	I31	C33	C34	C35	-38.7(7)
O1	C1	C2	N2	43.1(7)	O31	C31	C32	N32	41.4(7)
O1	C1	C2	C3	168.2(5)	O31	C31	C32	C33	168.7(5)

O5	C11	C12	C13	-169.0(4)		O35	C41	C42	C43	-171.4(4)	
O5	C11	C12	C24	75.5(5)		O35	C41	C42	C54	71.0(5)	
N1	C1	C2	N2	-140.6(4)		N31	C31	C32	N32	-142.6(4)	
N1	C1	C2	C3	-15.5(5)		N31	C31	C32	C33	-15.2(5)	
N1	C4	C5	C6	-39.4(5)		N31	C34	C35	C36	-39.0(7)	
N1	C7	C8	O2	-6.3(8)		N31	C37	C38	O32	-12.0(10)	
N1	C7	C8	O3	174.0(4)		N31	C37	C38	O33	169.6(5)	
N2	C2	C3	I1	-82.1(4)		N32	C32	C33	I31	-81.6(4)	
N2	C2	C3	C4	152.7(4)		N32	C32	C33	C34	152.6(4)	
C1	N1	C4	C3	19.6(5)		C31	N31	C34	C33	17.5(5)	
C1	N1	C4	C5	-107.9(4)		C31	N31	C34	C35	-108.4(5)	
C1	N1	C7	C6	128.1(5)		C31	N31	C37	C36	128.2(6)	
C1	N1	C7	C8	-109.4(5)		C31	N31	C37	C38	-109.1(6)	
C1	C2	C3	I1	152.2(3)		C31	C32	C33	I31	151.4(3)	
C1	C2	C3	C4	27.0(4)		C31	C32	C33	C34	25.5(5)	
C2	N2	C10	O4	-1.1(7)		C32	N32	C40	O34	8.8(8)	
C2	N2	C10	O5	-179.6(4)		C32	N32	C40	O35	-172.2(4)	
C2	C3	C4	N1	-28.3(4)		C32	C33	C34	N31	-26.1(5)	
C2	C3	C4	C5	85.9(5)		C32	C33	C34	C35	86.8(6)	
C3	C4	C5	C6	-153.4(5)		C33	C34	C35	C36	-151.5(6)	
C4	N1	C1	O1	173.7(4)		C34	N31	C31	O31	174.4(5)	
C4	N1	C1	C2	-2.6(5)		C34	N31	C31	C32	-1.6(6)	
C4	N1	C7	C6	-5.5(5)		C34	N31	C37	C36	-6.9(6)	
C4	N1	C7	C8	117.0(5)		C34	N31	C37	C38	115.8(5)	
C4	C5	C6	C7	36.7(5)		C34	C35	C36	C37	35.4(8)	
C5	C6	C7	N1	-19.8(5)		C35	C36	C37	N31	-18.1(7)	
C5	C6	C7	C8	-143.1(4)		C35	C36	C37	C38	-140.7(6)	
C6	C7	C8	O2	111.2(7)		C36	C37	C38	O32	105.6(8)	
C6	C7	C8	O3	-68.5(6)		C36	C37	C38	O33	-72.8(7)	
C7	N1	C1	O1	40.9(7)		C37	N31	C31	O31	40.6(7)	
C7	N1	C1	C2	-135.5(4)		C37	N31	C31	C32	-135.4(4)	
C7	N1	C4	C3	156.5(4)		C37	N31	C34	C33	155.3(4)	
C7	N1	C4	C5	29.0(5)		C37	N31	C34	C35	29.4(6)	
C9	O3	C8	O2	0.6(9)		C39	O33	C38	O32	-0.8(10)	
C9	O3	C8	C7	-179.7(5)		C39	O33	C38	C37	177.6(6)	
C10	O5	C11	C12	173.6(4)		C40	O35	C41	C42	-173.7(4)	
C10	N2	C2	C1	-120.3(5)		C40	N32	C32	C31	52.5(7)	
C10	N2	C2	C3	120.7(5)		C40	N32	C32	C33	-68.2(6)	
C11	O5	C10	O4	7.1(6)		C41	O35	C40	O34	-1.1(7)	
C11	O5	C10	N2	-174.4(4)		C41	O35	C40	N32	179.9(4)	
C11	C12	C13	C14	59.0(6)		C41	C42	C43	C44	49.9(7)	
C11	C12	C13	C18	-120.5(4)		C41	C42	C43	C48	-128.3(5)	
C11	C12	C24	C19	119.0(4)		C41	C42	C54	C49	125.6(5)	
C11	C12	C24	C23	-61.9(6)		C41	C42	C54	C53	-56.6(7)	
C12	C13	C14	C15	-179.2(5)		C42	C43	C44	C45	-177.4(5)	

C12 C13 C18 C17	178.5(4)	C42 C43 C48 C47	178.8(4)
C12 C13 C18 C19	-2.5(5)	C42 C43 C48 C49	0.7(5)
C13 C12 C24 C19	-1.9(5)	C43 C42 C54 C49	3.3(5)
C13 C12 C24 C23	177.2(5)	C43 C42 C54 C53	-178.9(5)
C13 C14 C15 C16	0.8(7)	C43 C44 C45 C46	-1.0(7)
C13 C18 C19 C20	-177.2(5)	C43 C48 C49 C50	-176.6(5)
C13 C18 C19 C24	1.2(5)	C43 C48 C49 C54	1.5(6)
C14 C13 C18 C17	-1.2(7)	C44 C43 C48 C47	0.4(7)
C14 C13 C18 C19	177.9(4)	C44 C43 C48 C49	-177.8(4)
C14 C15 C16 C17	-1.0(8)	C44 C45 C46 C47	0.2(7)
C15 C16 C17 C18	0.1(7)	C45 C46 C47 C48	0.9(7)
C16 C17 C18 C13	0.9(7)	C46 C47 C48 C43	-1.1(7)
C16 C17 C18 C19	-177.9(5)	C46 C47 C48 C49	176.5(5)
C17 C18 C19 C20	1.8(9)	C47 C48 C49 C50	5.5(9)
C17 C18 C19 C24	-179.9(5)	C47 C48 C49 C54	-176.4(5)
C18 C13 C14 C15	0.3(7)	C48 C43 C44 C45	0.7(7)
C18 C19 C20 C21	177.5(5)	C48 C49 C50 C51	178.9(5)
C18 C19 C24 C12	0.5(5)	C48 C49 C54 C42	-3.1(6)
C18 C19 C24 C23	-178.7(4)	C48 C49 C54 C53	178.9(5)
C19 C20 C21 C22	0.2(8)	C49 C50 C51 C52	2.4(8)
C20 C19 C24 C12	179.1(4)	C50 C49 C54 C42	175.2(5)
C20 C19 C24 C23	-0.1(7)	C50 C49 C54 C53	-2.8(8)
C20 C21 C22 C23	1.1(8)	C50 C51 C52 C53	-4.1(9)
C21 C22 C23 C24	-1.9(8)	C51 C52 C53 C54	2.3(8)
C22 C23 C24 C12	-177.7(5)	C52 C53 C54 C42	-176.5(5)
C22 C23 C24 C19	1.4(7)	C52 C53 C54 C49	1.1(8)
C24 C12 C13 C14	-177.7(4)	C54 C42 C43 C44	175.9(5)
C24 C12 C13 C18	2.7(5)	C54 C42 C43 C48	-2.3(5)
C24 C19 C20 C21	-0.7(8)	C54 C49 C50 C51	1.1(8)

Table 8 Hydrogen Atom Coordinates (Å×10^4) and Isotropic Displacement Parameters (Å^2×10^3) for LUBE80.

Atom	*x*	*y*	*z*	U(eq)
H2	9770(100)	3910(20)	5381(10)	10(13)
H2A	6890	3115	5704	26
H3	11402	2713	5413	30
H4	12690	2024	5761	33
H5A	9558	1308	5931	40
H5B	7675	1929	6007	40
H6A	12322	1576	6306	50
H6B	9635	1760	6452	50
H7	10243	2888	6408	35
H9A	15623	2672	7104	81

H9B	16909	3113	6855	81
H9C	17285	2310	6861	81
H11A	3651	5079	5219	30
H11B	3387	4586	4945	30
H12	6977	5683	4953	28
H14	2336	6332	5179	35
H15	-754	7064	4991	40
H16	-1507	7101	4495	43
H17	865	6439	4180	40
H20	4249	5632	3914	44
H21	7513	4888	3783	51
H22	10010	4369	4130	44
H23	9207	4551	4622	36
H32	12330(160)	6440(30)	3329(15)	60(20)
H32A	12477	5723	3009	35
H33	7981	5243	3273	32
H34	6606	4687	2885	43
H35A	9693	4015	2676	69
H35B	11658	4639	2646	69
H36A	7107	4421	2311	86
H36B	9847	4646	2190	86
H37	9222	5743	2297	47
H39A	3752	5813	1600	90
H39B	2477	6154	1877	90
H39C	2169	5359	1822	90
H41A	6262	7090	3869	42
H41B	6129	7598	3598	42
H42	9692	7766	4061	36
H44	4504	7538	4325	35
H45	1578	8253	4557	37
H46	1779	9412	4493	39
H47	4843	9901	4198	39
H50	8614	10194	3841	44
H51	11986	10222	3513	51
H52	13593	9217	3323	51
H53	12196	8164	3502	47
H62A	7502	7649	7507	152
H62B	10317	7921	7566	152
H62C	9109	7355	7771	152
H63A	11903	6805	7015	155
H63B	10985	7575	7044	155
H63C	8954	6989	6983	155
H62D	-2698	7120	7179	152
H62E	-580	7558	7016	152
H62F	-1247	7714	7345	152

H63D	3682	7199	7041	155
H63E	1858	6658	6890	155
H63F	3870	6415	7127	155

Table 9 Atomic Occupancy for LUBE80.

Atom	*Occupancy*	Atom	*Occupancy*	Atom	*Occupancy*
O61A	0.655(8)	C61A	0.655(8)	C62A	0.655(8)
H62A	0.655(8)	H62B	0.655(8)	H62C	0.655(8)
C63A	0.655(8)	H63A	0.655(8)	H63B	0.655(8)
H63C	0.655(8)	O61B	0.345(8)	C61B	0.345(8)
C62B	0.345(8)	H62D	0.345(8)	H62E	0.345(8)
H62F	0.345(8)	C63B	0.345(8)	H63D	0.345(8)
H63E	0.345(8)	H63F	0.345(8)		

Experimental

Crystals of $C_{51}H_{52}I_2N_4O_{11}$ LUBE80 (**2.3**) were grown in acetone-hexane, a suitable crystal was selected and mounted on the **Bruker Microstar X8** diffractometer. The crystal was kept at 150 K during data collection. Using Olex2 [1], the structure was solved with the XT [2] structure solution program using Direct Methods and refined with the XL [3] refinement package using Least Squares minimisation.

1. Dolomanov, O.V., Bourhis, L.J., Gildea, R.J, Howard, J.A.K. & Puschmann, H. (2009), J. Appl. Cryst. 42, 339-341.
2. Sheldrick, G.M. (2008). Acta Cryst. A64, 112-122.
3. Sheldrick, G.M. (2008). Acta Cryst. A64, 112-122.

Crystal structure determination of [LUBE80]

Crystal Data for $C_{51}H_{52}I_2N_4O_{11}$ (M =1150.76 g/mol): orthorhombic, space group $P2_12_12_1$ (no. 19), a = 5.2638(2) Å, b = 19.7530(8) Å, c = 46.4372(18) Å, V = 4828.3(3) Å^3, Z = 4, T = 150 K, μ(CuKα) = 10.774 mm^{-1}, *Dcalc* = 1.583 g/cm^3, 90175 reflections measured (3.806° ≤ 2Θ ≤ 141.26°), 9214 unique (R_{int} = 0.0737, R_{sigma} = 0.0441) which were used in all calculations. The final R_1 was 0.0301 (I > 2σ(I)) and wR_2 was 0.0752 (all data).

Refinement model description

Number of restraints - 14, number of constraints - unknown.

Details:

```
1. Fixed Uiso
 At 1.2 times of:
  All C(H) groups, All C(H,H) groups
 At 1.5 times of:
  All C(H,H,H) groups
2. Restrained distances
 O61B-C61B ≈ O61A-C61A
 with sigma of 0.01
 C61B-C62B ≈ C61B-C63B ≈ C61A-C62A ≈ C61A-C63A
 with sigma of 0.01
 O61B-C62B ≈ O61B-C63B ≈ O61A-C62A ≈ O61A-C63A
 with sigma of 0.04
 C63B-C62B ≈ C63A-C62A
 with sigma of 0.04
3. Uiso/Uaniso restraints and constraints
: with sigma of 0.04 and sigma for terminal atoms of 0.08
Uiso(O61A) = Uiso(O61B)
Uiso(C61A) = Uiso(C61B)
Uiso(C62A) = Uiso(C62B)
Uiso(C63A) = Uiso(C63B)
4. Others
```

```
 Sof(O61B)=Sof(C61B)=Sof(C62B)=Sof(H62D)=Sof(H62E)=Sof(H62F)=Sof(C63B)=
 Sof(H63D)=Sof(H63E)=Sof(H63F)=1-FVAR(1)
 Sof(O61A)=Sof(C61A)=Sof(C62A)=Sof(H62A)=Sof(H62B)=Sof(H62C)=Sof(C63A)=
 Sof(H63A)=Sof(H63B)=Sof(H63C)=FVAR(1)
5.a Ternary CH refined with riding coordinates:
 C2(H2A), C3(H3), C4(H4), C7(H7), C12(H12), C32(H32A), C33(H33), C34(H34),
 C37(H37), C42(H42)
5.b Secondary CH2 refined with riding coordinates:
 C5(H5A,H5B), C6(H6A,H6B), C11(H11A,H11B), C35(H35A,H35B), C36(H36A,H36B),
 C41(H41A,H41B)
5.c Aromatic/amide H refined with riding coordinates:
 C14(H14), C15(H15), C16(H16), C17(H17), C20(H20), C21(H21), C22(H22),
 C23(H23), C44(H44), C45(H45), C46(H46), C47(H47), C50(H50), C51(H51), C52(H52),
  C53(H53)
5.d Idealised Me refined as rotating group:
 C9(H9A,H9B,H9C), C39(H39A,H39B,H39C), C62A(H62A,H62B,H62C), C63A(H63A,H63B,
 H63C), C62B(H62D,H62E,H62F), C63B(H63D,H63E,H63F)
```

This report has been created with Olex2, compiled on 2014.09.19 svn.r3010 for OlexSys. Please let us know if there are any errors or if you would like to have additional features.

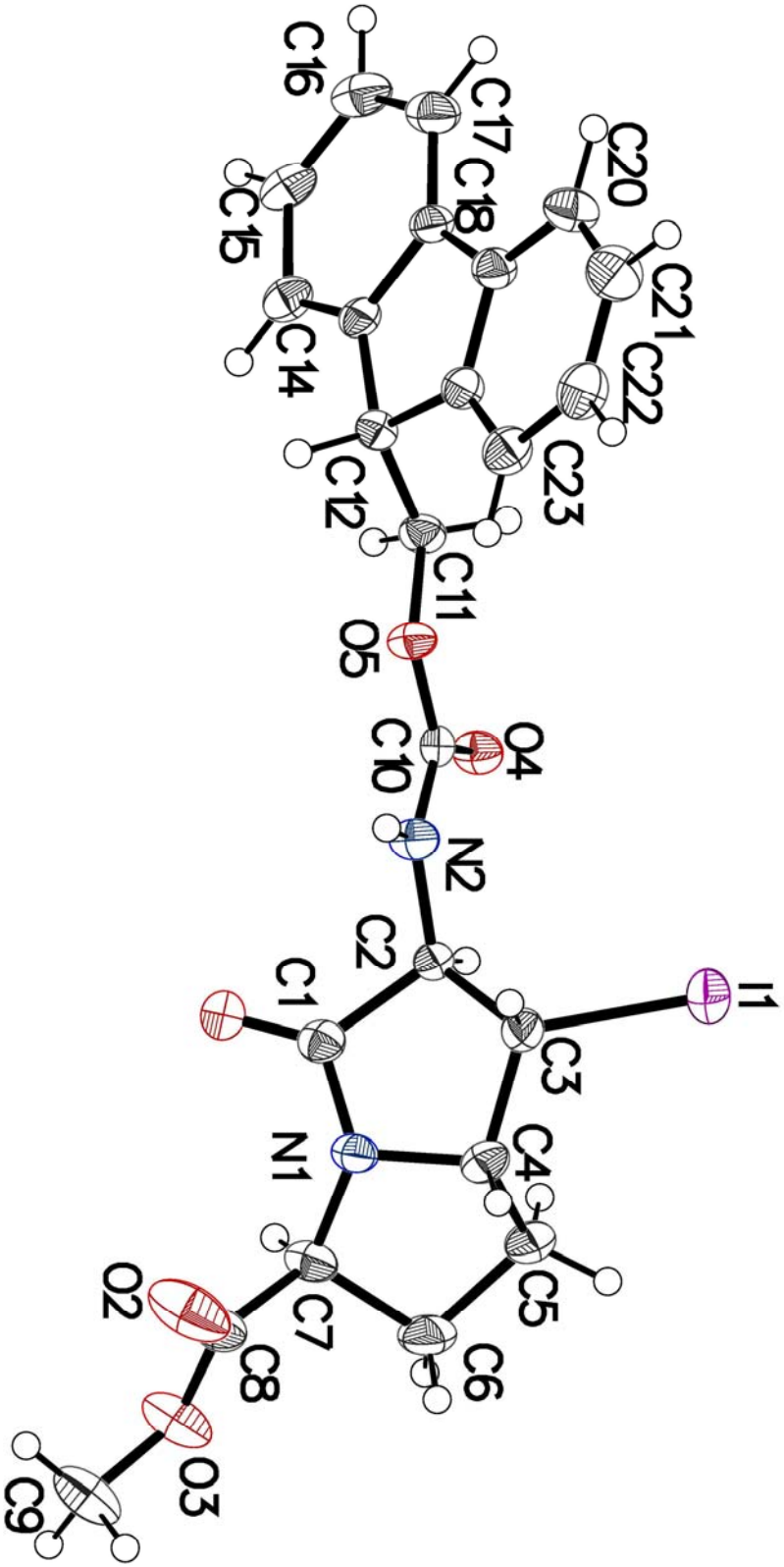
C16
C17
C18
C20
C15
C21
C14
C22
C12
C23
C11
O5
C10
O4
N2
C2
C1
I1
C3
N1
C4
O2
C7
C5
C8
C6
O3
C9

lube84: **(2.5)**

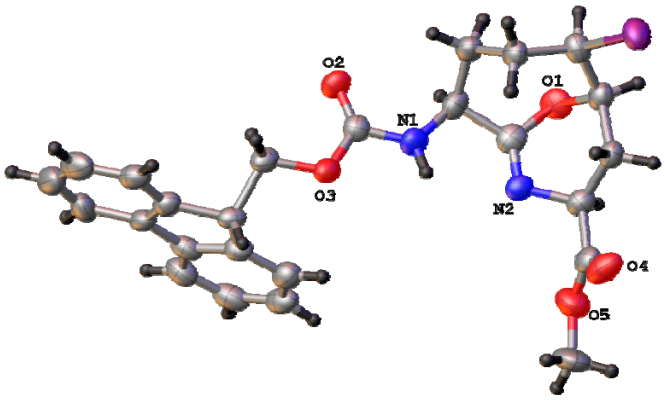

Table 1 Crystal data and structure refinement for lube84.

Identification code	lube84
Empirical formula	$C_{25}H_{25}IN_2O_5$
Formula weight	560.37
Temperature/K	100
Crystal system	orthorhombic
Space group	$P2_12_12_1$
a/Å	4.9813(6)
b/Å	15.1860(17)
c/Å	30.852(4)
α/°	90
β/°	90
γ/°	90
Volume/Å^3	2333.8(5)
Z	4
ρ_{calc}g/cm^3	1.595
μ/mm^{-1}	7.434
F(000)	1128.0
Crystal size/mm^3	0.15 × 0.02 × 0.02
Radiation	GaKα (λ = 1.34139)
2Θ range for data collection/°	4.984 to 109.91
Index ranges	$-5 \leq h \leq 4$, $-18 \leq k \leq 18$, $-37 \leq l \leq 36$
Reflections collected	15863
Independent reflections	4368 [R_{int} = 0.0965, R_{sigma} = 0.0845]
Data/restraints/parameters	4368/0/300
Goodness-of-fit on F^2	1.012
Final R indexes [I>=2σ (I)]	R_1 = 0.0562, wR_2 = 0.1352
Final R indexes [all data]	R_1 = 0.0699, wR_2 = 0.1418
Largest diff. peak/hole / e Å^{-3}	0.67/-0.94
Flack parameter	0.208(9)

Table 2 Fractional Atomic Coordinates ($\times 10^4$) and Equivalent Isotropic Displacement Parameters ($Å^2 \times 10^3$) for lube84. U_{eq} is defined as 1/3 of of the trace of the orthogonalised U_{IJ} tensor.

Atom	*x*	*y*	*z*	U(eq)
I1	9629.3(14)	6424.5(4)	3319.6(2)	55.6(3)
O1	5130(11)	5290(4)	4389(2)	45.9(15)
O2	9374(13)	6646(4)	5765.2(19)	44.4(15)
O3	12634(13)	5597(4)	5834.1(19)	42.9(15)
O4	11812(15)	3123(5)	3982(3)	62(2)
O5	9103(18)	2501(5)	4481(2)	70(2)
N1	9910(15)	5549(5)	5271(2)	44.1(17)
N2	8454(14)	4381(5)	4658(2)	38.4(17)
C1	7585(18)	5796(6)	5014(3)	45(2)
C2	7075(18)	5060(6)	4695(3)	44(2)
C3	6351(18)	5348(6)	3952(3)	42(2)
C4	7570(18)	6255(7)	3937(3)	44(2)
C5	9474(18)	6520(6)	4310(3)	41.3(19)
C6	7971(19)	6637(6)	4748(3)	46(2)
C7	7935(19)	3915(6)	4252(3)	42(2)
C8	8300(20)	4566(6)	3882(3)	41(2)
C9	10535(18)	5985(6)	5640(3)	38.6(18)
C10	13540(20)	6037(6)	6231(3)	42(2)
C11	14654(17)	5345(5)	6549(2)	35.3(17)
C12	15363(18)	5825(6)	6969(3)	39.0(19)
C13	17212(18)	6487(6)	7037(3)	48(2)
C14	17440(20)	6859(8)	7438(4)	63(3)
C15	15750(30)	6593(7)	7776(4)	64(3)
C16	13880(20)	5940(7)	7715(3)	53(3)
C17	13704(19)	5533(6)	7300(3)	41(2)
C18	11979(18)	4839(6)	7141(3)	43(2)
C19	10020(20)	4345(7)	7356(3)	51(2)
C20	8740(20)	3701(7)	7124(4)	57(3)
C21	9329(19)	3519(6)	6702(4)	53(2)
C22	11272(18)	4030(6)	6478(3)	48(2)
C23	12539(15)	4690(5)	6704(3)	38.8(18)
C24	9830(20)	3151(6)	4217(3)	44(2)
C25	10970(30)	1761(8)	4503(5)	88(4)

Table 3 Anisotropic Displacement Parameters ($Å^2×10^3$) for lube84. The Anisotropic displacement factor exponent takes the form: $-2\pi^2[h^2a^{*2}U_{11}+2hka^*b^*U_{12}+\ldots]$.

Atom	U_{11}	U_{22}	U_{33}	U_{23}	U_{13}	U_{12}
I1	68.6(4)	55.2(4)	42.9(3)	6.6(3)	-6.4(3)	-12.5(3)
O1	21(3)	57(4)	60(4)	-1(3)	-1(3)	-1(2)
O2	42(3)	44(4)	48(3)	-9(3)	6(3)	7(3)
O3	60(4)	35(4)	34(3)	0(3)	5(3)	4(3)
O4	49(4)	48(4)	90(6)	-20(4)	-1(4)	2(3)
O5	90(6)	57(5)	63(5)	17(4)	-14(4)	1(4)
N1	48(5)	44(4)	40(4)	-5(3)	5(3)	8(3)
N2	38(4)	35(4)	42(4)	-1(3)	6(3)	2(3)
C1	50(5)	46(6)	41(5)	-12(4)	5(4)	-1(4)
C2	37(5)	46(6)	49(5)	1(4)	8(4)	-8(4)
C3	38(5)	44(6)	44(5)	-9(4)	-7(4)	2(4)
C4	41(5)	54(6)	38(5)	1(4)	-3(4)	0(4)
C5	43(4)	38(5)	42(4)	-4(4)	-9(4)	-1(4)
C6	50(5)	39(6)	50(5)	-4(4)	-8(4)	8(4)
C7	41(5)	39(5)	48(6)	-5(4)	3(4)	0(4)
C8	45(5)	40(5)	37(5)	-6(4)	-2(4)	0(4)
C9	35(4)	40(5)	41(4)	1(4)	2(4)	-2(4)
C10	51(5)	34(5)	42(5)	1(4)	5(4)	-2(4)
C11	38(4)	27(4)	40(4)	5(3)	6(3)	2(3)
C12	36(4)	35(5)	45(5)	-3(4)	-2(4)	3(4)
C13	45(5)	35(5)	66(6)	2(5)	-11(4)	3(4)
C14	53(6)	52(7)	85(9)	1(6)	-31(6)	4(5)
C15	79(8)	50(7)	64(7)	-8(5)	-34(6)	9(6)
C16	64(7)	60(7)	35(5)	-1(5)	-11(4)	18(5)
C17	48(5)	28(5)	46(5)	0(4)	-12(4)	4(4)
C18	36(5)	44(6)	50(6)	16(4)	-4(4)	4(4)
C19	48(6)	56(6)	49(5)	15(5)	-4(5)	-1(4)
C20	42(5)	56(7)	71(7)	25(6)	-5(4)	2(4)
C21	45(4)	37(5)	76(7)	2(5)	-17(5)	-4(4)
C22	46(5)	43(6)	55(6)	-2(5)	-9(4)	3(4)
C23	37(4)	35(5)	45(5)	6(4)	0(4)	-2(3)
C24	47(6)	36(5)	49(5)	-8(4)	-8(5)	-5(4)
C25	126(12)	48(7)	91(9)	20(7)	-33(9)	19(7)

Table 4 Bond Lengths for lube84.

Atom	Atom	Length/Å	Atom	Atom	Length/Å
I1	C4	2.180(9)	C7	C8	1.521(13)
O1	C2	1.398(11)	C7	C24	1.499(13)
O1	C3	1.480(11)	C10	C11	1.542(12)
O2	C9	1.220(10)	C11	C12	1.528(12)
O3	C9	1.341(11)	C11	C23	1.525(11)
O3	C10	1.465(11)	C12	C13	1.379(13)
O4	C24	1.225(12)	C12	C17	1.388(13)
O5	C24	1.331(11)	C13	C14	1.366(15)
O5	C25	1.461(15)	C14	C15	1.399(18)
N1	C1	1.453(12)	C15	C16	1.375(16)
N1	C9	1.356(11)	C16	C17	1.424(14)
N2	C2	1.244(12)	C17	C18	1.444(13)
N2	C7	1.463(11)	C18	C19	1.397(13)
C1	C2	1.510(13)	C18	C23	1.395(14)
C1	C6	1.530(14)	C19	C20	1.368(15)
C3	C4	1.505(14)	C20	C21	1.364(15)
C3	C8	1.551(12)	C21	C22	1.419(14)
C4	C5	1.543(12)	C22	C23	1.374(13)
C5	C6	1.556(13)			

Table 5 Bond Angles for lube84.

Atom	Atom	Atom	Angle/°	Atom	Atom	Atom	Angle/°
C2	O1	C3	110.2(6)	C12	C11	C10	107.3(7)
C9	O3	C10	114.3(7)	C23	C11	C10	113.3(7)
C24	O5	C25	115.2(10)	C23	C11	C12	101.8(7)
C9	N1	C1	121.1(7)	C13	C12	C11	129.2(8)
C2	N2	C7	112.5(8)	C13	C12	C17	121.2(8)
N1	C1	C2	107.4(7)	C17	C12	C11	109.5(7)
N1	C1	C6	114.1(8)	C14	C13	C12	119.6(10)
C2	C1	C6	106.8(7)	C13	C14	C15	120.5(10)
O1	C2	C1	111.9(8)	C16	C15	C14	120.9(10)
N2	C2	O1	121.8(9)	C15	C16	C17	118.5(10)
N2	C2	C1	125.4(9)	C12	C17	C16	119.2(9)
O1	C3	C4	104.4(7)	C12	C17	C18	109.8(8)
O1	C3	C8	109.8(7)	C16	C17	C18	131.1(10)
C4	C3	C8	116.3(8)	C19	C18	C17	130.2(9)
C3	C4	I1	108.9(6)	C23	C18	C17	109.1(8)
C3	C4	C5	117.6(8)	C23	C18	C19	120.7(9)
C5	C4	I1	109.3(6)	C20	C19	C18	117.5(9)
C4	C5	C6	112.4(7)	C21	C20	C19	123.0(10)
C1	C6	C5	115.6(7)	C20	C21	C22	119.9(9)
N2	C7	C8	107.8(7)	C23	C22	C21	117.8(9)
N2	C7	C24	108.9(7)	C18	C23	C11	109.6(8)
C24	C7	C8	111.9(7)	C22	C23	C11	129.3(9)
C7	C8	C3	108.6(7)	C22	C23	C18	121.1(9)
O2	C9	O3	126.2(8)	O4	C24	O5	123.8(10)
O2	C9	N1	123.9(8)	O4	C24	C7	125.2(9)
O3	C9	N1	109.8(7)	O5	C24	C7	111.0(8)
O3	C10	C11	109.4(7)				

Table 6 Torsion Angles for lube84.

A	B	C	D	Angle/°	A	B	C	D	Angle/°
I1	C4	C5	C6	166.1(6)	C10	C11	C12	C13	-62.1(12)
O1	C3	C4	I1	177.4(5)	C10	C11	C12	C17	114.5(8)
O1	C3	C4	C5	52.3(10)	C10	C11	C23	C18	-110.3(8)
O1	C3	C8	C7	10.0(9)	C10	C11	C23	C22	70.1(11)
O3	C10	C11	C12	-175.7(7)	C11	C12	C13	C14	176.7(9)
O3	C10	C11	C23	-64.1(10)	C11	C12	C17	C16	-175.4(8)
N1	C1	C2	O1	-171.0(7)	C11	C12	C17	C18	3.2(10)
N1	C1	C2	N2	-1.4(12)	C12	C11	C23	C18	4.6(9)
N1	C1	C6	C5	82.0(10)	C12	C11	C23	C22	-175.0(9)
N2	C7	C8	C3	-58.1(9)	C12	C13	C14	C15	-2.0(15)
N2	C7	C24	O4	-104.6(10)	C12	C17	C18	C19	179.2(9)
N2	C7	C24	O5	74.7(9)	C12	C17	C18	C23	-0.2(10)
C1	N1	C9	O2	-6.2(13)	C13	C12	C17	C16	1.6(13)
C1	N1	C9	O3	175.6(7)	C13	C12	C17	C18	-179.9(8)
C2	O1	C3	C4	-82.6(8)	C13	C14	C15	C16	1.5(16)
C2	O1	C3	C8	42.8(9)	C14	C15	C16	C17	0.6(15)
C2	N2	C7	C8	53.7(10)	C15	C16	C17	C12	-2.1(13)
C2	N2	C7	C24	175.3(8)	C15	C16	C17	C18	179.7(9)
C2	C1	C6	C5	-36.5(10)	C16	C17	C18	C19	-2.4(16)
C3	O1	C2	N2	-56.4(11)	C16	C17	C18	C23	178.2(9)
C3	O1	C2	C1	113.7(8)	C17	C12	C13	C14	0.5(14)
C3	C4	C5	C6	-69.0(10)	C17	C18	C19	C20	-177.8(9)
C4	C3	C8	C7	128.2(9)	C17	C18	C23	C11	-3.0(9)
C4	C5	C6	C1	85.8(10)	C17	C18	C23	C22	176.6(8)
C6	C1	C2	O1	-48.3(9)	C18	C19	C20	C21	1.1(15)
C6	C1	C2	N2	121.4(10)	C19	C18	C23	C11	177.6(8)
C7	N2	C2	O1	4.4(12)	C19	C18	C23	C22	-2.8(13)
C7	N2	C2	C1	-164.3(8)	C19	C20	C21	C22	-2.4(15)
C8	C3	C4	I1	56.3(9)	C20	C21	C22	C23	1.1(13)
C8	C3	C4	C5	-68.8(11)	C21	C22	C23	C11	-179.0(8)
C8	C7	C24	O4	14.5(12)	C21	C22	C23	C18	1.5(13)
C8	C7	C24	O5	-166.2(8)	C23	C11	C12	C13	178.7(9)
C9	O3	C10	C11	147.8(7)	C23	C11	C12	C17	-4.7(9)
C9	N1	C1	C2	-166.4(8)	C23	C18	C19	C20	1.5(14)
C9	N1	C1	C6	75.4(10)	C24	C7	C8	C3	-177.9(7)
C10	O3	C9	O2	-0.2(12)	C25	O5	C24	O4	5.0(14)
C10	O3	C9	N1	178.0(7)	C25	O5	C24	C7	-174.3(9)

Table 7 Hydrogen Atom Coordinates (Å×10⁴) and Isotropic Displacement Parameters (Å²×10³) for lube84.

Atom	*x*	*y*	*z*	U(eq)
H1	10928	5109	5185	20(20)
H1A	5990	5865	5208	54
H3	4891	5314	3730	50
H4	6046	6684	3941	53
H5A	10380	7079	4234	50
H5B	10873	6062	4343	50
H6A	8977	7066	4927	56
H6B	6182	6893	4688	56
H7	6045	3692	4251	51
H8A	7919	4276	3602	49
H8B	10180	4781	3877	49
H10A	12017	6354	6366	51
H10B	14953	6472	6160	51
H11	16252	5035	6425	42
H13	18324	6683	6806	58
H14	18748	7301	7488	76
H15	15900	6867	8052	77
H16	12721	5764	7944	64
H19	9598	4451	7651	61
H20	7387	3366	7264	68
H21	8436	3051	6557	63
H22	11683	3920	6183	58
H25A	11047	1468	4220	132
H25B	10357	1341	4723	132
H25C	12762	1977	4580	132

Experimental

Crystals of $C_{25}H_{25}IN_2O_5$ lube84 (**2.5**) were grown in dichloromethane-hexane, a suitable crystal was selected and mounted on the **Bruker Venture Metaljet** diffractometer. The crystal was kept at 100 K during data collection. Using Olex2 [1], the structure was solved with the ShelXT [2] structure solution program using Direct Methods and refined with the XL [3] refinement package using Least Squares minimisation.

1. Dolomanov, O.V., Bourhis, L.J., Gildea, R.J, Howard, J.A.K. & Puschmann, H. (2009), J. Appl. Cryst. 42, 339-341.
2. Sheldrick, G.M. (2008). Acta Cryst. A64, 112-122.
3. Sheldrick, G.M. (2008). Acta Cryst. A64, 112-122.

Crystal structure determination of [lube84]

Crystal Data for $C_{25}H_{25}IN_2O_5$ (M =560.37 g/mol): orthorhombic, space group $P2_12_12_1$ (no. 19), a = 4.9813(6) Å, b = 15.1860(17) Å, c = 30.852(4) Å, V = 2333.8(5) Å^3, Z = 4, T = 100 K, μ(GaKα) = 7.434 mm^{-1}, *Dcalc* = 1.595 g/cm^3, 15863 reflections measured (4.984° ≤ 2Θ ≤ 109.91°), 4368 unique (R_{int} = 0.0965, R_{sigma} = 0.0845) which were used in all calculations. The final R_1 was 0.0562 (I > 2σ(I)) and wR_2 was 0.1418 (all data).

Refinement model description

Number of restraints - 0, number of constraints - unknown.
Details:

```
1. Fixed Uiso
 At 1.2 times of:
  All C(H) groups, All C(H,H) groups
 At 1.5 times of:
  All C(H,H,H) groups
2.a Ternary CH refined with riding coordinates:
 C1(H1A), C3(H3), C4(H4), C7(H7), C11(H11)
2.b Secondary CH2 refined with riding coordinates:
 C5(H5A,H5B), C6(H6A,H6B), C8(H8A,H8B), C10(H10A,H10B)
2.c Aromatic/amide H refined with riding coordinates:
 N1(H1), C13(H13), C14(H14), C15(H15), C16(H16), C19(H19), C20(H20), C21(H21),
 C22(H22)
2.d Idealised Me refined as rotating group:
 C25(H25A,H25B,H25C)
```

This report has been created with Olex2, compiled on 2014.09.19 svn.r3010 for OlexSys. Please let us know if there are any errors or if you would like to have additional features.

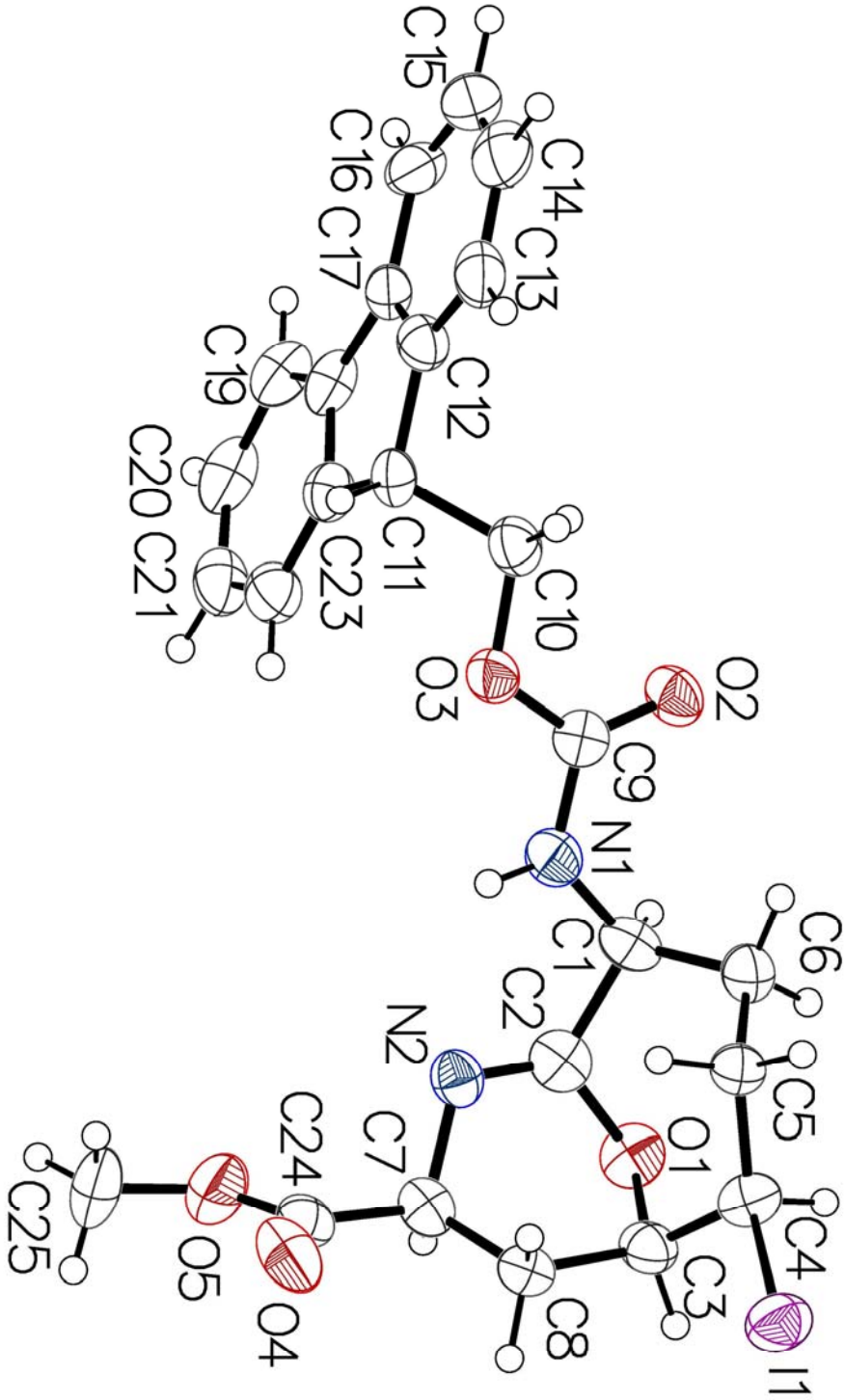
C15
C16
C17
C14
C13
C12
C19
C20
C21
C23
C11
C10
O3
O2
C9
N1
C1
C6
C2
N2
C5
C7
C24
O1
C4
C25
O5
O4
C8
C3
I1